

**DESIGN, SYNTHESIS AND BIOLOGICAL  
VALIDATION OF EPIGENETIC MODULATORS  
OF HISTONE/PROTEIN DEACETYLATION AND  
METHYLATION.**

Candidato: SERGIO VALENTE

Dottorato di Ricerca in Scienze Pasteuriane  
XIX Ciclo

**DESIGN, SYNTHESIS AND BIOLOGICAL VALIDATION OF EPIGENETIC MODULATORS OF HISTONE/PROTEIN DEACETYLATION AND METHYLATION.**

**Candidate: SERGIO VALENTE**

**Academic year 2005-2006  
XIX cycle**

**Ph.D. program: “SMALL MOLECULES AS EPIGENETIC MODULATORS”  
Department of Pharmaceutical Studies  
UNIVERSITY OF ROME “LA SAPIENZA”**

**Director of doctoral program:**

**Prof. Marco Tripodi (professor of Molecular Genetics)**

Department of Cellular Biotechnology and Hematology, University of Rome “La Sapienza”

**Scientific Tutor:**

**Prof. Antonello Mai (professor of Medicinal Chemistry)**

Department of Pharmaceuticals Studies, University of Rome “La Sapienza”

**Board of examiners:**

**Prof. Gino Lucente**

Department of Pharmaceuticals Studies, University of Rome “La Sapienza”

**Prof. Paolo Arese**

Department of Genetics, Biology and Biochemistry, University of Torin

**Prof. Mauro Piacentini**

Department of Biology, University of Rome “Tor Vergata”

**Acknowledgements**

I thank my Tutor, prof. Antonello Mai that has followed me since I was a graduated student. I am also grateful to the prof. Marino Artico for introducing in the research project work and my parents for their support.

## **Index**

1. Epigenetics.....	5
2. DNA methylation.....	6
3. Chromatin remodelling.....	9
4. Histone phosphorylation.....	14
5. Histone ubiquitylation.....	15
6. Histone acetylation status and gene expression.....	16
6.1. Histone acetyltransferase.....	17
6.2. Histone deacetylase.....	20
6.3. Histone deacetylase family: class I.....	23
6.4. Histone deacetylase family: class II.....	26
6.5. Biological role of histone deacetylases class IIa: MEF2 interaction.....	29
6.6. Regulation of histone deacetylase activities.....	32
7. Histone deacetylase and cancer.....	34
8. HDAC inhibitors in epigenetics: not only for cancer diseases.....	41
9. TSA/HDLP complex: mechanism of deacetylation.....	42
10. Histone methylation.....	45
10.1. Arginine methylation.....	46
10.2. Lysine methylation.....	55
11. Possible Arginine Demethylation by Amine Oxidases.....	59
12. Histone Methyltransferases and Cancer.....	60
13. HDAC inhibitors: mechanism of inhibition and pharmacophore model.....	61
14. HDAC inhibitors.....	65
14.1. Small molecule hydroxamic acid.....	66
14.2. Carboxylates.....	76
14.3. Benzamides.....	78
14.4. Electrophilic ketones.....	80
14.5. Cyclic peptide inhibitors.....	82
14.6. Thiol based inhibitors.....	87
15. Sirtuins' Inhibitors.....	88
16. Research project.....	89

16.1. First lead optimization.....	92
16.2. Chemistry.....	93
16.3 Experimental Section.....	102
16.4. Molecular modeling and docking studies.....	106
Binding mode of 4u.....	108
Binding mode of 4t.....	109
Docking of 4t and 4u.....	109
16.5. Biological evaluation.....	110
16.5.1. Anti-HD2 Activity and Structure-Activity Relationships (SARs).....	115
16.5.2. HD1-B and HD1-A Inhibitory Effects: Class Selectivity Assessment.....	116
16.5.3. Anti-mouse HDAC1 Activity of Selected Compounds.....	117
16.5.4. In Vitro Maize HD2, HD1-B, and HD1-A Enzyme Inhibition.....	118
16.5.5. Mouse HDAC1 Enzyme Assay.....	118
16.5.6. Growth Inhibition and Cell Differentiation Assay. Cell Culture and Reagents.....	118
16.5.7. Cell Viability and Growth Inhibition Assay.....	119
16.5.8. Cell Differentiation Assay.....	119
16.5.9. Antiproliferative and Cytodifferentiating Activities of 4b on Human Acute Promyelocytic Leukemia HL-60 Cells.....	120
16.5.10. Antiproliferative effect of 4b on human leukemia HL-60 cells.....	120
16.5.11. Differentiating activity of 4b on human leukemia HL-60 cells.....	122
16.5.12. Conclusions.....	123
17. Second lead optimizzation.....	124
17.1. Antiproliferative and Cytodifferentiating Effects of 4 on Friend Murine Erythroleukemia (MEL) Cells.....	129
18. Third lead optimization.....	131
18.1. Chemistry.....	132
18.3. Experimental Section.....	137
18.4. Biological evaluation.....	142
18.5. Modification of the connection unit and aromatic spacer.....	146
18.6. Chemistry.....	148
18.6. Experimental section.....	154
18.7. Biological evaluation, results and discussion.....	156

18.8. Conclusions.....	160
18.9. Optimizzation’s study of 3b.....	161
18.10. Chemistry.....	163
18.11. Experimental section.....	173
19. Biological evaluation.....	176
19.1. Granulocytic Differentiation on human U937 leukemia Cells.....	178
19.2. Effects on human U937 leukemia cells cycle.....	183
19.3 p21 Induction and $\alpha$ -Tubulin Acetylation.....	187
20. HMT inhibitors design.....	188
20.1. Chemistry.....	190
20.2. Experimental Section.....	205
20.3. Biological evaluation.....	210
20.3.1. Preparation of GST-RmtA Fusion Proteins.....	218
20.3.2. RmtA Inhibitory assay.....	219
20.3.3. PRMT1, CARM1/PRMT4, and SET7 Inhibitory Assay.....	219
20.4. Docking study of the compounds 1c, 1d and 1k.....	220
20.4.1. Molecular Docking.....	221
20.5. Results and discussion.....	221
References.....	223

## **Introduction.**

The epigenetic of human cancer has always been in the shadows of human cancer genetic but this area has become increasingly visible with a growing understanding of specific epigenetic mechanism.

If the disruption of the balance of epigenetic networks can cause several major pathologies, including cancer and syndromes involving chromosomal instabilities and mental retardation, great potential lies in the development of “epigenetic therapies”: several inhibitors of enzymes controlling epigenetic modifications, specifically histone deacetylases, have shown promising anti-tumorogenic effects for some malignancies.

### ***1. Epigenetics.***

Many phenomena suggest that gene expression is not determined solely by the DNA code itself. Instead, as it is now well known by cell and molecular biologists, this activity also depends on a host of so-called epigenetic phenomena-defined as any gene-regulating activity that does not involve changes to the DNA code and that can persist through one or more generations. Specifically, the most current interpretation of epigenetics combines the concept of changes in gene expression and the implication of mitotic inheritance with the use of DNA as a reference point and the implication of generational, including meiotic, inheritance to give rise to the current, and most widely accepted definition: the study of changes in gene function that are mitotically and/or meiotically heritable and that do not entail a change in DNA sequence.<sup>1,2</sup>

Although the mechanism of inheritance for epigenetic modifications has yet to be identified, the most important difference between an epigenetic mechanism and a genetic mechanism is that the epigenetic changes can be reversed by chemical agents.<sup>3</sup> Over the past 10 years, researchers have shown that gene activity is influenced by the proteins that package the DNA into chromatin, the protein-DNA complex that helps the genome fit nicely into the nucleus; by enzymes that modify both those proteins and the DNA itself; and even by RNAs.<sup>4</sup> As we will see in detail below, the two major mechanisms, sometimes strictly interdependent, in the epigenetic regulation of genes involve changes in the structure (remodeling) of chromatin, through covalent modifications of histone proteins and DNA methylation. These mechanisms have an important role in biological research and affect many different areas of study including cancer biology,<sup>5,6</sup> viral latency,<sup>7-10</sup> activity of mobile elements,<sup>11</sup> somatic

gene therapy,<sup>12-17</sup> cloning and transgenic technologies, shutting down of one copy of the X chromosome that occurs in female mammals,<sup>18</sup> genomic parental "imprinting" (in which a gene's activity depends on whether it is inherited from the mother or the father),<sup>19</sup> and developmental abnormalities.<sup>19</sup> Now, some researchers are beginning to investigate whether subtle modifications to the genome that do not alter its DNA sequence (i.e., epigenetic changes) may also underline common diseases such as diabetes, obesity, heart disease, and a host of psychiatric disorders like manic depression and schizophrenia. Many features of these conditions, such as the differences between pairs of twins in which only one suffers from schizophrenia,<sup>20</sup> cannot be explained readily by DNA-sequence variation. Although some psychiatric disorders seem to run in families, the chance of succumbing depends in some cases on whether this story is on the mother's or the father's side, suggesting that parental imprinting is involved. Moreover, in the mentioned case of twins, substantial differences in their patterns of DNA methylation have been found.<sup>20</sup> Some factors, such as lifestyle and diet, undoubtedly influence human susceptibility to disease and there is mounting speculation that they leave a trail of epigenetic footprints across human genome.<sup>21</sup> Furthermore, some researchers argue that changes in diet could activate certain biochemical pathways that leave an epigenetic imprint that is passed to the next generation too.<sup>22,23</sup> Now, the emerging evidence that epigenetic changes can be inherited, make it possible to argue that similar modifications, and not just mutations in DNA sequence, could lie at the root of inherited diseases.<sup>24,25</sup>

## **2. DNA methylation.**

The best-known epigenetic signal is DNA methylation, which tags cytosine, one of the four chemical bases that make up the genetic code, with a methyl group at C<sub>5</sub>-pyrimidine position. Recent advances have led to the cloning and preliminary characterization of the three known active DNA cytosine methyltransferases (DNMT 1, 3a and 3b).<sup>26,27</sup>

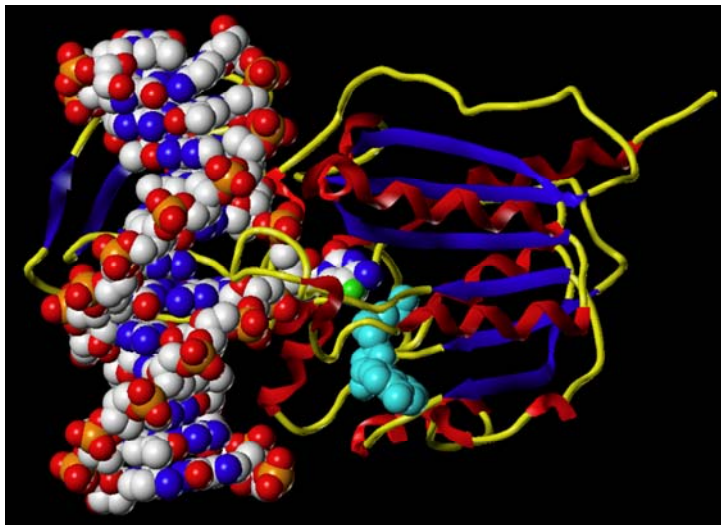


**Figure 1.** A methylating enzyme binds to its target site on DNA.

This post-synthetic addition's reaction alters the appearance of the major groove of DNA to which the DNA binding proteins bind. These epigenetic “markers” on DNA can be copied after DNA synthesis, resulting in heritable changes in chromatin structure. The sites of almost all methylation in mammals are the so-called CpG islands, regions of DNA where the bases cytosine and guanine alternate with one another (Fig. 1). These islands are often found in association with genes, most often in the promoters and first exons but also in regions more toward the 3' end.<sup>28</sup> Methylation of CpG-rich promoters is used by mammals to prevent transcriptional initiation and to ensure the silencing of genes on the inactive X chromosome, imprinted genes and in the long-term silencing of non-coding DNA in the genome, which contains a very substantial portion of repetitive elements (parasitic DNAs). The potential role of methylation in tissue-specific gene expression or in the regulation of CpG-poor promoters is less well established. There is also tantalizing evidence that normal chromosome structure may be affected by methylation and that human diseases, including cancer, are caused and impacted by abnormal methylation. Although it is often said that “methylation blocks gene



expression,” this statement is an oversimplification. Methylation changes the interactions between proteins and DNA, which leads to alterations in chromatin structure and either a decrease or an increase in the rate of transcription, depending on whether positive or negative regulatory elements of the genes are involved. Especially, methylation of a promoter CpG island leads to binding of several proteins (methylated CpG binding proteins MBD 1, 2, 3, and methylated DNA binding protein MECP 2), which can recruit HDACs and other transcriptional repressors to form tightly condensed chromatin structures and so to block the transcription initiation because the transcription factors (TFs), which normally regulate gene expression, are not able to access the promoter.<sup>29,30</sup> On the other hand, methylation of silencer<sup>31,32</sup> or insulator<sup>33</sup> elements blocks the binding of the cognate binding proteins, potentially abolishing their repressive activities on gene expression. Cytosine methylation is a major contributor to the generation of disease-causing germline mutations<sup>34</sup> and somatic mutations that cause cancer.<sup>35</sup> Moreover, recent works have shown that the abnormal methylation of the promoters of regulatory genes causes their silencing or overexpression, and it is a substantial pathway to cancer development and of comparable importance to gene mutations for the initiation and propagation of carcinogenesis. Many tumor suppressor genes, that are inactivated in particular tumor types, have highly methylated promoters; under normal conditions, the promoter regions are unmethylated and the relative genes are transcribed.<sup>36-42</sup> Some studies have also shown low DNAmethylation of proto-oncogenes in various human cancer cells.<sup>43-46</sup> As underlined above, the integration of DNA methylation with chromatin organization and the regulation of histone acetylation and deacetylation may be an important part of the overall carcinogenic effect. The links between DNA methylation and histone modifications have encouraged some researchers to investigate about dual therapies combining DNA methylation inhibitors (i.e., 5-azacitidine) with HDAC inhibitors (see below).<sup>47-50</sup> The molecular mechanisms of how hypermethylation of promoter regions participate in gene silencing and how loss of methylation alters chromosome structure are not fully elucidated yet. However, these epigenetic changes are potentially good therapeutic targets because of their reversibility and as tumor biomarkers may also be very useful for monitoring of the onset and progression of cancer.<sup>51</sup>

### **3. Chromatin remodelling.**

Another very important mechanism in the epigenetic regulation of gene expression is the chromatin remodelling.

Indeed, all of the human genome is packaged into chromatin, which is a dynamic macromolecular complex that consists of DNA, histones and non-histone proteins.<sup>52</sup>

Distinct levels of chromatin organization are dependent on the dynamic higher order structuring of nucleosomes, which represent the basic repeating units of chromatin.

In each nucleosome, roughly two super-helical turns of DNA containing about 146 base pairs wrap around an octamer of core histone proteins formed by four histone partners: an H3-H4 tetramer and two H2A-H2B dimers.<sup>53</sup>

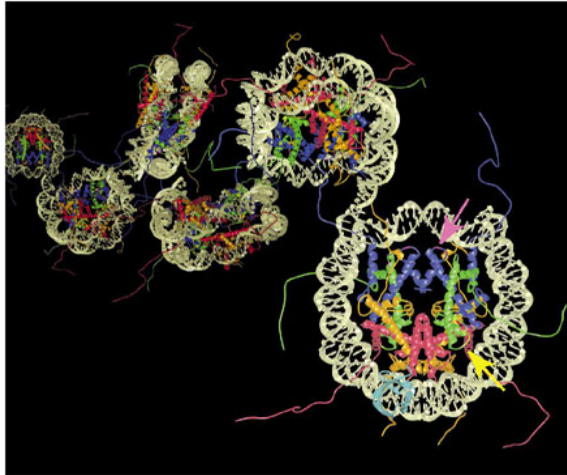


**Figure 2.** Nucleosomes.

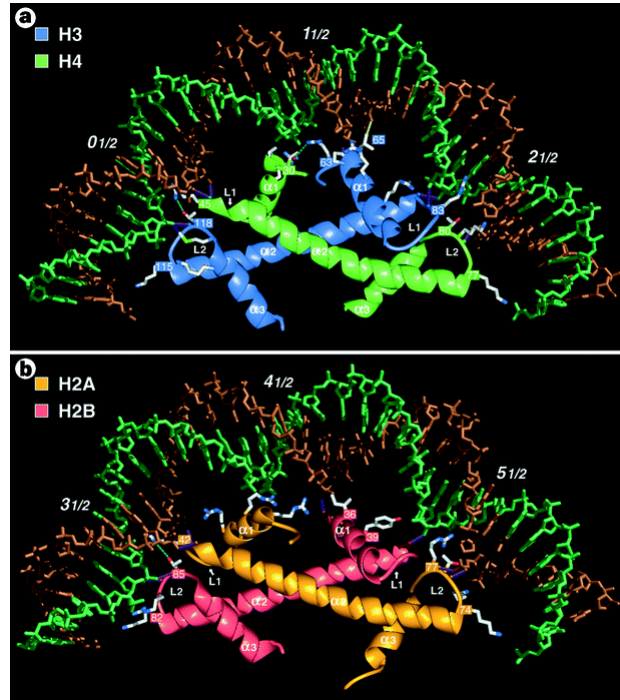


**Figure 3.** DNA wrapped around histones H3 and H4 (a), H2A and H2B (b).

Histones are small basic proteins consisting of a globular domain and a more flexible and charged NH<sub>2</sub>-terminus (so called histone ‘tail’) protruding from the nucleosome.

How the nucleosomal arrays containing the linker-histone H1 could twist and fold this chromatin fiber into increasingly more compacted filaments, leading to defined higher-order structures, is still unclear.

Certainly, H1 plays an important role in determining the level of DNA condensation, stabilizing the higher-order folding by electrostatic neutralization of the linker DNA segments through a positively charged carboxy-terminal domain.

So, this dynamic higher-order structure of nucleosomes defines distinct levels of chromatin organization and, subsequently, gene activity .

In general, condensed chromatin (also called “heterochromatin”) mediates transcriptional repression, whereas transcriptionally active genes are in areas of open chromatin (so called “euchromatin”).<sup>54</sup>

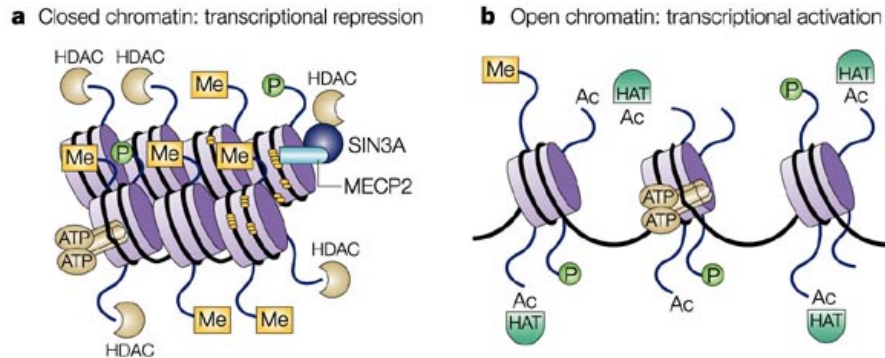


**Figure 4.** Heterochromatin (condensed or closed chromatin) and euchromatin (open chromatin).

An oversimplified view is that *trans*-acting, DNA-binding transcription factors have greater access to naked DNA in an open chromatin conformation compared with a condensed conformation.

However, it is important to remember that nucleosomes are not static, and their dynamic nature, allowing nucleosomal DNA to transiently unwrap and rebind the histone octamer, can give transcription factor access to DNA, albeit at various rates.

Nuclear histones, once thought as static, non-participating structural elements, are now known as integral and dynamic components of the machinery responsible for regulating not only gene transcription, but also other DNA-templated processes such as replication, repair, recombination and chromosome segregation.

An extensive literature shows an elaborate collection of post-translational modifications including acetylation, phosphorylation, methylation, ubiquitylation and ADP-ribosylation that take place on the ‘tail’ domains of histones.<sup>54-56</sup>

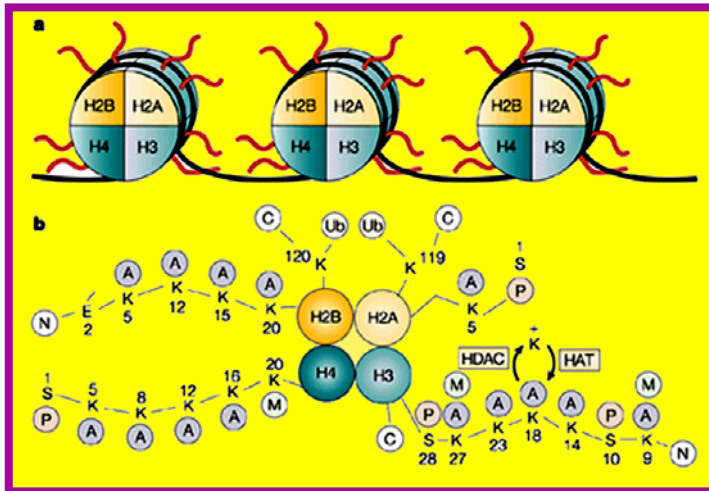


**Figure 5.** Covalent modifications of amino-terminal tails of core histones. A, acetyl; C, carboxyl terminus; E, glutamic acid; M, methyl; N, aminoterminal; P, phosphate; S, serine; Ub, ubiquitin.

Design, synthesis and biological validation of epigenetic modulators of histone/protein deacetylation and methylation.

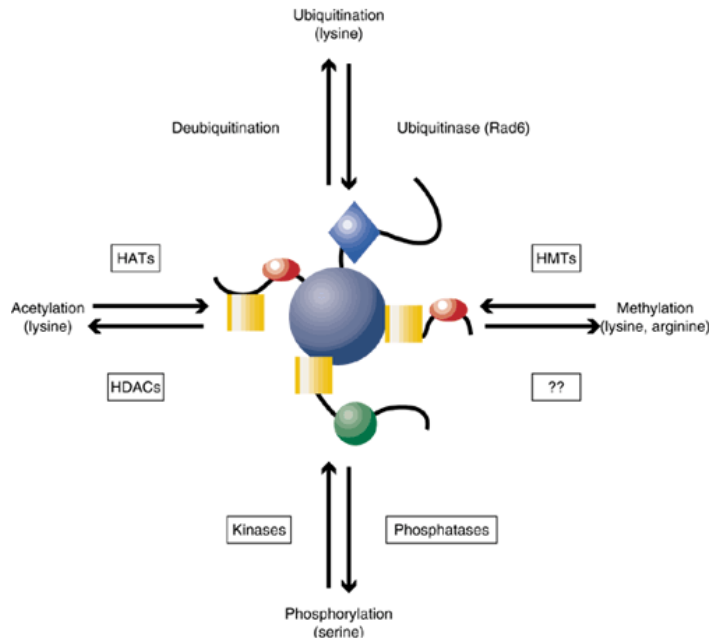


**Figure 6.** Reversible status of histone modifications.

These tails, which protrude from the surface of the chromatin polymer and are protease sensitive, comprise ~25-30% of the mass of individual histones,<sup>57</sup> thus providing an exposed surface for potential interactions with other proteins.<sup>58,59</sup>

Specifically, the tail of histone H4 appears to extend into the adjacent nucleosome to interact with the H2A-H2B complex, thereby indicating that the histone tails might regulate higher-order chromatin structure.<sup>53</sup>

Histone tails of H3 and H4 particularly are targeted for the mentioned covalent modifications. These modifications performed by histone acetyltransferases (HATs), deacetylases (HDACs), methyltransferases (HMTs) and kinases (HKs) offer a mechanism by which upstream signalling pathways can converge on common targets to regulate gene expression.

Infact, it has been proposed that there is a 'histone code' or 'epigenetic code' defined by the modifications that regulate the transcriptional activity of specific genes.<sup>60-63</sup>

The hypothesis is that the multiprotein complexes of transcription factors that activate or repress gene expression ‘read the code’.

Specifically, there are mounting evidences that distinct histone amino-terminal modifications, on one or more tails, can act sequentially or in combination and generate synergistic or antagonistic interaction affinities for chromatin-associated proteins, which in turn dictate dynamic transitions between transcriptionally active (euchromatic) or silent (heterochromatic) chromatin states.

The combinatorial nature of these modifications seems to reveal that the histone code considerably extends the information potential of the genetic (DNA) code.

In the attempt to understand rules and consequences of this novel code, it is of capital importance to identify and to characterize the enzyme systems that add or subtract these modifications.

#### ***4. Histone phosphorylation.***

Histone phosphorylation involving Ser-10 of histone H3 (the reaction is catalyzed by Aurora B kinase) has also emerged as an important modification, both in transcriptional activation and in chromosome condensation during mitosis.

As chromosome condensation and transcription are expected to involve opposing physical alterations of chromatin (i.e. closing of chromatin during mitosis and opening during transcription), the finding that the same modification is involved in both processes is circumstantial support for considering these modifications as binding surfaces rather than direct alteration of chromatin.

In fact as the outcome of histone modifications has been examined, two non-exclusive models have emerged. One is that histone modifications affect chromatin structure directly.

The second model is that modifications present a special surface for interaction with other proteins. Either model can be reconciled with the “histone code hypothesis”, both may operate simultaneously, and both have great explanatory power regarding the relationship between histone modification and gene control.

## 5. Histone ubiquitylation.

Two recent developments indicate that histone ubiquitylation is joining the ranks of important modifications.

First, in *S.cerevisiae* lysine 123 within the H2B carboxy-terminal tail is a substrate for the Rad6 ubiquitin ligase. This modification is critical to mitotic and meiotic growth, although it is not yet clear whether it is involved in transcription.

Second, TAF<sub>II</sub>250 in the TBP-associated complex TFIID has been shown to possess histone H1 ubiquitylation activity, adding to its long list of enzymatic activities (kinase and HAT activities), which may be involved in transcription.

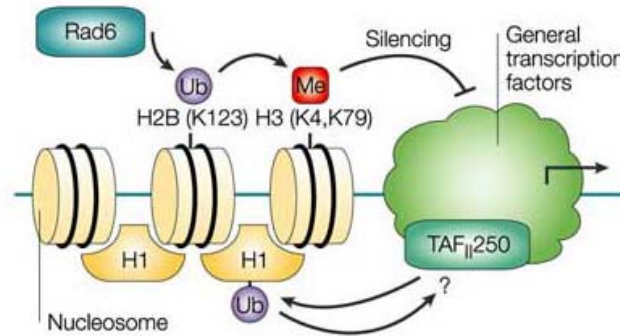


**Figure 7.** Control of chromatin by ubiquitin. The ubiquitin (Ub)-conjugating enzyme Rad6 ubiquitylates lysine 123 (K123) in the core of histone H2B. Through an unknown mechanism, this modification promotes the methylation of another histone, H3, at two positions, lysine 4 (K4) and lysine 79 (K79). These H3 modifications, in turn, are required for telomeric-gene silencing. In addition, TAF<sub>II</sub>250, which is a component of the general transcription factor TFIID, can ubiquitylate the linker histone H1; the significance of this ubiquitylation is unknown, but it might relate to the role of this TATA-binding protein (TBP)-



*associated factor (TAF) in transcriptional activation.*

### **6. Histone acetylation status and gene expression.**

Among post-translational histones modification, acetylation has been the most studied and appreciated.<sup>64</sup> The acetylation status of core histones is controlled by the competitive activities of HAT and HDAC superfamilies of enzymes.<sup>65,66</sup> The  $\epsilon$ -amino groups of lysine residues in the N-terminal regions of histones are substrates for HATs and HDACs.

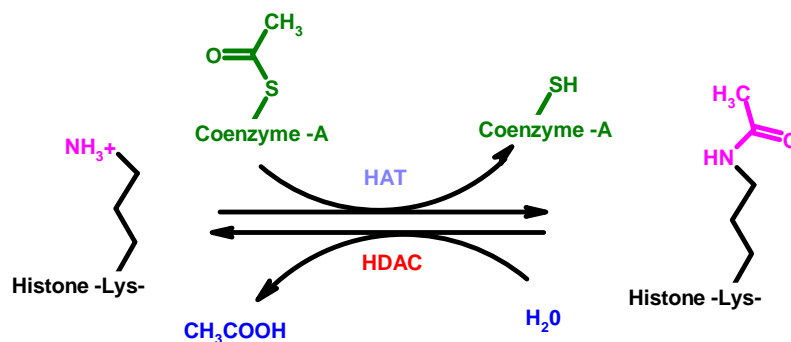


**Figure 8.** *Acetylation/deacetylation reactions on lysine  $\epsilon$ -amino groups.*

Generally, transcriptionally active genes are associated with highly acetylated core histones whereas transcriptional repression is associated with low levels of histone acetylation. Within the nucleosome, positively charged hypoacetylated histones are tightly bound to the phosphate backbone of DNA, maintaining chromatin in a transcriptionally silent state.

Acetylation neutralizes the positive charge on histones, disrupting higher-order structures in chromatin, thereby enhancing access of transcription factors, transcriptional regulatory complexes and RNA polymerases to promoter regions of DNA.

Histone deacetylation restores a positive charge on lysine residues of core histones, allowing chromatin to condense into a tightly supercoiled, transcriptionally silent conformation.<sup>67,68</sup> Nevertheless, in some cases histone acetylation is involved in transcriptional repression but not surprisingly: indeed the ‘histone code’ hypothesis itself offers a possible explanation for these situations.<sup>69-70</sup>

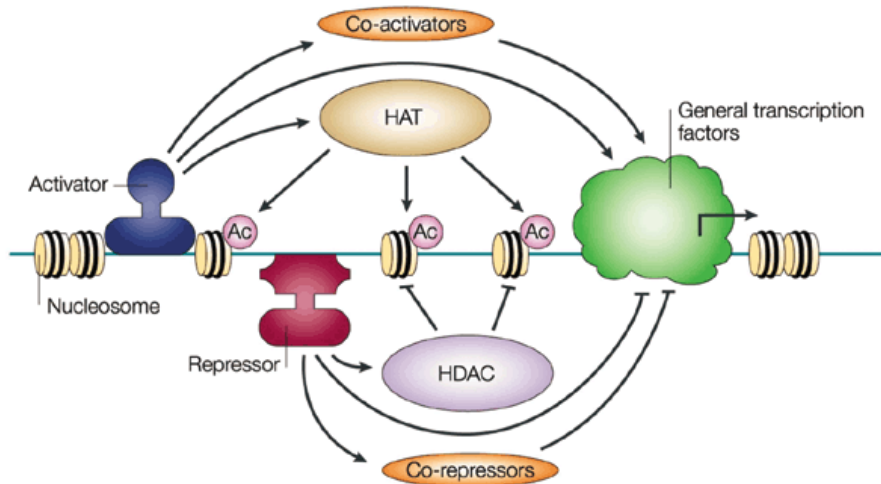


**Figure 9.** HAT/HDAC and transcriptional regulation.

### 6.1. Histone acetyltransferase.

It has been over three decades since Allfrey and coworkers proposed that the acetylation state of histones within chromatin influence gene expression.<sup>71</sup>

Despite the time since these initial studies, the enzymes that mediate histone acetylation and deacetylation have been identified and characterized only over the past few years. A breakthrough came with the cloning of a HAT enzyme from *Tetrahymena*<sup>71</sup>, which turned out

to be a homologue of the previously identified Gcn5 transcriptional co-activator/adaptor from yeast.

Subsequently, a flurry of studies led to the discovery of numerous HATs that were previously identified as transcriptional co-activators, such as the global regulator of transcription, the CREB (cyclic AMP response element binding protein)-binding protein (CBP)/p300 (a 300-kDa protein homologous to CBP), and the TAFII250 TBP-associated factor of the TFIID general transcription factor complex.<sup>72</sup>

Proteins that contain HAT modules fall into distinct families. There is high sequence similarity within these families, but poor to no sequence similarity between them. The HAT families are found in eukaryotes from yeast to humans and include the Gcn5/PCAF (p300/CBP-associated factor), CBP/p300, TAFII250/TAFII130, and the steroid-receptor co-activator (SRC) families, among others.<sup>73</sup>

The size of the HAT module differs between families, and HAT modules themselves occur in the context of other conserved protein modules. Moreover, different HAT families seem to elicit distinct biological activities.

For example, the Gcn5/PCAF (p300/CBP-associated factor) HAT family are co-activators for a subset of genes, whereas members of the CBP/p300 HAT family are more global activators of gene expression. By contrast, some members of the MYST (MOZ, YBF2/SAS3, SAS2, Tip60) family of HATs are involved in gene silencing.

Finally, different HAT families have specific and distinct histone substrate specificities. For example, recombinant Gcn5/PCAF family members will preferentially acetylate lysine 14 on histone H3, whereas the MYST family members have a preference for several lysines on histone H4.

As well as catalysing histone acetylation, several HATs, including CBP/p300 and PCAF, have intrinsic transcription-factor acetyltransferase activity and, in many of these cases, acetylation enhances the DNA-binding affinity of the affected protein.

Despite the differences between the various HAT families, there are some unifying themes.

First, all of the HAT proteins that have been characterized *in vivo* are associated with large multiprotein complexes. For example, Gcn5 is part of at least two multiprotein complexes, Ada and SAGA51, and Esa1, a member of the MYST family of proteins, is the catalytic subunit of the histone H4-specific NuA4 (nucleosome acetyltransferase of histone H4) HAT complex.

Second, although the recombinant proteins can acetylate free histones, nucleosomal acetylation occurs only in the context of *in vivo* HAT complexes, and substrate specificity is modulated in the context of these complexes. For example, recombinant Gcn5 preferentially acetylates Lys14 on histone H3, but it will also acetylate (to a lesser extent) Lys8 and Lys16 of histone H4.

Insights into the histone-binding properties of HAT proteins were revealed in the recent structure determinations of the Gcn5/PCAF and Esa1 HAT domains in various ligand-bound forms.<sup>73</sup>

A comparison of the HAT domains from the Gcn5/PCAF family, the MYST family (for example, Esa1) and the nucleosome-deposition-related HAT, HAT1, reveals structural homology within a central core domain that is important for acetyl-coenzyme-A cofactor binding and catalysis. Overall, protein regions amino- and carboxyterminal to this core domain show structural divergence.

However, despite the overall structural differences within the amino- and carboxy-terminal segments of the three HAT proteins, an  $\alpha$ -helix-loop region just amino-terminal to the core domain and an  $\alpha$ -helix-loop region just carboxy-terminal to the core domain superimpose well, indicating a related mode for histone substrate binding.

The structure of *Tetrahymena* Gcn5, in complex with CoA and a histone H3 peptide, reveals that these structurally conserved regions are indeed important for histone substrate binding. Specifically, the structure shows that the 11-amino-acid histone H3 peptide (centred around the Lys14 target of histone H3) adopts a random coil structure and is bound in a pronounced protein cleft of the Gcn5 protein above the core domain, and flanked on opposite sites by the amino- and carboxy-terminal protein segments (figure 10).

An extrapolation of this result suggests that the core histone-binding scaffold for other more sequence-divergent HAT modules might be structurally conserved, whereas the sequence divergence within this scaffold might mediate histone substrate binding specificity.

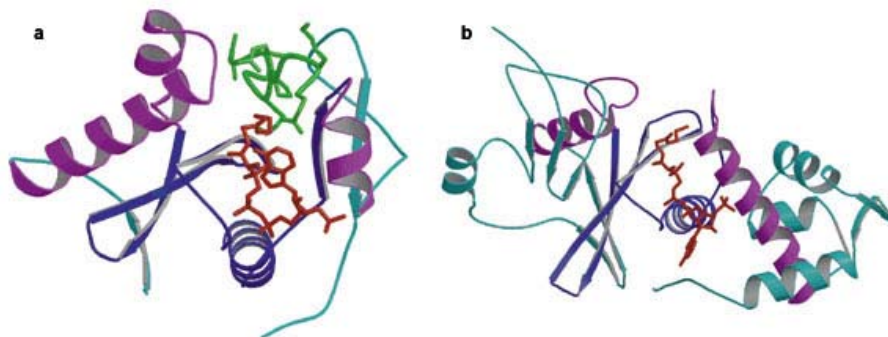


**Figure 10.** Overall structure of HAT domain module. **a:** Structure of the *Tetrahymena* Gcn5–CoA–histone-H3 peptide complex. The CoA cofactor is shown in red and the histone H3 peptide is shown in green. The central core domain responsible for CoA binding and catalysis is blue. **b:** Structure of the MYST HAT family member yeast *Esa1*, bound to CoA. Colour coding is the same as in (a).

## 6.2. Histone deacetylase.

Eighteen mammalian deacetylase enzymes have been identified to date, and these can be divided into two families: the histone deacetylase, properly named HDACs, and the ySir2-like deacetylases, or sirtuins (also named class III HDACs).

The HDAC family members can be divided into two classes based on their primary structure, size and similarity to *Saccharomyces cerevisiae* histone deacetylases: those with homology to the yeast's transcriptional regulator Rpd3 (reduced potassium dependency 3), or class I HDACs (HDAC1-3,8,11), and those with greater similarity to Hda1, or class II HDACs (HDAC 4-7,9,10).<sup>74,75,76</sup>

All of these enzymes possess a highly conserved catalytic domain of approximately 390 amino acids, and appear deacetylate their substrates by the same  $Zn^{2+}$ -dependent mechanism, but the class II proteins are two to three times larger in size than the class I proteins (120-130

kDa and 42-55 kDa, respectively) and there are certain conserved sequence motifs in the catalytic domain that differ between the two classes.<sup>150</sup> In addition, based on sequence homology among their deacetylase domains, class II can be further divided into two subclasses, namely IIa (HDAC4, HDAC5, HDAC7 and HDAC9) and IIb (HDAC6, containing as unique feature two homologous deacetylase domains, and HDAC10, more similar to HDAC6 than to HDAC4-7 and HDAC9).<sup>75-77</sup>

### HDAC families.

HDAC	CLASS	INTERACTIONS	CELLULAR LOCALIZATION	TISSUE EXPRESSION
HDAC1	I	DNMT1, ATM, BRCA1, MECP2, MYOD, p53, pRb, NF-kB	nuclear	ubiquit.
HDAC2	I	DNMT1, BRCA1, pRb, NF-kB, GATA2	nuclear	ubiquit.
HDAC3	I	pRb, NF-kB	nucl/cytopls	ubiquit.
HDAC8	I	a-SMA	nucl/cytopls	ubiquit.
HDAC11	IV	HDAC6	nuclear	ubiquit.
HDAC4	IIa	14-3-3, MEF2, calmodulin	shuttling n/c	heart, muscle, brain
HDAC5	IIa	14-3-3, MEF2, calmodulin	shuttling n/c	heart, muscle, brain
HDAC6	IIb	tubulin, PP1, dynactin, HDAC11	nucl/cytopls	testis
HDAC7	IIa	14-3-3, MEF2, calmodulin	shuttling n/c	CD4/CD8++thymocytes
HDAC9	IIa	14-3-3, MEF2, calmodulin	shuttling n/c	heart, muscle, brain
HDAC10	IIb	PP1, LcoR	nucl/cytopls	liver, spleen, kidney
SIRT1	III	FOXO, p53, p300	nuclear	ND
SIRT2	III	tubulin	cytoplasmic	ND
SIRT3	III	ND	mitocondr.	ND
SIRT4	III	ND	ND	ND
SIRT5	III	ND	ND	ND
SIRT6	III	ND	ND	ND
SIRT7	III	ND	ND	ND

Like the class I HDACs, members of class II HDACs function in the context of other protein subunits *in vivo*, and are sensitive to inhibition by TSA, SAHA, and related compounds. However, class II proteins appear to interact with a different set of proteins *in vivo* than class I proteins. Indeed, class II HDACs are not part of the above mentioned Sin3-HDAC and NuRD-Mi2-NRD complexes, but interact with one or more DNA-binding transcription factors including MEF2, BCL6, PLZF and TR2; with transcriptional co-repressors such as N-CoR, SMRT, B-CoR, and CtBP, and with the methyllysine-binding protein HP1.<sup>78,79</sup> Among these interactions, the most studied is that with myocyte enhancer factor 2 (MEF2). Class IIa HDACs inhibit MEF2-dependent transcription in reporter gene assay and regulate myogenesis in muscle differentiation models *in vitro*.<sup>78-80</sup> Moreover, in HDAC9 nude mice the development of age-dependent cardiac hypertrophy has been observed, strongly implicating class IIa members as important regulators of myogenesis.<sup>81</sup> In addition, class II HDACs differ from class I proteins depending on their tissue expression, subcellular localization and consequently biological roles.

Class I HDACs are ubiquitously expressed, whereas class II enzymes display tissue-specific expression in humans and mice (for example, human HDAC4 is the most abundant in skeletal muscle, modest in brain, heart and ovary, but not detectable in liver, lung, spleen and placenta, and HDAC5 is expressed in mouse heart, brain, liver and skeletal muscle but not in spleen).<sup>78-80</sup> In contrast to class I HDACs, which are mainly nuclear enzymes (except HDAC3),<sup>82</sup> under different cellular conditions class II HDACs localize either to the cell nucleus or to the cytoplasm, depending on their phosphorylation extent and subsequent binding of 14-3-3 chaperone proteins. For example, HDAC4 is actively shuttled between the nucleus and the cytoplasm *in vivo*, and phosphorylation and/or overexpression of 14-3-3 chaperons promote its cytoplasmic accumulation.<sup>80</sup>

*S. cerevisiae* has five sirtuins, including the founding member, Sir2, and four homologues, Hst1-4 (homologue of Sir two). Seven sirtuins (SIRT1-7) have been identified in humans. The sirtuins family can be divided into five classes, based on their primary structure.<sup>83</sup> All the five yeast sirtuins are class I proteins, as well as the human SIRT1-3. SIRT4 is a class II sirtuin, SIRT5 is in class III, and SIRT6 and SIRT7 are class IV proteins. The sirtuin deacetylases contain a conserved 275 amino acids catalytic domain, which is unrelated to that of HDACs (classes I and II), and operate by a very different mechanism that requires NAD<sup>+</sup> as cosubstrate.<sup>84</sup>

Despite these structural and mechanistic differences, proteins from both families have been shown to silence transcription at specific promoters or chromosomal domains by localized histone deacetylation and function in other cellular processes with non-histone substrates. To date, cellular functions have been assigned to only human SIRT1 that has been shown to deacetylate p53 at the carboxy terminus and inhibit p53-mediated transcriptional activation and apoptosis.<sup>85,86</sup> Their subcellular localization is not fully understood but seems that some of them are prevalently nuclear and others cytoplasmic.<sup>83,87</sup>

### *6.3. Histone deacetylase family: class I.*

HDAC1 and HDAC2 are highly similar enzymes, with an overall sequence identity of approx. 82%. The catalytic domain on the N-terminus forms the major part of the protein.

HDAC1 and HDAC2 are inactive when produced by recombinant techniques, implying that cofactors are necessary for HDAC activity to occur. These complexes consist of proteins necessary for modulating their deacetylase activity and for binding DNA, together with proteins that mediate the recruitment of HDACs to the promoters of genes.

Three protein complexes have been characterized that contain both HDAC1 and HDAC2: Sin3, NuRD (nucleosoma remodelling and deacetylating) and Co-REST. Both the Sin3 complex (named after its characteristic element mSin3A) and the NuRD complex consist of a core complex containing HDAC1, HDAC2, Rb-associated protein 48 (RbAp48, which binds histone H4 directly) and RbAp46. In addition to functioning through these complexes, HDAC1 and HDAC2 can also bind directly to DNA binding proteins such as YY1 (Yin and Yang 1, a cellular nuclear matrix regulatory protein), Rb binding protein-1 and Sp1.<sup>88-92</sup>

In addition to the regulation of HDAC1 and HDAC2 activity by the availability of co-repressors, a second means of regulating activity is via post-translational modifications. Both activity and complex-formation are regulated by phosphorylation. HDAC1 and HDAC2 are phosphorylated at a low steady-state level in resting cells. Hyperphosphorylation of HDAC1 and HDAC2 leads to a slight but significant increase in deacetylase activity, and at the same time to disruption of complex-formation between HDAC1 and HDAC2 and between HDAC1 and mSin3A/YY1.

When hypophosphorylation of HDAC1 and HDAC2 occurs, the activity of HDAC1 and HDAC2 decreases, but complex formation is increased. The apparently contradictory consequences of phosphorylation maintain HDAC activity at a certain optimal level.



Mutational analysis of HDAC1 shows that Ser-421 and Ser-423 are crucial phosphorylation sites; when they are mutated, complex-formation is hampered and HDAC activity is decreased.<sup>93</sup>

HDAC3 is evolutionarily most closely related to HDAC8, with 34% overall sequence identity, and HDAC3 has the same domain structure as all class I HDACs.

In HDAC1 and HDAC2, the regions that correspond to amino acids 181-333 of HDAC3 are very similar to each other (93% identity). However, the corresponding region in HDAC3 has only 68% identity with HDAC1 and HDAC2. Surprisingly, the non-conserved C-terminal region of HDAC3 is required for both deacetylase activity and transcriptional repression. In addition to the nuclear localization signal (*NLS*) that other class I HDACs possess, a *NES* (nuclear export signal) is also present in HDAC3 (amino acids 180-313).

The balance between these two signals is probably dependent on cell type and on environmental conditions. HDAC3 shares structural and functional features with other class I HDACs, but it exists in multisubunit complexes that are different from other known HDAC complexes. This could imply that individual HDACs have distinct functions due to their complex specificity.

SMRT (silencing mediator for retinoic acid and thyroid hormone receptors) and N-CoR (nuclear receptor co-repressor) are necessary factors for HDAC3 activity.<sup>94</sup>

N-CoR and SMRT are two distinct, but highly related, proteins that share similar domain structure and function. Both act as co-repressors, both have a conserved deacetylase-activating domain for HDAC3 activation.<sup>94</sup>

Of all the class I HDACs, HDAC8 is most similar to HDAC3 (34% identity). HDAC8 consists largely of the catalytic domain with an NLS in the centre.<sup>95</sup> Due to its very recent discovery, it is not yet known whether HDAC8 function is regulated by a co-repressor complex of proteins.

Recently the crystal structure of human HDAC8 in complex with a hydroxamic acid inhibitor was reported by Vannini *et al.*<sup>96</sup> Similar to bacterial HDAC-like protein, HDAC8 folds in a single  $\alpha/\beta$  domain. The inhibitor and the zinc-binding sites are similar in both proteins. However, significant differences are observed in the length and structure of the loops surrounding the active site, including the presence of two potassium ions in HDAC8 structure, one of which interacts with key catalytic residues. CD data suggest a direct role of potassium in the fold stabilization of HDAC8.

Knockdown of HDAC8 by RNA interference inhibits growth of human lung, colon, and cervical cancer cell lines, highlighting the importance of this HDAC subtype for tumor cell proliferation.

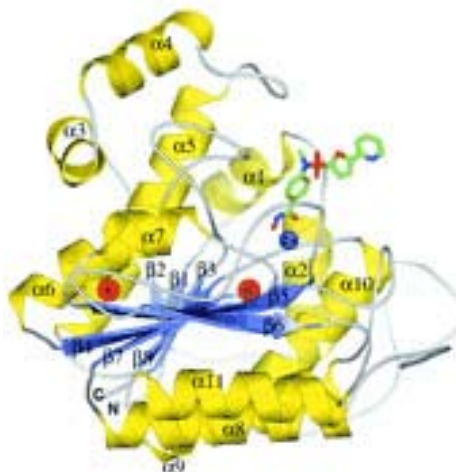


**Figure 11.** Ribbon diagram of human HDAC8 monomer with  $\alpha$ -helices and  $\beta$ -strands labeled and colored yellow and indigo, respectively. The inhibitor is drawn in stick representation (Vannini et al <sup>96</sup>).

From the phylogenetic analysis, it appears that HDAC11 is most closely related to HDAC3 and HDAC8, suggesting that it might be more closely related to the class I HDACs than to the class II HDACs (but in general its overall sequence identity with the other HDACs is limited). HDAC11 contains a catalytic domain situated at the N-terminus, with proven HDAC activity that can be inhibited by trapoxin (a TSA analogue). HDAC11 was found not to reside in any of the known HDAC complexes (Sin3, N-CoR/SMRT), possibly indicating a biochemically distinct function of HDAC11.

#### 6.4. Histone deacetylase family: class II.

HDAC4, HDAC5 and HDAC7 are found in the same region of the phylogenetic tree, and represent a subgroup within the class II HDACs. HDAC4 and HDAC5 are most similar to each other (overall similarity 70%), but HDAC7 is also closely related (58 and 57% overall similarity respectively).

All three HDACs have their catalytic domain on the C-terminal half of the protein, and the *NLS* is situated close to the N-terminus. Binding domains for C-terminal binding protein (CtBP), myocyte enhancer factor 2 (MEF2) and 14-3-3 proteins are conserved in all three HDACs on the N-terminus.

Furthermore, HDAC5 has a NES within the catalytic domain, suggesting nuclear/cytoplasmic trafficking. HDAC4, HDAC5 and HDAC7 are able to interact with SMRT/N-CoR, and the co-repressors BCoR (Bcl-6-interacting co-repressor) and CtBP. The N-termini of HDAC4, HDAC5 and HDAC7 interact specifically with and repress the myogenic transcription factor MEF2. MEF2 plays an essential role, as a DNA binding transcription factor, in muscle differentiation.

When MEF2 is associated with HDAC4, 5 or 7, the function of MEF2 as a transcription factor is inhibited, thus blocking muscle cell differentiation. CaMK activity overcomes this inhibition by dissociating the MEF2/HDAC complex due to phosphorylation of HDAC4/5/7.

Subsequently, transport (along with the cellular export factor CRM1) of the HDAC out of the nucleus can occur, illustrating another type of regulation of HDAC activity. Interestingly, HDAC4, 5 and 7 associate with HDAC3 *in vivo* via co-recruitment to the SMRT/N-CoR factors in the nucleus, with an absence of HDAC3 leading to inactivity. This suggests that HDAC4, 5, and 7 function as a link between DNA-binding recruiters and the HDAC3-containing HDAC complex.<sup>91</sup>

The subcellular localization of HDAC5 and HDAC7 differs from that of HDAC4 at the different stages of muscle cell differentiation. These HDACs might complement each other in order to control the differential regulation of gene expression during the various stages of differentiation in muscle cells.

These three HDACs are able to "fine tune" the repression of gene expression due to the need for co-repressors for their activity, and even more intriguingly via their ability to change localization in response to a specific signal, thus providing a carefully regulated sequence of changes in gene expression during differentiation.<sup>91</sup>

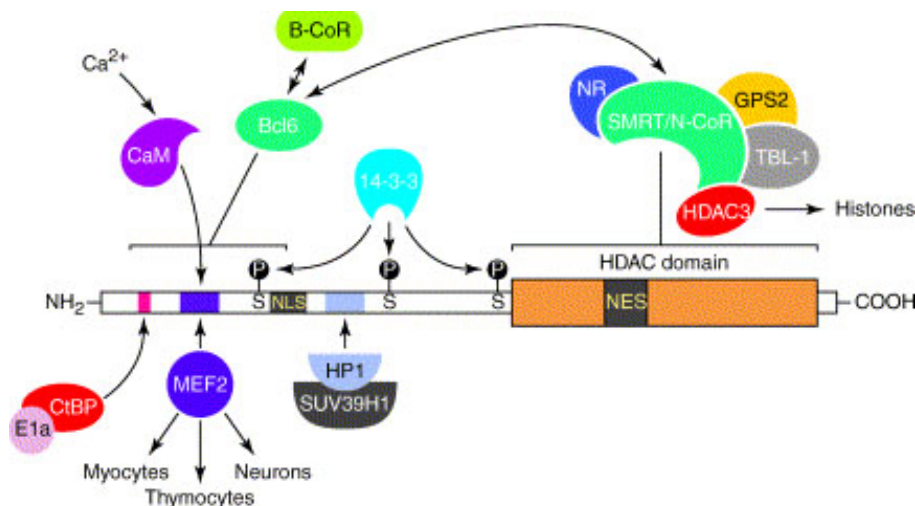


**Figure 12.** Interaction partners of class IIa histone deacetylases (HDACs). Class IIa HDACs interact with several partners through distinct domains. The N-terminal domain is used primarily as a targeting domain for distinct promoters by the MEF2 transcription factors. Interaction of class IIa HDACs with HP1, CtBP and the SMRT/N-CoR and B-CoR co-repressor complexes mediates the transcriptional repressive activities of class II HDACs.

The phylogenetic tree shows that HDAC9 splice variants are clustered as a separate group related to HDAC4/5/7 within class II of the classical HDAC family. The HDAC9 catalytic domain is located on the N-terminus, as for the class I HDACs.<sup>97</sup>

There are three known splice variants, HDAC9a, HDAC9b and HDRP/HDAC9c, but more variants are suspected. HDAC9c/HDRP lacks the catalytic domain and is 50% similar to the N-terminus of HDAC4 and HDAC5.

By analogy with HDAC4/5/7, HDRP is able to recruit HDAC3, thus circumventing the lack of a catalytic domain. In addition, HDAC9 is also able to interact with MEF2, CaMK, 14-3-3 proteins, indicating that HDAC9 may have an important function in muscle differentiation. The alternative splicing might also represent another way of fine-tuning HDAC activity. Certain cell types might express one isoform, while others express the other.<sup>97</sup>

The phylogenetic tree shows that HDAC6 is evolutionarily most closely related to HDAC10. In general the identity of HDAC6 with other human HDACs is low, with some resemblance to yeast HDA1 indicating an early separation from the other HDACs in evolution.

HDAC6 is a rather unique enzyme within the classical family of HDACs, because it contains two catalytic domains arranged in tandem. Another unique feature of HDAC6 is the presence of a HUB (HDAC6-, USP3-, and Brap2-related zinc finger motif) domain on the C-terminus. This domain is a signal for ubiquitylation, suggesting that this HDAC is particularly prone to degradation.<sup>98</sup> The catalytic domains of HDAC6 are most similar to the catalytic domain of HDAC9. HDAC6 functions as a tubulin deacetylase, regulating microtubule-dependent cell motility.

In 2003 Schreiber *et al.* used a multidimensional, chemical genetic screen of 7.392 small molecules to discover “tubacin” which inhibits  $\alpha$ -tubulin deacetylation in mammalian cells.<sup>99</sup>

Tubacin does not affect the level of histone acetylation, gene-expression patterns, or cell-cycle progression. They evidenced that class II histone deacetylase is the intracellular target of tubacin.

Only one of the two catalytic domains of HDAC6 possesses tubulin deacetylase activity, and only this domain is bound by tubacin. These results highlight the role of  $\alpha$ -tubulin acetylation in mediating the localization of microtubule associated proteins and the effect on cell motility. Given the dependence of metastasis and angiogenesis on cell movement, increasing  $\alpha$ -tubulin acetylation may be an important component to the antimetastatic and antiangiogenic properties of HDAC inhibitors.

Conversely, decreasing  $\alpha$ -tubulin acetylation by HDAC6 overexpression may be the cause of the reduced  $\alpha$ -tubulin acetylation levels observed in neurodegenerative disorders such as Alzheimer’s disease.

In addition, both suberoylanilide hydroxamic acid (SAHA) and butyrate, HDAC inhibitors used to suppress neurotoxicity in polyglutamine-repeat disorders, also inhibit  $\alpha$ -tubulin deacetylation.

Besides altering the expression levels of genes important for neuronal viability, the therapeutic effect of HDAC inhibitors in neurodegenerative disorders may involve increased  $\alpha$ -tubulin acetylation. By uncoupling the effects of deacetylase inhibitors on the cytoskeleton and chromatin, tubacin allows new applications of deacetylase inhibitors and improved versions of current ones having increased selectivity to be envisioned.

HDAC10 is the most recently discovered member of the class II HDACs. Two mRNA species, with a slight difference in length, have been found, suggesting the existence of two splice variants of HDAC10. Analysis of protein sequence identity shows that HDAC10 is most closely related (37% overall similarity) to HDAC6.<sup>100</sup>

HDAC10 has a catalytic domain on its N-terminus, and a NES and a putative second catalytic domain on the C-terminus. Also, two putative Rb binding domains have been found on HDAC10, suggesting a role in regulation of the cell cycle. Furthermore, HDAC10 is found to interact with HDACs 1, 2 and 3 (and/or SMRT) and HDACs 4, 5 and 7, but not with HDAC6, although some contradictory results are presented in the literature.<sup>100</sup> The fact that HDAC10 is able to associate with many other HDACs indicates that it might function as a recruiter rather than as a deacetylase.

#### *6.5. Biological role of histone deacetylases class IIa: MEF2 interaction.*

The many interactions between class IIa HDACs and transcriptional regulators suggest a wide variety of potential biological roles. However, most of these interactions have not been examined in a biological context.

By contrast, the importance of interactions between MEF2 and class IIa HDACs has been demonstrated in several tissue culture and animal models. MEF2 plays a significant transcriptional regulatory role in myogenesis, in negative selection of developing thymocytes, and in the transcriptional regulation of Epstein–Barr virus (EBV).

The striking similarity of MEF2 regulation in neurons and its role in neuronal resistance to excitotoxicity suggests that class IIa HDACs also play a significant role in neurons.

Class IIa HDACs inhibit myogenesis by binding to MEF2 at several promoters critical for the muscle differentiation program. Members of the MyoD family of basic helix-loop-helix

(bHLH) proteins as MyoD, Myf5, myogenin, and MRF4 act at multiple steps in the myogenic pathway to control the establishment of the myogenic lineage and the activation of differentiation genes. Recent studies have revealed that myogenic bHLH and MEF2 proteins control the activation and repression of muscle-specific genes by associating with HATs and HDACs, respectively, which act in an opposing manner to control the acetylation state of nucleosomal histones.<sup>101</sup>

It is now clear that HDAC4, -5, and -7 associate with MEF2 and act as potent inhibitors of MEF2-dependent transcription. Binding of these HDACs to MEF2 is mediated by 18 conserved amino acids in the amino-terminal extensions of HDAC4, -5, and -7.

Class I HDACs lack this domain and fail to directly associate with or regulate the activity of MEF2.

McKinsey *et al.* reported that when early muscle cells are encouraged to differentiate by the removal of serum from their culture medium, histone deacetylase-5 (HDAC5) exits the nucleus. MEF2 is left behind, where it promotes the transcription of genes essential for muscle differentiation.<sup>101</sup> This response is thought to be mediated largely by  $\text{Ca}^{2+}$  signals generated at the cell surface: in fact two  $\text{Ca}^{2+}$ /calmodulin-dependent protein kinases (CaMKI and CaMKIV) are known to induce the export of added histone deacetylase 4/5 from the nucleus.

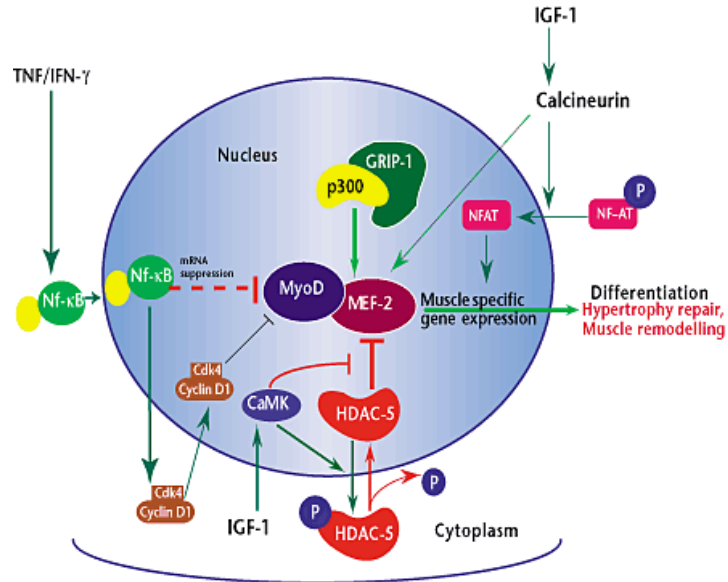


**Figure 13.** Muscle cells differentiation and HDAC5 shuttling.

All these data suggest how the pathway in early muscle cells might work: binding of an extracellular molecule to its receptor on the cell surface leads to an increase in cellular  $\text{Ca}^{2+}$ . This then activates  $\text{Ca}^{2+}$ /calmodulin-dependent kinases, which in turn phosphorylate histone deacetylase-4 and -5. These enzymes then detach themselves from MEF2, exposing their nuclear export signal. This signal consists of a sequence of amino acids that acts as an address label, allowing the proteins to be sent out of the nucleus. Alone in the nucleus, MEF2 works together with muscle-specific transcription factors to enhance the expression of muscle specific genes, allowing differentiation of the cell into a muscle fibre.



### *6.6. Regulation of histone deacetylase activities.*

The activity of HDACs can be separated into two areas, enzymatic activity (the ability to deacetylate histones or other non-histone protein substrates), and functional activity (the ability to regulate transcription, for example). As expected with proteins that occupy an essential physiological role, the activities of the HDAC proteins are highly regulated by multiple distinct mechanisms.

A first regulation mechanism is through protein complex formation: several HDACs exist as a component in stable large multi-subunit complexes, and most if not all HDACs interact with other cellular proteins.

Results from many studies in different laboratories suggest that with the exceptions of yeast HOS3 and mammalian HDAC8, most purified recombinant HDACs are enzymatically inactive. Any protein that associates with HDACs, therefore, has the potential to activate or inhibit the enzymatic activity of HDACs. Likewise, HDACs, in general, have no DNA binding activity, therefore, any DNA-binding protein that targets HDACs to DNA or to histones potentially can affect HDAC function.

For example, as we underlined before, human HDAC1 and HDAC2 exist together in at least three distinct multi-protein complexes: Sin3, the NuRD/NRD/Mi2, and the CoREST complexes.

Perhaps the best example of HDAC regulation by protein–protein interaction emanated from studies of HDAC3. Data from early studies suggested that nuclear receptor corepressors, silencing mediator of retinoid and thyroid receptor (SMRT) and nuclear receptor corepressor (N-CoR), function as platforms for recruitment of HDACs.

Surprisingly however, the interaction between HDAC3 and SMRT/N-CoR resulted in the stimulation of HDAC3 enzymatic activity. No enhancement of HDAC3 activity was seen with an N-CoR mutant that did not bind HDAC3. Thus, it appears that the enzymatic activity of HDAC3 is specifically regulated by the availability of interacting SMRT/N-CoR. The activation of HDAC3 is mediated by a deacetylase-activating domain (DAD) present in SMRT and N-CoR. This domain was found to be necessary and sufficient for HDAC3 enzymatic activation in reconstitution experiments using purified components.

Phosphorylation is a leading post-translational mechanism for controlling many enzyme activities.

All mammalian HDACs possess potential phosphorylation sites and many of them have been found to be phosphorylated *in vitro* and *in vivo*. In one study, hHDAC1 was analyzed by ion trap mass spectrometry, and two phosphorylated residues, Ser421 and Ser423, located in the protein's C-terminal, were identified.<sup>102</sup>

Site directed mutations of Ser-421 and Ser-423 to alanine in HDAC1 reduced enzymatic as well as transcriptional repression activity, and similar results were obtained with a C-terminal deletion mutant of HDAC1.<sup>102</sup> Importantly, complex formation, including association with RbAp48, MTA-2, mSin3A, and CoREST, is severely impaired in these mutants.

There are two non-mutually exclusive possibilities to explain how phosphorylation can affect HDAC activity. Conceivably, phosphorylation of HDAC1 can alter its conformation into a more favorable enzymatically active form. Alternatively, phosphorylation might increase the ability of HDAC1 to interact with proteins, such as MTA2 and SDS3, which can activate its activity and consequently enhance its enzymatic activity.

Besides phosphorylation, another post-translational modification that has been shown to regulate HDAC activity and function is the conjugation of small ubiquitin-related modifier (SUMO-1). Unlike the protein degradation effects of ubiquitylation, SUMO-1 modification exerts varied effects on the target protein, including subcellular localization, protein-protein interaction, and enzymatic activity modulation.

Two independent studies identified HDAC1 as a substrate for SUMO-1 modification *in vitro* and *in vivo* at Lys444 and Lys476.<sup>103,104</sup>

In order to deacetylate histones and to repress transcription, HDACs must reside in the nucleus. Therefore, signals that enhance HDAC nuclear localization positively regulate HDAC activities. In contrast, signals that increase cytoplasmic localization of HDACs negatively regulate their activities. HDAC1, 2, and 8 are predominantly nuclear proteins, and at this time, it appears that these three class I HDACs are not regulated by subcellular localization.

In contrast, HDAC3 can be found both in the nucleus and cytoplasm and the nuclear/cytoplasmic ratio depends on cell types and stimuli.

In response to IL-1 $\beta$  signaling, the N-CoR/ TAB2/HDAC3 corepressor complex undergoes nuclear to cytoplasmic translocation, resulting in derepression of a specific subset of NF-kB regulated genes.

Class II HDACs 4, 5, 7, and 9 shuttle between the nucleus and the cytoplasm. The binding of HDACs to 14-3-3 is absolutely dependent on phosphorylation of conserved N-terminal serine residues of HDACs, and the association results in sequestration of HDACs to the cytoplasm.<sup>101</sup>

The nuclear export sequences of HDACs 4, 5, and 7 are signal-responsive and are activated upon CaMK-dependent binding of 14-3-3 proteins to the N-terminal phospho-serine residues of class II HDACs.

Unlike class I and II HDACs, the SIR2-like enzymes that comprise class III HDACs require the coenzyme NAD<sup>+</sup> for catalytic activity.

In this reaction, nicotinamide is liberated from NAD<sup>+</sup> while the acetyl group of the substrate is transferred to cleaved NAD<sup>+</sup>, generating O-acetyl-ADP-ribose.

The exact physiological regulator of the SIR2 enzymes has not been confirmed as yet. However, studies have suggested two alternative models of SIR2 activation: (i) increasing the NAD<sup>+</sup>/NADH ratio by increasing NAD<sup>+</sup> or by reducing the level of NADH, a competitive inhibitor of SIR2,<sup>105</sup> or (ii) decreasing the level of nicotinamide, an inhibitory product of SIR2.<sup>106</sup> Whatever the case, the requirement of NAD<sup>+</sup> for SIR2 activity provides a unique mechanism for regulating class III HDACs in response to the metabolic status of the cell.

### **7. Histone deacetylase and cancer.**

It is now well documented that the aberrant transcription (*ie* epigenetic modulation) of genes that regulate cellular differentiation, cell cycle, and apoptosis is due to altered expression or mutation of genes that encode HATs, HDACs, or their binding and recruiting partners. Such modifications are key events in the tumour onset and progression.<sup>107-110</sup> Cell development and differentiation is governed by a hierarchical order of sequential gene activation, which is controlled at the level of chromatin structure.<sup>111</sup> The removal of cells from the cell cycle and regulation of apoptosis are integrated into the differentiation programme. So, disruptions in chromatin remodelling leading to aberrant gene expression can disrupt this highly-ordered process, and induce the proliferation of undifferentiated cells and cancer.

HATs and HDACs are involved in acetylation and deacetylation not only of chromatin proteins which can lead to altered regulation of transcription of genes but also of non-histone proteins themselves controlling cell cycle progression, differentiation and/or apoptosis. It has become increasingly clear that there is 'cross-talk' between the epigenetic regulation of gene

expression and the post-translational modifications of cell cycle proteins, and that HDACs and HATs play an important role at both levels of regulation of cell proliferation.<sup>112-115</sup>

Specifically, genes encoding HATs have been found translocated, amplified, overexpressed and/or mutated in different human cancers, both epithelial and haematological. Mutations in the p300 gene, either missense or encoding truncated p300, have been identified in colorectal and primary gastric tumours and other epithelial cancers.<sup>116,117</sup>

Mutations in the transcriptional co-activator CBP are present in Rubinstein-Taybi syndrome, which has an increased risk of cancer development.<sup>118</sup> Inactivation of HATs due to the inhibitory action of viral proteins is associated with cancer too.<sup>119</sup> Infact, oncogenic viral proteins, such as adenovirus E1A and the SV40 T-antigen, can bind p300, CBP and PCAF, antagonizing in this manner the expression of cellular genes that are normally activated by p300 or CBP, either by directly inhibiting HAT activity or by blocking the interaction of the co-activators with DNA-binding proteins or basal transcription factors.<sup>119</sup> Translocations resulting in in-frame fusions of the p300 or CBP genes with other genes are well described in several haematological malignancies.<sup>116</sup>

Such translocations can have dual effect. First, they can inactivate the wild-type function of HAT, thereby disrupting the transcription of genes that are regulated by that particular HAT. In addition, fusion of HAT to a DNA-binding protein result in aberrant transcriptional activation of genes, that otherwise might not be expressed.

Whilst specific alterations in HDAC genes have not been reported in human cancers, there are associations between HDACs and well-characterized oncogenes or tumour suppressor genes.<sup>120,121</sup> For example, the retinoblastoma tumour suppressor protein recruits HDAC1,<sup>122,123</sup> p53 protein complexes with Sin3-HDAC<sup>124</sup> and BRCA1, the breast cancer susceptibility protein, associates with HDAC1 and 2.<sup>125</sup>

There are several examples in which HDACs are functionally involved in oncogenic translocation products in specific forms of leukaemia and lymphoma.<sup>126,127</sup> The link between altered HDAC activity and tumorigenesis is best shown in acute promyelocytic leukaemia (APL) that serves as a model for several other haematological malignancies.

The retinoic acid (RA) receptor (RAR) is a transcriptional regulator that is important for myeloid differentiation. RAR $\alpha$  and its heterodimerization partner RXR bind to retinoic-acid response elements (RAREs), and, in the absence of retinoids, repress transcription by recruiting Sin3/HDAC through N-CoR and SMRT.

Addition of endogenous ligand releases the HDAC complexes from RAR $\alpha$ -RXR, and allows subsequent binding of HATs, such as TIF2 and CBP, to activate transcription.<sup>108-110</sup> So, the coordinated activation and repression of genes that contain functional RAREs is important for myeloid-cell normal differentiation and development. In APL, chromosomal translocations produce fusion proteins that contain RAR $\alpha$  and PML (promyelocytic-leukaemia protein) [t(15;17)], and RAR $\alpha$  and PLZF (promyelocytic zinc finger) [t(11;17)].

These aberrant proteins bind to RAREs, recruit HDACs with high affinity, are not responsive to physiological concentrations of retinoids, and behave like constitutive transcriptional repressors of RAR-targeted genes, blocking normal promyelocytes' differentiation and leading to APL.

It is not known yet which RAR-targeted genes are sufficient and/or necessary to regulate myeloid differentiation, or whether RAR $\alpha$ -containing fusion proteins target a different subset of genes compared with wild-type RAR $\alpha$ . However, as discussed below, addition of HDAC inhibitors can restore sensitivity of APL cells to RA, indicating that aberrant histone deacetylation is a key process in leukaemogenesis (figure 14).

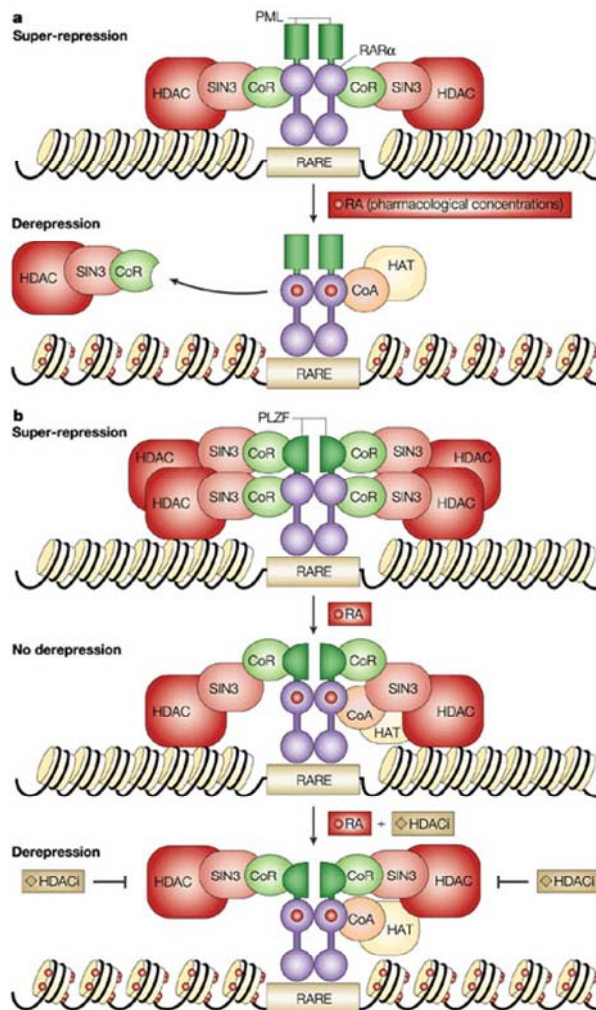


**Figure 14.** In APL, chromosomal translocations produce fusion proteins that contain RAR $\alpha$  and PML (a) and RAR $\alpha$  and PLZF (b). These aberrant proteins bind to retinoic-acid response elements (RAREs), recruit HDACs with high affinity, are not responsive to physiological concentrations of retinoids (RA), and behave like constitutive transcriptional repressors of RAR-targeted genes. Addition of HDAC inhibitors can restore sensitivity of APL cells to RA.

Transformed cells, characterized by inappropriate cell proliferation, do not necessarily lose the capacity to undergo growth arrest under certain stimuli.<sup>128,129</sup>

To date, several inhibitors of HDACs with different chemical features have been reported active both *in vitro* and *in vivo* in arresting cancer cell growth, with little toxicity.

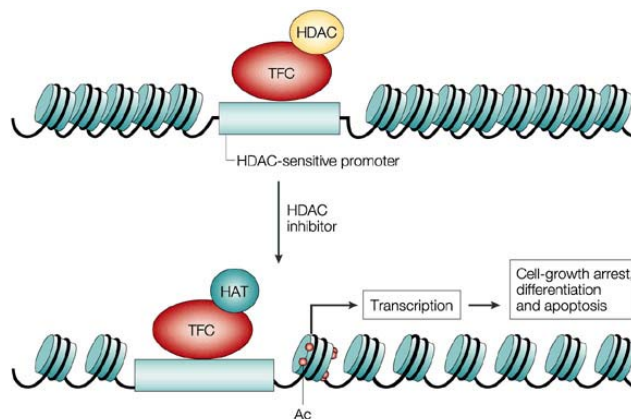


**Figure 15.** Biochemical effect of HDAC inhibitors.

These compounds have been shown to inhibit the activity of partially purified HDACs, to cause reversion of transformed morphology and inhibition of cell proliferation by induction of cell cycle arrest in G1 and/or G2 phase, terminal differentiation and/or apoptosis of transformed cells in culture for a large range of transformed cell types including solid tumour and haematological neoplastic cell lines.

Moreover, they inhibit the growth of several types of cancers in tumour bearing models, being some of them actually in clinical trials.<sup>129-132</sup> The anticancer potential of HDAC inhibitors stems from their ability to affect several cellular processes, that are dysregulated in neoplastic cells.

For the most part, activation of differentiation programmes, inhibition of the cell cycle, and induction of apoptosis are the key antitumour activities of HDAC inhibitors. In addition,

activation of the host immune response and inhibition of angiogenesis might also have important roles in HDAC-inhibitor mediated tumour regression *in vivo* (figure 16).

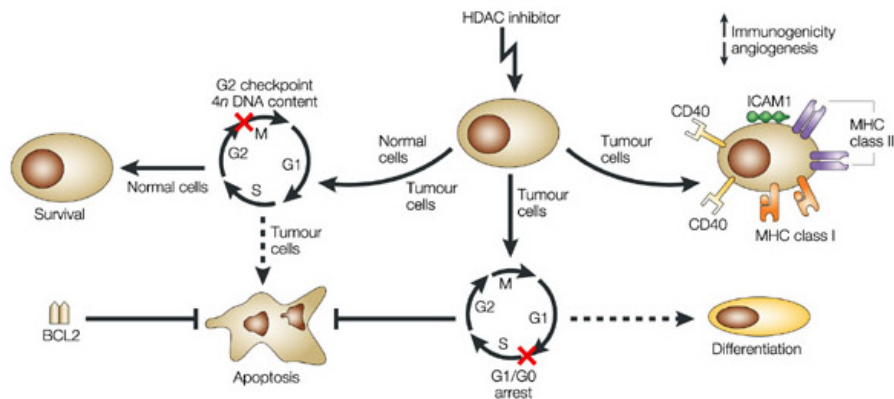


**Figure 16.** Regulation of cell growth and survival by HDAC inhibitors.

The treatment of normal and tumour cells with HDAC inhibitors causes a similar accumulation of acetylated histones H4, H3, H2A and H2B.<sup>129,131,132</sup>

Nevertheless, tumour cells appear to be much more sensitive to the growth inhibition and apoptotic effects of these agents than normal cells.<sup>133-136</sup> In clinical trials the accumulation of acetylated histone in normal and tumour tissue may be used as a marker of biological activity. Another important characteristic of HDAC inhibitors is their selectivity in altering gene expression in transformed cells.<sup>137-139</sup>

These compounds induce accumulation of hyperacetylated histones in most regions of chromatin, but only a small subset of expressed genes show a change in transcription patterns. Initial studies using differential display techniques estimate that less than 2% of genes are affected; however more recent analyses using DNA microarrays put this number closer to 10%.<sup>139</sup> The basis of this selectivity is not fully elucidated. It appears that specific sequences, such as NFY or Sp1 sites in the promoter region of genes may be required for these effects.<sup>140-141</sup>



In addition, this selectivity might relate to other covalent modifications of histone tails that can similarly affect gene expression, confirming in this way the 'histone code' hypothesis.<sup>142</sup> In particular, histone methylation, which proceeds after deacetylation of histone tails, can induce heterochromatin and euchromatin gene silencing.

In this case, the addition of HDAC inhibitors would not be sufficient to reactivate the silenced gene.<sup>142</sup>

Among the genes whose expression is increased by different HDAC inhibitors in several transformed cell lines, there is the CDK-NIA gene which encodes the cyclin-dependent kinase inhibitor WAF (p21).<sup>136,143</sup>

This tumour suppressor protein binds and inhibits the activity of CDKs, leading to hypophosphorylation of pocket proteins pRb, p107 and p130, suppression of cell proliferation, and cell cycle arrest in G1 phase.

Among other genes whose transcription is selectively altered there is the thioredoxin-binding protein 2 (TBP2). Its expression is low in a number of human cancers.<sup>144</sup> Suberoylanilide hydroxamic acid (SAHA), a well known HDAC inhibitor, selectively increases the expression of TBP2, which in turn binds reduced thioredoxin and inactivates this important cellular redox regulatory protein, increasing sensitivity to oxidative stress and apoptosis.<sup>144</sup>

The activation of TBP2 and probably other genes repressed in tumour cells by HDAC inhibitors could contribute to cell growth arrest, terminal differentiation and/or apoptosis caused by these agents. HDAC inhibitors induce transcriptional activation of a subset of genes such as p21<sup>WAF</sup> but does not necessarily account for maximal activation.

Furthermore, these compounds induce repression of an equal or larger number of genes such as cyclins A and D. The mechanism of gene repression is poorly understood and may be the result of recruitment and/or activation of co-repressors and/or acetylation of non-histone protein substrates. The latter event has varying functional effects and may also explain tumour growth arrest caused by HDAC inhibitors through mechanisms, in addition to affecting gene expression.<sup>145</sup>

These agents can cause accumulation of acetylated proteins that are important regulators of cell cycle progression, for example, pRb, transcription factors, such as p53, and hormone receptors, such as glucocorticoid and thyroid hormone receptors.

The exact contribution to anticancer activity of such HDAC inhibitors' different effects, as well as that exerted by other effects still to be discovered, require further investigation. In

addition to directly affecting cancer-cell growth and survival, HDAC inhibitors might have supplementary activities that indirectly affect tumour development. These agents can transcriptionally activate major histocompatibility complex (MHC) class I and II proteins, the co-stimulatory molecules CD40, CD80 and CD86, the intercellular adhesion molecule ICAM1, and type I and II interferons, to potentially augment immune-cell recognition and activation.<sup>145,146</sup>

In support of this hypothesis, addition of HDAC inhibitors sensitizes tumour cells for destruction in an allogeneic mixed-leukocyte reaction.<sup>147</sup> Moreover, the growth and survival of rapidly expanding solid tumours requires a continuous oxygen and nutrient supply to be maintained by the tumour neovasculature.

Trichostatin A (TSA) can inhibit hypoxia-induced expression of vascular endothelial growth factor (VEGF) and suppress angiogenesis, both *in vitro* and *in vivo*.<sup>148-150</sup> So, augmentation of the host immune response and inhibition of tumour angiogenesis might markedly suppress the growth of primary tumours and impede metastasis.

### **8. HDAC inhibitors in epigenetics: not only for cancer diseases.**

Besides angiogenesis, it is now emerging that the histone proteins and the enzymes that regulate their acetylation's state are important for chemotherapy too. In fact, the histones that are present in abundance, are antigenic and may have a role to play in the pathology of the parasitosis.<sup>151</sup>

The histones of *P. falciparum* have recently been proposed as targets for drug treatment of blood stage parasites.<sup>151</sup> They also play important role in chromatin remodelling in trypanosomatids, which include leishmania and trypanosomes.<sup>153</sup> Apicidin itself, a cyclic tetrapeptide isolated from *Fusarium* spp, was firstly reported as reversible inhibitor of *in vitro* development of *Apicomplexan* parasites, acting by inhibition of parasite (including *Plasmodium* species) HDAC enzyme,<sup>152</sup> and only later showed antiproliferative and cytodifferentiating effects on mammalian cells.<sup>154</sup>

To date, there are some reports that highlight the potential use of HDAC inhibitors with selective toxicity for protozoan parasites, and also as a new class of antimalarial agents.<sup>155</sup>

Epigenetic phenomena are also involved in many psychiatric disorders. For example, HDAC inhibitors have recently been proposed as therapeutic agents in mitigating vulnerability to schizophrenia among high-risk individuals.

More in detail, in the adult mammalian brain GABAergic interneurons release a protein named reelin (RELN) into the extracellular matrix. In this site RELN binds with high affinity to the integrin receptors, and likely plays a role in synaptic plasticity.

Because there is a great deficit (~50%) in the RELN content in specific areas of brains from schizophrenic individuals<sup>156</sup>, and this protein is normally operational during embryonic corticogenesis and throughout the patient's lifespan, the morbidity risk of schizophrenia has been proposed arising as a consequence of compromised reelin expression. This is totally in accordance with the suggestion that embryonic factors contribute to the etiology of schizophrenia.<sup>157</sup>

The deregulation of the RELN gene might well result from hypermethylation of the promoter and, because in heterozygous reeler mice (haploinsufficient in RELN) HDAC inhibitors increase DNA demethylase activity and restore RELN expression, they have been proposed for the treatment of schizophrenia.<sup>158</sup> Furthermore, HDACs and their inhibitors are involved in mental retardation<sup>159</sup> and neurodegeneration in *Drosophila*, respectively.<sup>160</sup>

Recent evidence points out that HDACs are involved in the ageing too. Indeed, it has been identified a senescence-specific form of HDAC2.<sup>161</sup> Furthermore, it has been reported that these enzymes regulate the lifespan in some animal models.<sup>162</sup>

Last but not least, nicotinamide, an inhibitor of class III deacetylases (sirtuins), is often used to self-treat anxiety, osteoarthritis, psychosis, and is in clinical trials for treatment of some cancers and type I diabetes.<sup>163</sup>

### **9. TSA/HDLP complex: mechanism of deacetylation.**

In 1999, the X-ray crystal structure of a deacetylase protein from the hyperthermophilic bacterium *Aquifex aeolicus* with sequence homology to the class I and II HDACs (termed histone deacetylase-like protein, HDLP) has been determined alone and in complex with two inhibitors, (*R*)-TSA and SAHA (figure 17).<sup>164</sup>

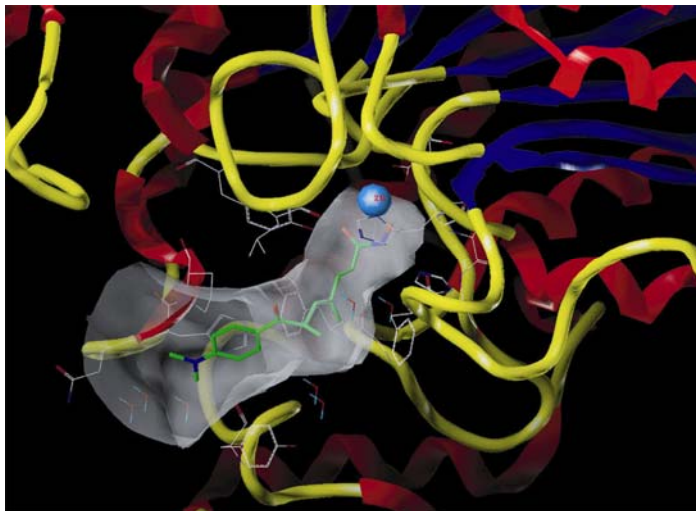


**Figure 17.** Computational representation of TSA in the active-site pocket of HDLP.<sup>164</sup>

These crystal structures have suggested a mechanism for the deacetylation reaction (figure 18).<sup>164</sup> The carbonyl oxygen of the N-acetylamide bond is thought to coordinate to the zinc cation and to thereby position it closely to a bound water molecule and activate it for a nucleophilic attack by the water.

The nucleophilicity of the water molecule, in turn, could be enhanced by an interaction with the negative charge of the buried Asp166-His131 charge-relay system to which the water is hydrogen bonded.

The attack of the water molecule on the carbonyl carbon would produce an oxy-anion intermediate, stabilized by the zinc ion, and by hydrogen bond to Tyr297. The collapse of this intermediate would result in cleavage of the carbon-nitrogen bond, with the nitrogen accepting a proton from the His132 residue, and would thereby produce the observed acetate and lysine products.<sup>164</sup>

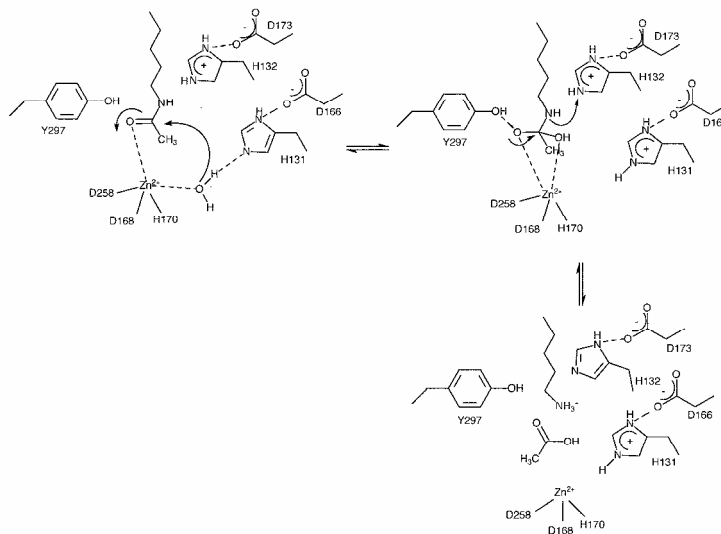


**Figure 18.** Proposed mechanism for HDAC deacetylation.

The NAD<sup>+</sup>-dependent mechanism of deacetylation performed by sirtuins involves the cleavage of the nicotinamide-ribose glycosidic bond of NAD<sup>+</sup>, joined with the transfer of the acetyl group of acetyllysine to the ADP-ribose molecule: the result is the production of an O-acetyl-ADP-ribose together with the free Lys residue (figure 19).

The formation of a labile 1'-acetylated-ADP-ribose, which is in turn converted into the 2'-O-acetyl-ADP-ribose, has been observed during the enzyme-catalyzed reaction.

This product subsequently equilibrates with the 3'-acetylated-isomer in solution, through a nonenzymatic intramolecular transesterification reaction.<sup>84</sup>

Although the physiological role of O-acetyl-ADP-ribose is still unclear, microinjection of such product results in delay/block in oocyte maturation, and in a delay/block of embryo cell division,<sup>165</sup> providing further evidence for its important function in cell signalling or metabolism.

This unusual mechanism, proposed respect yeast Sir2 protein, reveals that  $\text{NAD}^+$  serves as a true stoichiometric cofactor rather than as a component of the catalytic machinery or as an allosteric regulator of the enzyme.

Indeed, only one acetyl-lysine residue can be deacetylated for each  $\text{NAD}^+$  molecule, and hence the amount of Sir2 activity would be tightly linked to the cellular  $\text{NAD}^+$  concentrations and to the metabolic state of the cell. With this mechanism, Sir2 and likely the other sirtuins truly would function as ‘sensors’ of the metabolic conditions of the cell.

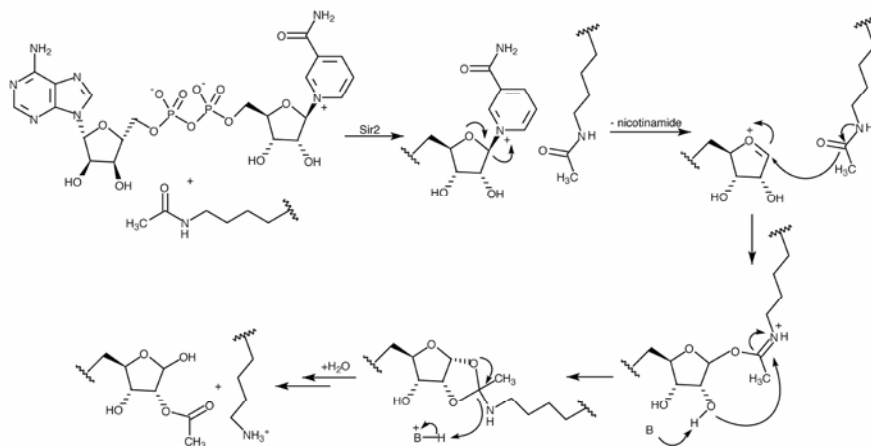


**Figure 19.** Proposed mechanism for sirtuin deacetylation.

## 10. Histone methylation.

Although acetylation/deacetylation remain the most studied post-translational histone modification, in the last years it is emerging new regulators of protein function: HMT (histone methyltransferase) that methylate arginine residues (PRMTs) and lysine residues (HKMTs) on the histone tails.

### 10.1. Arginine methylation.

Methylation of arginine residues is catalyzed by Type I and Type II Protein arginine *N*-methyltransferases (PRMTs), both types catalyze the formation of monomethylarginine(MMA) as an intermediate, but Type I facilitate the formation of asymmetric  $\omega$ - $N^G$ , $N^G$ -dimethylarginine (aDMA) residues, and Type II enzymes generate symmetric  $\omega$ - $N^G$ , $N^G$ -dimethylarginine (sDMA) residues.<sup>166</sup>

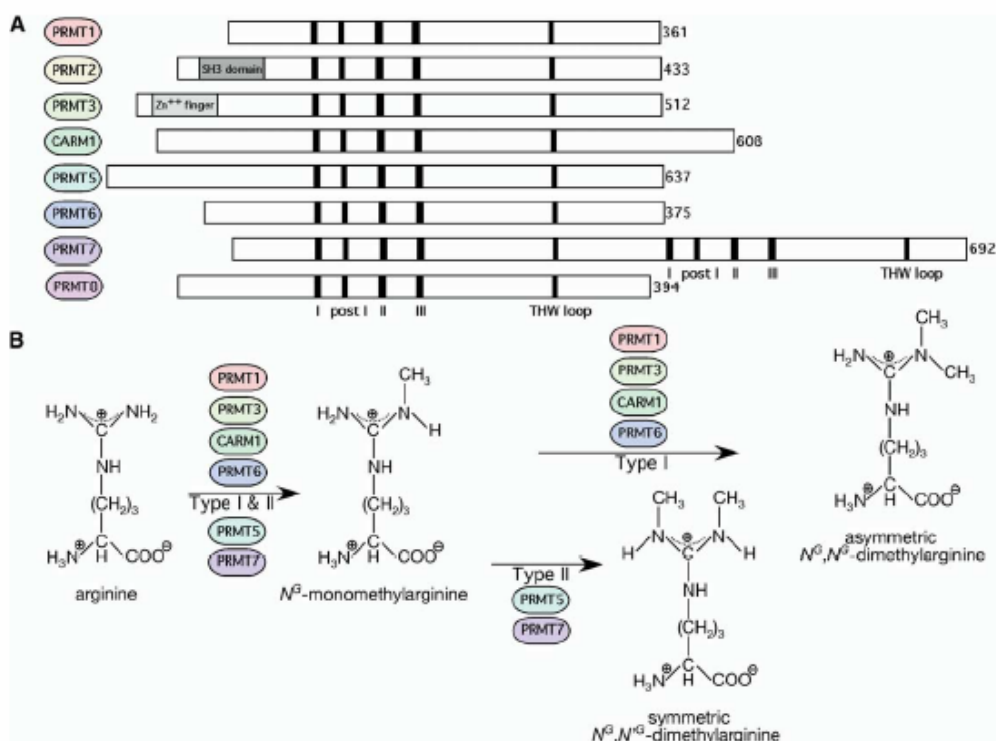


**Figure 20 . The Protein Arginine Methyltransferase Family.**

(A) There are currently eight mammalian members of the PRMT family, which harbor signature motifs I; post I, post II, and post III; and the conserved THW loop (in black). PRMT7 has a duplication of these motifs. PRMT2 and PRMT3 have an SH3 domain and a Zn<sup>2+</sup> finger, respectively, which likely facilitate substrate recognition. The accession numbers for the PRMTs are as follows: AAF62893 for hPRMT1, AAH00727 for hPRMT2, AAC39837 for hPRMT3, NP\_954592 for CARM1, AAF04502 for hPRMT5, Q96LA8 for hPRMT6, NP\_061896 for hPRMT7, and DAA01382 for mPRMT8. The number of residues is indicated at the C terminus of the PRMTs. (B) Type I and type II PRMTs generate monomethylarginine. The generation of asymmetric dimethylarginine is catalyzed by type I, and the production of symmetric dimethylarginine is catalyzed by the type II enzymes.

Currently, known mammalian Type I enzymes include PRMT1,<sup>167,168</sup> the zinc finger-containing enzyme PRMT3,<sup>169</sup> the coactivator-associated arginine methyltransferase PRMT4/CARM1,<sup>170</sup> and the nuclear enzyme PRMT6.<sup>171</sup> Methyltransferases catalyze the addition of methyl groups to nitrogen, carbon, sulfur, and oxygen atoms of small molecules, lipids, protein, and nucleic acids. Currently, eight mammalian protein arginine methyltransferases (PRMT) have been identified. Six have been shown to catalyze the transfer of a methyl group from S-adenosylmethionine (AdoMet) to a guanidino nitrogen of arginine, resulting in S-adenosylhomocysteine (AdoHcy) and methylarginine. No activity has been demonstrated for PRMT2 and PRMT8. The PRMTs are ubiquitously expressed enzymes, and they may achieve a degree of tissue specificity by alternative splicing.<sup>172</sup> Little data exist about the regulation of the expression or the stability of the PRMTs.

It has long been known that proteins that harbor glycine and arginine-rich (GAR) motifs are often targets for PRMTs.<sup>173</sup> Three enzymes that methylate GAR motifs have been crystallized, and their core structures have proven very similar.<sup>174-176</sup> The crystal structure of PRMT1 in complex with the re-action product AdoHcy and a GAR motif has been described,<sup>175</sup> and it reveals three different peptide binding channels, possibly reflecting alternate docking orientations for different GAR motif-containing substrates. RNA binding proteins (RBPs) represent major targets for PRMTs, but also histone H3, H4, p300/CBP, ILF3, HIV tat are known PRMT substrates. It was proposed that arginine methylation might



serve as a maturation signal.<sup>177</sup> It was recognized early on that histones were substrates of methyltransferases,<sup>178</sup> and it is now known that histones are substrates of PRMT1, CARM1, and PRMT5.<sup>179,180</sup> The posttranslational modification of histones is known to regulate gene expression and contribute to the histone code.<sup>181</sup>

Protein arginine *N*-methyltransferases (PRMTs) have been implicated in a variety of processes, including nuclear receptor-regulated transcription and protein trafficking.<sup>182</sup>

There are numerous transcription factors, including p53,<sup>183</sup> YY1,<sup>184</sup> and NF- $\kappa$ B,<sup>185</sup> that contribute to the recruitment of the PRMTs to promoters.<sup>186</sup> In addition to the histones, PRMTs have been shown to methylate coactivators including CBP/p300.<sup>187,188</sup> Signaling is governed by posttranslational modifications that alter protein function in part by altering protein-protein interactions. Methylated arginines have been shown to block some interactions and to promote others.<sup>179</sup>

Design, synthesis and biological validation of epigenetic modulators of histone/protein deacetylation and methylation.

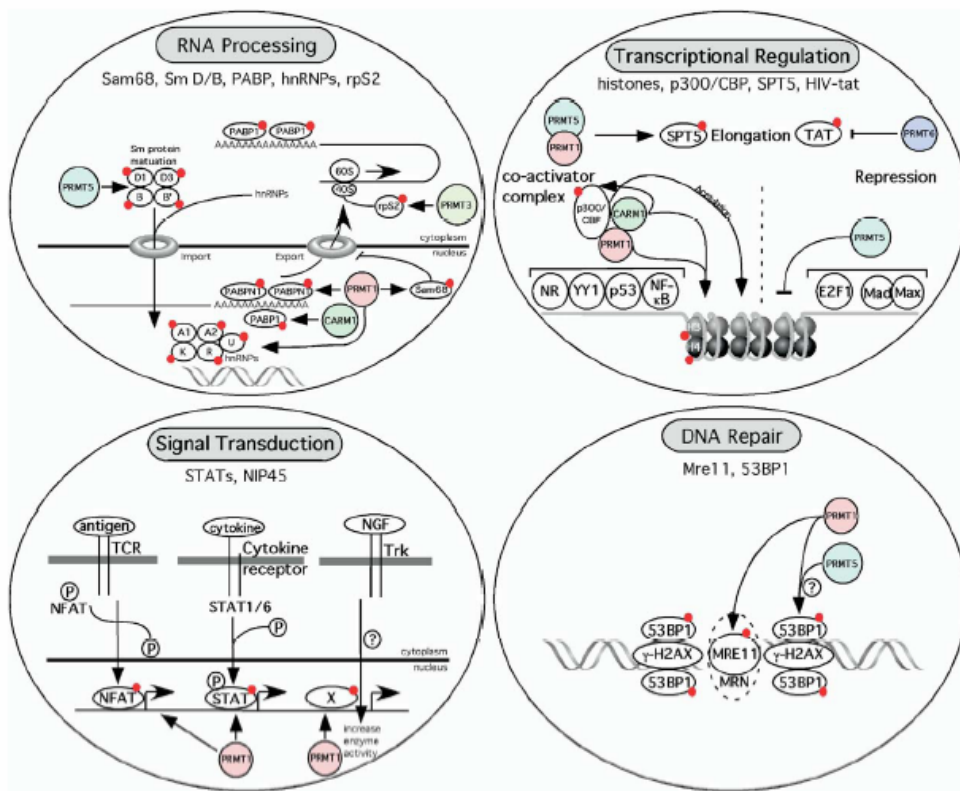


**Figure 21.** Cellular Processes Regulated by Arginine Methylation. PRMTs have been implicated in a number of basic cellular actions, including RNA processing, transcriptional regulation, signal transduction, and DNA repair. Methylarginines are denoted by a red dot.

There are several pathways that have been shown to utilize arginine methylation as a tag for signal transduction downstream of the interferon receptor, the T cell receptor, cytokine

receptors, and nerve growth factor (NGF) receptor. In addition, many cell surface receptors and signaling proteins were identified by proteomic analysis.<sup>189</sup> PRMT1 was the first enzyme in this family to be linked to signal transduction, with the finding that it binds the cytoplasmic region of the type I interferon receptor,<sup>190</sup> while binding of the tumor suppressor DAL-1 to PRMT3 acts as an inhibitor of enzyme activity, both in *in vitro* reactions and in cell lines.<sup>191</sup> Two well-studied enzymes, PRMT1 and PRMT4/CARM1, methylate histones H3,<sup>192,170,193,194</sup> H4,<sup>195,196</sup> and H2B,<sup>183</sup> in addition to many other substrates. Histone arginine methylation is a component of the histone code that directs a variety of processes involving chromatin.<sup>197,198</sup> For example, methylation of Arg-3 of histone H4 by PRMT1 facilitates H4 acetylation and enhances transcriptional activation by nuclear hormone receptors synergistically with CARM1,<sup>188,196,199,200</sup> in that CARM1 prefers acetylated histone tails in generating H3 Arg-17 methylation.<sup>196,200</sup>

PRMT1 is the predominant type I PRMT in mammalian cells, accounting for 85% of cellular PRMT activity.<sup>201</sup> It is essential for early postimplantation development, the expression is highest in developing neural structures in embryos<sup>202</sup> and PRMT1 has been implicated in neuronal differentiation.<sup>203</sup> The best-known substrates for PRMT1 are RNA-binding proteins involved in various aspects of RNA processing and/or transport, such as hnRNPs, fibrillarin, nucleolin,<sup>166</sup> and poly(A)-binding protein II.<sup>204</sup> A growing number of other proteins were found to be substrates of PRMT1, including high-molecular-weight fibroblast growth factor-2 (HMWFGF-2), a nuclear growth factor,<sup>205</sup> interleukin enhancer-binding factor 3 (ILF3),<sup>201</sup> STAT1, a transcription factor activated by extracellular signals,<sup>206</sup> SPT5, a regulator of transcriptional elongation,<sup>207</sup> and histones H4<sup>195,196</sup> and H2B.<sup>183</sup> PRMT4 was discovered as a transcriptional coactivator-associated arginine (R) MTase (CARM1).<sup>170</sup> CARM1 enhances gene activation by nuclear receptors in a synergistic collaboration with two other classes of coactivators: the p160 coactivators and the protein acetyltransferases p300/CBP.<sup>170,199</sup> CARM1 can methylate specific arginine residues in the N-terminal tail of histone H3.<sup>170,192-194</sup> Both CARM1 as well as PRMT1 act in concert with the acetyltransferase CBP/p300, along with the p160 coactivator family to enhance transcription from hormone-responsive promoters.<sup>208,209</sup> Similarly, CARM1 and PRMT1 act as coactivators in the tumor suppressor protein p53-mediated transcription, via direct interactions with p53 and its associated coactivator partner p300.<sup>183</sup> Three crystal structures of PRMTs are currently available: rat PRMT1,<sup>175</sup> the rat PRMT3 catalytic core<sup>176</sup> and yeast RMT1/Hmt1.<sup>174</sup> These structures

reflect a striking structural conservation of the PRMT catalytic core. The overall monomeric structure of the PRMT core can be divided into three parts: an MTase domain, a  $\beta$ -barrel, and a dimerization arm. The MTase domain has the consensus fold conserved in a class-I AdoMet-dependent MTase that harbors an AdoMet-binding site.<sup>210,211</sup> The  $\beta$ -barrel domain is unique to the PRMT family.<sup>176</sup> An identical hydrophobic dimer interface is observed in PRMT1,<sup>175</sup> the PRMT3 core,<sup>176</sup> and yeast RMT1/Hmt1,<sup>174</sup> despite different crystallization conditions, space groups, and cell dimensions. This observation supports the notion that dimer formation is a conserved feature in the PRMT family.<sup>176</sup>

It is conceivable that dimerization is required to engage the residues in the AdoMet-binding site in a manner in which they can interact with AdoMet properly. Interestingly, the higher order oligomerization of PRMT1<sup>168,175</sup> does not occur in the absence of dimerization.<sup>175</sup>

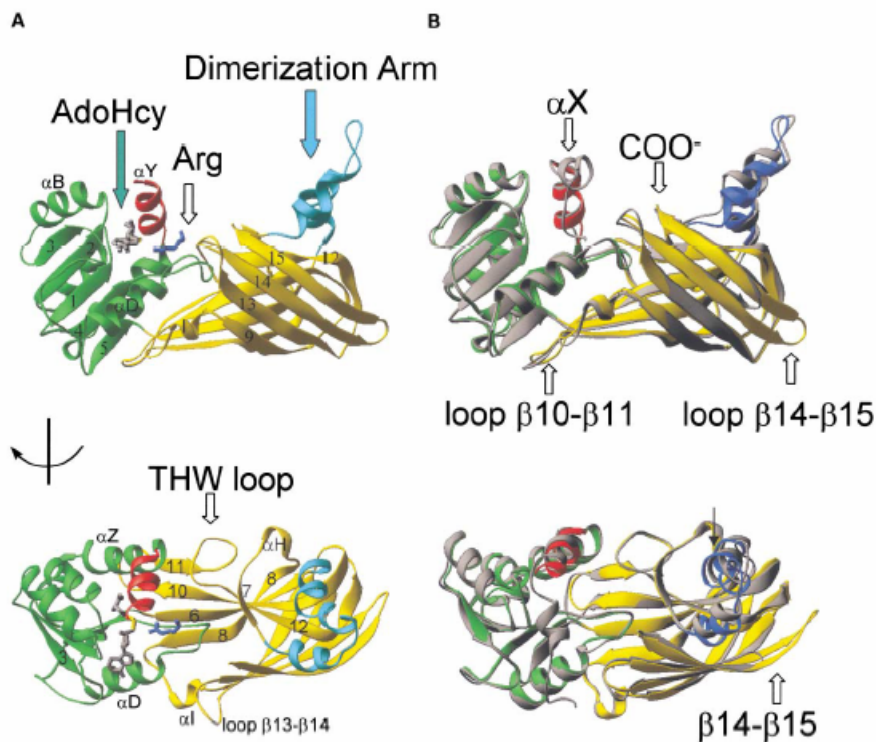


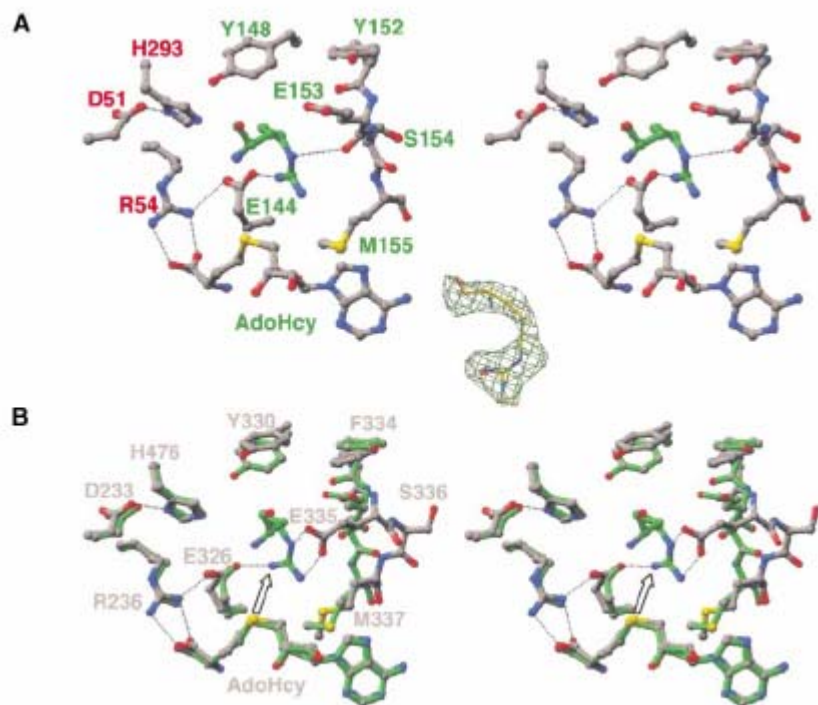
**Figure 22.** Structure of PRMT1.

(A) Two views (top and bottom panels) of monomer structure. The N-terminal helix  $\alpha Y$  is shown in red, and the AdoMet binding domain in green. The bound AdoHcy is shown in a stick model with the sulfur atom (where the transferable methyl group would be attached in AdoMet) shown in yellow. The  $\beta$ -barrel structure is shown in yellow, and the dimerization arm (which is inserted into the  $\beta$ -barrel) is in light blue. The bound arginine (blue) in the S14-AdoHcy-R3 ternary complex defines the active site, located between the AdoMet binding domain (green) and the  $\beta$ -barrel (yellow).

(B) Superposition of PRMT1 (residues 41–353) and PRMT3 core (residues 208–528, in gray). Besides deletion or insertion (located in loops between  $\beta$ -10 and  $\beta$ -11 and between  $\beta$ -14 and  $\beta$ -15), the two structures can be superimposed with less than 1 Å of root-mean-square deviation between them.

The target arginine is situated in a deep pocket between the AdoMet binding domain and the  $\beta$ -barrel domain. The residues that make up the active site are conserved across the PRMT family, and form a hairpin, that is called the “double-E loop” because it contains two invariant glutamates (E144 and E153;).

Design, synthesis and biological validation of epigenetic modulators of histone/protein deacetylation and methylation.



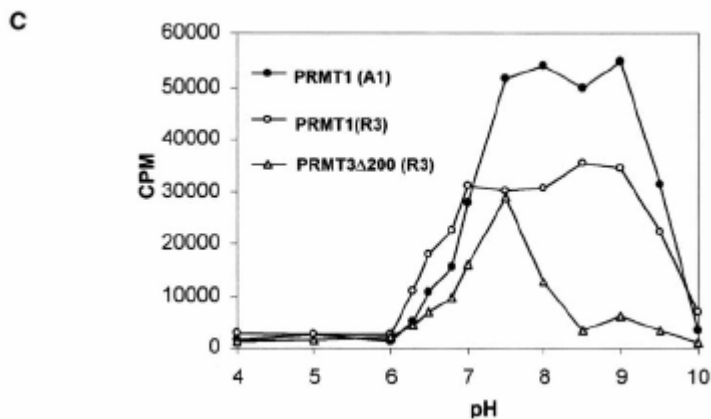


**Figure 23.** Active Sites of PRMT1 and PRMT3.

(A) PRMT1 active site with bound Arg in stereo. The annealed omit electron density map, contoured at  $5.0\sigma$  of the arginine, is shown as an insert.

(B) Superimposition of PRMT1 and PRMT3 (PDB ID code 1F3J) active sites in stereo. Only the PRMT3 residues are labeled. The arrow indicates transfer of the methyl group (attached to AdoHcy) to the bound Arg.

(C) pH dependence of PRMT1 and PRMT3 activities. Reactions ( $20\ \mu\text{l}$ ) contained  $5\ \mu\text{M}$  of purified hnRNP A1 or  $100\ \mu\text{M}$  of R3 peptide,  $10\ \mu\text{g/ml}$  of PRMT1 or  $50\ \mu\text{g/ml}$  of PRMT3 $\Delta$ 290,  $40\ \mu\text{M}$  [methyl- $^3\text{H}$ ]AdoMet ( $0.5\ \mu\text{Ci}$ ) in  $100\ \text{mM}$  buffer,  $200\ \text{mM}$  NaCl,  $2\ \text{mM}$  EDTA, and  $1\ \text{mM}$  dithiothreitol. The buffers used were sodium acetate (pH 4 and 5), MES (pH 6.0, 6.3, 6.5, and 6.8), HEPES (pH 7.0 and 7.5), Tris (pH 8.0 and 8.5), and glycine (pH 9.0, 9.5, and 10.0). After incubating at  $37^\circ\text{C}$  for 15 min,  $2.5\ \mu\text{l}$  of  $100\ \text{mg/ml}$  BSA was added, followed by  $0.5\ \text{ml}$  of 20% TCA. The samples were filtered and washed three times with 20% TCA through a GF/F filter (Millipore), dried, and subjected to liquid scintillation counting.

The hydrophobic methylene groups of the target arginine lie parallel to the plane of the Y148 aromatic ring, while the side chain of E144 and the main chain carbonyl oxygen of E153

hydrogen bond the guanidino group. Surprisingly, the side chain of E153 points away from, rather than toward, the bound guanidino group in the active site. It is noted that all three forms of PRMT1 were crystallized at low pH (~4.7); under this condition PRMT1 is inactive, perhaps due to protonation of one or both Glu side chains.<sup>176</sup>

### *10.2. Lysine methylation.*

Another substrate of methyltransferases is represented by histone lysine that is methylated by histone lysine (K) methyltransferases (HKMTs). This enzyme contains a SET domain that was originally identified in three *Drosophila* genes involved in epigenetic processes, the suppressor of position-effect variegation 3–9, Su(var)3–9; an enhancer of the eye color mutant zeste, En(zeste); and the homeotic gene regulator Trithorax.<sup>212</sup> Mammalian homologues of *Drosophila* Su(var) 3–9 were the first HKMTs identified, and they specifically methylate H3 at Lys-9.<sup>213</sup>



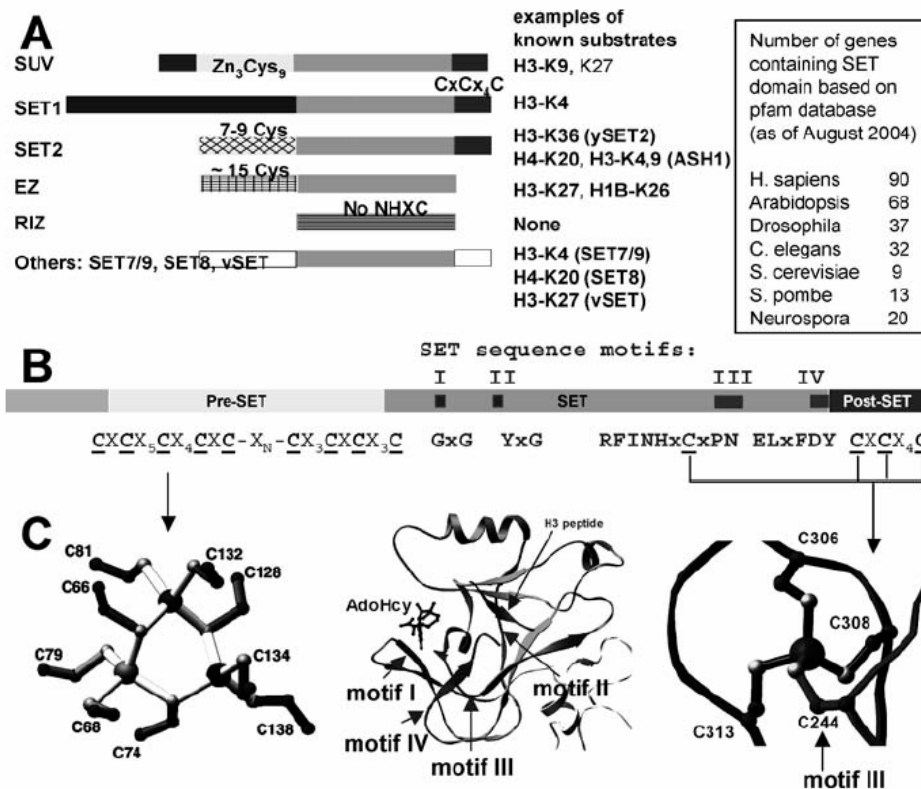


**Figure 24.** SET domain HKMTs.

(a) Domain structure of SET HKMT families. (b) DIM-5 protein (one of the smallest members of the SUV family) contains four segments: a weakly conserved N-terminal region, a pre-SET domain containing nine invariant cysteines, the SET region containing four signature motifs, and the post-SET domain containing three invariant cysteines. (c) Illustration of pre-SET Zn3Cys9 triangular zinc cluster (left panel); ribbon diagram of DIM-5 SET domain, with arrows indicating locations of conserved motifs, the cofactor binding and substrate histone H3 peptide, and the pseudo knot formed by motifs III and IV (middle panel); and post-SET zinc center (right panel).

So far, SET containing HKMTs that methylate Lys-4, -9, -27, or -36 of histone H3 and Lys-20 of histone H4 have been identified. HKMTs can be classified according to the presence or absence and the nature of sequences surrounding the SET domain that are conserved within families.<sup>197,214</sup> Representatives of the major families include SUV, SET1, SET2, EZ, and RIZ. The SET7/9 and SET8 proteins do not fit into these families. The SUV family includes the greatest number of HKMTs. The tertiary structure of SET proteins shows that these conserved residues are clustered together and involved in one of the three steps in the methylation reaction: AdoMet binding, catalysis of methyl transfer and formation of the hydrophobic target lysine-binding channel.

Currently known structures of SET proteins include the crystal structures of two SUV family proteins, *Neurospora crassa* DIM-5<sup>215,216</sup> and *Schizosaccharomyces pombe* Clr4,<sup>217</sup> four human SET7/9 structures in various configurations.<sup>218-221</sup> SET7/9 in a ternary complex with a peptide containing histone H3 Lys-4<sup>221</sup> revealed the target lysine is inserted into a narrow channel so that the target nitrogen lies in close proximity to the methyl donor AdoMet at the opposite end of the channel. At the bottom of the channel, the terminal  $\epsilon$ -amino group of the substrate lysine hydrogen bonds the hydroxyl of catalytic Tyr of SET domain.

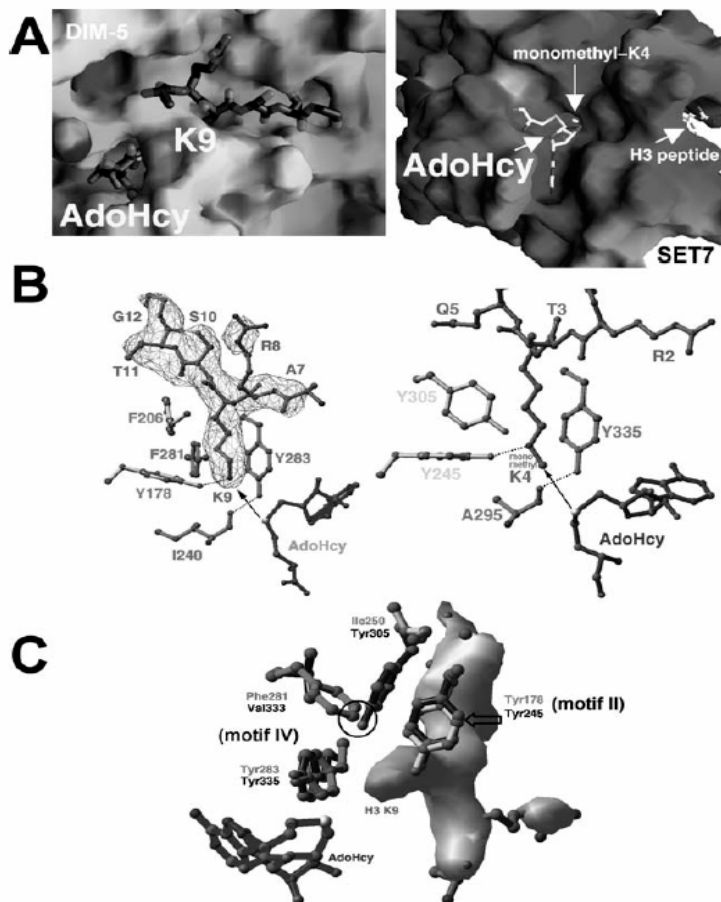


**Figure 25.** Active site of SET domain.  
(a) H3 peptide-binding site in DIM-5 with the target Lys-9 inserted into a channel (PDB 1PEG) (left panel), and the AdoHcy-binding site in SET7/9, located at the opposite end of the target lysine-binding channel (PDB 1O9S) (right panel).  
(b) The active sites in DIM-5 (PDB 1PEG) (left panel) and SET7/9 (PDB 1MT6) (right panel). The arrow indicates the

*movement of the methyl group transferred from the AdoMet methylsulfonium group to the target amino group. (c) Structural comparison of active sites in DIM-5 and SET7/9: either two tyrosines and one phenylalanine (DIM-5) or three tyrosines (SET7/9) surrounds the target lysine.*

HKMTs differ both in their substrate specificity for the various acceptor lysines and in their product specificity for the number of methyl groups (one, two or three) they transfer. The *Saccharomyces cerevisiae* SET1 protein can catalyze di- and trimethylation of H3 Lys-4, and trimethylation of Lys-4 is thought to be present exclusively in active genes.<sup>222</sup> Human SET7/9 protein, on the other hand, generates exclusively monomethyl Lys-4 of H3.<sup>216,221</sup> Considering that different methylation products might have different signaling properties,<sup>222-224</sup> it is important to understand the structural basis for this product specificity.<sup>216</sup>

A very important factor is that SET-domain-containing HKMTs such as DIM-5 and SET7, which have a narrower pH range (active at pH 8 or higher) and an unusually high pH optimum (~10).<sup>215,225</sup> At pH 10, the amino group of the target lysine should be partially deprotonated. Only the deprotonated target lysine has a free lone pair of electrons capable of nucleophilic attack on the AdoMet methyl group, this is probably a necessary condition for catalytic activity.

### ***11. Possible Arginine Demethylation by Amine Oxidases.***

Recently, it was demonstrated that a common component of a number of corepressor complexes possesses lysine demethylase activity<sup>226</sup>. The enzyme responsible for this activity, LSD1, is an amine oxidase that can specifically remove the methyl groups from dimethylated H3-K4. Although not yet confirmed, members within this family of enzymes may also be able to demethylate arginine residues. These enzymes are very likely the long sought after, bona fide lysine and arginine demethylases.

## ***12.Histone Methyltransferases and Cancer.***

Prostate and breast cancers are common tumors that are often hormone dependent. The fact that PRMTs are known coactivators for nuclear receptors makes them likely candidates to be overexpressed in these cancer types. Indeed, it has been found that increased expression of CARM1 correlates with androgen independence in human prostate carcinoma.<sup>227</sup> Importantly, small molecules that inhibit both PRMT1 and CARM1 can suppress estrogen and androgen receptor-mediated transcriptional activation,<sup>228</sup> and, in mouse embryonic fibroblast cell lines derived from *Carm1* null embryos, estrogen receptor-mediated transactivation is dramatically attenuated.<sup>229</sup> In addition, the ability of PRMT5, when over-expressed, to promote anchorage-independent cell growth also points to this enzyme as a candidate for deregulation in transformed cellular states.<sup>230</sup> PRMT5 may achieve this task by inhibiting the expression of tumor suppressors. Although the PRMTs have not been convincingly identified as oncogenes or tumor suppressors, a precedent has been set by the lysine methyltransferases for the involvement of protein methylation in transformation.<sup>231,232</sup> Moreover, the involvement of arginine methylation in the DNA damage response may identify examples of cancer in which there is genomic instability caused by the deregulation of arginine methylation.

Cellular differentiation is governed by changes in gene expression, but at the same time, a cell's identity needs to be maintained through multiple cell divisions during maturation. In myeloid cell lines, retinoids induce gene expression and a well-characterized two-step lineage-specific differentiation. To identify mechanisms that contribute to cellular transcriptional memory, some researchers studied the epigenetic changes taking place on regulatory regions of tissue transglutaminase, a gene whose expression is tightly linked to retinoid-induced differentiation. They reported that the induction of an intermediary or "primed" state of myeloid differentiation is associated with increased H4 arginine 3 and decreased H3 lysine 4 methylation. These modifications occur before transcription and appear to prime the chromatin for subsequent hormone-regulated transcription. Moreover, inhibition of methyltransferase activity, preacetylation, attenuated retinoid-regulated gene expression, while overexpression of PRMT1, a methyltransferase, enhanced retinoid responsiveness. Taken together, our results suggest that H4 arginine 3 methylation is a bona fide positive epigenetic marker and regulator of transcriptional responsiveness as well as a signal integration mechanism during cell differentiation and, as such, may provide epigenetic memory.<sup>233</sup>

The tumor suppressor DAL-1/4.1B, which suppresses growth in multiple cell types, interacts with PRMT5 and modifies its ability, either positively or negatively, to methylate cellular substrates in vitro and in cultured cells. How the PRMT5/DAL-1/4.1B interaction directly or indirectly relates to DAL-1/4.1B growth suppression may partially be explained through the altered methylation of known cellular substrates including the splicing-related Sm proteins and/or cyclin E1 as well as other cellular proteins as yet identified, regulating their ability to function in pathways important in controlling cell growth. This would be a unique mechanism for such tumor suppressor gene function in mammalian cells.<sup>234</sup>

Despite recent advances in identifying MTases, we still know little about what regulates their activities or determines their specificity. This is evident by a recent report that SET7/9 activity is not limited to histones; it also methylates the tumor suppressor p53.<sup>235</sup> With the increasing interest in protein (histone) methylation as a mechanism for gene regulation, we will undoubtedly discover other exciting roles for MTases and the cellular processes that they direct.

### ***13. HDAC inhibitors: mechanism of inhibition and pharmacophore model.***

As we have underlined above, the HDLP deacetylase core X-ray structure, together with the resolution of HDLP/TSA and HDLP/SAHA complexes, have revealed the active site of the enzyme but have also elucidated the mechanism of HDAC inhibition by hydroxamic-acid based inhibitors.<sup>164</sup>

HDLP has a single domain structure related to the open  $\alpha/\beta$  class of folds. It contains a central eight-stranded parallel  $\beta$  sheet, with four  $\alpha$  helices packed on either face. Eight additional  $\alpha$  helices and large loops in the  $\beta$  sheet further extend the structure and result in the formation of a deep, narrow pocket with an adjacent internal cavity. Concisely, the catalytic core has an  $\alpha/\beta$  motif and the active site consists of a tubular pocket with a zinc-binding site and two Asp-His charge-relay systems (His 131/Asp 166 and His132/Asp173) that facilitate the acetyl cleavage of substrate by weakening the amide bond.

The zinc cation required for the enzymatic activity is positioned near the bottom of the pocket and is coordinated by several histidine and aspartate residues too. Hydrophobic residues surround the channel leading to the bottom of the pocket, which is presumably where the aliphatic chain of the acetyl-lysine residue is nestled. TSA and SAHA act as substrate mimics;

the aliphatic chain and hydroxamic acid of each inhibitor are analogous to the lysine side chain and acetyl group of the substrate, respectively.

These inhibitors bind inside the pocket by inserting the aliphatic chain into the tube, making contact with the residues at the rim, walls and at the bottom of the pocket. Specifically, TSA contains a cap group, an aliphatic chain and a terminal hydroxamic acid functional group.

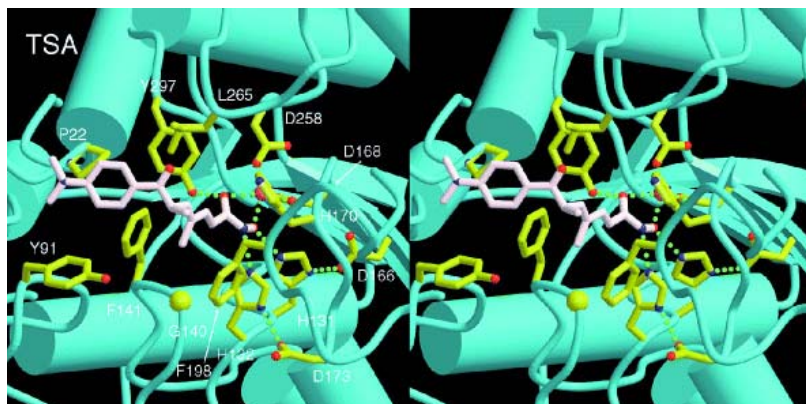


**Figure 26.** HDLP residues that interact with TSA in the tubular pocket.

The hydroxamic acid coordinates the zinc cation in a bidentate fashion (through CO and OH groups) and also contacts active-site residues (forming two hydrogen-bonds between its NH and OH groups and the two charge-relay systems His131/Asp166 and His132/Asp173, and another one between its CO and the Tyr297 hydroxyl group).

Moreover, hydroxamic acid function replaces the zinc-bound water molecule of the active structure with its OH group.<sup>236</sup> Fitting snugly into the channel, the aliphatic chain makes several Van der Waals contacts with the channel residues.

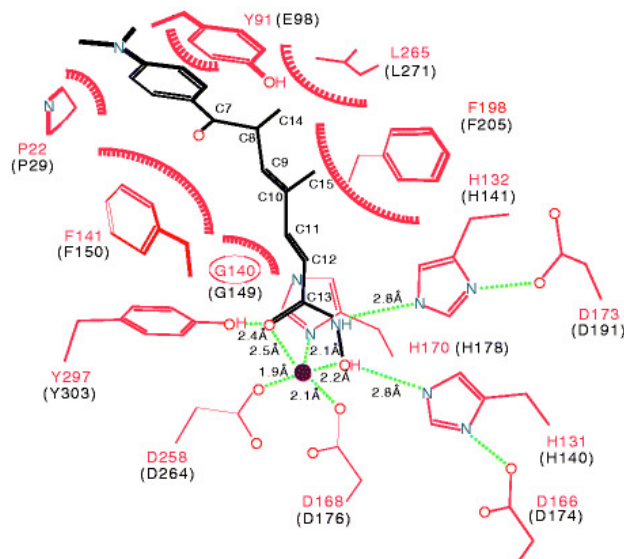


**Figure 27.** TSA binds inside the pocket making contacts to residues at the rim, walls and bottom of the pocket.

The dimethylaminophenyl group acts as a cap to pack the inhibitor at the rim of the tubular pocket-like active site.

Indeed, this cap group contacts the residues of Pro22 and Tyr91 on the rim of the pocket and possibly mimics the amino acids adjacent to the acetylated lysine residue in the histone.

The binding of TSA causes a conformational change in a tyrosine residue on this rim (Tyr91) and thereby allows tighter packing of the cap group. It has been postulated that this insertion and binding in the catalytic site blocks substrate access to the active zinc ion and, thereby, inhibits the deacetylase activity.

Conservation of the amino acid sequences of the loops that form the active site pocket among HDLP and class I and II mammalian HDACs strongly suggests that the catalytic reaction and mechanism of inhibition by TSA and SAHA are the same in HDACs as HDLP.<sup>236</sup>



The catalytic domains of the known class I and II human HDACs are very well conserved, but there are certain differences that may allow for the production of specific inhibitors.

Most of the residues that are seen in the HDLP structure to interact directly with TSA are completely conserved among all of the HDACs, but there is less conservation in the surrounding residues, with significant differences apparent between the class I and class II HDACs.<sup>237</sup> Notably, there is a striking divergence in the region of Tyr91 of HDLP, and this tyrosine residue itself is very poorly conserved among the human HDACs.

This is particularly interesting in that Tyr91 is positioned on the rim of the channel and interacts directly with the cap group of TSA, and it is the only residue that shifts its conformation upon TSA binding.<sup>236</sup>

Thus, the considerably diversity in the region of the protein suggests that it would be possible to develop more potent and/or specific inhibitors by altering the structure of this cap group.

From the TSA/HDLP complex data, we can elaborate a structural model (common pharmacophore) for class I/II HDAC inhibition. This pharmacophore consists of a metal binding domain, which interacts with the active site, a linker domain, which occupies the channel, and a surface recognition domain, which interacts with residues on the rim of the active site.

Indeed, in all known natural or synthetic inhibitors it is possible to see an extremely variable cap group.

This moiety contacts residues on the rim of the catalytic pocket and is generally connected to an electronegative group (connection unit, CU) that is able to interact by hydrogen bond with other residues.

Such CU portion is bound to an hydrocarbon linker interacting with the channel residues of the active site of the enzyme and finishing with the enzyme inhibiting group (EIG), that in many cases chelate the zinc cation near the bottom of the catalytic pocket.

The cap groups can be, for example, represented by substituted benzene rings, pyridine, pyridylmethyl groups, a portion of tricyclic systems or of cyclic tetrapeptides. The electronegative group is generally a ketone, an amide, a reverse amide, a carbamate, or a sulfonamide.

The linker is a saturated or unsaturated aliphatic chain, which mimics that of the lysine substrate, with an optimal length of 4-6 carbon residues. In some cases, it is possible to find an aromatic or heteroaromatic ring inserted into the hydrocarbon chain.

To date, the most useful EIG is the hydroxamic acid moiety but also ethyl ketone, trifluoromethyl ketone,  $\alpha$ -ketoamide, 2-aminoanilide, thiol and its acetyl derivative (which *in vivo* is rapidly hydrolyzed) are effectively able to chelate the zinc ion.

The epoxyketone and epoxy groups of some natural inhibitors seem to react irreversibly with some nucleophilic residues of the catalytic pocket of the HDAC enzymes, but the ketone group can also interact in its hydrate form as ligand with the metal ion (figure 28).

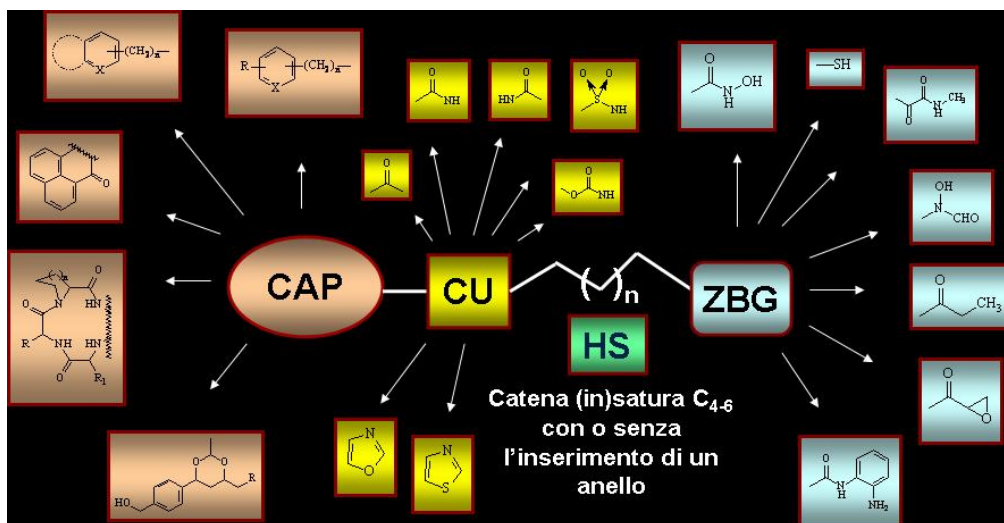


Figure 28. Pharmacophore model for HDAC inhibitors.

#### 14. HDAC inhibitors.

In the last ten years, a number of HDAC inhibitors have been reported as useful tools for the study of function of chromatin acetylation and deacetylation, and gene expression. These compounds can be natural or synthetic. Among former ones, TSA,<sup>238</sup> a cyclic tetrapeptide

family including trapoxins A and B (TPX),<sup>239</sup> chlamydocin,<sup>240</sup> HC-toxin,<sup>236</sup> Cyl-2,<sup>241</sup> WF-3161,<sup>242</sup> apicidin,<sup>154</sup> the more recent depsipeptide FK-228 (FR901228)<sup>243</sup>, and depudecin<sup>244</sup> have been isolated from cultures of fungal strains. Differently, sodium butyrate (NaB)<sup>245</sup> is a fiber-derived fermentation product generated by anaerobic bacteria in the lumen of intestine. On the other hand SAHA, its aza-analogue pyroxamide and the related second-generation hybrid polar compounds (HPCs),<sup>246</sup> straight chain TSA- and SAHA-like analogues,<sup>247-249</sup> 1,4-cyclohexylene- and 1,4-phenylene-N-hydroxycarboxamides,<sup>250</sup> scriptaid,<sup>251</sup> oxamflatin<sup>252</sup> and related compounds,<sup>253</sup> cyclic hydroxamic acid-containing peptides (CHAPs),<sup>254</sup> NVP-LAQ824 and related compounds,<sup>255</sup> benzamide derivatives with MS-275 as lead compound,<sup>256</sup> trifluoromethyl and other electrophilic ketones ( $\alpha$ -ketoamides and heterocyclic ketones),<sup>257,258</sup> and short chain and aromatic fatty acids (such as 4-phenylbutyrate<sup>259</sup> and valproic acid<sup>260</sup>) were obtained by synthetic pathways.

A useful classification of HDAC inhibitors could be made on the basis of the chemical structure that allow us to identify the different possibilities of the pharmacophore model.

Seven main classes are described:

- 1 small molecule hydroxamic acids,
- 2 carboxylates,
- 3 benzamides,
- 4 electrophilic ketones,
- 5 cyclic peptide inhibitors,
- 6 thiol based inhibitors,
- 7 miscellaneous.

#### *14.1. Small molecule hydroxamic acid.*

Hydroxamic acid based differentiating and antiproliferative agents were among the first compounds to be identified as histone deacetylase inhibitors, and these agents helped to define the pharmacophore model for HDAC inhibitors. The linker domain can consist of linear or cyclic structures, either saturated or unsaturated, and the surface recognition domain is generally a hydrophobic group, most often aromatic. Hydroxamic acids carrying cyclic peptide surface recognition domain structures are described in section 5.

TSA (**2**) and its glucopyranosyl derivative trichostatin C were first isolated from cultures of *Streptomyces hygroscopicus* as antifungal antibiotics active against *Trichophyton* species.<sup>261,262</sup>

Many years later, the trichostatins were found to have potent antiproliferative and differentiating activity at nanomolar concentrations against Friend murine erythroleukemia cells in culture.<sup>263</sup>

Whilst dimethylsulfoxide and sodium butyrate were previously known to induce differentiation in this cell line, TSA was orders of magnitude more potent.<sup>264</sup> Stereoselective synthesis of the enantiomers of TSA and subsequent analysis showed that the natural configuration is (*R*)-TSA and (*S*)-TSA is 70-fold less potent as an inducer of Friend erythroleukemia cell differentiation.<sup>265</sup>

The extremely potent biological activity and the chiral specificity of (*R*)-TSA suggested the binding of the molecule to a specific molecular target. In later studies, TSA was active in a number of normal and tumour cell lines, arresting the growth of rat fibroblast cells in G1 and G2 phases of the cell cycle.<sup>266</sup>

Nuclear histones from cells treated with TSA were highly acetylated and on pulse-chase analysis this was not due to increased acetylation but rather, to decreased deacetylation.<sup>238</sup> In experiments using partially purified mouse HDAC, TSA was a potent, reversible, non-competitive inhibitor with  $K_i = 3.4$  nM, closely related to the effective antiproliferative concentration in cell lines.

Furthermore, the  $K_i$  was 10-fold higher for HDAC purified from a mutant cell line resistant to TSA, suggesting that HDAC was the likely primary target of TSA.<sup>238</sup>

SAHA (**1**) is the prototype in a series of synthetic hydroxamic acid-based HPCs with nanomolar HDAC inhibitory potency also including pyroxamide.<sup>246</sup>

Structure-activity studies of HPCs have shown that the hydroxamic acid is the crucial moiety to obtain high inhibiting activity, since substitution or modification at this site reduces their anti-HDAC effect.<sup>267</sup> SAHA is in phase II development, and is reported to be active in patients with solid tumours and with Hodgkin's disease at non-toxic doses.<sup>268</sup>

Histone hyperacetylation was detected in tumour biopsies and in peripheral mononuclear cells after administration of SAHA at doses substantially below those at which antitumour efficacy was seen. SAHA also had good oral bioavailability and early phase clinical studies were reported to be ongoing in patients with both solid tumours and haematological cancers.<sup>268</sup> In

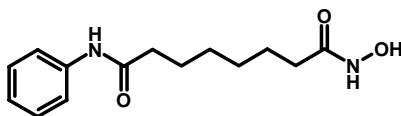
phase I studies, the closely related compound pyroxamide was initially evaluated as a continuous intravenous infusion for 5-7 days, but severe fatigue and transient hepatic toxicity limit the dose. Shorter infusional schedules are now being investigated.<sup>268</sup>

Hydroxamate SAHA analogues are represented by CBHA (**3**), pyroxamide (**4**) and 3-Cl-UCHA (**5**).<sup>269,270</sup> These agents have been shown to be effective HDAC inhibitors and antiproliferative agents, both *in vitro* and *in vivo*.

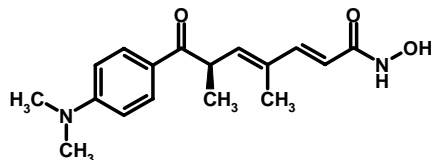
SAHA (**1**), TSA (**2**), and CBHA (**3**), which represent the paradigmatic hydroxamate HDAC inhibitors, have been instrumental in guiding the design of hydroxamate-derived HDAC inhibitors.

Constituents of the hydroxamate class are herein divided into two categories based on the structures of their linkers:

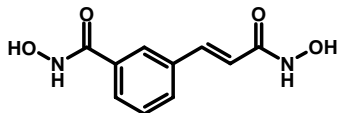
- i inhibitors with linear linkers (TSA and SAHA-like),
- ii inhibitors with linkers consisting of carbo- or heterocycles (CBHA-like).



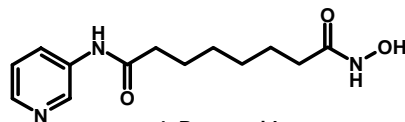
1: SAHA



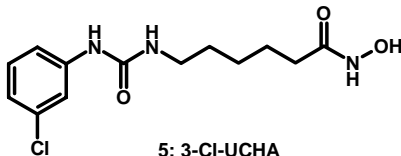
2: TSA



3: CBHA



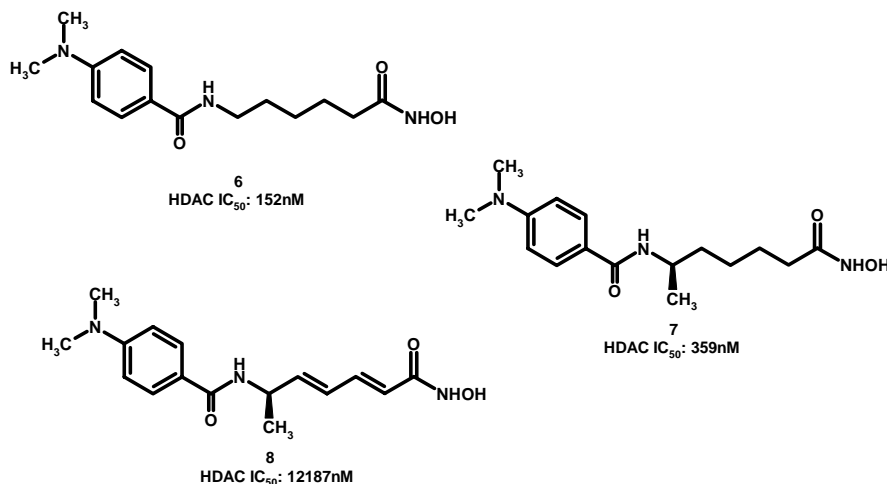
4: Pyroxamide



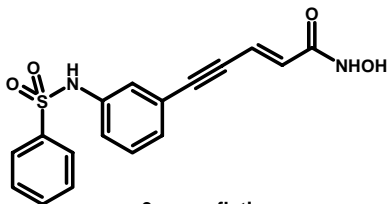
5: 3-Cl-UCHA

Design, synthesis and biological validation of epigenetic modulators of histone/protein deacetylation and methylation.

*Inhibitors containing linear linker domain structures.* In an effort to understand the importance of the methyl-substituted olefinic linker in TSA hybrids, the synthesis and evaluation of the compounds **7** and **8** has been performed.<sup>271</sup> These agents, along with related analogue **6**, demonstrate a highly sensitive and limited SAR profile. For example, the sequential addition of a methyl group (**7**) and two double bonds (**8**) caused a 2.3- and 33-fold reduction in activity, respectively, relative to the linear alkyl (**6**).

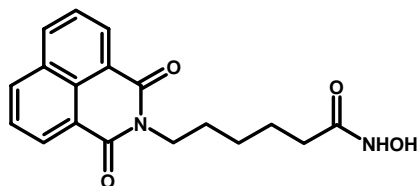


Oxamflatin (**9**) was prepared by researchers at Shionogi Laboratories in 1996.<sup>272,273</sup> Oxamflatin was found to be a potent HDAC inhibitor of partially purified mouse HDAC (IC<sub>50</sub>=15.7 nM), although it was found to be less potent than TSA (**2**) (IC<sub>50</sub>=1.44 nM) in the same assay.

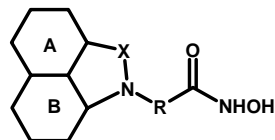


9: oxamflatin

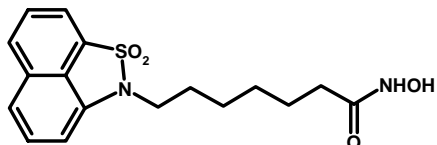
Scriptaid (**10**), which was identified *via* highthroughput screening for transcriptional activators, was also found to inhibit HDAC and cause the induction of histone hyperacetylation.<sup>274</sup> A series of tricyclic molecules related to scriptaid (**10**) and corresponding to the general formula **11** were recently reported. The most potent analogue, **12**, has IC<sub>90</sub>=10 nM.



10: Scriptaid



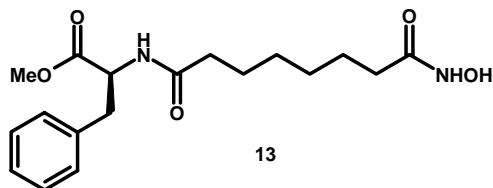
11



12

Jung and co-workers synthesized a group of phenylalanine-containing SAHA analogues, including **13** and other derivatives.<sup>275,276</sup> These agents were tested against both maize histone deacetylase (HD-2) and partially purified rat liver HDAC.

Design, synthesis and biological validation of epigenetic modulators of histone/protein deacetylation and methylation.

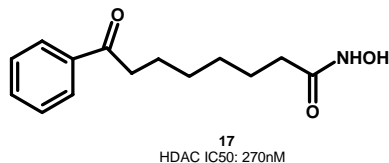
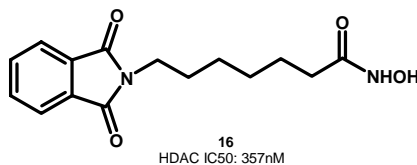
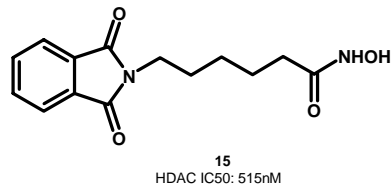
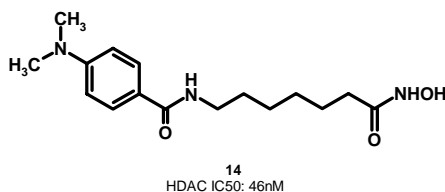


This series provides insight into the nature of inhibitor-enzyme interactions. The trends in activity against HD-2 are different from those observed in mammalian HDAC.

For example SAHA (**1**) appears to be a poor inhibitor of HD-2; furthermore HD-2 does not discriminate between the five- and six-methylene linkers, while HDAC favors the six-methylene linker.

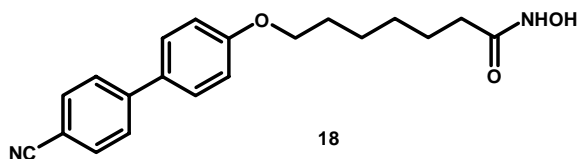
Compounds of this series with bulky hydrophobic residues (naphthyl or indolyl groups) in the side chains appear to be among the best inhibitors and differentiating agents. Finally, inversion of the phenylalanine chiral center did not affect inhibitor activity against the enzyme or in cells.

The same group also reported reverse amide SAHA derivatives.<sup>277,278</sup> This study confirmed the earlier observation that compounds with five- and six methylene spacers (**6** and **14**) are the most active. This series of compounds was expanded further to include scriptaid analogues **15** and **16** and SAHA analogue **17**.



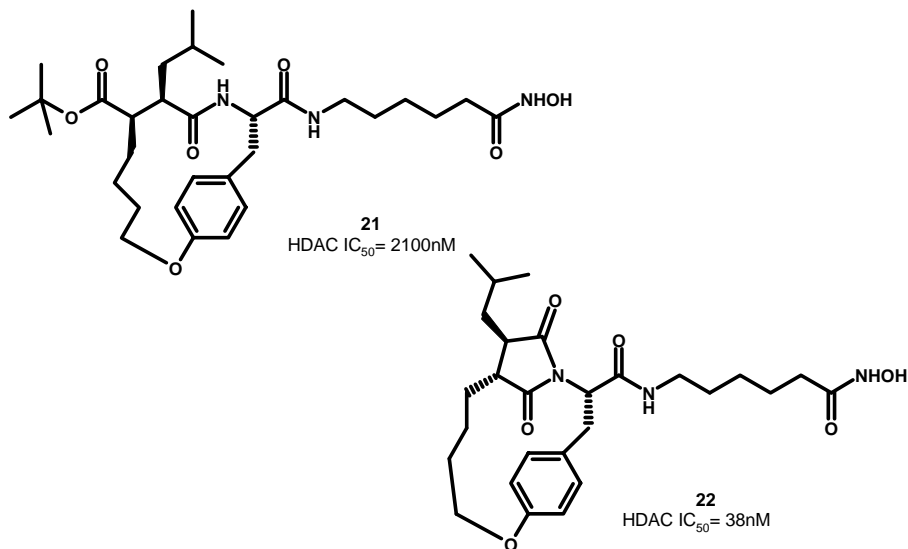


Biaryl ether hydroxamate **18** was identified by Glaser and co-workers as a mimic of transforming growth factor  $\alpha$  (TGF- $\alpha$ ) with proliferation inhibitory properties. This agent was further shown to inhibit a mixture containing human HDAC1, HDAC2, and HDAC3 ( $IC_{50}$ = 9 nM) and to cause histone hyperacetylation and p21 induction.<sup>279</sup>

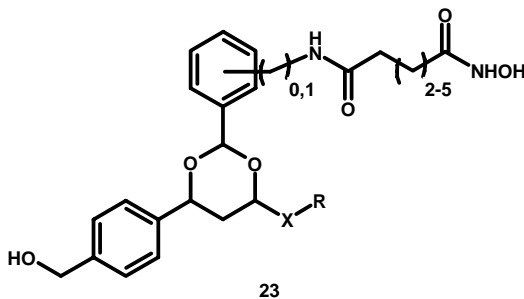


In a more recent paper, Curtin and co-workers reported the synthesis and HDAC1 inhibitory activity of **21** and reaction byproduct succinimide **22**, both of which contain a macrocyclic surface recognition domain.<sup>280</sup> A related series of succinimide hydroxamic acids were prepared and assayed against human HDAC1. The number, identity, and disposition of macrocycle substituents appear to be critical for activity. The removal of the succinimide substituents or the phenylalanine side chain depresses activity. Replacement of the succinimide with a lactam or phthalimide also led to reduced activity. The length of the linker domain alkyl group was also found to be critical, with the five-methylene analogue showing maximal activity.

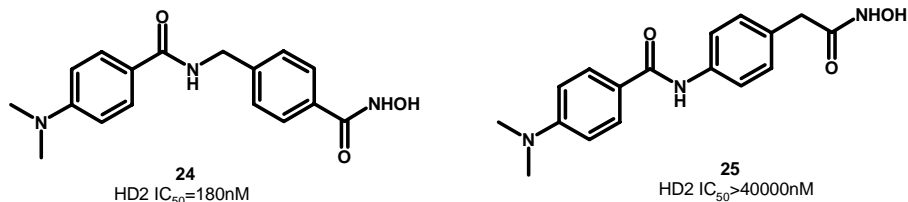
Design, synthesis and biological validation of epigenetic modulators of histone/protein deacetylation and methylation.



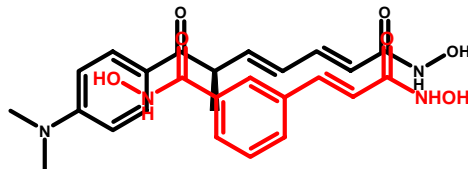
Schreiber and co-workers reported the synthesis of a library of SAHA-derived HDAC inhibitors including hydroxamates (**23**), benzamides, and carboxylates.<sup>281</sup> This set of compounds was aimed at the exploration of the chemical space in the rim region of the HDAC enzymes.



*Inhibitors containing cyclic linker domain substructures.* One of the earliest papers reporting compounds with aromatic linkers presented the activity of compounds **24** and **25** together with compounds with linear linkers.<sup>275</sup> These studies demonstrate the importance of the proper orientation of the linker, underscoring the importance of conformation and arrangement of substructures for HDAC inhibition.

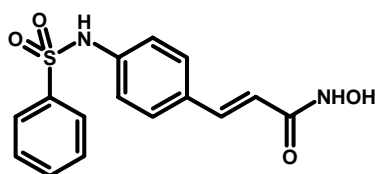


The discovery of CBHA (**3**) as an HDAC inhibitor demonstrated toleration of aromatic rings in the linker domain.<sup>269,270</sup> This observation, and the olefinmethyl arrangement found in TSA (**2**), suggests an isosteric relationship between these agents.

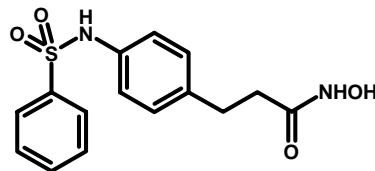


Oxamflatin-CBHA derived compounds have also been disclosed.<sup>282</sup> Compounds containing cinnamic (**26**) and hydrocinnamic (**27**) linkers were determined to be the best in a series consisting of various lengths.

Design, synthesis and biological validation of epigenetic modulators of histone/protein deacetylation and methylation.



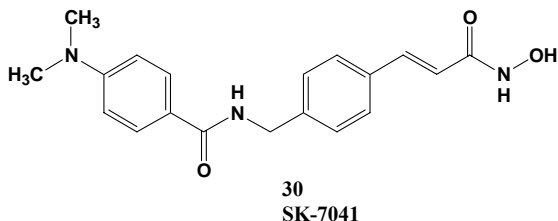
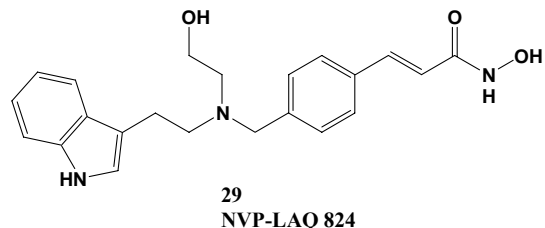
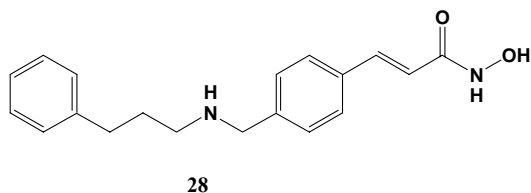
26



27

This result was interpreted in terms of effect of the chain length but could also stem from the geometries the compounds can assume, as seen for **24** and **25**. The presence of the double bond has little effect on activity, while substitution R to the hydroxamate dramatically decreased activity. A 3-fold decrease in HDAC inhibitory activity was observed upon methylation of the sulfonamide nitrogen.<sup>282</sup>

Finally, screening of a compound library yielded CBHA derivative **28** which was found to inhibit HDAC, induce p21, and inhibit proliferation. A series of agents based on **28** led to NVP-LAQ824 (**29**)<sup>283</sup> and SK-7041,<sup>284</sup> that is in preclinical studies.

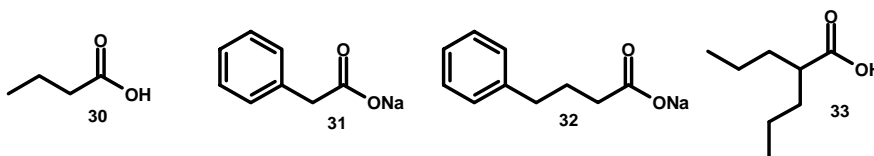


Hydroxamic acids constitute the largest class of HDAC inhibitors, with new examples being added at a rapid pace both in the literature and in patent disclosures. These agents are among the most potent HDAC inhibitors, with many examples of low nanomolar activity, and the search for even more potent compounds in this class will presumably continue for the foreseeable future. In addition, *in vivo* efficacy studies have demonstrated that the hydroxamate class has great therapeutic potential. There are currently two HDAC inhibitors from the hydroxamate class in clinical trials, the most advanced of which is SAHA (Vorinostat, phase III).

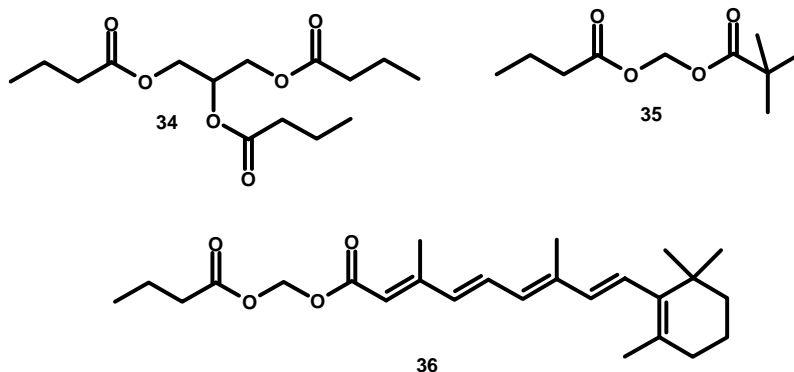
#### 14.2. Carboxylates.

The study of the SAR of the carboxylate class<sup>285</sup>, which is defined as possessing a carboxylate in the metal binding domain, has been limited as a result of poor HDAC inhibitory activity. With some exceptions like a CHAP carboxylic acid analogue corresponding to trapoxin B (IC<sub>50</sub>=100 nM), these agents possess millimolar HDAC inhibitory activities. The activity of the CHAP carboxylic acid analogue illustrates the importance of the surface recognition domain to HDAC inhibitory activity. However, most carboxylates reported to date have been

limited to simple alkyl chains. Nonetheless, these agents are being studied in the clinic for the treatment of cancer, albeit at doses required to achieve high concentrations of drug. For example, butyric acid (BA, **30**), a natural product generated in man by metabolism of fatty acids and bacterial fermentation of fiber in the colon, has long been known to be an antiproliferative and differentiating agent.<sup>285,286</sup> The first report of anticancer activity of BA on solid tumors in 1933 was followed by the observation that it possesses differentiating activity at high micromolar concentrations on several cancer cell types.<sup>287</sup> It was later determined that BA is a millimolar HDAC inhibitor, and this observation is thought to explain its mechanism of action. Other short-chain fatty acid analogues of BA, such as sodium phenylacetate (**31**), sodium phenylbutyrate (**32**), and the anticonvulsant valproic acid (**33**), have also been identified as antiproliferative agents and HDAC inhibitors.<sup>285</sup>



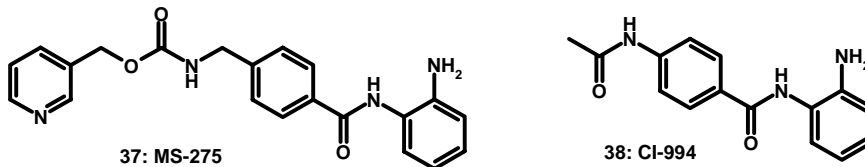
Despite poor enzymatic inhibitory activity, a number of carboxylates, including butyric (**30**) and phenylbutyric acid (**31**), are in clinical trials for cancer treatment alone and in combination with other agents.<sup>288</sup> A combination of phenylbutyrate and all-trans retinoic acid (ATRA), for example, induced histone hyperacetylation and complete remission in a case of highly resistant promyelocytic leukemia before relapse occurred after 7 months.<sup>289</sup> The high concentration of BA and analogues needed for clinical use, coupled with poor bioavailability and rapid metabolic degradation, has led to the exploration of prodrugs such as **34** and **35**.<sup>290</sup> Compound **34**, also known as tributyrin, can deliver 3 equivalents of BA upon hydrolysis. Compound **36** is a prodrug of both BA and ATRA. These agents show better absorption and have a more favorable metabolic profile than the corresponding parent compounds.<sup>290</sup>



Overall, the carboxylate class possesses limited HDAC inhibitory activity. Advances in generating carboxylates with improved HDAC inhibitory potency have provided important insights into the field of HDAC inhibitor design. However, a great deal of work remains to be done before potent carboxylates can be routinely generated as HDAC inhibitors. Nonetheless, the clinical utility of modestly active constituents of the carboxylate class is under investigation and promising results have been obtained, thereby accentuating the validity of HDAC inhibition as a potential treatment for cancer.

### 14.3. Benzamides.

The benzamide class, which is generally less potent than the corresponding hydroxamate and cyclic tetrapeptide classes, includes MS-275<sup>291</sup> (**37**) and CI-994<sup>292, 293</sup> (**38**).



In 1999, Suzuki and coworkers identified MS-275 (**37**) from a series of synthetic benzamide-based HDAC inhibitors.<sup>291</sup> The SAR of the benzanilide functionality revealed that a 2'-amino (**37**) or 2'-hydroxyl moiety is critical for inhibitory activity against partially purified histone deacetylase.

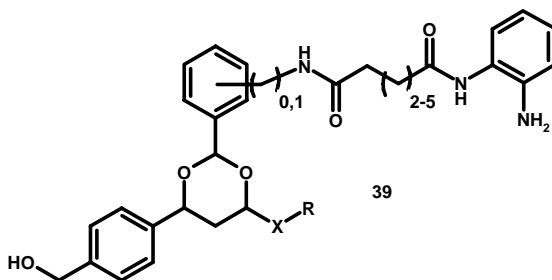
Removing or repositioning the amino group on the aryl substituent or capping with acetate generates inactive agents.

Substitution at the 3', 4', and 5' positions attenuated enzymatic activity, apparently because of increased steric interactions, given that electronic contributions of substituents at these positions appeared to have little effect. Additional evaluation of MS-275 demonstrated that it could inhibit partially purified human HDAC preparations and cause hyperacetylation of nuclear histones in various cell lines.<sup>294</sup> When administered orally to nude mice implanted with tumor lines, seven out of eight lines were strongly inhibited.<sup>294</sup>

Importantly, an inactive MS-275 structural analogue was devoid of both in vitro and in vivo activity, further suggesting that the beneficial biological effects are a result of HDAC inhibition. MS-275 is currently in phase II clinical trials.

CI-99455 (**38**) is an acetylated derivative of dinaline initially developed as a potential anticonvulsive agent. The mechanism for the antitumor activity of CI-994 is currently unclear but may involve the modulation histone deacetylation, although no information on HDAC inhibitory activity has been published to date. Phase II trials for non-small-cell lung cancer revealed activity, and trials comparing gemcitabine alone to gemcitabine in combination with CI-994 have been initiated.<sup>295</sup>

The benzamide moiety of MS-275 (**37**) was also explored in a library of SAHA derivatives related to **23** (generic formula **39**).





These inhibitors, which were based on a 1,3-dioxane diversity structure, were synthesized on polystyrene beads and assayed for biological activity in a "one beadone stock solution format".<sup>281</sup> These elegant studies led to the identification of molecules that appear to selectively inhibit HDAC1 over HDAC6.<sup>296</sup>

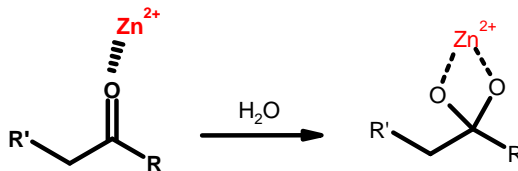
The exact mechanism by which the benzamides exert their antiproliferative effects has not been fully elucidated.

However, it has been clearly demonstrated that certain members of the benzamide class possess antitumor activity that correlates with HDAC inhibitory activity, although the nature of this activity appears to differ significantly from that of the small-molecule hydroxamates, as measured by changes in gene expression.

Additional unanswered questions include whether benzamide-induced HDAC inhibition occurs at the active site, as demonstrated for hydroxamates, and if so, the exact nature of the benzamide moiety interaction with the active site zinc of the enzyme remains to be characterized. Additional studies will be required in order to understand the mechanistic differences between the benzamide and hydroxamic acid classes with regard to HDAC inhibition.

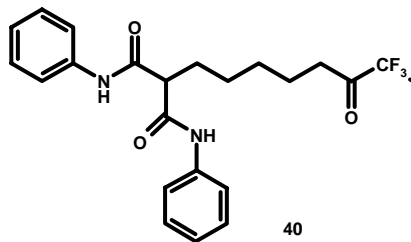
#### *14.4. Electrophilic ketones.*

Numerous electrophilic ketones are known inhibitors of proteases, including metal-dependent hydrolytic enzymes such as carboxypeptidase A and metallo- $\beta$ -lactamase.<sup>297, 298</sup> Studies have demonstrated that the hydrated form of the ketone acts as a transition-state analogue and coordinates the zinc ion in the active site of carboxypeptidase A.<sup>297</sup>

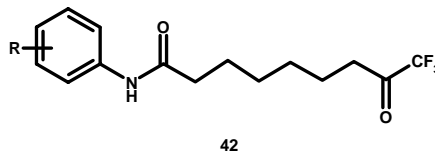
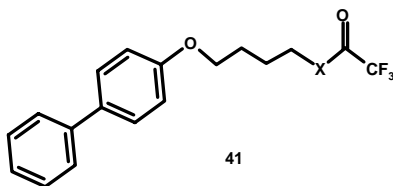


It seems likely that a similar mechanism is operative for HDAC inhibition by the electrophilic ketone class. The first constituent discovered in this newly defined class of HDAC inhibitors was trifluoromethyl ketone **40**.<sup>278</sup>

Design, synthesis and biological validation of epigenetic modulators of histone/protein deacetylation and methylation.



The synthesis of various linear molecules based on this structure comprising an aromatic in the surface recognition domain, connected *via* ether or amide bonds to an aliphatic chain in the linker domain and carrying a trifluoromethyl ketone in the metal binding domain, was recently disclosed (generic formula **41**, **42**).<sup>299</sup>



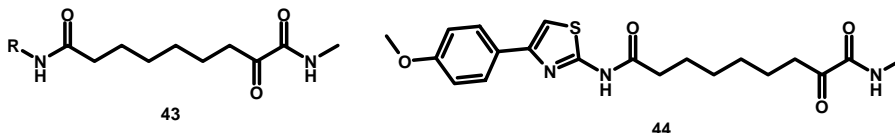
These agents were tested against a mixture of HDAC1 and HDAC2 and showed inhibition at low micromolar/high nanomolar concentrations. These agents also possess antiproliferative activities *in vitro* and induce histone hyperacetylation and p21 gene expression.

Both the five- and six-methylene linkers showed optimal activity in the ether series. Compounds carrying meta or para substituents were found to be significantly more potent than the corresponding ortho analogues (**42** series), and an aromatic moiety can be accommodated in the linker. The trifluoromethyl ketone is essential for the inhibitory activity of these compounds.

A simple ketone, a trifluoromethylcarbinol and a pentafluoroethyl ketone showed no inhibition up to 50  $\mu$ M, although some simple ketones in the cyclic peptide class possess potent HDAC inhibitory properties. The trifluoromethyl ketones studied exhibit short half-

lives both *in vivo* and *in vitro* by rapid reduction to the corresponding alcohol, which occurs *in vitro* in the presence of whole blood or cells.

The same group recently presented R-ketoamides as HDAC inhibitors.<sup>300</sup> The compounds of general structure **43** were chosen as the best candidates among other electrophilic ketones, including various R-ketoacids and ketoesters. Compound **44** is an HDAC inhibitor (IC<sub>50</sub>=9 nM) that shows antiproliferative activity *in vitro*, as well as efficacy in a tumor model *in vivo*.



This series of compounds, as might be expected, was also rapidly metabolized to the corresponding alcohol both *in vivo* and *in vitro* in whole blood.

The antiproliferative activity and *in vivo* efficacy of electrophilic ketones, despite their metabolic instability, were rationalized by the hypothesis that a brief exposure to HDAC inhibitors can induce a biological response.<sup>300</sup>

The electrophilic ketone class represents a new design that has not yet been fully exploited. Current challenges include the need to develop additional structural variants in order to assess optimal design parameters and tolerances, as well as the application of the wealth of information available about the linker and surface recognition domains from other structural classes to the electrophilic ketone class. Nonetheless, the electrophilic ketone class contains potent inhibitors of HDAC that, despite apparent poor stability, possess antitumor effects in animal models.

#### 14.5. Cyclic peptide inhibitors.

Cyclic peptide containing HDAC inhibitors, which constitute the most structurally complex class of HDAC inhibitors, are herein divided into two subclasses: inhibitors bearing (*S*)-2-amino-9,10-epoxy-8-oxodecanoic acid (L-Aoe), which contains an epoxy ketone, and inhibitors without the L-Aoe moiety.

All of the agents from each subclass conform to the pharmacophore model for HDAC inhibitors and possess a macrocycle containing hydrophobic amino acids in the surface

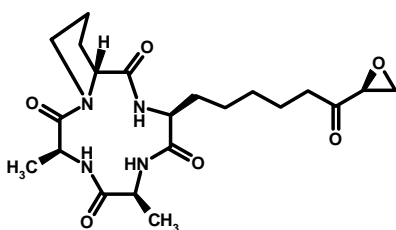
recognition domain, an alkyl chain in the linker domain, and a functional group in the metal binding domain.

Constituents of the cyclic peptide class typically possess nanomolar levels of HDAC inhibitory activity; however, their general utility in the treatment of cancer remains largely unproven, with the possible exception of FK-228 (**45**, aka depsipeptide, see below).<sup>301</sup>

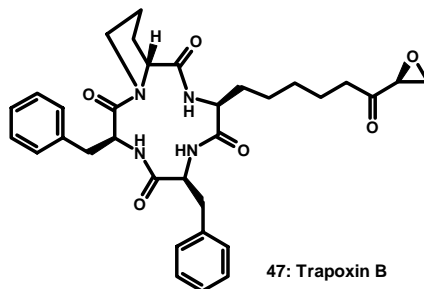
It is believed that cyclic peptide HDAC inhibitors bind to the HDAC enzyme in a manner consistent with the X-ray crystallographic findings with hydroxamates. By this model, the aliphatic linker passes down the enzyme's tubelike channel, positioning the binding moiety in proximity to the active site zinc, while the macrocyclic portion binds to the rim of the active site. However, the mechanism of action differs between the Aoe-containing inhibitors, which are typically classified as irreversible HDAC inhibitors, and those without the Aoe moiety, which are reversible inhibitors.

However, the irreversible nature of Aoe-containing inhibitors is still in question and mechanistic possibilities include both direct covalent modification via nucleophilic attack on the reactive epoxy ketone in the active site and noncovalent binding with slow dissociation of the inhibitor from the active site.<sup>302</sup>

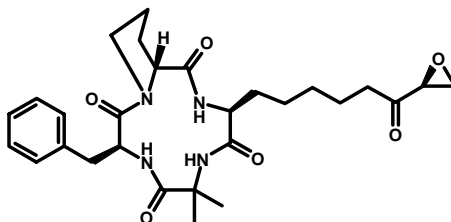
The first examples of the cyclic peptide class arose from screening natural products for antiparasitic or antiproliferation activity, with the Aoe-containing cyclic peptides being the first subclass isolated. These compounds include HC-toxins (**46**),<sup>303</sup> trapoxin B (**47**),<sup>304</sup> and chlamydocin (**48**)<sup>305</sup>.



46: HC-toxin



47: Trapoxin B



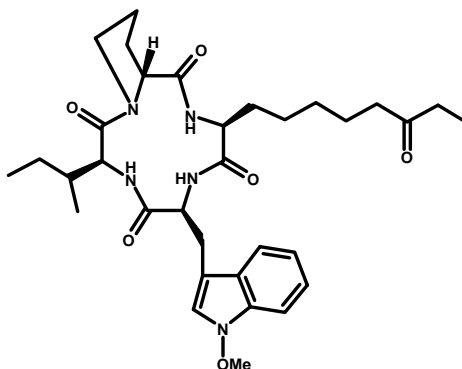
48: Chlamydomycin A

The isosteric nature of the Aoe side chain with acetylated lysine suggests it mimics the natural substrate. Some Aoe-containing inhibitors appear to operate exclusively by an irreversible mechanism and require the epoxy ketone functionality for their effects. For example, the 9,10-diol analogue of HC-toxin (**46**) is devoid of activity. Reduction of the C8-ketone of chlamydomycin (**48**) to the alcohol or replacement of the epoxide with  $\text{CH}_2=\text{CH}_2$ ,  $\text{CH}_2\text{CH}_3$ , or  $\text{CH}_2\text{CH}_2\text{OH}$  leads to reduced HDAC inhibitory activity.<sup>305</sup>

Within the subclass of cyclic tetrapeptides classified as reversible inhibitors are active variants of the Aoe-containing natural products lacking the epoxy ketone functionality.

These agents demonstrate that the potentially reactive epoxy ketone moiety is not required for HDAC inhibition. Apicidin (**49**), a fungal metabolite, contains an (*S*)-2-amino-8-oxodecanyl side chain lacking an epoxide.<sup>306</sup>

It has broad spectrum activity (ranging from 4 to 125 ng/mL) against the apicomplexan family of parasites, presumably via inhibition of protozoan histone deacetylases ( $\text{IC}_{50}=1\text{-}2\text{ nM}$ ), and demonstrates efficacy against *Plasmodium berghei* malaria in mice.

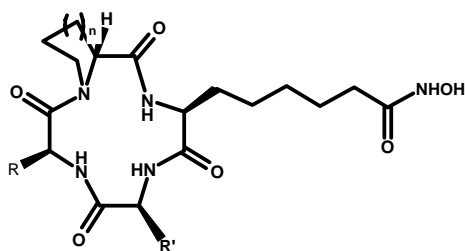


49: Apicidin

A systematic study into side chain derivatives of apicidin revealed several picomolar HDAC inhibitors.<sup>307</sup> These derivatives were tested for HDAC inhibition using partially purified extracts of both human HeLa cells and *Eimeria tenella* protozoa.

Potent HDAC inhibitors maintaining a tetrapeptide macrocycle and linear linker, but incorporating the known zinc chelating ability of hydroxamic acids, have been explored extensively by Yoshida and co-workers.<sup>308</sup>

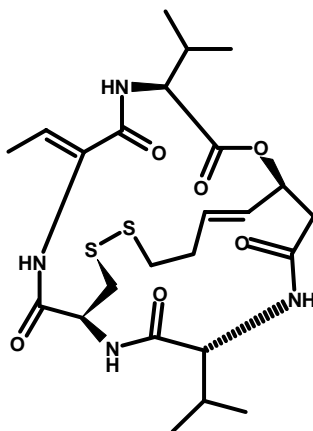
These synthetic hybrids of the hydroxamate and cyclic tetrapeptide classes, termed CHAPs (**50**), resulted in reversible inhibitors of HDAC1 that are active at low nanomolar concentrations. Studies of chain length between the macrocycle and the hydroxamic acid revealed that the optimal linker for HDAC1 inhibitory activity was five-methylene units, relative to four- and seven-methylene units. It is interesting to note that a CHAP carboxylic acid analogue corresponding to trapoxin B had significant activity ( $IC_{50}=100$  nM).



50: CHAPs

Other studies investigating the biological effects of synthetically modified macrocyclics have been performed. In their efforts to identify parasite-selective HDAC inhibitors, Merck researchers generated indole-modified apidicin analogues possessing picomolar enzyme activity, as well as tryptophan-replacement analogues displaying 20- to 100-fold parasite selectivity.<sup>309</sup>

FK228 (**45**) which was discovered from a fermentation broth of *Chromobacterium violaceum*,<sup>310</sup> differs structurally from other constituents of the cyclic peptide class. FK228 contains a unique bicyclic structure with four amino acids and a  $\beta$ -hydroxyamide moiety, which collectively form a 16-membered lactone with a disulfide bridge. FK228 (Romidepsin) is currently the only member of the cyclic peptide class in clinical trials (phase III).



45: Depsipeptide

Cyclic peptides comprise a diverse class of HDAC inhibitors possessing modes of enzyme inactivation ranging from reversible to irreversible inhibition.

This class of HDAC inhibitors has aided in the understanding of the factors governing HDAC inhibitor activity and selectivity. Further investigations probing binding interactions on the outer rim of the HDAC enzymes will hopefully lead to a greater understanding of essential inhibitor-enzyme contacts and ultimately to the identification of selective inhibitors with more druglike qualities.

#### 14.6. Thiol based inhibitors.

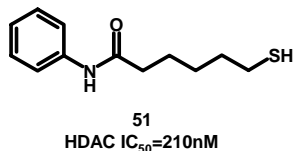
In the search for a suitable hydroxamic acid replacement, thiols seemed to be reasonable targets, because they have been reported to inhibit zinc-dependent enzymes such as angiotensin converting enzyme (ACE) and matrix metalloproteinase (MMPs).

Recently, Furumai *et al.* demonstrated that the disulfide bond of FK228 (**45**), a cyclic peptide HDAC inhibitor, is reduced in the cellular environment, releasing the free thiol analogue as the active species.<sup>311</sup>

Prompted by these data, T. Suzuki *et al.* synthesized thiol-based SAHA analogues.<sup>312</sup>



Compound **51**, in which the hydroxamic acid of SAHA was replaced by a thiol, was found to be as potent as SAHA.



They shown that the potency is related to chain length, and the amide and reversed amide were preferred as the group attaching the phenyl moiety. The conversion of the phenyl group of compound **51** to other aromatic groups led to the identification of inhibitors more potent than SAHA. The SAR results within the thiol series indicate that thiols inhibit HDACs in a manner similar to that of hydroxamates.

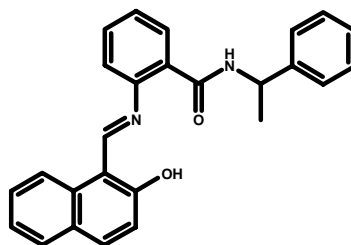
### ***15. Sirtuins' Inhibitors.***

To date, only a few molecules have been discovered as inhibitors of sirtuins.

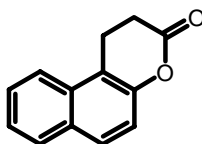
Among them, the so called sirtinol (Sir two inhibitor naph

) was identified by a high throughput phenotypic screening in cells.<sup>313</sup>

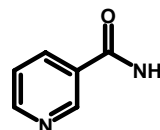
The splitomicin was discovered by screening of other libraries,<sup>314</sup> and last but not least the vitamin nicotinamide was recognized able to inhibit the sirtuins without competing with NAD<sup>+</sup>.<sup>163</sup>



Sirtinol



Splitomicina



Nicotinamide

### ***16. Research project.***

A large number of natural and synthetic class I/II HDAC inhibitors have been reported so far, and the majority of them do not discriminate between the different classes of enzymes.<sup>315-322</sup> The only exceptions are sodium valproate (VPA),<sup>323</sup> some 2'-aminoanilides (such as MS-275,<sup>324,325</sup> histacin,<sup>326</sup> and pimeloyl-anilide orthoaminoanilide (PAOA)<sup>326</sup> a few cinnamyl hydroxamates (SK-7041 and SK-7068),<sup>327</sup> and depsipeptide FK-228,<sup>328</sup> which are class I-selective HDAC inhibitors. Trapoxins (TPXs), cyclic hydroxamic acidcontaining peptide 1 (CHAP1), and sodium butyrate (NaB) are ineffective in inhibiting HDAC6,<sup>329,330</sup> whereas tubacin<sup>331-333</sup> and some aryloxopropenyl-pyrrolyl hydroxyamides<sup>334</sup> are class IIb- and class II (IIa)-selective HDAC inhibitors, respectively (Figure 28).

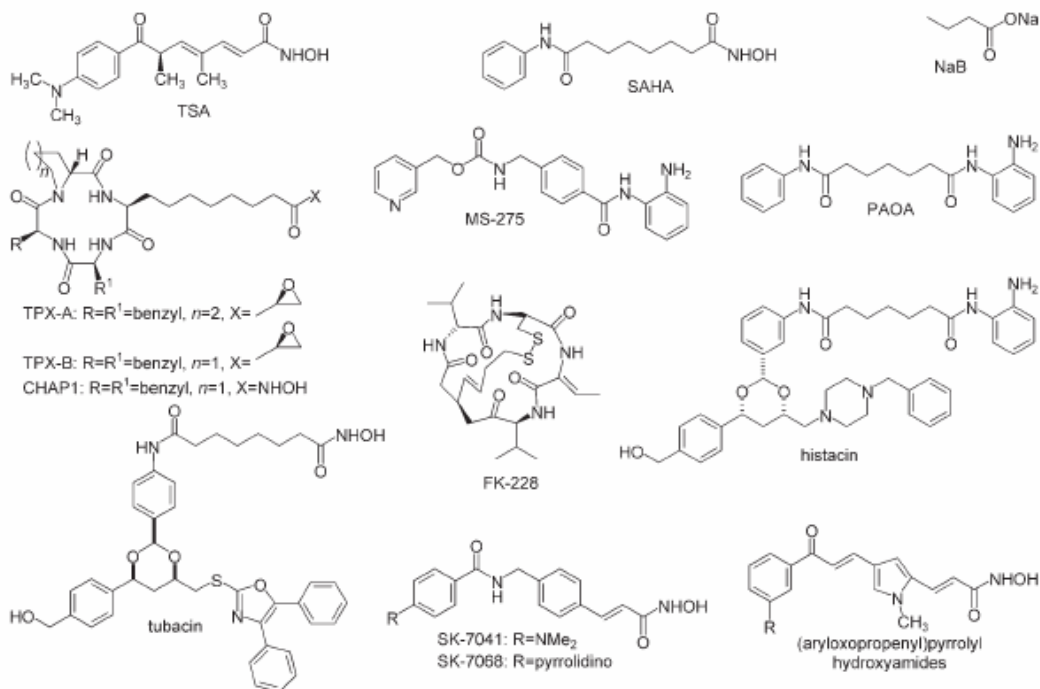


**Figure 28.** Structures of known HDAC inhibitors.

According to these findings, we undertook synthetic and biological efforts to improve the HDAC inhibitory activity of the aroyl-pyrrolyl hydroxyamides (APHAs) recently reported by us (Figure 29).<sup>335-339</sup>

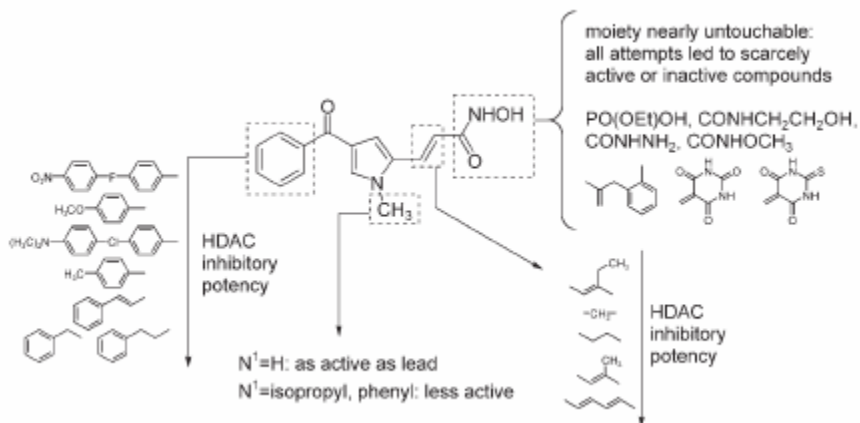


**Figure 29.** Structure–activity relationship (SAR) summary of aroyl-pyrrolyl hydroxyamides (APHAs).

Starting from the first lead compound, 3-(4-benzoyl-1-methyl-1H-pyrrol-2-yl)-Nhydroxy-2-propenamide (1) (Figure 30),<sup>335,336</sup> we performed some chemical modifications on the structure of 1 to increase its anti-HDAC activity. Among the modifications described, only the insertion of a phenylacetyl/phenylpropionyl moiety at the C4 position of the pyrrole ring led to an improved anti-HDAC potency of the inhibitors, affording compounds 2 and 3 (Figure 30).<sup>337,338</sup> Furthermore, 2 and 3 were tested against maize HD1-B<sup>340,341</sup> and HD1-A,<sup>342,343</sup> two mammalian class I and class II HDAC homologues, to explore their potential class-selectivity. In these tests, 2 and 3 showed similar activities (2: IC<sub>50</sub>(HD1-B)= 150 nM, IC<sub>50</sub>(HD1-A)=50 nM; 3: IC<sub>50</sub>(HD1-B)=120 nM, IC<sub>50</sub>(HD1-A)= 60 nM), with 2 having higher selectivity for class II than 3 (selectivity for class II HDACs: 2, 3-fold; 3, 2-fold). Compounds 2 and 3 showed similar antiproliferative and cytodifferentiation properties in assays with Friends murine erythroleukemia (MEL) cells.<sup>338</sup>

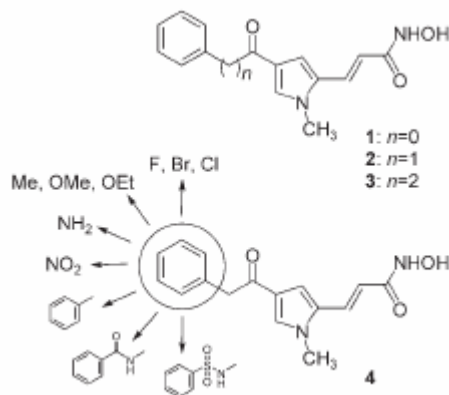
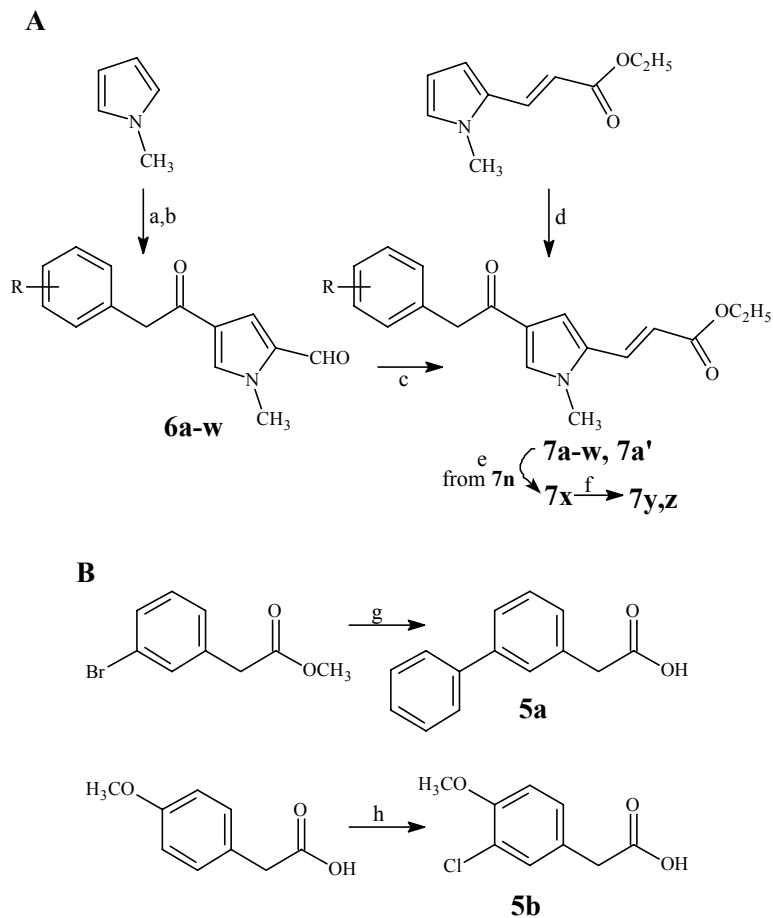


**Figure 30.** APHA lead compounds and new designed derivatives.

### 16.1. First lead optimization.

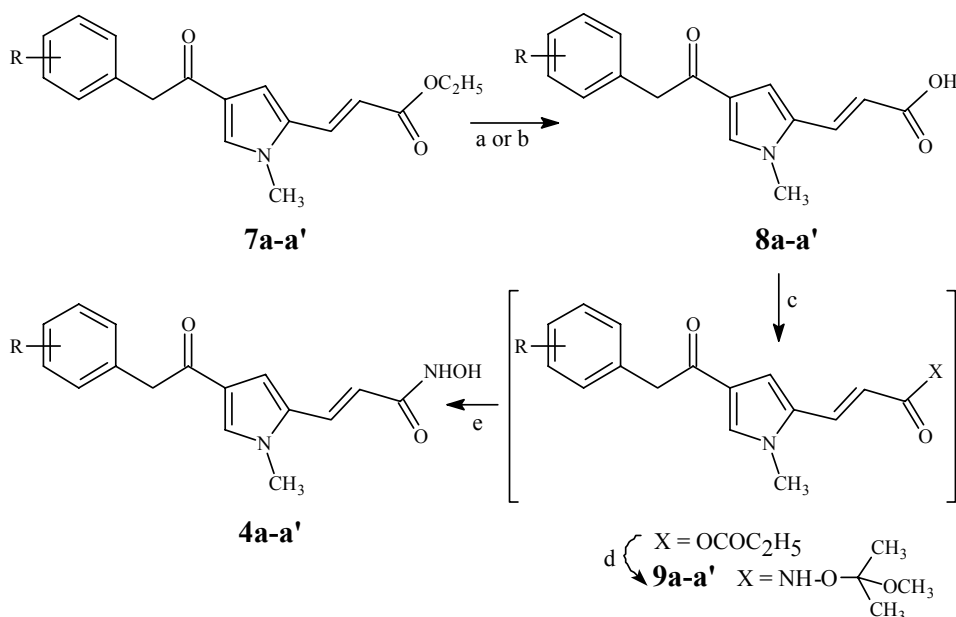
As 2 and 3 showed similar behaviors both *in vitro* and *in vivo*, we chose the phenylacetylpyrrolyl hydroxypropenamido template of 2 for chemical investigation. In particular, we introduced various substituents ranging between electron-donating and electron-withdrawing groups, in the ortho, meta, or para positions of the benzene ring (compounds 4, Figure 30). The influence of such insertions on the inhibitory activities toward HD2 as well as HD1-B and HD1-A was evaluated, and the potential class-selectivity of the novel derivatives was assessed. Selected title compounds 4b,k were tested against mouse HDAC1 in comparison with 2 and SAHA. Homology models, molecular modeling, and docking studies were performed on the most selective derivatives against HD1-B (compound 4u) and HD1-A (compound 4t), to gain insight about their binding mode. Finally, the most potent compound, 4b, was evaluated as an antiproliferative and cytodifferentiation agent in human acute promyelocytic leukemia HL-60 cells.

16.2. Chemistry.



**Scheme 1.** a) Oxalyl chloride, DMF, RT; b) 1. R-Ph-CH<sub>2</sub>COCl, AlCl<sub>3</sub>, 1,2-dichloroethane, RT, 2. KOH, H<sub>2</sub>O, RT; c) (C<sub>2</sub>H<sub>5</sub>O)<sub>2</sub>OPCH<sub>2</sub>COOC<sub>2</sub>H<sub>5</sub>, K<sub>2</sub>CO<sub>3</sub>, C<sub>2</sub>H<sub>5</sub>OH, 80°C; d) **5b**, SOCl<sub>2</sub>, AlCl<sub>3</sub>, 1,2-dichloroethane, RT; e) NaHPO<sub>2</sub>, K<sub>2</sub>CO<sub>3</sub>, Pd/C, THF/H<sub>2</sub>O, RT; f) benzoyl chloride or benzenesulfonyl chloride, (C<sub>2</sub>H<sub>5</sub>)<sub>3</sub>N, dichloromethane, RT; g) 1. phenylboronic acid, Na<sub>2</sub>CO<sub>3</sub>,

tetrakis(triphenylphosphine) palladium, Ph-CH<sub>3</sub>/C<sub>2</sub>H<sub>5</sub>OH, 80°C, 2. KOH, H<sub>2</sub>O, RT; h) potassium peroxymonosulfate (oxone), NaCl, acetone/H<sub>2</sub>O, RT.



**Scheme 2.** a) KOH, C<sub>2</sub>H<sub>5</sub>OH, H<sub>2</sub>O, 70°C; b) LiOH, H<sub>2</sub>O, RT; c) ClCOOC<sub>2</sub>H<sub>5</sub>, (C<sub>2</sub>H<sub>5</sub>)<sub>3</sub>N, THF, 0°C; d) NH<sub>2</sub>OC(CH<sub>3</sub>)<sub>2</sub>OCH<sub>3</sub>, RT; e) Amberlyst 15, CH<sub>3</sub>OH, RT.

Ethyl 3-[1-methyl-4-(substituted)phenylacetyl-1H-pyrrol-2-yl]-2-propenoates **7a-w**, key intermediates for the synthesis of the hydroxamates **4**, were prepared by the one-pot Vilsmeier-Haack/Friedel-Crafts reaction performed on 1-methyl-1H-pyrrole with oxalyl chloride/*N,N*-dimethylformamide and (substituted) phenylacetyl chloride/aluminum trichloride, followed by Wittig-Horner reaction of the obtained aroyl-pyrrolecarboxaldehydes **6a-w** with triethylphosphonoacetate and potassium carbonate (Scheme 1 a). 3-Ethoxyphenylacetic acid, useful for the synthesis of the pyrrolealdehyde **6r**, was prepared as

reported.<sup>344</sup> A Suzuki coupling reaction between methyl 3-bromophenylacetate and phenylboronic acid in the presence of tetrakis(triphenylphosphine)palladium and sodium carbonate followed by alkaline hydrolysis afforded, with a simple twostep method, the 3-biphenylacetic acid **5a**,<sup>345</sup> which was used for the synthesis of **6t** (Scheme 1 b). A single-step, high-yielding reaction of 4-methoxyphenylacetic acid with potassium peroxymonosulfate (oxone) and sodium chloride led to the 3-chloro-4-methoxyphenylacetic acid **5b**<sup>346</sup> (Scheme 1 b), which was useful in the preparation of the ethyl 3-[4-(3-chloro-4-methoxyphenylacetyl)-1-methyl-1H-pyrrol-2-yl]-2-propenoate **7a'**. Such compounds, the preparation of which failed with the Vilsmeier–Haack/Friedel–Crafts procedure, was obtained by acylation of ethyl (1-methyl-1H-pyrrol-2-yl)-2-propenoate<sup>347</sup> with aluminum trichloride and 3-chloro-4-methoxyphenylacetyl chloride (Scheme 1 a). Ethyl 3-[4-(3-benzoylamino- and 3-benzenesulfonylamino)phenylacetyl)-1-methyl-1H-pyrrol-2-yl]-2-propenoates **7y,z** were prepared by the reaction of benzoyl chloride or benzenesulfonyl chloride with ethyl 3-[4-(3-aminophenylacetyl)-1-methyl-1H-pyrrol-2-yl]-2-propenoate **7x**, previously obtained by reduction of the 3-nitro analogue **7n** with sodium hypophosphite and potassium carbonate (Scheme 1 a). Alkaline hydrolysis of the ethyl pyrrole-propenoates **7a–a'** furnished the pyrrole-propenoic acids **8a–a'**, which were in turn converted into the corresponding hydroxamates **4a–a'** through reaction with ethyl chloroformate and O-(2-methoxy-2-propyl)hydroxylamine,<sup>348</sup> followed by acid hydrolysis of the N-(1-methoxy-1-methylethoxy)propenamides **9a–a'** with the Amberlyst 15 ion-exchange resin (Scheme 2). The O-protected hydroxamates **9** were hydrolyzed without further purification as soon as they were obtained.

Chemical and physical data for compounds **4a–a'** are listed in Table 1. Chemical and physical data for the intermediate compounds **5–8** are listed in Table 2.



**Table 1.** Chemical and physical data for compounds **4a–a'**.

compound	R	mp, ° C	recrystallization solvent	% yield
<b>4a</b>	2-Cl	> 250	acetonitrile	58
<b>4b</b>	3-Cl	162-163	benzene/acetonitrile	52
<b>4c</b>	4-Cl	175-177	acetonitrile	66
<b>4d</b>	2-F	188-190	benzene/acetonitrile	54
<b>4e</b>	3-F	199-201	acetonitrile/benzene	57
<b>4f</b>	4-F	178-179	benzene/acetonitrile	68
<b>4g</b>	2-Br	180-182	benzene/acetonitrile	49
<b>4h</b>	3-Br	163-165	benzene/acetonitrile	55
<b>4i</b>	4-Br	153-154	benzene/acetonitrile	64
<b>4j</b>	2-Me	> 250	acetonitrile	52
<b>4k</b>	3-Me	210-212	acetonitrile/benzene	57
<b>4l</b>	4-Me	>250	acetonitrile	54
<b>4m</b>	2-NO <sub>2</sub>	180-182	benzene/acetonitrile	45
<b>4n</b>	3-NO <sub>2</sub>	228-230	acetonitrile	58
<b>4o</b>	4-NO <sub>2</sub>	118-120	benzene/acetonitrile	59
<b>4p</b>	3-OMe	148-150	benzene/acetonitrile	43
<b>4q</b>	4-OMe	178-180	benzene/acetonitrile	56
<b>4r</b>	3-OEt	100-102	benzene	48
<b>4s</b>	4-OEt	190-192	benzene/acetonitrile	44
<b>4t</b>	3-Ph	117-118	benzene	42
<b>4u</b>	4-Ph	199-201	benzene/acetonitrile	58
<b>4v</b>	3,5-Me <sub>2</sub>	194-196	acetonitrile/ethanol	58

Design, synthesis and biological validation of epigenetic modulators of histone/protein deacetylation and methylation.

<b>4w</b>	3,5-F <sub>2</sub>	143-145	benzene/acetonitrile	56
<b>4x</b>	3-NH <sub>2</sub>	201-202	benzene/acetonitrile	53
<b>4y</b>	3-NHCOPh	222-225	benzene/acetonitrile	40
<b>4z</b>	3-NHSO <sub>2</sub> Ph	75-77	diethyl ether	42
<b>4a'</b>	3-Cl-4-OMe	100-102	diethyl ether	55

**Table 2.** Chemical and physical data for compounds **5-8**.

compound	R	mp, ° C	recrystallization solvent	% yield
<b>5a</b>		141-143	benzene/cyclohexane	84
<b>5b</b>		98-100	benzene/cyclohexane	90
<b>6a</b>	2-Cl	101-102	benzene/cyclohexane	56
<b>6b</b>	3-Cl	86-88	diethyl ether	41
<b>6c</b>	4-Cl	110-111	benzene	57
<b>6d</b>	2-F	89-91	cyclohexane/benzene	65
<b>6e</b>	3-F	48-50	diethyl ether	70
<b>6f</b>	4-F	85-87	benzene/cyclohexane	83
<b>6g</b>	2-Br	94-95	benzene/cyclohexane	54
<b>6h</b>	3-Br	104-105	benzene/cyclohexane	64
<b>6i</b>	4-Br	128-130	benzene/cyclohexane	72
<b>6j</b>	2-Me	111-112	cyclohexane	42
<b>6k</b>	3-Me	54-55	cyclohexane	58
<b>6l</b>	4-Me	110-111	benzene/cyclohexane	90
<b>6m</b>	2-NO <sub>2</sub>	134-136	benzene	38
<b>6n</b>	3-NO <sub>2</sub>	126-128	benzene/cyclohexane	87
<b>6o</b>	4-NO <sub>2</sub>	135-136	benzene/cyclohexane	76
<b>6p</b>	3-OMe	88-90	benzene/cyclohexane	58
<b>6q</b>	4-OMe	149-151	benzene/cyclohexane	66
<b>6r</b>	3-OEt	94-95	cyclohexane	42
<b>6s</b>	4-OEt	125-127	benzene/cyclohexane	53

*Design, synthesis and biological validation of epigenetic modulators of histone/protein deacetylation and methylation.*

---

<b>6t</b>	4-Ph	78-80	diethyl ether	41
<b>6u</b>	3,5-Me <sub>2</sub>	oil		62
<b>6v</b>	3,5-F <sub>2</sub>	146-147	benzene/cyclohexane	57
<b>7a</b>	2-Cl	209-210	benzene/cyclohexane	42
<b>7b</b>	3-Cl	oil		95
<b>7c</b>	4-Cl	oil		73
<b>7d</b>	2-F	95-97	benzene/cyclohexane	88
<b>7e</b>	3-F	oil		86
<b>7f</b>	4-F	93-94	benzene/cyclohexane	91
<b>7g</b>	2-Br	99-101	benzene/cyclohexane	75
<b>7h</b>	3-Br	111-112	benzene/cyclohexane	79
<b>7i</b>	4-Br	136-137	benzene/cyclohexane	89
<b>7j</b>	2-Me	124-126	benzene/acetonitrile	68
<b>7k</b>	3-Me	80-82	cyclohexane	77
<b>7l</b>	4-Me	54-56	cyclohexane	95
<b>7m</b>	2-NO <sub>2</sub>	94-96	diethyl ether	81
<b>7n</b>	3-NO <sub>2</sub>	128-130	benzene/cyclohexane	87
<b>7o</b>	4-NO <sub>2</sub>	129-131	benzene/cyclohexane	78
<b>7p</b>	3-OMe	91-93	benzene	60
<b>7q</b>	4-OMe	85-87	diethyleter	72
<b>7r</b>	3-OEt	99-100	benzene/cyclohexane	67
<b>7s</b>	4-OEt	73-75	cyclohexane	63

---

---

<b>7t</b>	3-Ph	oil		45
<b>7u</b>	4-Ph	130-132	benzene/cyclohexane	74
<b>7v</b>	3,5-Me <sub>2</sub>	oil		59
<b>7w</b>	3,5-F <sub>2</sub>	154-156	benzene	63
<b>7x</b>	3-NH <sub>2</sub>	oil		63
<b>7y</b>	3- NHCOPh	oil		53
<b>7z</b>	3- NHSO <sub>2</sub> Ph	oil		59
<b>7a'</b>	3-Cl-4- OMe	104-105	benzene/cyclohexane	67
<b>8a</b>	2-Cl	210-212	benzene/cyclohexane	74
<b>8b</b>	3-Cl	195-196	acetonitrile	65
<b>8c</b>	4-Cl	207-209	acetonitrile	74
<b>8d</b>	2-F	185-187	benzene/acetonitrile	78
<b>8e</b>	3-F	105-107	benzene	67
<b>8f</b>	4-F	169-171	benzene/cetonitrile	73
<b>8g</b>	2-Br	210-211	benzene/acetonitrile	81
<b>8h</b>	3-Br	209-210	benzene/acetonitrile	84
<b>8i</b>	4-Br	178-180	benzene/acetonitrile	87
<b>8j</b>	2-Me	204-205	acetonitrile	75
<b>8k</b>	3-Me	160-161	acetonitrile	79
<b>8l</b>	4-Me	189-190	acetonitrile	77
<b>8m</b>	2-NO <sub>2</sub>	230-232	benzene/acetonitrile	68
<b>8n</b>	3-NO <sub>2</sub>	260-262	acetonitrile	85

---

*Design, synthesis and biological validation of epigenetic modulators of histone/protein deacetylation and methylation.*

<b>8o</b>	4-NO <sub>2</sub>	210-212	benzene/acetonitrile	76
<b>8p</b>	3-OMe	150-152	benzene	69
<b>8q</b>	4-OMe	174-176	benzene/acetonitrile	72
<b>8r</b>	3-OEt	102-103	benzene	74
<b>8s</b>	4-OEt	178-180	benzene/acetonitrile	83
<b>8t</b>	3-Ph	135-136	benzene/acetonitrile	80
<b>8u</b>	4-Ph	190-192	benzene/acetonitrile	73
<b>8v</b>	3,5-Me <sub>2</sub>	81-83	diethyl ether	87
<b>8w</b>	3,5-F <sub>2</sub>	238-239	benzene/acetonitrile	81
<b>8x</b>	3-NH <sub>2</sub>	182-183	benzene	64
<b>8y</b>	3- NHCOPh	182-183	benzene	75
<b>8z</b>	3- NHSO <sub>2</sub> Ph	81-83	diethyl ether	87
<b>8a'</b>	3-Cl-4- OMe	239-240	acetonitrile	62

### 16.3 Experimental Section.

*Chemistry.* Melting points were determined on a Büchi 530 melting point apparatus and are uncorrected. Infrared (IR) spectra (KBr) were recorded on a Perkin-Elmer Spectrum One instrument. <sup>1</sup>H NMR spectra were recorded at 200 MHz on a Bruker AC 200 spectrometer; chemical shifts are reported in  $\delta$  (ppm) units relative to the internal reference tetramethylsilane (Me<sub>4</sub>Si). All compounds were routinely checked by TLC and <sup>1</sup>H NMR. TLC was performed on aluminum-backed silica gel plates (Merck DC-Alufolien Kieselgel 60 F<sub>254</sub>) with spots visualized by UV light. All solvents were reagent grade and, when necessary, were purified and dried by standard methods. Concentration of solutions after reactions and extractions involved the use of a rotary evaporator operating at a reduced pressure of *ca.* 20 Torr. Organic solutions were dried over anhydrous sodium sulfate. Analytical results are within  $\pm 0.40\%$  of the theoretical values. A SAHA sample for biological assays was prepared as previously reported by us.<sup>349</sup> All chemicals were purchased from Aldrich Chimica, Milan (Italy) or Lancaster Synthesis GmbH, Milan (Italy) and were of the highest purity.

**3-Biphenylacetic acid (5a).** To a mixture of phenylboronic acid (13.4 mmol; 1.6 g) and methyl 3-bromophenylacetate (13.4 mmol, 3.1 g) dissolved in toluene/ethanol (70 mL/6 mL) an aqueous solution of 2 M sodium carbonate (28.2 mmol; 3.0 g dissolved in 14 mL of water) was added. After the resulting mixture was degassed for 10 min by nitrogen, tetrakis(triphenylphosphine)palladium (0.7 mmol, 0.8 g) was added, and the reaction was heated at 80 °C for 16 h. After, it was cooled until room temperature, the suspension was filtered and the solvent was evaporated under reduced pressure. The residue was partitioned between water (50 mL) and ethyl acetate (50 mL), the organic layer was separated, and the aqueous one was extracted with ethyl acetate (2 x 50 mL). The organic layer was washed with brine (3 x 50 mL), dried, and concentrated in vacuo. The residue was purified by column chromatography on silica gel by eluting with ethyl acetate:chloroform 1:1. The crude methyl 3-biphenylacetate was then dissolved in ethanol and treated with 2 N KOH (26.9 mmol, 1.5 g, 13.5 mL). After being stirred at room temperature for 5 h, the solution was poured into water (100 mL), and extracted with ethyl acetate (2 x 50 mL). To the aqueous layer, a sample of 2 N HCl was added until the pH was 2, and the precipitate was filtered and purified by crystallization. <sup>1</sup>H NMR (CDCl<sub>3</sub>)  $\delta$  3.42 (s, 2 H, CH<sub>2</sub>), 7.05 (m, 1 H, benzene H-4'), 7.17 (m,

1 H, benzene H-6), 7.30 (m, 5 H, benzene H-5,2',3',5',6'), 7.47 (m, 2 H, benzene H-2,4), 8.55 (bs, 1 H, OH). Anal. (C<sub>14</sub>H<sub>12</sub>O<sub>2</sub>) C, H.

**3-Chloro-4-methoxyphenylacetic acid (5b).** To a solution of 4-methoxyphenylacetic acid (12.0 mmol; 2.0 g) dissolved in acetone (20 mL) potassium peroxydisulfate (OXONE<sup>®</sup>) (12.0 mmol; 7.4 g) was added, and the suspension was stirred at room temperature for 15 min. Afterward, sodium chloride solution (48.1 mmol; 2.8 g in 20 mL of water) was added, and the resulting mixture was stirred for 6 h. When the reaction was finished (TLC control: SiO<sub>2</sub>/ethyl acetate), the solvent was evaporated under reduced pressure, and the residue was diluted with water (100 mL), and extracted with ethyl acetate (3 x 50 mL). The organic layer was washed with sodium chloride solution (3 x 50 mL), dried, and concentrated. The residue was a solid that was recrystallized by cyclohexane/benzene. <sup>1</sup>H NMR (CDCl<sub>3</sub>) δ 3.56 (s, 2 H, CH<sub>2</sub>), 3.87 (s, 3 H, CH<sub>3</sub>), 6.88 (m, 1 H, benzene H-5), 7.14 (m, 1 H, benzene H-6), 7.30 (m, 1 H, benzene H-2), 9.00 (bs, 1 H, OH). Anal. (C<sub>9</sub>H<sub>9</sub>ClO<sub>3</sub>) C, H, Cl.

**General Procedure for the Synthesis of 4-Aroyl-1-methyl-1H-pyrrole-2-carboxaldehydes 6a-w. Example: 4-(4'-Methylphenylacetyl)-1-methyl-1H-pyrrole-2-carboxaldehyde (6l).** A 1,2-dichloroethane (20 mL) solution of oxalyl chloride (18.4 mmol, 1.4 mL) was added to a cooled (0-5 °C) solution of *N,N*-dimethylformamide (18.4 mmol, 1.6 mL) in 1,2-dichloroethane (20 mL) over a period of 5-10 min. After being stirred at room temperature for 15 min, the suspension was cooled (0-5 °C) again and treated with a solution of 1-methyl-1H-pyrrole (18.4 mmol, 1.5 g) in 1,2-dichloroethane (20 mL). The mixture was stirred at room temperature for 15 min, and then was treated with aluminum trichloride (40.6 mmol, 5.4 g) and 4-tolylacetyl chloride (previously prepared by heating the corresponding acid (18.4 mmol, 2.8 g) with SOCl<sub>2</sub> (20 mL) for 1 h at 50 °C). After 3 h, the reaction mixture was poured onto crushed ice (100 g) containing 50% NaOH (20 mL) and stirred for 10 min. The pH of the solution was adjusted to 4 with 37% HCl, the organic layer was separated, and the aqueous one was extracted with chloroform (2 x 20 mL). The combined organic solutions were washed with water (3 x 50 mL), dried, and evaporated to dryness. The residual oil was purified by column chromatography on silica gel eluting with ethyl acetate:chloroform 1:5. The obtained solid was recrystallized from cyclohexane/benzene to give pure **6l**. <sup>1</sup>H NMR (CDCl<sub>3</sub>) δ 2.27 (s, 3 H, PhCH<sub>3</sub>), 3.90 (s, 3 H, NCH<sub>3</sub>), 3.96 (s, 2 H, PhCH<sub>2</sub>CO), 7.10 (dd, 4 H, benzene H),



7.27 (m, 1 H, pyrrole  $\beta$ -proton), 7.39 (m, 1 H, pyrrole  $\alpha$ -proton), 9.54 (s, 1 H, CHO). Anal. (C<sub>15</sub>H<sub>15</sub>NO<sub>2</sub>) C, H, N.

**General Procedure for the Synthesis of Ethyl 3-(4-Aroyl-1-methyl-1*H*-pyrrol-2-yl)-2-propenoates 7a-w. Example: Ethyl 3-[4-(3'-methoxyphenylacetyl)-1-methyl-1*H*-pyrrol-2-yl]-2-propenoate (7p).** A suspension of **6p** (1.7 mmol, 0.6 g) in absolute ethanol (20 mL) was added in one portion to a mixture of triethyl phosphonoacetate (2.1 mmol, 0.4 mL) and anhydrous potassium carbonate (3.5 mmol, 0.5 g). After being stirred at 70 °C for 2 h, the reaction mixture was cooled to room temperature, diluted with water (50 mL), and extracted with ethyl acetate (3 x 50 mL). The organic layer was washed with water, dried, and evaporated to dryness, and the solid residue was recrystallized to furnish pure **7p**. <sup>1</sup>H NMR (CDCl<sub>3</sub>)  $\delta$  1.36 (t, 3 H, COOCH<sub>2</sub>CH<sub>3</sub>), 3.74 (s, 3 H, NCH<sub>3</sub>), 3.81 (s, 3 H, OCH<sub>3</sub>), 4.01 (s, 2 H CH<sub>2</sub>CO), 4.27 (q, 2 H, COOCH<sub>2</sub>CH<sub>3</sub>), 6.25 (d, 1 H, CH=CHCO), 6.90 (m, 3 H, benzene H-2,4,6), 7.10 (m, 1 H, pyrrole  $\beta$ -proton), 7.26 (m, 1 H, benzene H-5), 7.40 (m, 1 H, pyrrole  $\alpha$ -proton), 7.55 (d, 1 H, CH=CHCO). Anal. (C<sub>19</sub>H<sub>21</sub>NO<sub>4</sub>) C, H, N.

**Ethyl 3-[4-(3'-aminophenylacetyl)-1-methyl-1*H*-pyrrol-2-yl]-2-propenoate (7x).** Potassium carbonate (4.1 mmol, 0.6 g) and 10% palladium on carbon (20 mg) were slowly added to a solution of ethyl 3-[4-(3'-nitrophenylacetyl)-1-methyl-1*H*-pyrrol-2-yl]-2-propenoate **7n** (5.8 mmol, 2.0 g) in a mixture of water (4 mL) and THF (5 mL). After being stirred at room temperature for 10 min, a solution of sodium hypophosphite (22.2 mmol, 2.4 g) in water (30 mL) was added. After stirring at room temperature for 2 h, the reaction mixture was filtered, the organic layer was separated, and the aqueous one was extracted with ethyl acetate (3 x 50 mL). The combined organic solution was washed with water (2 x 100 mL), dried, and evaporated to dryness. The residual oil was purified through column chromatography on silica gel by eluting with a 1:1 mixture of ethyl acetate and chloroform. Compound **7x** was obtained as pure oil. <sup>1</sup>H NMR (CDCl<sub>3</sub>)  $\delta$  1.30 (t, 3 H, COOCH<sub>2</sub>CH<sub>3</sub>), 3.72 (s, 3 H, NCH<sub>3</sub>), 3.90 (s, 2 H CH<sub>2</sub>CO), 4.24 (q, 2 H, COOCH<sub>2</sub>CH<sub>3</sub>), 6.25 (d, 1 H, CH=CHCO), 6.64 (m, 2 H, NH<sub>2</sub>), 6.70 (m, 4 H, benzene H-2,4,6 and pyrrole  $\beta$ -proton), 7.09 (m, 1 H, benzene H-5), 7.36 (m, 1 H, pyrrole  $\alpha$ -proton), 7.49 (d, 1 H, CH=CHCO). Anal. (C<sub>18</sub>H<sub>20</sub>N<sub>2</sub>O<sub>3</sub>) C, H, N.

**General Procedure for the Synthesis of Ethyl 3-[4-(3'-benzoyl- and -benzenesulfonylamino)phenylacetyl]-1-methyl-1*H*-pyrrol-2-yl]-2-propenoates 7<sub>y,z</sub>.**

**Example: Ethyl 3-[4-(3'-benzenesulfonylamino)phenylacetyl]-1-methyl-1*H*-pyrrol-2-yl]-2-propenoate (7<sub>z</sub>).** Benzenesulfonyl chloride (6.8 mmol, 2.1 g) and triethylamine (10.2 mmol, 1.4 mL) were added to a solution of 3-[4-(3'-aminophenylacetyl)-1-methyl-1*H*-pyrrol-2-yl]-2-propenoate (7<sub>x</sub>) (6.8 mmol, 2.1 g) in dichloromethane (20 mL). After being stirred at room temperature for 1 h, the reaction mixture was poured into water (50 mL), the organic layer was separated, and the aqueous one was extracted with chloroform (2 x 50 mL). The combined organic solution was washed with water (100 mL) and brine (100 mL), and was dried and evaporated to dryness. The residual oil was purified through column chromatography on silica gel by eluting with a 1:1 mixture of ethyl acetate and chloroform. Compound 7<sub>z</sub> was obtained as pure oil. <sup>1</sup>H NMR (CDCl<sub>3</sub>) δ 1.28 (t, 3 H, COOCH<sub>2</sub>CH<sub>3</sub>), 3.72 (s, 3 H, NCH<sub>3</sub>), 3.90 (s, 2 H CH<sub>2</sub>CO), 4.20 (q, 2 H, COOCH<sub>2</sub>CH<sub>3</sub>), 6.25 (d, 1 H, CH=CHCO), 6.90-7.95 (m, 12 H, pyrrole protons, benzene protons, and CH=CHCO). Anal. (C<sub>24</sub>H<sub>24</sub>N<sub>2</sub>O<sub>5</sub>S) C, H, N, S.

**Ethyl 3-[4-(3'-chloro-4'-methoxyphenylacetyl)-1-methyl-1*H*-pyrrol-2-yl]-2-propenoate (7<sub>a'</sub>).** Aluminum trichloride (15.0 mmol, 2.0 g) was slowly added to a cooled (0-5 °C) solution of ethyl (1-methyl-1*H*-pyrrol-2-yl)-2-propenoate<sup>[53]</sup> (7.5 mmol, 1.3 g) and 3-chloro-4-methoxyphenylacetyl chloride (previously prepared by heating 5<sub>b</sub> (15.0 mmol, 3.0 g) with SOCl<sub>2</sub> (20 mL) for 1 h at 50 °C) in 1,2-dichloroethane (100 mL). After being stirred at room temperature for 30 min, the reaction mixture was poured onto crushed ice (100 g) and the pH of the solution was adjusted to 4 with 37% HCl. The organic layer was separated, and the aqueous one was extracted with chloroform (3 x 50 mL). The combined organic solution was washed with water (100 mL), dried and evaporated to dryness. The residual oil was purified through column chromatography on silica gel by eluting with a 1:20 mixture of ethyl acetate and chloroform. Compound 7<sub>a'</sub> was obtained as pure solid. <sup>1</sup>H NMR (CDCl<sub>3</sub>) δ 1.32 (t, 3 H, COOCH<sub>2</sub>CH<sub>3</sub>), 3.71 (s, 3 H, NCH<sub>3</sub>), 3.87 (s, 3 H, OCH<sub>3</sub>), 3.93 (s, 2 H CH<sub>2</sub>CO), 4.25 (q, 2 H, COOCH<sub>2</sub>CH<sub>3</sub>), 6.25 (d, 1 H, CH=CHCO), 6.88 (m, 1 H, benzene H-5), 7.03 (m, 1 H, pyrrole β-proton), 7.13 (m, 2 H, benzene H-6), 7.30 (m, 1 H, benzene H-2), 7.35 (m, 1 H, pyrrole α-proton), 7.52 (d, 1 H, CH=CHCO). Anal. (C<sub>19</sub>H<sub>20</sub>ClNO<sub>4</sub>) C, H, Cl, N.

**General Procedure for the Synthesis of 3-(4-Aroyl-1-methyl-1H-pyrrol-2-yl)-2-propenoic Acids 8a-a'. Example: 3-[4-(4'-Chlorophenylacetyl)-1H-pyrrol-2-yl]-2-propenoic acid (8c).** A mixture of **7c** (4.3 mmol, 1.4 g), 2 N KOH (17.2 mmol, 1.0 g, 8.6 mL), and ethanol (15 mL) was stirred at room temperature overnight. Afterward, the solution was poured into water (50 mL) and extracted with ethyl acetate (3 x 20 mL). A sample of 2 N HCl was added to the aqueous layer until the pH was 5, and the obtained precipitate was filtered and recrystallized from benzene/acetonitrile to give the pure compound **8c**. <sup>1</sup>H NMR (DMSO-*d*<sub>6</sub>) δ 3.70 (s, 3 H, NCH<sub>3</sub>), 3.98 (s, 2 H, CH<sub>2</sub>CO), 6.25 (d, 1 H, CH=CHCO), 7.28 (m, 6 H, benzene and pyrrole protons), 7.40 (d, 1 H, CH=CHCO), 12.10 (bs, 1 H, OH). Anal. (C<sub>16</sub>H<sub>14</sub>ClNO<sub>3</sub>) C, H, Cl, N.

**General Procedure for the Synthesis of 3-(4-Aroyl-1-methyl-1H-pyrrol-2-yl)-N-hydroxy-2-propenamides 4a-a'. Example: 3-[4-(2'-Fluorophenylacetyl)-1-methyl-1H-pyrrol-2-yl]-N-hydroxy-2-propenamide (4d).** Ethyl chloroformate (1.9 mmol, 0.2 mL) and triethylamine (2.0 mmol, 0.3 mL) were added to a cooled (0 °C) solution of **3d** (1.6 mmol, 0.5 g) in dry THF (10 mL), and the mixture was stirred for 10 min. The solid was filtered off, and *O*-(2-methoxy-2-propyl)hydroxylamine (4.7 mmol, 0.4 mL)<sup>[54]</sup> was added to the filtrate. The solution was stirred for 15 min at 0 °C, then was evaporated under reduced pressure, and the residue was diluted in methanol (10 mL). Amberlyst<sup>®</sup> 15 ion-exchange resin (0.2 g) was added to the solution of the *O*-protected hydroxamate, and the mixture was stirred at 45 °C for 1 h. Afterward, the reaction was filtered and the filtrate was concentrated in vacuo to give the crude **4d**, which was purified by crystallization. <sup>1</sup>H NMR (DMSO-*d*<sub>6</sub>) δ 3.78 (s, 3 H, NCH<sub>3</sub>), 4.15 (s, 2 H, CH<sub>2</sub>CO), 6.33 (d, 1 H, CH=CHCO), 6.99 (m, 1 H, pyrrole β-proton), 7.38 (m, 5 H, benzene protons and pyrrole α-proton), 7.85 (m, 1 H, CH=CHCO), 9.01 (bs, 1 H, NH), 10.72 (bs, 1 H, OH). Anal. (C<sub>16</sub>H<sub>15</sub>FN<sub>2</sub>O<sub>3</sub>) C, H, F, N.

#### 16.4. Molecular modeling and docking studies.

Homology models for the HD1-A<sup>342,243,350</sup> and HD1-B<sup>340,341</sup> sequences were derived by using the CPHmodels 2.0 Server<sup>351</sup> with structural data from the HDAC8-TSA complex<sup>352</sup> (PDB code: 1T64). The models were refined with a molecular dynamics (MD) protocol (Experimental Section) by using the program AMBER 8.0<sup>353,354</sup>. The Autodock<sup>355</sup> program was used to explore the binding mode of derivatives 4u and 4t, the most selective derivatives

against HD1-B and HD1-A, respectively. In general, the docked conformations obtained with the two enzymes differ mainly in that the molecules are placed deeper in the HD1-A pocket, where they partially occupy the acetyl escape channel,<sup>356</sup> whereas in HD1-B, the docked conformations adopt different conformations (Figure 31 and Figure 32).

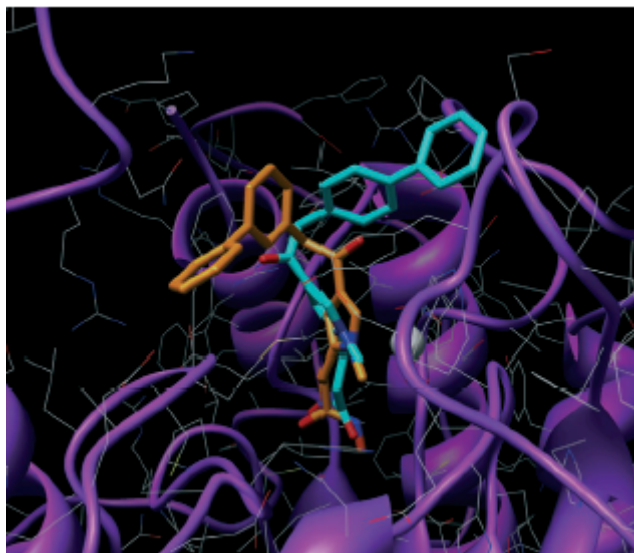


**Figure 31.** Derivatives **4t** (orange) and **4u** (cyan) docked into HD1-A. The enzyme is shown in tube representation (violet), and side chains are in gray.

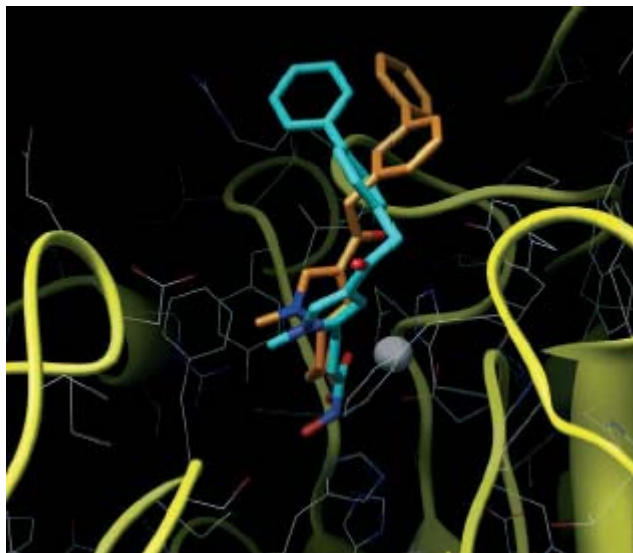


**Figure 32.** Derivatives **4t** (orange) and **4u** (cyan) docked into HD1-B. The enzyme is shown in tube representation (yellow), and side chains are in gray.

#### *Binding mode of 4u.*

The Autodock lowest-energy pose for derivative 4u in HD1-A shows a deep position inside the catalytic channel. Inspection of the binding mode reveals several positive interactions: the hydroxyl oxygen atom is positioned within hydrogen-bonding distance from either the carbonyl oxygen atom of Ala 277 ( $d=2.62$  M) or that of Pro 106 ( $d=2.73$  M); the hydroxyamide carbonyl oxygen atom is within weak hydrogen-bonding distance from His 109 NH ( $d=3.20$  M); a weak hydrogen bond is present between the phenylacetyl carbonyl oxygen atom and the phenol group of Tyr 180 ( $O\_O$  distance= $3.74$  M). Finally, positive hydrophobic interactions ( $<4$  M) are possible between the 4-biphenyl group of 4u and the benzyl side chain of Tyr 180 and one of the methyl groups of Leu249. In contrast to HD1-A, the acetyl escape

is narrower in the HD1-B model and places the hydroxyamide portion of 4u close to the catalytic zinc ion (Supporting Information). This scenario reveals that the hydroxyamide carbonyl oxygen approaches the zinc ion at an effective chelating distance ( $Zn^{2+} \cdots O=C$   $d=1.88$  M) that could explain the slightly improved selectivity toward HD1-B. Along with the chelation, further contributing interactions can be observed: the hydroxy oxygen atom is positioned within a weak hydrogen-bonding distance from the carbonyl oxygen atom of Gly 268 ( $d=3.87$  M); the hydroxyamide nitrogen atom at a hydrogen-bonding distance from the carbonyl oxygen atom of Asp144 ( $d=2.90$  M). Furthermore, positive hydrophobic interactions may take place between the pyrrole group of 4u and the benzyl side chain of Phe173, and between the 4-phenyl substituent of 4u and the side chain of Arg 238.

#### *Binding mode of 4t.*

Similar to 4u, the lowest-energy docked conformation of 4t is placed deep inside the HD1-A catalytic tunnel, and the pyrrolyl hydroxypropenamide moiety is nicely superimposed with that of 4u (with some slight differences), whereas the biphenyl group of 4u is swiveled  $\sim 110^\circ$ . This rotation of the biphenyl group leads to the disruption of the previously observed hydrophobic interactions for 4u and creates new interactions with the Phe118 side chain. In contrast to 4u, the hydroxyamide group is rotated roughly  $180^\circ$ , and only weak hydrogen-bond interactions are displayed between the hydroxy oxygen atom and the carbonyl oxygen atom of Asp149 ( $d=3.59$  M), and between the hydroxyamide carbonyl oxygen atom and the amide group of His 109 ( $d=3.79$  M). The lowest-energy docked conformation of 4t in HD1-B is shifted back from the catalytic channel with an overall decrease in the contributing favorable interactions that could explain the slight selectivity of 4t toward HD1-A. Moreover, comparison of the binding mode of 4t with that of 4u in the HD1-B catalytic pocket shows that whereas the latter is placed optimally to chelate  $Zn^{2+}$ , the former does not show any effective chelating distance between the hydroxyamide group and the zinc ion ( $Zn \cdots O=C$   $d=2.76$  M,  $Zn \cdots O\_N$   $d=3.02$  M).

#### *Docking of 4t and 4u.*

The docking studies were performed using Autodock 3.0.5. The molecular structures of derivatives **4t** and **4u** were drawn using the PRODGR software which give directly the

molecule ready to be used by Autodock. The AutodockTools package was employed to generate the docking input files and to analyze the docking results, the same procedure as described in the manual was followed. All the nonpolar hydrogens and the water molecules were removed. The Kollmann charges were loaded for the proteins while the charges applied by the PRODRG program were retained in the ligand. A grid box size of  $40 \times 40 \times 60$  points with a spacing of  $0.375 \text{ \AA}$  between the grid points was implemented and covered most of the catalytic channel of either enzymes. The grid was centered on the mass center of the bound TSA. For all the inhibitors, the single bonds including the amide bonds were treated as active torsional bonds. One hundred structures, *ie* 30 runs, were generated by using genetic algorithm searches. A default protocol was applied, with an initial population of 50 randomly placed individuals, a maximum number of  $2.5 \times 10^5$  energy evaluations, and a maximum number of  $2.7 \times 10^4$  generations. A mutation rate of 0.02 and a crossover rate of 0.8 were used. In a parallel docking experiment the bound TSA molecules extracted from either average MD equilibrated complexes were docked back. Autodock proved to reposition the TSA with a minimal rmsd error ( $\text{rmsd}_{\text{TSA-HD1-A}} = 1.29$ ,  $\text{rmsd}_{\text{TSA-HD1-B}} = 0.95$ ).

### *16.5. Biological evaluation.*

The novel APHA compounds 4a–a' (Figure 30) were evaluated for their ability to inhibit maize HDACs. The maize system offers the advantage that three different types of HDACs can be biochemically separated: class I (HD1-B) and class II (HD1-A) enzymes, and the plant-specific form HD2. Two short-chain fatty acids (NaB and VPA), two hydroxamic acids (TSA and SAHA), two cyclic tetrapeptides (TPX and HC-toxin), PAOA (a class I-selective inhibitor), and tubacin (an in-cell class IIB-selective inhibitor) have been reported as reference drugs in anti-HD2 assays. The results, expressed as the percent inhibition at a fixed dose and IC<sub>50</sub> (50% inhibitory concentration) values, are reported in Table 3. In assays for HD1-B and HD1-A inhibition, TSA, SAHA, PAOA, tubacin, 2, and 3 were also tested for the purpose of comparison (Table 4). Selected compounds (3'-chloro (compound 4b) and 3'-methyl (compound 4k) derivatives) were tested against mouse HDAC1 in comparison with 2 and SAHA (Table 5).

**Table 3.** Maize HD2 Inhibitory Activity of Compounds **4a-a**<sup>1a</sup>

compound	R	% inhibition (at fixed dose, $\mu\text{M}$ )	IC <sub>50</sub> $\pm$ SD ( $\mu\text{M}$ )
<b>4a</b>	2-Cl	94.3 (24.1)	0.09 $\pm$ 0.004
<b>4b</b>	3-Cl	97.2 (24.1)	0.05 $\pm$ 0.001
<b>4c</b>	4-Cl	96.8 (24.1)	0.10 $\pm$ 0.005
<b>4d</b>	2-F	96 (25.4)	0.13 $\pm$ 0.006
<b>4e</b>	3-F	96.9 (25.4)	0.07 $\pm$ 0.003
<b>4f</b>	4-F	93.9 (25.4)	0.15 $\pm$ 0.007
<b>4g</b>	2-Br	91.1 (21.2)	0.18 $\pm$ 0.009
<b>4h</b>	3-Br	98 (21.2)	0.08 $\pm$ 0.004
<b>4i</b>	4-Br	93.7 (21.2)	0.15 $\pm$ 0.007
<b>4j</b>	2-Me	95 (25.8)	0.21 $\pm$ 0.01
<b>4k</b>	3-Me	96.6 (25.8)	0.06 $\pm$ 0.003
<b>4l</b>	4-Me	83 (1.3)	0.23 $\pm$ 0.009
<b>4m</b>	2-NO <sub>2</sub>	96 (23.4)	0.16 $\pm$ 0.005
<b>4n</b>	3-NO <sub>2</sub>	97 (23.4)	0.13 $\pm$ 0.005
<b>4o</b>	4-NO <sub>2</sub>	97.2 (23.4)	0.18 $\pm$ 0.005
<b>4p</b>	3-OMe	96.5 (24.5)	0.07 $\pm$ 0.003
<b>4q</b>	4-OMe	93.7 (24.5)	0.06 $\pm$ 0.001
<b>4r</b>	3-OEt	91.2 (23.4)	0.34 $\pm$ 0.02
<b>4s</b>	4-OEt	93.6 (23.4)	0.18 $\pm$ 0.005
<b>4t</b>	3-Ph	95 (21.3)	0.25 $\pm$ 0.01
<b>4u</b>	4-Ph	97 (21.3)	0.09 $\pm$ 0.004
<b>4v</b>	3,5-Me <sub>2</sub>	97 (23.4)	0.07 $\pm$ 0.003
<b>4w</b>	3,5-F <sub>2</sub>	95 (24)	0.12 $\pm$ 0.004
<b>4x</b>	3-NH <sub>2</sub>	88.5 (25.5)	1.84 $\pm$ 0.07



*Ph.D. program: "Small Molecules as Epigenetic Modulators"*

<b>4y</b>	3-NHCOPh	94.1 (19.1)	$0.10 \pm 0.002$
<b>4z</b>	3-NHSO <sub>2</sub> Ph	94.3 (17.5)	$0.09 \pm 0.003$
<b>4a'</b>	3-Cl-4-OMe	95 (22.1)	$0.08 \pm 0.002$
<b>2<sup>b</sup></b>		96 (29)	$0.10 \pm 0.004$
<b>3<sup>c</sup></b>		98 (25.7)	$0.05 \pm 0.003$
NaB		35 (5000)	ND <sup>d</sup>
VPA			$128 \pm 3.8$
TSA			$0.007 \pm 0.0002$
SAHA			$0.05 \pm 0.001$
TPX			$0.01 \pm 0.0003$
HC-toxin			$0.11 \pm 0.004$
PAOA			$292 \pm 8.8$
tubacin		92.9 (40)	$2.0 \pm 0.1$

---

<sup>a</sup>Data represent mean values of at least three separate experiments. <sup>b</sup>Ref. 45.  
<sup>c</sup>Ref. 46. <sup>d</sup>ND, not determined.

**Table 4.** Maize HD1-B and HD1-A Inhibitory Activities of Compounds **4a-a'**<sup>a</sup>

compound	R	IC <sub>50</sub> ± SD (μM)		fold selectivity	
		HD1-B	HD1-A	class I	class II
<b>4a</b>	2-Cl	0.13 ± 0.005	0.12 ± 0.005		
<b>4b</b>	3-Cl	0.03 ± 0.0007	0.03 ± 0.001		
<b>4c</b>	4-Cl	0.07 ± 0.003	0.06 ± 0.002		
<b>4d</b>	2-F	0.04 ± 0.001	0.02 ± 0.0005		
<b>4e</b>	3-F	0.04 ± 0.001	0.03 ± 0.0005		
<b>4f</b>	4-F	0.06 ± 0.002	0.07 ± 0.003		
<b>4g</b>	2-Br	0.29 ± 0.015	0.21 ± 0.011		
<b>4h</b>	3-Br	0.04 ± 0.001	0.03 ± 0.001		
<b>4i</b>	4-Br	0.06 ± 0.002	0.05 ± 0.002		
<b>4j</b>	2-Me	0.10 ± 0.004	0.11 ± 0.004		
<b>4k</b>	3-Me	0.02 ± 0.0005	0.03 ± 0.0008		
<b>4l</b>	4-Me	ND <sup>b</sup>	ND		
<b>4m</b>	2-NO <sub>2</sub>	0.07 ± 0.003	0.08 ± 0.003		
<b>4n</b>	3-NO <sub>2</sub>	0.07 ± 0.003	0.13 ± 0.004		
<b>4o</b>	4-NO <sub>2</sub>	0.06 ± 0.001	0.12 ± 0.005	2	
<b>4p</b>	3-OMe	0.05 ± 0.002	0.04 ± 0.001		
<b>4q</b>	4-OMe	0.06 ± 0.002	0.09 ± 0.004		
<b>4r</b>	3-OEt	0.15 ± 0.004	0.13 ± 0.005		
<b>4s</b>	4-OEt	0.06 ± 0.002	0.06 ± 0.002		

<b>4t</b>	3-Ph	1.16 ± 0.07	0.32 ± 0.013		3.6
<b>4u</b>	4-Ph	0.02 ± 0.0005	0.05 ± 0.002	2.5	
<b>4v</b>	3,5-Me <sub>2</sub>	ND	ND		
<b>4w</b>	3,5-F <sub>2</sub>	ND	ND		
<b>4x</b>	3-NH <sub>2</sub>	ND	ND		
<b>4y</b>	3-NHCOPh	0.08 ± 0.004	0.05 ± 0.003		
<b>4z</b>	3-NHSO <sub>2</sub> Ph	0.10 ± 0.006	0.05 ± 0.003		2
<b>4a'</b>	3-Cl-4-OMe	0.10 ± 0.006	0.04 ± 0.001		2.5
<b>2</b>		0.15 ± 0.004	0.05 ± 0.001		3
<b>3</b>		0.12 ± 0.006	0.06 ± 0.002		2
TSA		0.0004 ± 0.00001	0.0008 ± 0.00003	2	
SAHA		0.03 ± 0.001	0.2 ± 0.009	6.7	
PAOA		150 ± 4.5	756 ± 30.2	5	
tubacin		0.98 ± 0.04	0.45 ± 0.02		2.2

<sup>a</sup>Data represent mean values of at least three separate experiments. <sup>b</sup>ND, not determined.

**Table 5.** Mouse HDAC1 Inhibitory Activities of Compounds **4b** and **4k**<sup>a</sup>

compd	R	IC <sub>50</sub> ± SD (μM)
<b>4b</b>	3-Cl	0.23 ± 0.01
<b>4k</b>	3-Me	0.31 ± 0.01
<b>2</b> <sup>b</sup>		0.51 ± 0.02
SAHA		0.11 ± 0.004

<sup>a</sup>Data represent mean values of at least three separate experiments. <sup>b</sup>Ref. 45.

### 16.5.1. Anti-HD2 Activity and Structure-Activity Relationships (SARs)

Starting from the recently reported findings about the APHA compounds,<sup>337-340</sup> we chose the 3-(1-methyl-4-phenylacetyl-1H-pyrrol-2-yl)-N-hydroxy-2-propenamide **2** as lead compound, and we introduced various substituents (*ie* chloro, fluorine, bromo, methyl, nitro, amino, benzoylamino, benzenesulfonylamino, methoxy, ethoxy, phenyl groups) at *ortho*, *meta*, and *para* positions of the benzene ring to determine the effect of such substitutions on anti-HD2 activity (Table 3).

Halogen and methyl substitutions at both *ortho* and *para* positions of the benzene ring of the pyrrole-C<sub>4</sub> phenylacetyl moiety of **2** left unaltered (**4a,c**) or lowered (**4d,f,g,i,j,l**) the HDAC inhibitory activity of the new derivatives. Conversely, the 3'-chloro- (**4b**), 3'-fluoro- (**4e**), and 3'-bromo- (**4h**) as well as 3'-methylsubstituted (**4k**) pyrroles were endowed with higher anti-HD2 activity than **2**. With the insertion of a nitro group (at whatever position of benzene ring) only low-active compounds (**4m-o**) were obtained. Differently, the introduction of a methoxy (but no ethoxy!) group at either 3'- or 4'-position of the benzene ring led to more potent compounds (**4p,q**) than **2**, while the bulky phenyl substituent was well tolerated at *para* (**4u**) but it was not at *meta* position (**4t**). Reduction of 3'-nitro to 3'-amino function (from **4n** to **4x**) strongly abated the HD2 inhibiting activity of the derivative, but this activity was promptly restored when an amide function (**4y,z**) replaced the amine group (**4x**). 3',5'-Difluoro- (**4w**)

and 3',5'-dimethyl- (**4v**) as well as 3'-chloro-4'-methoxyphenyl (**4a'**) substitutions at the pyrrole-C<sub>4</sub> phenylacetyl moiety, that were designed by taking together two equal or diverse groups efficient in increasing the anti-HD2 activity of APHA compounds, did not significantly improve the inhibitory potency of the derivatives.

#### *16.5.2. HD1-B and HD1-A Inhibitory Effects: Class Selectivity Assessment.*

3-[1-Methyl-4-phenylacetyl- and -4-(3-phenylpropionyl)-1*H*-pyrrol-2-yl]-*N*-hydroxy-2-propenamides **2** and **3**, when tested against the maize deacetylases homologues of mammalian class I (HD1-B) and class II (HD1-A) HDACs, showed in both cases submicromolar inhibitory activities, they being more potent against HD1-A than HD1-B enzyme (class II fold selectivity: **2** = 3; **3** = 2) (Table 4). In order to study the inhibiting action of the new pyrrole compounds against these two enzymes, and to explore the effect of substituent insertion on HDAC class selectivity, we assayed **4a-a'** against HD1-B and HD1-A, in comparison with TSA, SAHA, PAOA (class I-selective inhibitor), and tubacin (in cell class Iib-selective inhibitor) (Table 4).

Halogen as well as methyl substitution at the 3'- (**4b,e,h,k**) or 4'-position (**4c,f,i**) of the pyrrole-C<sub>4</sub> phenylacetyl moiety led to compounds with higher inhibiting activity against HD1-B than **2**, while 2'-substituted analogues were as active as (**4j**) or less active than (**4a,g**) the pyrrole reference, with the exception of the 2'-fluoroderivative **4d**, which was 3-4 times more potent than **2** against HD1-B.

Against HD1-A enzyme, a little effect of benzene ring substitution on inhibiting activity was observed, 4'-substituted derivatives (**4c,f,i**) showing the same activity and the 3'-analogues (**4b,e,h,k**) being 2-fold more potent than **2**. 2'-Chloro, 2'-bromo, and 2'-methylsubstituted derivatives **4a,g,j** were from 2 to 4 times less potent than the pyrrole reference, while again the 2'-fluoro analogue **4d** showed an increase of two-fold in HD1-A inhibiting activity if compared with **2**.

To determinate the potential class selectivity of the described compounds, the IC<sub>50-HD1-A</sub>/IC<sub>50-HD1-B</sub> ratio for class I-selectivity and the IC<sub>50-HD1-B</sub>/IC<sub>50-HD1-A</sub> ratio for class II-selectivity have been calculated. Only selectivity values  $\geq 2$  have been reported. As a result of the HD1-B/HD1-A inhibitory trend, all the halogen- and methyl-substituted compounds did not show any class selectivity. Nitro-substituted compounds **4m-o** displayed a opposite pattern of HD1-B/HD1-A inhibition when it is compared with that of **2**, **4m-o** being more potent against

HD1-B than HD1-A. However, just **4o** showed little class I selectivity value (class I fold selectivity = 2). The 3'-methoxy-, 4'-methoxy-, and 4'-ethoxyphenylacetyl compounds **4p,q,s** were efficient HD1-B and HD1-A inhibitors, with IC<sub>50</sub> values ranging from 40 to 90 nM, but lacked selectivity. The introduction of phenyl substituent at the 3'-position of the benzene ring (compound **4t**) highly decreased the anti-HD1-B and, to a lesser extent, the anti-HD1-A activities of the derivative. Nevertheless, **4t** showed 3.6-fold selectivity against class II deacetylase, while its 4'-phenyl counterpart **4u** was very potent against both the enzymes and showed little class I selectivity ratio (class I fold selectivity = 2.5). The 3'-amide analogues **4y,z** and the 3'-chloro-4'-methoxyderivative **4a'** were still endowed with interesting inhibiting activities, they being more active than (HD1-B) and as active as (HD1-A) the pyrrole reference **2**. However, only **4z** and **4a'** showed little class II selectivity values (class II fold selectivity = 2 and 2.5, respectively).

TSA and SAHA in anti-HD1-B assay were endowed with strong inhibiting activity, TSA being inhibitor at subnanomolar concentration (IC<sub>50</sub> = 0.4 nM), and SAHA showing an IC<sub>50</sub> = 30 nM. Compared with SAHA, 3'-chloro- (**4b**), 2'-fluoro- (**4d**), 3'-bromo- (**4h**), 3'-methyl- (**4k**), and 4'-phenylsubstituted (**4u**) APHAs displayed similar inhibiting activity.

Against HD1-A, TSA was still a very potent inhibitor (IC<sub>50</sub> = 0.8 nM), while SAHA exhibited submicromolar activity (IC<sub>50</sub> = 0.2 μM), showing 6.7-fold selectivity towards class I HDACs. The APHA derivatives described herein, when compared with SAHA, were all more potent in inhibiting HD1-A enzyme, with the sole exceptions of the 2'-bromo (**4g**) and the 3'-phenyl (**4t**) derivatives.

### *16.5.3. Anti-mouse HDAC1 Activity of Selected Compounds.*

Among the title compounds, 3'-chloro (**4b**) and 3'-methyl (**4k**) derivatives were from 2 to 7.5 times more potent than **2** in maize system (HD2, HD1-B, and HD1-A). Thus, we tested them against mouse HDAC1, in comparison with **2** and SAHA (Table 5). Similarly to that obtained with maize HD2, **4b** and **4k** were 2-fold more potent than **2**, and 2 or 3 times less potent than SAHA in inhibiting mouse HDAC1.

*16.5.4. In Vitro Maize HD2, HD1-B, and HD1-A Enzyme Inhibition.*

Radioactively labeled chicken core histones were used as the enzyme substrate according to established procedures. The enzyme liberated tritiated acetic acid from the substrate, which was quantified by scintillation counting. IC<sub>50</sub> values are results of triple determinations. A 50 µL sample of maize enzyme (at 30 °C) was incubated (30 min) with 10 µL of total [<sup>3</sup>H]acetate-prelabeled chicken reticulocyte histones (1 mg/mL). Reaction was stopped by addition of 36 µL of 1 M HCl/0.4 M acetate and 800 µL of ethyl acetate. After centrifugation (10 000g, 5 min), an aliquot of 600 µL of the upper phase was counted for radioactivity in 3 mL of liquid scintillation cocktail. The compounds were tested at a starting concentration of 40 µM, and active substances were diluted further. NaB, VPA, TSA, SAHA, TPX, HC-toxin, PAOA, and tubacin were used as the reference compounds, and blank solvents were used as negative controls.

*16.5.5. Mouse HDAC1 Enzyme Assay.*

For inhibition assay, partially purified HDAC1 from mouse A20 cells (ATCC: TIB-208) (anion exchange chromatography, affinity chromatography was used as enzyme source. HDAC activity was determined as described using [<sup>3</sup>H]acetate-prelabeled chicken reticulocyte histones as substrate. 50 µL of mouse HDAC1 were incubated with different concentrations of compounds for 15 min on ice and 10 µL of total [<sup>3</sup>H]acetate-prelabeled chicken reticulocyte histones (4 mg/mL) were added, resulting in a concentration of 41 µM. The mixture was incubated at 37 °C for 1 h. The reaction was stopped by addition of 50 µL of 1 M HCl/0.4 M acetylacetate and 1 mL ethyl acetate. After centrifugation at 10 000g for 5 min an aliquot of 600 µL of the upper phase was counted for radioactivity in 3 mL liquid scintillation cocktail.

*16.5.6. Growth Inhibition and Cell Differentiation Assay. Cell Culture and Reagents.*

Human acute promyelocytic leukemia HL-60 cells were obtained from Interlab Cell Line Collection (CBA, Genoa, Italy). Cells were maintained at 37 °C under a humidified atmosphere of 5% CO<sub>2</sub> in RPMI 1640 Hepes modified medium supplemented with 10% (v/v) heat inactivated fetal calf serum, 2 mmol/L glutamine, 100 IU/mL penicillin and 100 µg/mL

streptomycin. Unless indicated all chemicals and reagents (cell culture grade) were obtained from Sigma Chemical Co., Milan, Italy.

#### *16.5.7. Cell Viability and Growth Inhibition Assay.*

Cell number was determined using a Neubauer hemocytometer, and viability was assessed by their ability to exclude trypan blue. The stock solutions were prepared immediately before use. TSA and **4b** were dissolved in DMSO. HL-60 exponentially growing cells ( $2 \times 10^5$  cells/mL) were set at day 0 in media containing various concentrations of drugs for 96 h. The final concentrations of the drugs were as follows: TSA, 30 nM; **4b**, 2.5, 5, 10, and 20  $\mu$ M. The final concentration of DMSO, used as a vehicle, was the same (0.1% v/v) in all samples during the experiments.

#### *16.5.8. Cell Differentiation Assay.*

Phorbol-12-myristate-13-acetate- (PMA-) stimulated reactive oxygen species (ROS) production, mostly due to the activity of NADPH oxidase system, was used as a marker of differentiation in the human myeloid cell line HL-60. ROS metabolism was studied by a chemiluminescence (CL) assay as already described. Briefly, assays were performed in triplicate in an automatic luminometer (Autolumat LB 953, EG&G, Turku, Finland) at 25 °C for 120 min with cycles of five minutes each. The CL system contained  $1 \times 10^5$  cells, without treatment (control), or treated with 0.1% DMSO (vehicle alone), or cells treated with different differentiating factors, 100 nmol of luminol, 150 pmol of PMA adjusted to a final volume of 1.0 mL with KRP solution. Unstimulated activity was measured without any addition of stimulus. Stimulated CL was evaluated through calculation of a CL index as follows: Area (expressed as counts/cell/120 min)<sub>stimulated cells</sub>/Area (expressed as counts/cell/120 min)<sub>unstimulated cells</sub>.

#### *Statistical Analysis.*

All results are expressed as the mean  $\pm$  SEM. The group mean values were compared by analysis of variance (ANOVA) followed by a multiple comparison of means by the Dunnet test.  $p < 0.05$  was considered significant.



*16.5.9. Antiproliferative and Cytodifferentiating Activities of 4b on Human Acute Promyelocytic Leukemia HL-60 Cells.*

Among the APHA derivatives showing the highest inhibitory values against the three maize enzymes (the 3'-substituted phenylacetylpyrroles **4b,e,h,k,p**), we chose the 3[4-(3'-chlorophenylacetyl)-1-methyl-1*H*-pyrrol-2-yl]-*N*-hydroxy-2-propenamide **4b** to test as antiproliferative and cytodifferentiating agent in human acute promyelocytic leukemia HL-60 cells.

*16.5.10. Antiproliferative effect of 4b on human leukemia HL-60 cells.*

The capability of **4b** to induce growth inhibition on human leukemia cell line was evaluated in comparison with TSA (30 nM). Figure 5A shows the effect of **4b** on the growth of HL-60 cells, cultured for 96 h with different concentrations of drug. The APHA compound **4b** showed a significant dose-dependent inhibitory effect on the growth rate of the cell line. In particular, the growth curve of cells is inhibited by the presence of 2.5, 5, 10 and 20  $\mu$ M of **4b** by 15% ( $p < 0.05$ ), 36% ( $p < 0.01$ ), 49% ( $p < 0.01$ ), and 86% ( $p < 0.01$ ), with respect to vehicle (Figure 33a). This **4b** inhibitory effect does not seem to depend on a direct cytotoxic action of the drug. In fact, the viability index (VI) appears significantly modified by **4b** only at 20  $\mu$ M (VI = 64%) (Figure 33b).

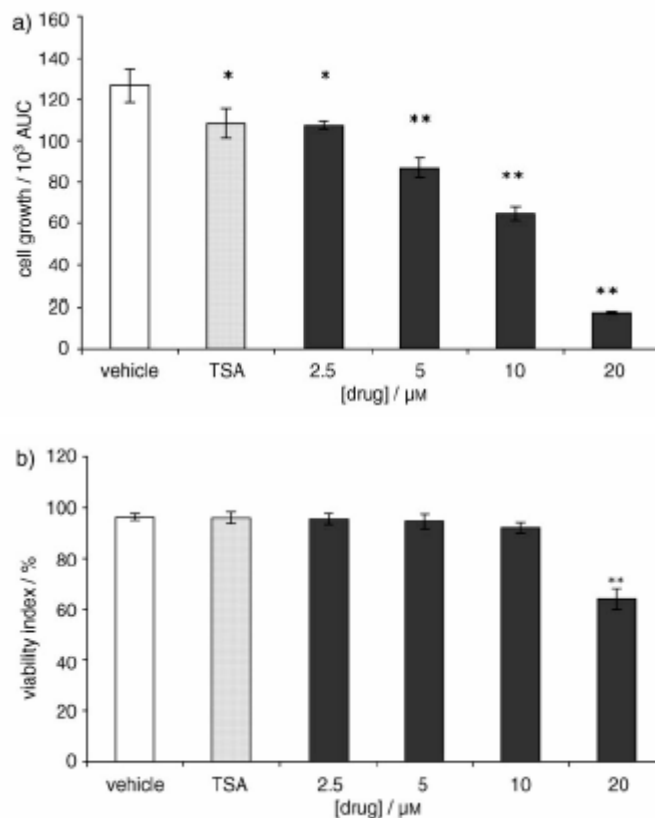


**Figure 33.** a) Effect of various concentrations of 4b (in dark grey) on the growth of human leukemia cells cultured for 96 h in comparison with TSA (30 nm); data are expressed as cell number (mean  $\pm$  SEM,  $n=4$ ); \* $p<0.05$ , \*\* $p<0.01$ . b) Cytotoxic effect in human leukemia cells cultured for 96 h with various concentrations of 4b (in dark grey); each point represents the mean  $\pm$  SEM ( $n=4$ ); \*\* $p<0.01$ .

*16.5.11. Differentiating activity of 4b on human leukemia HL-60 cells.*

The restoration of so-called respiratory burst was evaluated as fundamental functional marker of differentiation in human leukemia cell lines. This aspect of the phagocytes oxidative metabolism has been analyzed by chemiluminescence (CL) in HL-60 cells, incubated with different concentrations of **4b** for 96 hours, and stimulated by phorbol-12-myristate-13-acetate (PMA). In particular, the presence of PMA-induced CL seems to demonstrate an acquired right assembly of the NADPH oxidase system.

Results clearly showed a dose-dependent recovery of reactive oxygen species (ROS) metabolism when the cells were stimulated by PMA, reaching the maximum CL activity ( $p < 0.01$ ) at **4b** concentration = 20  $\mu\text{M}$  (Figure 34).

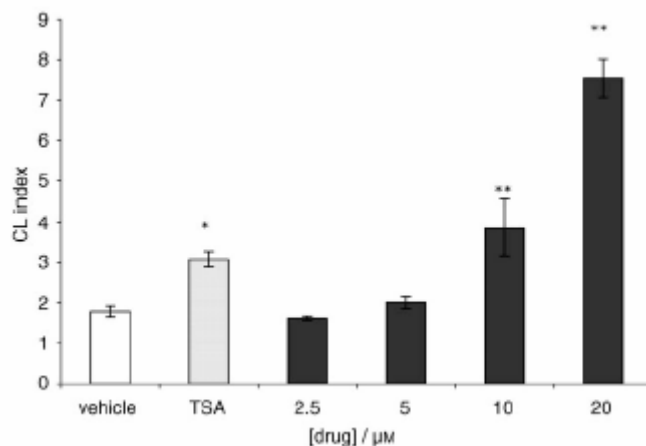


**Figure 34.** Concentration-dependent effect of **4b** on the differentiation of HL-60 cells with TSA (30 nm) as a reference. Cells were cultured with various concentrations of **4b** (in dark grey) for 96 h. Differentiation-inducing activity was measured by chemiluminescence (CL) as described in the Experimental Section. Each

point represents the mean  $\pm$  SEM (n=4);  
\* $p$ <0.05; \*\* $p$ <0.01.

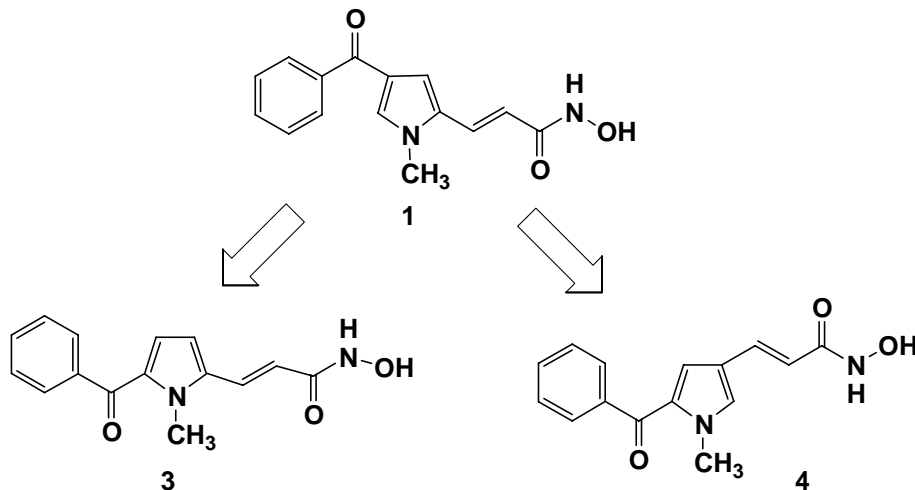
#### 16.5.12. Conclusions.

A new series of aroyl-pyrrolyl hydroxyamides (compounds **4–4a'**) have been described and are analogues of the lead compound 3-(1-methyl-4-phenylacetyl-1H-pyrrol-2-yl)-N-hydroxy-2-propenamide (**2**). The phenyl ring of **2** was substituted with a wide range of electron-donating and electron-withdrawing groups, and the effects were evaluated with three maize histone deacetylases: HD2, HD1-B (class I HDAC), and HD1-A (class II HDAC). HD2 inhibition data (Table 3) shows that the insertion of substituents such as halogen or methyl groups at the 3' position of the benzene ring increases the inhibitory effect of the derivatives **4b**, **4e**, **4h**, and **4k** up to 2-fold. The highest inhibiting activity was showed by the 3-[4-(3'-chlorophenylacetyl)-1-methyl-1H-pyrrol-2-yl]-N-hydroxy-2-propenamide (**4b**, IC<sub>50</sub>= 0.05 mm) and its 3'-methyl analogue **4k** (IC<sub>50</sub>=0.06 mm), which were more potent than VPA, HC-toxin, and **2**. Moreover, they showed the same activity as SAHA and were 7–5-fold less active than TSA and TPX. In assays against mouse HDAC1 in comparison with **2**, **4b** and **4k** showed inhibition data in agreement with those obtained in the anti-HD2 assay. Assays for the inhibition of HD1-B and HD1-A (Table 4) performed with **4a–4a'** confirmed the inhibition trend observed with HD2 above. The introduction of various substituents at the 3' and, to a lesser extent, at the 4' positions of the benzene ring of **2** led to compounds up to 6-fold more active than **2** against HD1-B (with the exception of the 3'-ethoxy and 3'-phenyl compounds **4r** and **4t**), whereas their anti-HD1-A activity remained the same as **2**. The 3- and 2-fold selectivity ratios toward class II (HD1-A) enzymes displayed by **2** and **3**, respectively, was lost by the insertion of substituents at the benzene ring; exceptions include the 3'-phenyl (compound **4t**), 3'-benzenesulfonamido (compound **4z**), and the 3'-chloro-4'-methoxy (compound **4a'**) derivatives, which showed selectivity ratios from **2** to 3.6 in favor of class II. Two compounds, the 4-nitro and the 4-phenyl derivatives **4o** and **4u** displayed an opposite pattern of HD1-B/HD1-A inhibition, as both are slightly more potent against HD1-B than HD1-A. Molecular modeling studies based on HD1-B and HD1-A homology models have been performed to gather insight on the observed inhibition differences. In tests with human

acute promyelocytic leucemia HL-60 cells, **4b** showed interesting, dose-dependent antiproliferative and cytodifferentiation properties.

### 17. Second lead optimization.

In parallel with the study of the influence of Pyrrole C4-phenylacetyl substitution on Histone Deacetylase inhibition we applied a different approach on the **1** structure to discover novel leads, using structure-based drug design and docking procedures. Particularly, we designed two isomers of **1**, 3-(2-benzoyl-1-methyl-1*H*-pyrrol-5-yl)-*N*-hydroxy-2-propenamide **3** and 3-(2-benzoyl-1-methyl-1*H*-pyrrol-4-yl)-*N*-hydroxy-2-propenamide **4**, and we performed computational studies to predict their HDAC inhibiting activity.



In the chemical structure of the APHA lead compound **1**, virtual rotation of *N*-methylpyrrole ring between benzoyl and *N*-hydroxy-2-propenamide moieties allowed us to design two isomers of **1**, 3-(2-benzoyl-1-methyl-1*H*-pyrrol-5-yl)-*N*-hydroxy-2-propenamide **3** and 3-(2-benzoyl-1-methyl-1*H*-pyrrol-4-yl)-*N*-hydroxy-2-propenamide **4**. Extensive binding mode analyses were undertaken to see if the HDAC1 enzyme inhibitory potency would be

influenced by the above different rearrangement of benzoyl and *N*-hydroxypropenamide substituents on the pyrrole ring.

Initially, binding mode analyses of **3** and **4** into the modeled HDAC1 structure were investigated using a semiautomatic dock (SAD) procedure, analogous to that reported for **1**. In parallel experiments, docking studies were performed on **3** and **4** structures by the mean of the DOCK 4.0.2 and Autodock 3.0.5 programs. The results of the automatic docking procedures (DOCK and Autodock) were energy rescored by a single point minimization by the MACROMODEL molecular mechanics program, using the AMBER all atom force fields and point charges calculated with the MOZYME routine as implemented in the MOPAC2000 program. From docking studies three bound conformations for both **3** and **4** were obtained, and their associated HDAC inhibitory potencies, expressed as p*K*<sub>i</sub> values, were predicted using our in house refined VALIDATE scoring function model. In Table 6 the p*K*<sub>i</sub> prediction values for APHA isomers **3** and **4** compared with their experimental p*C*<sub>50</sub> values (see below) are reported. For comparison purpose, **1**, TSA, and SAHA p*K*<sub>i</sub> prediction values are also shown. Among the minimized ligand/HDAC1 complexes, the most stable ones were those proposed by Autodock (Table 7). Similarly as previously observed, DOCK and Autodock results were in good agreement each other and with those obtained by the SAD procedure (Table 8). To compare the docked molecules (**1**, **3**, **4**, TSA, and SAHA), their binding conformations obtained by Autodock are depicted in Figure 35.

**Table 6.** VALIDATE and Autodock Predicted Anti-HDAC1 p*K*<sub>i</sub> Compared with Experimental p*C*<sub>50</sub> Values of APHA Isomers **1**, **3**, **4**, and TSA, and SAHA.

compd	predicted p <i>K</i> <sub>i</sub>				experimental p <i>C</i> <sub>50</sub>	
	VALIDATE			Autodock	HDAC1	HD2
	SAD	DOCK	Autodock			
<b>3</b>	5.87	7.31	7.76	5.29	6.64	6.60
<b>4</b>	7.13	7.55	7.47	5.73	6.11	7.30
<b>1</b>	5.76 <sup>27</sup>	4.76 <sup>28</sup>	7.31 <sup>28</sup>	5.65 <sup>28</sup>	5.31 <sup>27</sup>	5.42 <sup>27</sup>
TSA	8.61 <sup>a,27</sup>	7.26 <sup>28</sup>	7.92 <sup>28</sup>	7.41 <sup>28</sup>	8.70 <sup>27</sup>	8.15 <sup>27</sup>
SAHA	6.69 <sup>a,27</sup>	6.79 <sup>28</sup>	7.15 <sup>28</sup>	6.21 <sup>28</sup>	6.95 <sup>27</sup>	7.30 <sup>27</sup>

<sup>a</sup> Predicted from X-ray experimental data.

**Table 7.** Minimized Complex Steric Energies (kJ/mol) (AMBER force field) Relative to APHA Isomers **3** and **4** Obtained by DOCK, Autodock, and SAD Procedures into the Modeled HDAC1. For Direct Comparison the Same Values for **1**, TSA, and SAHA Are Reported.

docking method	<b>3</b>	<b>4</b>	<b>1</b> <sup>a</sup>	TSA <sup>a</sup>	SAHA <sup>a</sup>
DOCK	-7754.958	-7710.129	-7174.81	-8909.93	-7369.18
Autodock	-8737.534	-10161.400	-8913.90	-9976.13	-10363.13
SAD	-8581.698	-8457.775	-7828.92	ND <sup>b</sup>	ND <sup>b</sup>

**Table 8.** Comparison of Docking Studies Performed on **3** and **4**. Values Are the Root Mean Square Deviations (RMSDs) for All Non-H Atoms. For Direct Comparison, the Same Values for **1**, TSA, and SAHA Are Reported.

compd	SAD or Exp vs DOCK	SAD or Exp vs Autodock	DOCK vs Autodock
<b>3</b>	3.2	3.1	1.4
<b>4</b>	2.2	2.8	1.5
<b>1</b>	5.6	3.8	5.1
TSA	1.0	1.4	1.9
SAHA	1.5	2.3	2.0

**Table 9.** Antimaize HD2 and Antimouse HDAC1 Activities of Compounds **3** and **4**<sup>a</sup>.

compd	maize HD2		mouse HDAC1, IC <sub>50</sub> ± SD (μM)
	% inhbtn <sup>b</sup>	IC <sub>50</sub> ± SD (μM)	
<b>3</b>	95	0.28 ± 0.014	0.25 ± 0.01
<b>4</b>	97	0.05 ± 0.003	0.78 ± 0.04
<b>1</b> <sup>27</sup>	86	3.8 ± 0.1	4.9 ± 0.1
TSA <sup>27</sup>		0.0072 ± 0.0003	0.002 ± 0.00006
SAHA <sup>27</sup>		0.05 ± 0.002	0.112 ± 0.004

<sup>a</sup> Data represent mean values of at least three separate experiments.

<sup>b</sup> Percent of inhibition at 30 μM.

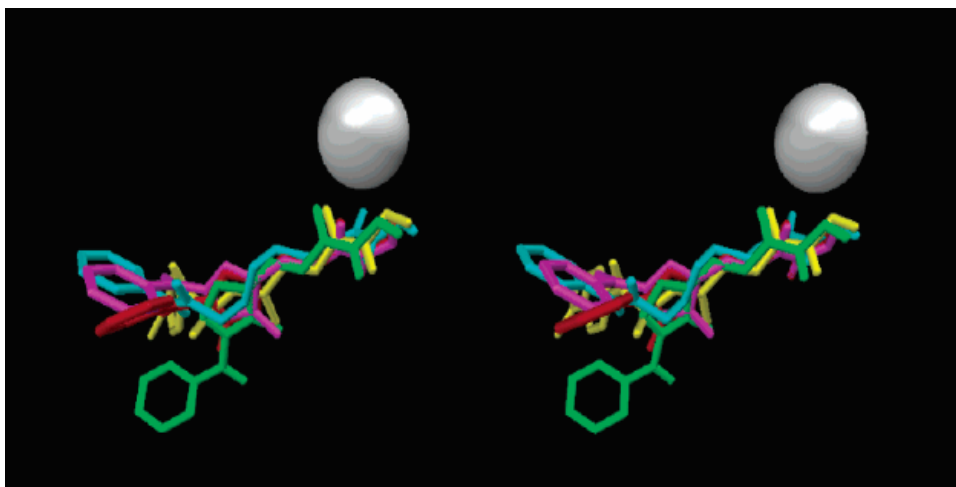


**Figure 35.** Stereoview of superimposition of the Autodock docked conformations of **1** (magenta), **3** (green), **4** (red), TSA (yellow), and SAHA (cyan). The gray ball represents the mean position of the zinc ion. HDAC1 pocket and nonessential hydrogen atoms are not shown for the sake of clarity.



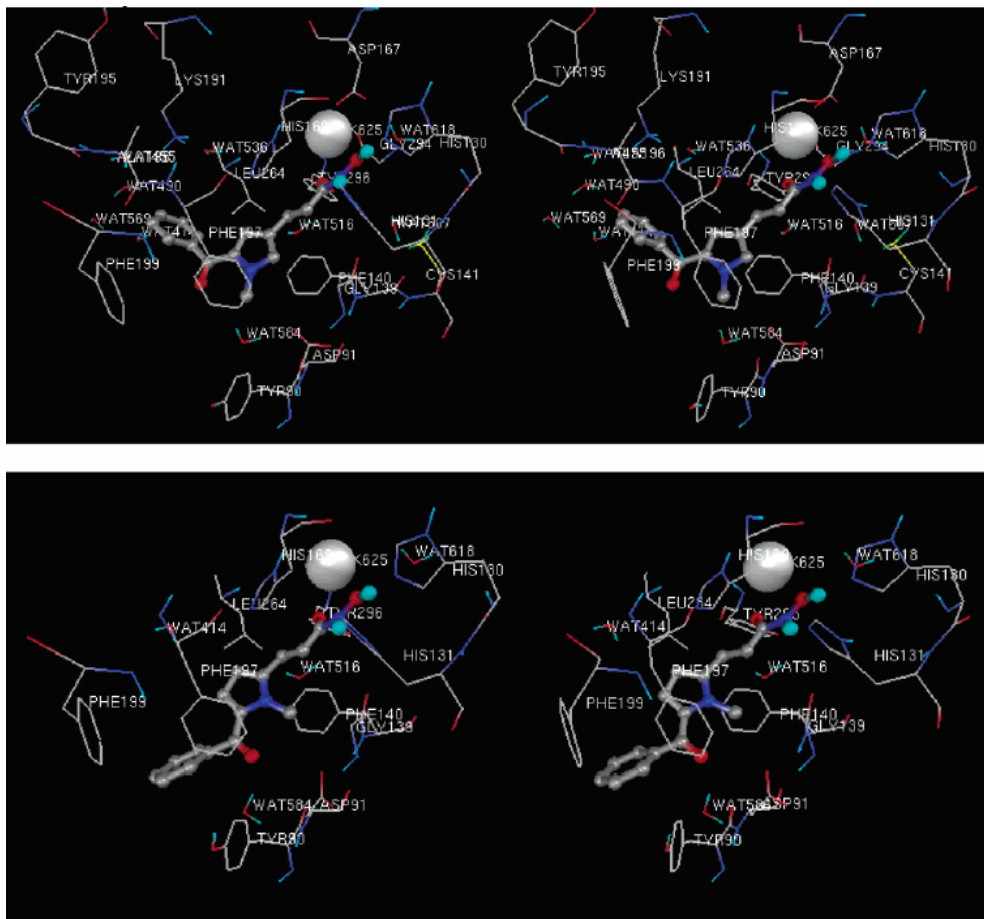


**Figure 36.** Autodock binding mode of APHA isomers **3** (bottom) and **4** (top). Inhibitors are drawn in ball-and-stick. For the sake of clarity, only a 3 Å core of the HDAC1 with essential hydrogen atoms is displayed. Residue numbering is reported for description without correction relative to the real HDAC1 sequence.

By comparing the docking studies performed on **3** and **4**, it is possible to observe that docking studies highly agree each other, displaying clustered binding conformations for either isomer

**3** or **4** (Figure 36). These data agree with our previous findings that low active compounds (i.e., isomer **1**) bind the deacetylase core in a lousy way and probably with a not fully defined binding conformation. On the other hand, in this study we found that the pyrrole ring rotation between benzoyl and *N*-hydroxy-2-propenamide moieties critically affects the binding mode of APHA isomers. In fact (Figure 36), while the *N*-hydroxy-2-propenamide tail maintains a similar conformation for either isomer **3** or **4**, the *N*-methylpyrrole and benzoyl moieties are clearly disposed in different ways (compare left side with right side of the Figure 36).

#### *17.1. Antiproliferative and Cytodifferentiating Effects of 4 on Friend Murine Erythroleukemia (MEL) Cells.*

In addition to in vitro enzyme assays, the capability of **4** to induce antiproliferative and cytodifferentiating effects in vivo on Friend MEL cells were evaluated. Figure 36A shows the effect of **4** on the growth of MEL cells, cultured for 48 h. Such compounds showed significant dose-dependent inhibitory effect on the growth rate of cell line ( $p < 0.01$ ). Moreover, after 48 h the inhibitor was not cytotoxic at the tested concentrations (data not shown). In MEL cells, benzidine staining reveals the  $\square$  hemoglobin accumulation rate, which is related to the activation of the cell line differentiation process. The results (Figure 36B) clearly indicate a dose-dependent increase of  $\square$  hemoglobin synthesis for **4** at the tested doses.

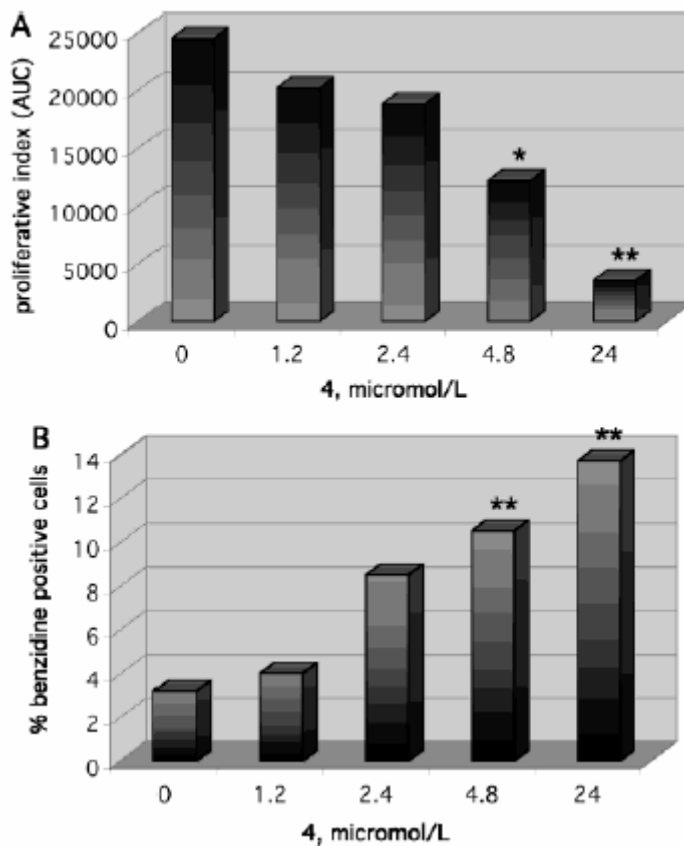


**Figure 36.** Antiproliferative and cytodifferentiating effects of **4** on MEL cell line. (A) Effects of **4** on cell growth of MEL cells, cultured for 48 h. Data are expressed as area under the curve (AUC) (mean ( SEM, n ) 4); \*,  $p < 0.05$ ; \*\*,  $p < 0.01$ . (B) Effects of **4** on differentiation of MEL cells. The cells were cultured with various concentrations of drug for 48 h. Each point is the mean ( SEM (n) 4); \*\*,  $p < 0.01$ .

### 18. Third lead optimization.

As the predicted  $pK_i$  values were in the submicromolar range, we synthesized and tested **3** and **4** against both maize HD2 and mouse HDAC1 enzymes.

Furthermore we performed various chemical modifications (as the introduction of different substituents on the benzene ring and the replacement of the benzene ring with a bulkier aromatic one) on these two APHA isomers in order to improve prototypes enzyme inhibiting activity .

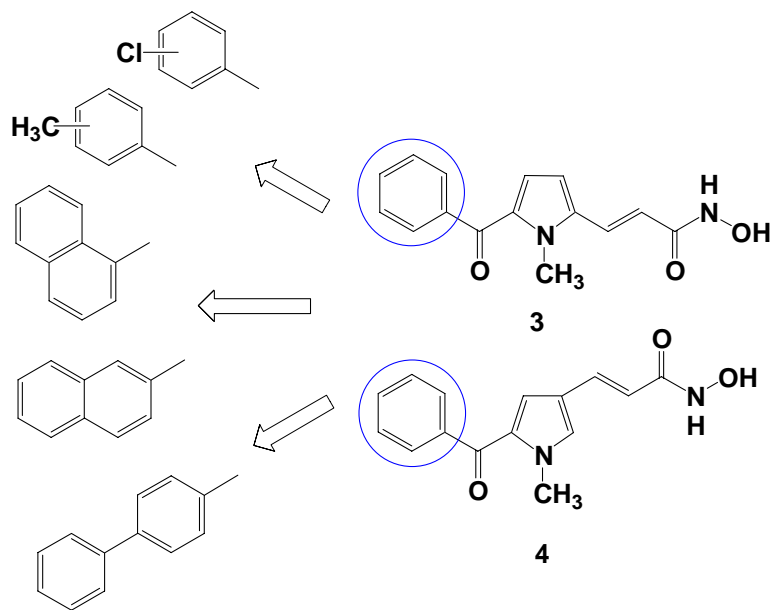
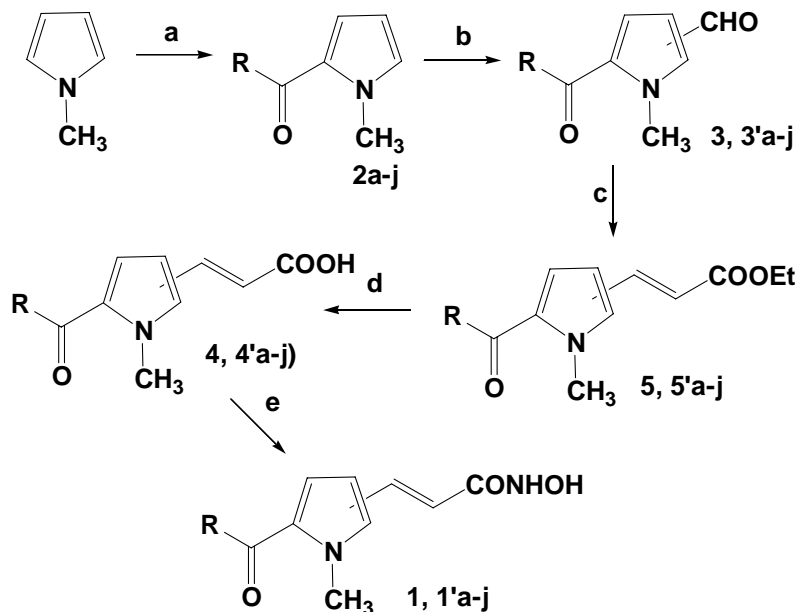


**Figure 37.** APHA (Aroyl pyrrolil hydroxyamides) isomers derivatives.

18.1. Chemistry.



**Scheme 1.**

**A:**  $\text{BF}_3\text{X Et}_2\text{O}$ ,  $\text{RCOCl}$ ,  $\text{CH}_2\text{Cl}_2$ , r.t., three days; **b:** 1) DMF,  $(\text{COCl})_2$ ,  $(\text{CH}_2)_2\text{Cl}_2$ ,  $0^\circ\text{C}$ , 1 h; 2) NaOH 50%, 15 min.; **c:**  $(\text{EtO})_2\text{POCH}_2\text{COOEt}$ , anhydrous  $\text{K}_2\text{CO}_3$ , EtOH,  $80^\circ\text{C}$ , 2 h; **d:** KOH 2N, EtOH, overnight; **e:** 1)  $\text{ClCOOEt}$ ,  $\text{Et}_3\text{N}$ , anhydrous THF,  $0^\circ\text{C}$ , 15 min.; 2)  $\text{CH}_3\text{OC}(\text{CH}_3)_2\text{ONH}_2$ , anhydrous THF,  $0^\circ\text{C}$ , 1 h; 3) Amberlist 15, MeOH, r.t., 1 h.

Chemical and physical data for compounds **1a-j** and **1'a-j** are listed in Table 10,11. Chemical and physical data for the intermediate compounds **5-8** are listed in Table 12, 13.

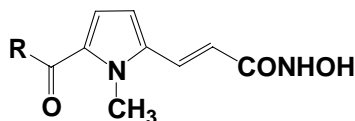


**Table 10.**

Compound	R	Melting point (°C)	recrystallization solvent	Yield (%)
<b>1a</b>	Ph	88-89	Benzene/acetonitrile	84.6
<b>1b</b>	2'-Cl-Ph	oil	Benzene/acetonitrile	77.9
<b>1c</b>	3'-Cl-Ph	100-101	Acetonitrile	85.3
<b>1d</b>	4'-Cl-Ph	132-133	Acetonitrile	98.0
<b>1e</b>	2'-CH <sub>3</sub> -Ph	114-115	Benzene	77.3
<b>1f</b>	3'-CH <sub>3</sub> -Ph	125-126	Benzene/acetonitrile	65.9
<b>1g</b>	4'-CH <sub>3</sub> -Ph	151-152	Benzene/acetonitrile	90.1
<b>1h</b>	1-naphthyl	oil	Benzene/acetonitrile	98.2
<b>1i</b>	2-naphthyl	126-127	Benzene/acetonitrile	78.4
<b>1j</b>	4-biphenyl	150-151	Acetonitrile	93.0

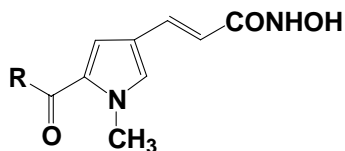


**Table 11.**

Compound	R	Melting point (°C)	recrystallization solvent	Yield (%)
<b>1'a</b>	Ph	144-145	Benzene	68.3
<b>1'b</b>	2'-Cl-Ph	146-148	Benzene	94.8
<b>1'c</b>	3'-Cl-Ph	164-165	Benzene/acetonitrile	89.1
<b>1'd</b>	4'-Cl-Ph	165-166	Benzene/acetonitrile	88.9
<b>1'e</b>	2'-CH <sub>3</sub> -Ph	218-220	Benzene/acetonitrile	97.8
<b>1'f</b>	3'-CH <sub>3</sub> -Ph	168-169	Benzene/acetonitrile	98.1
<b>1'g</b>	4'-CH <sub>3</sub> -Ph	168-169	Benzene/acetonitrile	98.9
<b>1'h</b>	1-naphthyl	140-141	Benzene	87.8
<b>1'i</b>	2-naphthyl	205-206	Benzene/acetonitrile	78.8
<b>1'j</b>	4-biphenyl	184-186	Acetonitrile	97.9

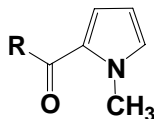


**Table 12.**

<b>Compound</b>	<b>R</b>	<b>Melting Point (°C)</b>	<b>Recrystallization solvent</b>	<b>Yield (%)</b>
<b>2a</b>	Ph	97-99	Cyclohexane	68.7
<b>2b</b>	2'-Cl-Ph	Oil	-	64
<b>2c</b>	3'-Cl-Ph	Oil	-	67
<b>2d</b>	4'-Cl-Ph	Oil	-	65.6
<b>2e</b>	2'-CH <sub>3</sub> -Ph	120-122	Cyclohexane	62
<b>2f</b>	3'-CH <sub>3</sub> -Ph	Oil	-	69.5
<b>2g</b>	4'-CH <sub>3</sub> -Ph	130-132	Cyclohexane/benzene	71
<b>2h</b>	1-naphthyl	116-118	Cyclohexane	63.8
<b>2i</b>	2-naphthyl	114-116	Cyclohexane	66.3
<b>2j</b>	4-biphenyl	81-83	Cyclohexane	63.4



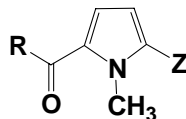


**Table 13.**

Compound	R	Z	Melting point (°C)	recrystallization solvent	Yield (%)
<b>3a</b>	Ph	CHO	88-89	Cyclohexane	84.6
<b>3b</b>	2'-Cl-Ph	CHO	oil	-	77.9
<b>3c</b>	3'-Cl-Ph	CHO	100-101	Cyclohexane	85.3
<b>3d</b>	4'-Cl-Ph	CHO	132-133	Cyclohexane/benzene	98.0
<b>3e</b>	2'-CH <sub>3</sub> -Ph	CHO	114-115	Cyclohexane/benzene	77.3
<b>3f</b>	3'-CH <sub>3</sub> -Ph	CHO	125-126	Cyclohexane	65.9
<b>3g</b>	4'-CH <sub>3</sub> -Ph	CHO	151-152	Cyclohexane/benzene	90.1
<b>3h</b>	1-naphthyl	CHO	oil	-	98.2
<b>3i</b>	2-naphthyl	CHO	126-127	Cyclohexane/benzene	78.4
<b>3j</b>	4-biphenyl	CHO	150-151	Cyclohexane/benzene	99.5
<b>4a</b>	Ph	CH=CHCOOEt	222-223	Benzene/acetonitrile	91.8
<b>4b</b>	2'-Cl-Ph	CH=CHCOOEt	163-164	Cyclohexane/benzene	93.0
<b>4c</b>	3'-Cl-Ph	CH=CHCOOEt	158-159	Benzene	89.6
<b>4d</b>	4'-Cl-Ph	CH=CHCOOEt	127-128	Benzene	87.3
<b>4e</b>	2'-CH <sub>3</sub> -Ph	CH=CHCOOEt	oil	-	68.7
<b>4f</b>	3'-CH <sub>3</sub> -Ph	CH=CHCOOEt	112-113	Cyclohexane	84.9

*Design, synthesis and biological validation of epigenetic modulators of histone/protein deacetylation and methylation.*

<b>4g</b>	4'-CH <sub>3</sub> -Ph	CH=CHCOOEt	129-130	Cyclohexane/benzene	95.3
<b>4h</b>	1-naphthyl	CH=CHCOOEt	oil	-	89.5
<b>4i</b>	2-naphthyl	CH=CHCOOEt	110-111	Cyclohexane	93.8
<b>4j</b>	4-biphenyl	CH=CHCOOEt	157-158	Cyclohexane/benzene	77.8
<b>5a</b>	Ph	CH=CHCOOH	188-189	Benzene	84.0
<b>5b</b>	2'-Cl-Ph	CH=CHCOOH	158-160	Acetonitrile	95.2
<b>5c</b>	3'-Cl-Ph	CH=CHCOOH	180-181	Acetonitrile	88.8
<b>5d</b>	4'-Cl-Ph	CH=CHCOOH	201-202	Acetonitrile	89.6
<b>5e</b>	2'-CH <sub>3</sub> -Ph	CH=CHCOOH	188-189	Acetonitrile	77.1
<b>5f</b>	3'-CH <sub>3</sub> -Ph	CH=CHCOOH	162-163	Acetonitrile	98.3
<b>5g</b>	4'-CH <sub>3</sub> -Ph	CH=CHCOOH	180-181	Acetonitrile	88.9
<b>5h</b>	1-naphthyl	CH=CHCOOH	199-200	Benzene	81.0
<b>5i</b>	2-naphthyl	CH=CHCOOH	237-238	Benzene/acetonitrile	87.9
<b>5j</b>	4-biphenyl	CH=CHCOOH	239-240	Benzene/acetonitrile	83.3

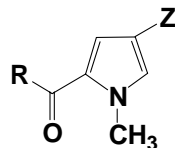


**Table 14.**

Compound	R	Z	Melting point (°C)	recrystallization solvent	Yield (%)
3'a	Ph	CHO	olio	-	75.0
3'b	2'-Cl-Ph	CHO	123-125	cyclohexane	79.3
3'c	3'-Cl-Ph	CHO	115-116	Cyclohexane/benzene	87.4
3'd	4'-Cl-Ph	CHO	148-149	Cyclohexane/benzene	94.1
3'e	2'-CH <sub>3</sub> -Ph	CHO	oil	-	84.2
3'f	3'-CH <sub>3</sub> -Ph	CHO	oil	-	82.9
3'g	4'-CH <sub>3</sub> -Ph	CHO	148-149	Cyclohexane/benzene	95.2
3'h	1-naphthyl	CHO	oil	-	98.0
3'i	2-naphthyl	CHO	145-146	cyclohexane	82.7
3'j	4-biphenyl	CHO	148-149	Cyclohexane/benzene	97.0
4'a	Ph	CH=CHCOOEt	178-179	Benzene	71.5
4'b	2'-Cl-Ph	CH=CHCOOEt	143-145	Cyclohexane/benzene	94.6
4'c	3'-Cl-Ph	CH=CHCOOEt	155-156	Benzene	84.2
4'd	4'-Cl-Ph	CH=CHCOOEt	135	Benzene	86.9
4'e	2'-CH <sub>3</sub> -Ph	CH=CHCOOEt	oil	-	75.9
4'f	3'-CH <sub>3</sub> -Ph	CH=CHCOOEt	109-110	Cyclohexane/benzene	89.2

4'g	4'-CH <sub>3</sub> -Ph	CH=CHCOOEt	135-136	Cyclohexane/benzene	97.0
4'h	1-naphthyl	CH=CHCOOEt	oil	-	92.7
4'i	2-naphthyl	CH=CHCOOEt	100-101	cyclohexane	91.0
4'j	4-biphenyl	CH=CHCOOEt	146-147	Cyclohexane/benzene	87.2
5'a	Ph	CH=CHCOOH	209-210	Benzene/acetonitrile	92.3
5'b	2'-Cl-Ph	CH=CHCOOH	193-195	Benzene/acetonitrile	98.8
5'c	3'-Cl-Ph	CH=CHCOOH	185-186	Acetonitrile	85.9
5'd	4'-Cl-Ph	CH=CHCOOH	228-229	Acetonitrile	91.5
5'e	2'-CH <sub>3</sub> -Ph	CH=CHCOOH	201-202	Benzene/acetonitrile	78.9
5'f	3'-CH <sub>3</sub> -Ph	CH=CHCOOH	159-160	Acetonitrile	98.7
5'g	4'-CH <sub>3</sub> -Ph	CH=CHCOOH	159-160	Acetonitrile	98.7
5'h	1-naphthyl	CH=CHCOOH	206-207	Acetonitrile	79.5
5'i	2-naphthyl	CH=CHCOOH	231-232	Benzene/acetonitrile	85..0
5'j	4-biphenyl	CH=CHCOOH	242-243	Benzene/acetonitrile	78.8

### 18.3. Experimental Section.

#### General procedure for the synthesis of 2-aryl-1-methyl-1H-pyrroles (2a-j).

##### Example: 2-(2'-chlorobenzoyl)-1-methyl-1H-pyrrole (2d).

1-methyl-1H-pyrrole (24.65 mmol; 2.2 ml) was added to a solution of 2-chlorobenzoylchloride (49.3 mmol; 6.32 ml) and BF<sub>3</sub>·Oet (49.3 mmol; 6.19 ml) in dichloromethane (100ml). After being stirred at room temperature for three days, water was slowly added to the reaction mixture. The organic layer was separated, and the aqueous one was extracted with chloroform (2 x 50 mL). The combined organic solutions were washed with water, dried, and evaporated to dryness. The residual oil (alpha+beta isomers) was chromatographed on silica gel eluting with ethyl acetate: n-hexane 1:10 to give as first eluate the pure desired compound **2d**. <sup>1</sup>H NMR (CDCl<sub>3</sub>) δ 4.08 (s, 3H, N-CH<sub>3</sub>), 6.10 (m, 1H, pyrrole H-4), 6.46 (d, 1H, pyrrole H-3), 6.93 (d, 1H, pyrrole H-5), 7.3-7.42 (m, 4H, benzene H-2-5).

**General procedure for the synthesis of 5-aryl-1-methyl-1H-pyrrole-2-carboxaldehyde (3a-j) and 5-aryl-1-methyl-1H-pyrrole-3-carboxaldehyde (3'a-j).**

**Example: 2-Benzoyl-1-methyl-1H-pyrrole-5-carboxaldehyde (3a) and 2-Benzoyl-1-methyl-1H-pyrrole-4-carboxaldehyde (3'a).**

A solution of oxalyl chloride (0.06 mol, 5.2 mL) in 1,2-dichloroethane was added to a cooled (0-5 °C) solution of *N,N*-dimethylformamide (0.06 mol, 4.6 mL) in 1,2-dichloroethane (50 mL) over a period of 5-10 min. After being stirred at room temperature for 15 min, the suspension was cooled (0-5 °C) again and treated with a solution of 2-benzoyl-1-methyl-1H-pyrrole (0.06 mol, 11.1 g) in 1,2-dichloroethane (50 mL). The mixture was stirred at room temperature for 1 h and then was poured onto crushed ice (200 g) containing 50% NaOH (50 mL) and stirred for 10 min. The pH of the solution was adjusted to 4 with 37% HCl, the organic layer was separated, and the aqueous one was extracted with chloroform (2 x 50 mL). The combined organic solutions were washed with water, dried, and evaporated to dryness. The residual oil was chromatographed on silica gel eluting with ethyl acetate:chloroform 1:10. The first eluates were collected and evaporated to afford **3a** as a pure solid; further elution gave **3a'** as a pure solid. **3a**: yield: 44%; mp: 90-91 °C, recrystallization solvent: cyclohexane; <sup>1</sup>H NMR (CDCl<sub>3</sub>) δ 4.23 (s, 3 H, CH<sub>3</sub>), 6.62 (m, 1 H, pyrrole β-proton), 6.87 (m, 1 H, pyrrole β-proton), 7.44 (m, 3 H, benzene H-3,4,5), 7.78 (m, 2 H, benzene H-2,6), 9.77 (s, 1 H, CHO). **3'a**: yield: 56%; mp: 108-109 °C, recrystallization solvent: cyclohexane; <sup>1</sup>H NMR (CDCl<sub>3</sub>) δ 4.04 (s, 3 H, CH<sub>3</sub>), 7.12 (d, 1 H, pyrrole β-proton), 7.47 (m, 4 H, pyrrole α-proton and benzene H-3,4,5), 7.76 (m, 2 H, benzene H-2,6), 9.74 (s, 1 H, CHO).

**General Procedure for the Synthesis of Ethyl 3-[(5-aryl)-1H-1-methyl-2-pyrrolyl]-propenoates and 3-[(5-aryl)-1H-1-methyl-3-pyrrolyl]-propenoates.**

**Example: Ethyl 3-[5-(2-naphthoyl)-1H-1-methyl-2-pyrrolyl]-propenoates (4i) and Ethyl 3-[5-(2-naphthoyl)-1H-1-methyl-3-pyrrolyl]-propenoates (4'i).**

A suspension of **3i** or **3'i** (1.03 mmol, 0.27 g) in absolute ethanol (20 mL) was added in one portion to a mixture of triethyl phosphonoacetate (1.2 eq, 1.24 mmol, 0.25 mL) and anhydrous potassium carbonate (2 eq, 2.06 mmol, 0.28 g). After stirring at 70 °C for 2 h, the reaction mixture was cooled to room temperature, diluted with water (50 mL) and extracted with ethyl acetate (3 x 30 mL). The organic layer was washed with water, dried with sodium sulfate and evaporated to dryness, the solid residue was recrystallized by cyclohexane to furnish pure **4i**

Yield: 93.8 %, mp: 110-111°C. <sup>1</sup>H NMR (CDCl<sub>3</sub>, 400 MHz, δ; ppm) δ 1.35 (m, 3H, CH<sub>2</sub>CH<sub>3</sub>), δ 4.10 (s, 3H, N-CH<sub>3</sub>), 4.28 (m, 3H, CH<sub>2</sub>CH<sub>3</sub>), 6.41 (d, 1H, CH=CHCOOEt), 6.65 (d, 1H, pyrrole *H*-3), 6.76 (d, 1H, d, 1H, pyrrole *H*-4), 7.57 (m, 2H, naphthalene *H*-6,7), 7.71 (d, 1H, CH=CHCOOEt), 7.90 (m, 4H, naphthalene *H*-3,4,5,8), 8.31 (s, 1H, naphthalene *H*-1) or **4'a** Yield: 91 %, mp: 100-101°C. NMR (CDCl<sub>3</sub>, 400 MHz, δ; ppm) δ 1.28 (m, 3H, CH<sub>2</sub>CH<sub>3</sub>), δ 4.06 (s, 3H, N-CH<sub>3</sub>), 4.21 (m, 3H, CH<sub>2</sub>CH<sub>3</sub>), 6.10 (d, 1H, CH=CHCOOEt), 6.96 (d, 1H, pyrrole *H*-4), 7.15 (s, 1H, pyrrole *H*-2), 7.53-7.61 (m, 3H, CH=CHCOOEt, naphthalene *H*-6,7), 7.87-7.97 (m, 4H, naphthalene *H*-3,4,5,8), 8.32 (s, 1H, naphthalene *H*-1).

**General Procedure for the Synthesis of 3-[(5-*aroyl*)-1*H*-1-methyl-2-pyrrolyl]-propenoic and 3-[(5-*aroyl*)-1*H*-1-methyl-3-pyrrolyl]-propenoic acids.**

**Example. 3-[5-(3'-methyl)-1*H*-1-methyl-2-pyrrolyl]-propenoic acid (5f) and Ethyl 3-[5-(2-naphthoyl)-1*H*-1-methyl-3-pyrrolyl]-propenoic acid (5'f).**

A mixture of **4f** or **4f'** (3.13 mmol, 0.93 g), 2 N KOH (4 eq, 12.52 mmol, 0.70 g, 6.26 ml H<sub>2</sub>O) and ethanol (15 mL) was stirred at room temperature overnight. Then the solution was poured into water (50 mL) and extracted with ethyl acetate (3 x 20 mL). To the aqueous layer 2 N HCl was added until the pH was 5, and the precipitate was filtered and recrystallized by acetonitrile to give pure compound **5f** Yield: 98.3 %, mp: 162-163 °C. NMR (DMSO-*d*<sub>6</sub>, 400 MHz, δ; ppm) δ 2.42 (s, 3H, CH<sub>3</sub>), 4.08 (s, 3H, N-CH<sub>3</sub>), 6.40 (d, 1H, CH=CHCOOH), 6.70 (m, 2H, pyrrole *H*-3,4) 7.35 (m, 2H, benzene *H*-3,4), 7.60 (m, 2H, benzene *H*-2,6), 7.79 (d, 1H, CH=CHCOOEt), 12 (s, 1H, COOH) or **5f'** Yield: 98.7%, mp: 159-160°C. NMR (DMSO-*d*<sub>6</sub>, 400 MHz, δ; ppm) δ 2.37 (s, 3H, CH<sub>3</sub>), 3.90 (s, 3H, N-CH<sub>3</sub>), 6.15 (d, 1H, CH=CHCOOH), 6.99 (s, 1H, pyrrole *H*-4), 7.34-7.43 (m, 3H: benzene *H*-3,4, CH=CHCOOEt), 7.53 (m, 2H, benzene *H*-2,6), 7.67 (s, 1H, pyrrole *H*-2), 12 (s, 1H, COOH).

**General Procedure for the Synthesis of 3-[(5-*aroyl*)-1*H*-1-methyl-2-pyrrolyl]-*N*-hydroxy-2-propenamide and 3-[5-*aroyl*)-1*H*-1-methyl-3-pyrrolyl]-*N*-hydroxy-2-propenamide.**

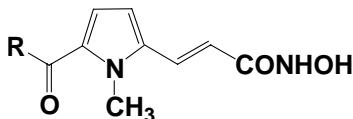
**Example. 3-[5-(4-biphenylcarbonyl)-1*H*-1-methyl-2-pyrrolyl]-*N*-hydroxy-2-propenamide (**1j**) and 3-[5-(4-biphenylcarbonyl)-1*H*-1-methyl-2-pyrrolyl]-*N*-hydroxy-2-propenamide (**1'j**).**

Ethyl chloroformate (1.2 eq, 1.88 mmol, 0.18 ml) and triethylamine (1.3 eq, 2.04 mmol, 0.28 ml) were added to a cooled (0 °C) solution of **5j** or **5'j** (1.57 mmol, 0.50 g) in dry THF (10 mL), and the mixture was stirred for 10 min. The solid was filtered off. To the filtrate was added O-(2-methoxypropyl)-hydroxylamine (3 eq, 4.71 mmol, 0.35 ml). The solution was stirred for 15 minutes at 0°C, then the mixture was evaporated under reduced pressure, the residue was eluted in methanol (10 ml) and to the solution of protected hydroxamate was added Amberlist 15 (157 mg) and the mixture was stirred at 45°C for 1 h. The resin was filtered and the filtrate was concentrated in vacuo to give compound **1j** recrystallized from acetonitrile. Yield: 93%, mp: 150-151°C. NMR (DMSO-*d*<sub>6</sub>, 400 MHz, δ; ppm) δ 3.98 (s, 3H, N-CH<sub>3</sub>), 6.45 (d, 1H, CH=CHCONHOH), 6.63 (d, 1H, pyrrole, *H*-3), 6.72 (d, 1H, pyrrole, *H*-4), 7.41-7.51 (m, 3H: CH=CHCOOEt, biphenyl *H*-3,5), 7.74 (d, 2H, biphenyl *H*-2,6), 7.81 (s, 5H, biphenyl *H*-2'-6'), 9 (s, 1H, NHOH), 10.75 (s, 1H, NHOH).

#### 18.4. Biological evaluation.

In anti-HD2 assay, **8a** and **9a** were 16- and 76-times more effective in inhibiting the enzyme than **1a**, **9a** being as potent as SAHA and 7-times less active than TSA.

Biological data related to HD2 also underlined as in 2,5 isomers (**8b-g**) the introduction of chloro or methyl groups was well tolerated in *para* but not in *orto* position; furthermore *meta* substitution improved HD2 inhibiting activity (**8c**: IC<sub>50</sub>(HD2)=0.09 μM).



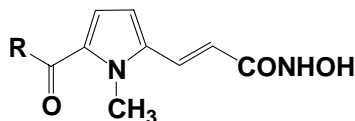


**Table 15.** Inhibiting activity of the compounds **1a-j**.

Compound	R	IC <sub>50</sub> (μM)		
		<i>zmHD</i> <sub>2</sub>	<i>zmHD</i> <sub>1-B</sub>	<i>zmHD</i> <sub>1-A</sub>
<b>1a</b>	Ph	0.23	0.176	0.093
<b>1b</b>	2 <sup>o</sup> -Cl-Ph	0.32	1.59	0.682
<b>1c</b>	3 <sup>o</sup> -Cl-Ph	0.09	1.04	0.104
<b>1d</b>	4 <sup>o</sup> -Cl-Ph	0.239	0.445	0.131
<b>1e</b>	2 <sup>o</sup> -CH <sub>3</sub> -Ph	0.312	0.413	0.309
<b>1f</b>	3 <sup>o</sup> -CH <sub>3</sub> -Ph	0.189	0.225	0.104
<b>1g</b>	4 <sup>o</sup> -CH <sub>3</sub> -Ph	0.192	0.391	0.093
<b>1h</b>	1-naphthyl	0.131	0.046	0.264
<b>1i</b>	2-naphthyl	0.668	0.56	0.812
<b>1j</b>	4-biphenyl	2.8	2.2	2.76
<b>1</b>	none	3.8	ND <sup>b</sup>	ND <sup>b</sup>
sodium valproate		128	-	-
TSA		0.0072	0.0004	0.0008
SAHA		0.05	0.028	0.178
trapoxin		0.01	-	-
HC-toxin		0.11	-	-

Data represent mean values of at least three separate experiments.



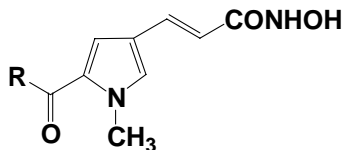


**Table 16.** Inhibiting activity of the compounds **1'a-j**.

Compound	R	IC <sub>50</sub> (μM)		
		<i>zmHD2</i>	<i>zmHD1-B</i>	<i>zmHD1-A</i>
<b>1'a</b>	Ph	0.05	0.152	0.02
<b>1'b</b>	2'-Cl-Ph	0.198	0.32	0.116
<b>1'c</b>	3'-Cl-Ph	0.178	0.24	0.053
<b>1'd</b>	4'-Cl-Ph	0.161	0.17	0.075
<b>1'e</b>	2'-CH <sub>3</sub> -Ph	0.061	0.133	0.011
<b>1'f</b>	3'-CH <sub>3</sub> -Ph	0.101	0.166	0.021
<b>1'g</b>	4'-CH <sub>3</sub> -Ph	0.146	0.068	0.168
<b>1'h</b>	1-naphthyl	0.013	0.012	0.075
<b>1'i</b>	2-naphthyl	0.049	0.089	0.043
<b>1'j</b>	4-biphenyl	0.048	0.031	0.146
<b>1</b>	none	3.8	ND <sup>b</sup>	ND <sup>b</sup>
sodium valproate		128	-	-
TSA		0.0072	0.0004	0.0008
SAHA		0.05	0.028	0.178
trapoxin		0.01	-	-
HC-toxin		0.11	-	-

Data represent mean values of at least three separate experiments.

In this series inhibiting activity decreased with the replacement of the phenyl ring with 2-naphthyl (**1i**) or biphenyl (**1j**) groups while 1-naphthyl derivative (**1h**) was 1.8 and 29-fold respectively more potent than **1a** and **1**.

2,4 isomers showed a different trend on HD2: only methyl substitution in *orto* (**1'e**: IC<sub>50</sub> HD2=0.061 μM) kept biological activity while all chloro derivatives (**1'b-d**) were less active than lead **1'a**.

As in 2,5 series, 1-naphthyl derivative **1h** was 4.6 fold more efficient than lead (**1h**: IC<sub>50</sub> HD2=0.013 μM); 2-naphthyl and biphenyl groups didn't affect inhibitory potency.

The two isomers **1a**, **1'a** were tested also on HD1-B (homologue of class I HDACs) and HD1-A (homologue of class II HDACs) to underline a possible class selectivity: both were selective towards class II, being **1'a** 7-fold more potent on HD1-A than HD1-B (IC<sub>50</sub> (HD1-B)=0.152 μM; IC<sub>50</sub>(HD1-A)=0.021 μM).

Biological screening on HD1-B showed as in 2,5 series chloro/methyl substitutions (in all positions) and replacement with 2-naphthyl or biphenyl groups led to an inhibiting activity decrease; whereas **1h** (1-naphthyl derivative) was 3.8 times more potent than **1a** on this enzyme.

In 2,4 series, chloro and methyl insertion in *para* position respectively kept or improves biological activity (**1'd**: IC<sub>50</sub> (HD1-B)=0.17 μM; **1'g**: IC<sub>50</sub> (HD1-B)=0.068 μM). 1-naphthyl (**1'h**), 2-naphthyl (**1'i**) and biphenyl (**1'j**) derivatives were all more potent than **1'a**: **1'h** IC<sub>50</sub> (HD1-B)=0.012 μM.

Finally enzymatic screening on HD1-A showed as in 2,5 series all compounds were less or as active (**1c,f,g**: respectively *meta*-Cl, *meta*-CH<sub>3</sub>, *para*-CH<sub>3</sub> derivatives) as lead **1a**.

In 2,4 series, methyl was well tolerated in *orto* and *meta* position (*orto*- CH<sub>3</sub> derivative **1'e** was 2-fold more potent than lead **1'a**); chloro substitution and big aromatic groups caused an inhibiting activity decrease.

In conclusion we can underline these SAR features:

(i) in 2,5 series, insertion of chloro or methyl groups was well tolerated in *meta* and *para* positions in all the enzymatic screening (HD2, HD1-B, HD1-A); *orto* substitution caused an inhibiting activity decrease. 2-naphthyl (**1i**) and 4-biphenyl (**1l**) derivatives were always less active than lead **1a**, while 1-naphthyl compound **1h** was more active on HD2 and HD1-B and less active on HD1-A.

(ii) in 2,4 series, insertion of a methyl group was favourable only in *orto* position (**1'e**); *meta* and *para* substitutions (**1'f,g**) led to less active derivative with the exception of *para*-methyl compound **1'g** on HD1-B.

Chlorine in all positions (**1'b-d**) caused a decrease of inhibiting activity.

With regard to 1/2 naphthyl and biphenyl derivatives (**1'h-l**), biological data showed that 1-naphthyl **1'h** was more active than lead **1'a** on HD2 and HD1-B but not on HD1-A; 2-naphthyl and biphenyl derivatives (**1'i,l**) were more active than lead only on HD1-B.

(iii) about class selectivity, the best selective compounds were **1c** (2,5 series; 3-Cl derivative; IC<sub>50</sub> (HD1-B)=1.04 μM; IC<sub>50</sub>(HD1-A)=0.1 μM) and **1'e** (2,4 series; 2- CH<sub>3</sub> derivative; IC<sub>50</sub> (HD1-B)=0.133 μM; IC<sub>50</sub>(HD1-A)=0.011 μM) respectively 10 and 11 fold more potent on class II than class I.

#### *18.5. Modification of the connection unit and aromatic spacer.*

Another development of the our HDAC inhibitors was the replacement of the connection unit and aromatic spacer common to all synthesized derivatives, in fact we have substituted the ketone (C.U) with the amidic function and the pyrrole (aromatic spacer) with the benzene ring, so obtaining the new acylaminocinnamyl *N*-hydroxyamides.

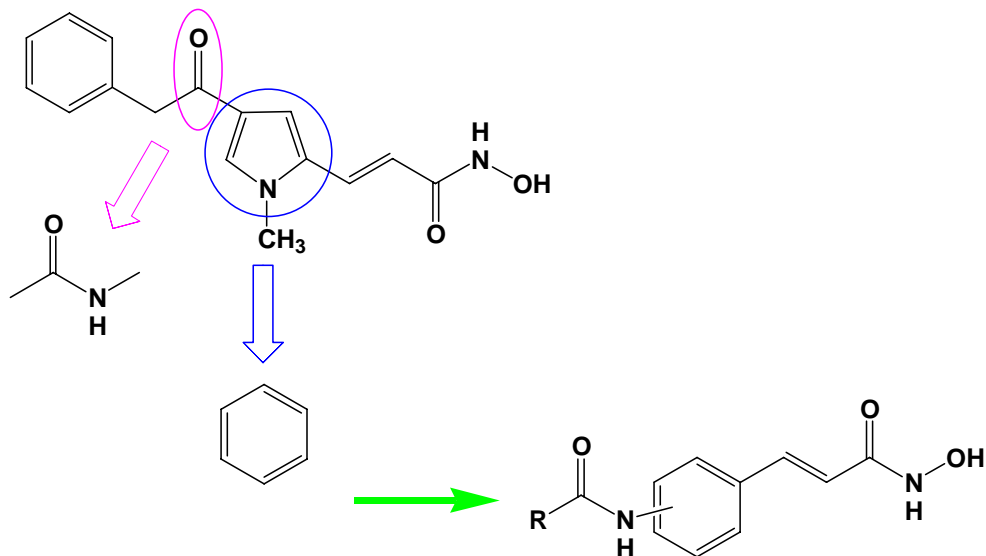
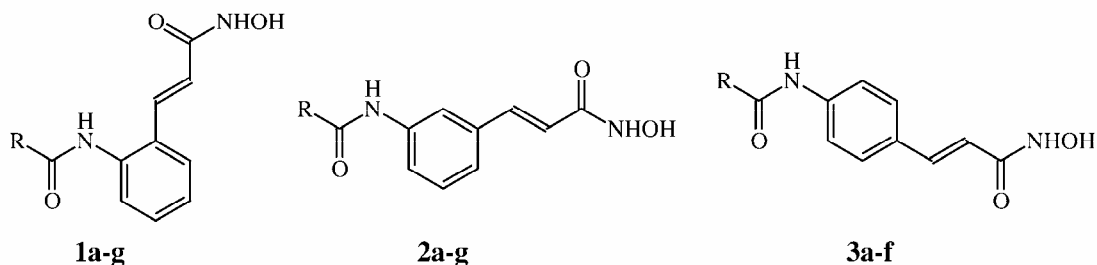


**Figure 38.** Rational design.

Then we synthesized a new class of compounds having a cinnamyl-hydroxamate (HS plus EIG) function linked to 2-, 3-, or 4-acylamino moiety (CAP plus CU) (compounds **1-3**, Fig. (39)), and the new derivatives were tested against three maize enzymes with deacetylase activity, *ie* HD2, HD1-B (homologue of mammalian class I HDACs), and HD1-A (homologue of mammalian class II HDACs).

Cinnamyl-hydroxyamides bearing acylamino substituents at the C2 position of the benzene ring (compounds **1a-g**) showed very low HDAC inhibiting activities, with  $IC_{50}$  values in the high micromolar range. By shifting the same acylamino groups from C2 to C3 (compounds **2a-g**) as well as C4 (compounds **3a-f**) position of the benzene ring, a number of highly potent HDAC inhibitors have been obtained.



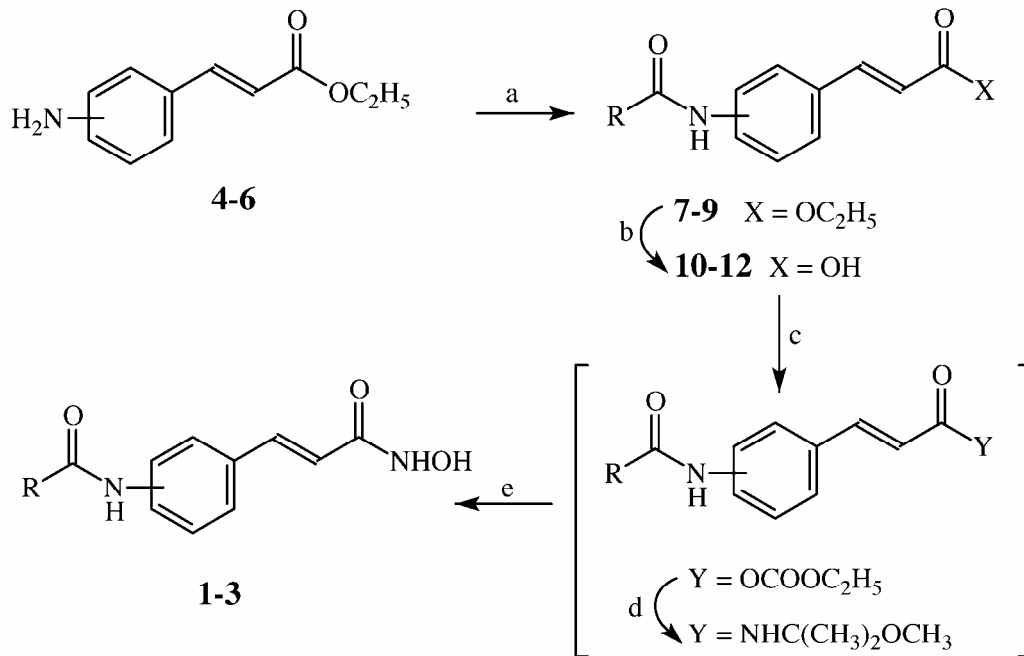
R = Ph, PhCH<sub>2</sub>, PhCH<sub>2</sub>CH<sub>2</sub>, PhCH=CH, 1-Naphthyl, 2-Naphthyl, 4-Biphenyl

**Figure 39.** 2-Acyloaminocinnamyl-*N*-hydroxyamides **1**, 3-acyloaminocinnamyl-*N*-hydroxyamides **2**, and 4-acyloaminocinnamyl-*N*-hydroxyamides **3**.

### 18.6. Chemistry.

Ethyl 2-, 3-, and 4-aminocinnamates **4-6** were treated with the appropriate acyl chloride in the presence of triethylamine to afford the amido-esters **7a-g**, **8a-g**, and **9a-g**, which were in turn hydrolyzed in alkaline medium to the corresponding carboxylic acids **10a-g**, **11a-g**, and **12a-f**. Strangely, the hydrolysis under basic conditions (NaOH, KOH, LiOH) of the ethyl 4-(4-biphenylcarbonylamino)cinnamate **9g** failed to give the corresponding cinnamic acid. Further conversion of **10-12** into the desired hydroxamates **1-3** has been accomplished by a one-pot, three step procedure involving (i) the formation of mixed anhydrides between **10-12** and ethyl chloroformate in the presence of triethylamine, (ii) the reaction of such activated anhydrides with *O*-(2-methoxy-2-propyl)hydroxylamine, and (iii) acidic hydrolysis of the *O*-(2-methoxy-2-propyl)hydroxamates with the Amberlyst<sup>®</sup> 15 ion-exchange resin (Scheme 1). All compounds were purified by crystallization.

Chemical and physical data of compounds **1-3** are listed in Table 17. Chemical and physical data of the intermediate compounds **7-12** are reported in Table 18.



**Scheme 1.** <sup>a</sup>(a) RCOCl, (C<sub>2</sub>H<sub>5</sub>)<sub>3</sub>N, CH<sub>2</sub>Cl<sub>2</sub>, room temp. (b) LiOH, H<sub>2</sub>O, room temp. (c) ClCOOC<sub>2</sub>H<sub>5</sub>, (C<sub>2</sub>H<sub>5</sub>)<sub>3</sub>N, THF, 0 °C. (d) NH<sub>2</sub>OC(CH<sub>3</sub>)<sub>2</sub>OCH<sub>3</sub>, room temp. (e) Amberlyst 15, CH<sub>3</sub>OH, room temp.

**Table 17.** Chemical and physical properties of compounds **1-3**.

compd	R	mp, °C	recrystall. solvent	yield, %
<b>1a</b>	Ph	170-172	benzene	53
<b>1b</b>	PhCH <sub>2</sub>	158-160	benzene	55
<b>1c</b>	PhCH <sub>2</sub> CH <sub>2</sub>	150-151	benzene	54
<b>1d</b>	PhCH=CH	128-130	benzene	47
<b>1e</b>	1-naphthyl	195-196	MeOH	65
<b>1f</b>	2-naphthyl	128-130	benzene	67
<b>1g</b>	4-biphenyl	124-125	benzene	48
<b>2a</b>	Ph	213-214	THF	51
<b>2b</b>	PhCH <sub>2</sub>	183-184	THF	50
<b>2c</b>	PhCH <sub>2</sub> CH <sub>2</sub>	179-180	THF	56
<b>2d</b>	PhCH=CH	86-87	Et <sub>2</sub> O	45
<b>2e</b>	1-naphthyl	191-192	MeOH	61
<b>2f</b>	2-naphthyl	182-183	MeOH	59
<b>2g</b>	4-biphenyl	213-214	MeOH	53
<b>3a</b>	Ph	212-213	THF	54

*Design, synthesis and biological validation of epigenetic modulators of histone/protein deacetylation and methylation.*

<b>3b</b>	PhCH <sub>2</sub>	198-199	THF	55
<b>3c</b>	PhCH <sub>2</sub> CH <sub>2</sub>	204-205	THF	51
<b>3d</b>	PhCH=CH	218-220	THF	49
<b>3e</b>	1-naphthyl	210-211	MeOH	63
<b>3f</b>	2-naphthyl	223-224	MeOH	58



**Table 18.** Chemical and physical properties of compounds **7-12**.

compd	R	X	mp, °C	recrystall. solvent	yield, %
<b>7a</b>	Ph	COOC <sub>2</sub> H <sub>5</sub>	137-139	toluene	73
<b>7b</b>	PhCH <sub>2</sub>	COOC <sub>2</sub> H <sub>5</sub>	123-124	toluene	58
<b>7c</b>	PhCH <sub>2</sub> CH <sub>2</sub>	COOC <sub>2</sub> H <sub>5</sub>	119-120	toluene	72
<b>7d</b>	PhCH=CH	COOC <sub>2</sub> H <sub>5</sub>	114-116	toluene	60
<b>7e</b>	1-naphthyl	COOC <sub>2</sub> H <sub>5</sub>	182-183	toluene	75
<b>7f</b>	2-naphthyl	COOC <sub>2</sub> H <sub>5</sub>	168-169	toluene	78
<b>7g</b>	4-biphenyl	COOC <sub>2</sub> H <sub>5</sub>	173-174	toluene	71
<b>8a</b>	Ph	COOC <sub>2</sub> H <sub>5</sub>	110-111	CH <sub>2</sub> Cl <sub>2</sub> / <i>n</i> -hexane	75
<b>8b</b>	PhCH <sub>2</sub>	COOC <sub>2</sub> H <sub>5</sub>	97-98	CH <sub>2</sub> Cl <sub>2</sub> / <i>n</i> -hexane	83
<b>8c</b>	PhCH <sub>2</sub> CH <sub>2</sub>	COOC <sub>2</sub> H <sub>5</sub>	90-92	CH <sub>2</sub> Cl <sub>2</sub> / <i>n</i> -hexane	80
<b>8d</b>	PhCH=CH	COOC <sub>2</sub> H <sub>5</sub>	94-95	CH <sub>2</sub> Cl <sub>2</sub> / <i>n</i> -hexane	68
<b>8e</b>	1-naphthyl	COOC <sub>2</sub> H <sub>5</sub>	155-156	toluene	81
<b>8f</b>	2-naphthyl	COOC <sub>2</sub> H <sub>5</sub>	115-116	toluene	83
<b>8g</b>	4-biphenyl	COOC <sub>2</sub> H <sub>5</sub>	174-175	toluene	69
<b>9a</b>	Ph	COOC <sub>2</sub> H <sub>5</sub>	144-146	CH <sub>2</sub> Cl <sub>2</sub> / <i>n</i> -hexane	71
<b>9b</b>	PhCH <sub>2</sub>	COOC <sub>2</sub> H <sub>5</sub>	158-160	CH <sub>2</sub> Cl <sub>2</sub> / <i>n</i> -hexane	78
<b>9c</b>	PhCH <sub>2</sub> CH <sub>2</sub>	COOC <sub>2</sub> H <sub>5</sub>	124-126	CH <sub>2</sub> Cl <sub>2</sub> / <i>n</i> -hexane	77
<b>9d</b>	PhCH=CH	COOC <sub>2</sub> H <sub>5</sub>	153-155	CH <sub>2</sub> Cl <sub>2</sub> / <i>n</i> -hexane	68
<b>9e</b>	1-naphthyl	COOC <sub>2</sub> H <sub>5</sub>	169-170	toluene	80

*Design, synthesis and biological validation of epigenetic modulators of histone/protein deacetylation and methylation.*

---

<b>9f</b>	2-naphthyl	COOC <sub>2</sub> H <sub>5</sub>	161-162	toluene	85
<b>9g</b>	4-biphenyl	COOC <sub>2</sub> H <sub>5</sub>	246-248	toluene	78
<b>10a</b>	Ph	COOH	185-186	MeOH	75
<b>10b</b>	PhCH <sub>2</sub>	COOH	207-208	MeOH	79
<b>10c</b>	PhCH <sub>2</sub> CH <sub>2</sub>	COOH	235-236	MeOH	78
<b>10d</b>	PhCH=CH	COOH	265-266	MeOH	65
<b>10e</b>	1-naphthyl	COOH	166-168	EtOH	83
<b>10f</b>	2-naphthyl	COOH	146-147	EtOH	79
<b>10g</b>	4-biphenyl	COOH	270-271	MeOH	75
<b>11a</b>	Ph	COOH	230-231	MeOH	74
<b>11b</b>	PhCH <sub>2</sub>	COOH	207-209	MeOH	80
<b>11c</b>	PhCH <sub>2</sub> CH <sub>2</sub>	COOH	196-198	MeOH	81
<b>11d</b>	PhCH=CH	COOH	>280	MeOH	71
<b>11e</b>	1-naphthyl	COOH	>280	EtOH	87
<b>11f</b>	2-naphthyl	COOH	236-237	EtOH	77
<b>11g</b>	4-biphenyl	COOH	>280	MeOH	74
<b>12a</b>	Ph	COOH	252-254	MeOH	78
<b>12b</b>	PhCH <sub>2</sub>	COOH	>280	MeOH	83
<b>12c</b>	PhCH <sub>2</sub> CH <sub>2</sub>	COOH	>280	MeOH	76
<b>12d</b>	PhCH=CH	COOH	260-262	MeOH	67
<b>12e</b>	1-naphthyl	COOH	248-249	MeOH	91

---

<b>12f</b>	2-naphthyl	COOH	>280	MeOH	84
------------	------------	------	------	------	----

### 18.6. Experimental section.

*Chemistry.* Melting points were determined on a Buchi 530 melting point apparatus and are uncorrected. Infrared (IR) spectra (KBr) were recorded on a Perkin- Elmer Spectrum One instrument. <sup>1</sup>H NMR spectra were recorded at 200 MHz on a Bruker AC 200 spectrometer; chemical shifts are reported in  $\delta$  (ppm) units relative to the internal reference tetramethylsilane (Me<sub>4</sub>Si). All compounds were routinely checked by TLC and <sup>1</sup>H NMR. Mass spectra (MS) were obtained on a JEOL JMS-HX 110 spectrometer. TLC was performed on aluminum-backed silica gel plates (Merck DC-Alufolien Kieselgel 60 F<sub>254</sub>) with spots visualized by UV light. All solvents were reagent grade and, when necessary, were purified and dried by standard methods. Concentration of solutions after reactions and extraction involved the use of a rotary evaporator operating at a reduced pressure of *ca.* 20 Torr. Organic solutions were dried over anhydrous sodium sulfate. Analytical results are within  $-0.40$  and  $+0.40\%$  of the theoretical values. All chemicals were purchased from Aldrich Chimica, Milan (Italy) or Lancaster Synthesis GmbH, Milan (Italy) and were of the highest purity.

**General procedure for the synthesis of ethyl 3-(2-acylaminophenyl)-2-propenoates 7a-g, ethyl 3-(3-acylaminophenyl)-2-propenoates 8a-g, and 4-(4-acylaminophenyl)-2-propenoates 9a-g. Example: Ethyl 3-[4-(3-phenylpropionyl)aminophenyl]-2-propenoate (9c).** 3-Phenylpropionyl chloride (3.7 mmol, 0.5 mL) and triethylamine (7.7 mmol, 1.1 mL) were added to a solution of ethyl 3-(4-aminophenyl)-2-propenoate hydrochloride **6** (3.1 mmol, 0.7 g) in dry dichloromethane (20 mL) at 0 °C under nitrogen atmosphere. After stirring at room temperature for 4 h, the reaction mixture was poured into water (50 mL), the organic layer was separated, and the aqueous one was extracted with chloroform (2 x 50 mL). The combined organic solution was washed with water (100 mL) and brine (100 mL), and was dried and evaporated to dryness. The residual solid was purified by crystallization from dichloromethane/*n*-hexane to yield pure **9c**. <sup>1</sup>H NMR (CDCl<sub>3</sub>)  $\delta$  1.31-1.34 (t, 3 H, COOCH<sub>2</sub>CH<sub>3</sub>), 2.66-2.70 (t, 2 H, PhCH<sub>2</sub>CH<sub>2</sub>CO), 3.02-3.06 (t, 2 H, PhCH<sub>2</sub>CH<sub>2</sub>CO), 4.22-

4.27 (q, 2 H, COOCH<sub>2</sub>CH<sub>3</sub>), 6.32-6.36 (d, 1 H, CH=CHCO), 7.21-7.23 (m, 2 H, benzene H-2,6), 7.27-7.29 (m, 2 H, benzene H-3,5), 7.42-7.50 (m, 5 H, benzene H-2'-6'), 7.59-7.63 (d, 1 H, CH=CHCO). Low resolution MS (EI<sup>+</sup>) *m/z* 324 (M<sup>+</sup>).

**General procedure for the synthesis of 3-(2-acylaminophenyl)-2-propenoic acids 10a-g, 3-(3-acylaminophenyl)-2-propenoic acids 11a-g, and 3-(4-acylaminophenyl)-2-propenoic acids 12a-f. Example: 3-[2-(3-Phenyl-2-propenoylamino)phenyl]-2-propenoic acid (10d).** A mixture of ethyl 3-[2-(3-phenyl-2-propenoylamino)phenyl]-2-propenoate (**7d**) (2.0 mmol, 0.6 g), lithium hydroxide hydrate (4.0 mmol, 0.17 g), and ethanol (15 mL) was stirred at room temperature. After 24 h, 2 N HCl was added to the mixture until the pH was 5, and the obtained solid was filtered and recrystallized from methanol to yield pure **10d**. <sup>1</sup>H NMR (DMSO-*d*<sub>6</sub>) δ 6.47-6.51 (d, 1H, CH=CHCOOH), 6.92-6.96 (d, 1H, CH=CHCONH), 7.23-7.27 (m, 1 H, benzene H-5), 7.40-7.46 (m, 3 H, benzene H-4,6,4'), 7.51-7.57 (m, 2 H, benzene H-3',5'), 7.61-7.64 (m, 3 H, benzene H-3,2',6'), 7.73-7.77 (d, 1H, CH=CHCOOH), 7.80-7.82 (d, 1 H, CH=CHCONH), 12.50 (bs, 1H, COOH exchangeable with D<sub>2</sub>O). Low resolution MS (EI<sup>+</sup>) *m/z* 294 (M<sup>+</sup>).

**General procedure for the synthesis of 3-(2-acylaminophenyl)-*N*-hydroxy-2-propenamides 1a-g, 3-(3-acylaminophenyl)-*N*-hydroxy-2-propenamides 2a-g, and 3-(4-acylaminophenyl)-*N*-hydroxy-2-propenamides 3a-f. Example: 3-[4-(2-Naphthoylamino)phenyl]-*N*-hydroxy-2-propenamide (3f).** Ethyl chloroformate (2.9 mmol, 0.3 mL) and triethylamine (3.1 mmol, 0.4 mL) were added to a cooled (0 °C) solution of 3-[4-(2-naphthoylamino)phenyl]-2-propenoic acid **12f** (1.5 mmol, 0.5 g) in dry THF (10 mL), and the mixture was stirred for 10 min. The solid was filtered off, and *O*-(2-methoxy-2-propyl)hydroxylamine (4.71 mmol, 0.35 mL) was added to the filtrate. The solution was stirred for 15 min at 0 °C, then was evaporated under reduced pressure, and the residue was diluted in methanol (10 mL). Amberlyst<sup>®</sup> 15 ion-exchange resin (0.16 g) was added to the solution of the *O*-protected hydroxamate, and the mixture was stirred at room temperature for 1 h. After, the reaction was filtered and the filtrate was concentrated in vacuo to give the crude **3f** which was purified by crystallization. <sup>1</sup>H NMR (DMSO-*d*<sub>6</sub>) δ 6.39-6.43 (d, 1 H, CH=CHCO), 7.42-7.46 (d, 1 H, CH=CHCO), 7.57-7.62 (m, 5 H, benzene H-2,6 and naphthalene H-5-7), 7.75-7.76 (d, 1 H, naphthalene H-8), 7.85-7.87 (d, 2 H, benzene H-3,5),

8.00-8.02 (m, 1 H, naphthalene H-4), 8.06-8.08 (d, 1 H, naphthalene H-3), 8.16-8.18 (m, 1 H, naphthalene H-1), 9.03 (bs, 1 H, OH exchangeable with D<sub>2</sub>O), 10.74 (s, 2 H, NH exchangeable with D<sub>2</sub>O). Low resolution MS (EI<sup>+</sup>) *m/z* 333 (M<sup>+</sup>).

*18.7. Biological evaluation, results and discussion.*

**Table 19.** HD2 inhibitory activity of compounds **1-3<sup>a</sup>**

compound	R	% inhbtn (fixed dose, $\mu$ M)	IC <sub>50</sub> $\pm$ SD ( $\mu$ M)
<b>1a</b>	Ph	43.9 (27.2)	33.6 $\pm$ 1344
<b>1b</b>	PhCH <sub>2</sub>	58 (26)	14.5 $\pm$ 725
<b>1c</b>	PhCH <sub>2</sub> CH <sub>2</sub>	28.4 (24.8)	48.2 $\pm$ 1928
<b>1d</b>	PhCH=CH	72.5 (25)	8.1 $\pm$ 405
<b>1e</b>	1-naphthyl	32 (23.1)	41.6 $\pm$ 2080
<b>1f</b>	2-naphthyl	48.6 (23.1)	24.8 $\pm$ 744
<b>1g</b>	4-biphenyl	54.2 (21.4)	19.3 $\pm$ 965
<b>2a</b>	Ph	94.7 (27.2)	0.130 $\pm$ 3.9
<b>2b</b>	PhCH <sub>2</sub>	97.4 (25.9)	0.085 $\pm$ 4.2
<b>2c</b>	PhCH <sub>2</sub> CH <sub>2</sub>	96.8 (24.8)	0.090 $\pm$ 2.7
<b>2d</b>	PhCH=CH	95.2 (24.9)	0.092 $\pm$ 2.8
<b>2e</b>	1-naphthyl	96.2 (23.1)	0.112 $\pm$ 3.4
<b>2f</b>	2-naphthyl	96.3 (23.1)	0.102 $\pm$ 4.1

<b>2g</b>	4-biphenyl	89.2 (21.4)	0.096 ± 4.8
<b>3a</b>	Ph	93.7 (27.2)	0.168 ± 6.7
<b>3b</b>	PhCH <sub>2</sub>	97.3 (26)	0.065 ± 3.2
<b>3c</b>	PhCH <sub>2</sub> CH <sub>2</sub>	98 (24.8)	0.011 ± 0.5
<b>3d</b>	PhCH=CH	94.3 (24.9)	0.077 ± 3.1
<b>3e</b>	1-naphthyl	96.4 (23.1)	0.69 ± 2.8
<b>3f</b>	2-naphthyl	96.3 (23.1)	0.84 ± 3.4
sodium butyrate		35 (5000)	-
sodium valproate			128 ± 3800
TSA			0.007.2 ± 0.2
SAHA			0.050 ± 1.5
trapoxin			0.010 ± 0.3
HC-toxin			0.110 ± 4.4

<sup>a</sup>Data represent mean values of at least three separate experiments

**Table 20.** HD1-B and HD1-A inhibitory activity of compounds **1-3<sup>a</sup>**

compd	R	IC <sub>50</sub> ± SD (μM)		class selectivity	
		HD1-B	HD1-A	class I	class II
<b>1a</b>	Ph	32.2 ± 1610	34.1 ± 1364		
<b>1b</b>	PhCH <sub>2</sub>	23.2 ± 696	23.0 ± 920		
<b>1c</b>	PhCH <sub>2</sub> CH <sub>2</sub>	42.0 ± 1680	NI <sup>b</sup>		

<b>1d</b>	PhCH=CH	13.0 ± 520	11.5 ± 690	
<b>1e</b>	1-naphthyl	52.0 ± 2080	17.8 ± 1068	2.9
<b>1f</b>	2-naphthyl	22.0 ± 1100	26.1 ± 1044	
<b>1g</b>	4-biphenyl	23.2 ± 1160	14.1 ± 423	1.6
<b>2a</b>	Ph	0.302 ± 15.1	0.070 ± 3.5	4.3
<b>2b</b>	PhCH <sub>2</sub>	0.192 ± 9.6	0.081 ± 3.2	2.4
<b>2c</b>	PhCH <sub>2</sub> CH <sub>2</sub>	0.114 ± 3.4	0.094 ± 3.8	
<b>2d</b>	PhCH=CH	0.232 ± 13.9	0.152 ± 6.1	
<b>2e</b>	1-naphthyl	0.216 ± 8.6	0.102 ± 5.1	2.1
<b>2f</b>	2-naphthyl	0.168 ± 5.0	0.090 ± 4.5	1.9
<b>2g</b>	4-biphenyl	0.206 ± 10.3	0.120 ± 3.6	1.7
<b>3a</b>	Ph	0.239 ± 7.1	0.130 ± 6.5	1.8
<b>3b</b>	PhCH <sub>2</sub>	0.092 ± 2.8	0.072 ± 3.6	
<b>3c</b>	PhCH <sub>2</sub> CH <sub>2</sub>	0.102 ± 6.1	0.076 ± 3.0	
<b>3d</b>	PhCH=CH	0.126 ± 5.0	0.101 ± 5.0	
<b>3e</b>	1-naphthyl	0.115 ± 4.6	0.059 ± 2.9	1.9
<b>3f</b>	2-naphthyl	0.036 ± 1.4	0.042 ± 1.3	
TSA		0.0004 ± 0.01	0.0008 ± 0.03	2
SAHA		0.030 ± 1.0	0.200 ± 9.0	6.7

<sup>a</sup>Data represent mean values of at least three separate experiments. <sup>b</sup>NI, no inhibition.

Compounds **1-3** have been evaluated for their inhibiting activities against three maize HDAC enzymes, namely HD2, HD1-B, and HD1-A. In the anti-HD2 assay, the percent of inhibition displayed by **1-3** at a fixed dose (ranged from 20 to 30  $\mu\text{M}$ , see Table 18) and their  $\text{IC}_{50}$  (50% inhibitory concentration) values in comparison with those of two short-chain fatty acids (sodium butyrate and sodium valproate), two hydroxamic acids (TSA and SAHA), and two cyclic tetrapeptides (trapoxin and HC-toxin) as reference drugs have been reported (Table 18). Table 19 shows the inhibiting effect ( $\text{IC}_{50}$  values) of **1-3** against HD1-B and HD1-A enzymes in comparison with TSA and SAHA, and the resulting fold-selectivity values (for class I HDACs:  $\text{IC}_{50\text{-HD1-A}}/\text{IC}_{50\text{-HD1-B}}$  ratio; for class II HDACs:  $\text{IC}_{50\text{-HD1-B}}/\text{IC}_{50\text{-HD1-A}}$  ratio) have been assessed. From both anti-HD2 and -HD1-B/-HD1-A assays, inhibitory data clearly showed that the 2-acylamino-cinnamyl-*N*-hydroxyamides **1a-g** are endowed with poor deacetylase inhibiting activity, their  $\text{IC}_{50}$  values being in the range 8.1-52.0  $\mu\text{M}$ . The most potent compound is the 2-cinnamoylamino derivative **1d**, its  $\text{IC}_{50}$  values being 8.1, 13.0, and 11.5  $\mu\text{M}$  against HD2, HD1-B, and HD1-A respectively.

Instead, the 3-acylamino- and the 4-acylamino-isomers **2** and **3** were very efficient in HDAC inhibition with inhibitory values in the nanomolar range. In particular, against HD2 the 3-acylamino-substituted compounds **2a-g** showed  $\text{IC}_{50}$  values from 85 to 130 nM. The less active derivative was the 3-benzoylamino **2a** ( $\text{IC}_{50} = 130$  nM). By insertion of one or two carbon atom units between the benzene ring and the carbonyl group of the **2a** benzoyl portion, as well as by replacement of the benzene ring with bulkier aromatic groups (1-naphthyl, 2-naphthyl, 4-biphenyl), highly potent compounds have been obtained (**2b-g**;  $\text{IC}_{50}$  values: 85-112 nM). The activities of **2a-g** against HD1-B and HD1-A enzymes were still in the nanomolar range ( $\text{IC}_{50}$  values = 70-302 nM), but while in the anti-HD1-B assay the same structure-activity relationships (SARs) as those described in the anti-HD2 assay have been observed, against HD1-A the 3-benzoylamino derivative **2a** was the most potent ( $\text{IC}_{50} = 70$  nM) and the most class II-selective (class II selectivity ratio: 4.3) compound among all the synthesized cinnamyl-hydroxyamides **1-3**. Molecular modeling and docking studies with 3D-QSAR models of HD1-B and HD1-A enzymes have been undertaken, also to provide an explanation for the **2a** activity data.

Against HD2, the 4-substituted series (compounds **3a-f**) resembled the same SAR profile as the 3-substituted counterparts, the 4-benzoylamino derivative **3a** and the 4-(3-phenylpropionylamino) derivative **3c** being, respectively, the least and the most potent



compound (**3a**:  $IC_{50} = 168$  nM; **3c**:  $IC_{50} = 11$  nM) of the series. In the anti-HD1-B and -HD1-A assays, again the 4-benzoylamino derivative **3a** was the less active compound, whilst the 4-(2-naphthoylamino)cinnamyl-*N*-hydroxyamide **3f** showed the highest inhibitory activity, with  $IC_{50-HD1-B} = 36$  nM and  $IC_{50-HD1-A} = 42$  nM.

### 18.8. Conclusions.

A new series of 2-, 3-, and 4-acylamino-cinnamyl-*N*-hydroxyamides **1-3** have been prepared, and their anti-HDAC (against maize HD2, HD1-B, and HD1-A enzymes) activities have been assessed. Cinnamyl-hydroxyamides bearing acylamino substituents at the C2 position of the benzene ring (compounds **1a-g**) showed very low HDAC inhibiting activities, with  $IC_{50}$  values in the high micromolar range. By shifting the same acylamino groups from C2 to C3 (compounds **2a-g**) as well as C4 (compounds **3a-f**) position of the benzene ring, a number of highly potent HDAC inhibitors have been obtained.

As a rule, the introduction of a benzoylamino moiety both at C3 or C4 position led to 3- and 4-benzoylamino-cinnamyl-*N*-hydroxyamides (**2a** and **3a**) with  $IC_{50}$  values in the range 130-302 nM (with the exception of the activity of **2a** against HD1-A,  $IC_{50} = 70$  nM). The insertion of 1-2 carbon atom units between the benzene and the carbonyl group of the benzoyl portion, as well as the replacement of the benzene with the bulkier 1-naphthyl, 2-naphthyl, or 4-biphenyl moiety increased up to 15-times the HDAC inhibitory activity of the derivatives (compare **3a**,  $IC_{50-HD2} = 168$  nM, with **3c**,  $IC_{50-HD2} = 11$  nM).

In the anti-HD2 assay **3c** ( $IC_{50} = 11$  nM) was the most potent compound, being >11600-, 4.5-, and 10-fold more potent than sodium valproate, SAHA, and HC-toxin, respectively, and showing the same activity as trapoxin and slightly lower (1.5-fold) activity than TSA. HD1-B and HD1-A assays have been performed to screen the inhibitory action of **1-3** against mammalian class I (HD1-B) and class II (HD1-A) HDAC homologous enzymes. From the corresponding  $IC_{50}$  data, a selectivity ratio has been calculated. In general, compounds **1-3** showed no or little selectivity towards the class II homologue HD1-A, the most selective being **2a** with class II selectivity ratio = 4.3. SAHA and, to a lesser extent, TSA were both class I selective (class I selectivity ratios: SAHA, 6.7; TSA, 2). About the inhibitory potency, the 4-(2-naphthoylamino)cinnamyl-*N*-hydroxyamide **3f** showed the highest inhibiting effect against the two enzymes. Even though it was 90- (HD1-B) and 52-fold (HD1-A) less potent

than TSA, **3f** showed the same activity as SAHA against HD1-B, and was 4.8-fold more potent than SAHA against HD1-A.

Selected **2** and **3** compounds will be evaluated to determine their antiproliferative and cytodifferentiating activities on human acute promyelocytic leukemia HL-60 cells.

#### *18.9. Optimizzation's study of **3b**.*

The 4-acylaminocinnamyl-*N*-hydroxyamides series resulted the most potent against the HD1-B and HD1-A enzymes, in particular the compound **3b**. That induced us to effect chemical manipulations on such derivatives. Then we made stiff **3b** and then we studied the branching effect at methylene group between the benzene ring and the carbonilic group. Afterwards, on the MS-275's stuctural basis, we replaced the idroxammic function (EIG) with a 2-aminoanilide function. Furthermore we replaced the cinnamylic benzene ring with an heteroaromatic ring, that is with the pyridin ring. At last we introduced on the acylic moiety bulky groupas 1 and 2-naphthyl groups, for improving the interactions between the CAP group and the rhyme of enzyme's tubular pocket.

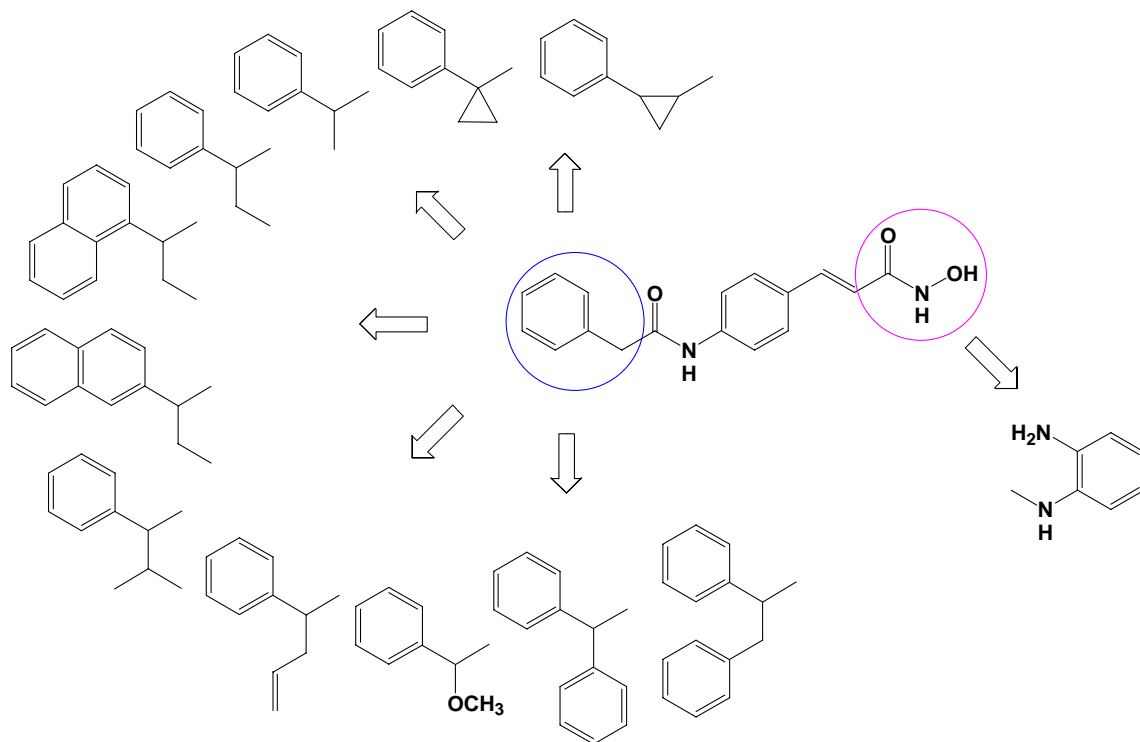
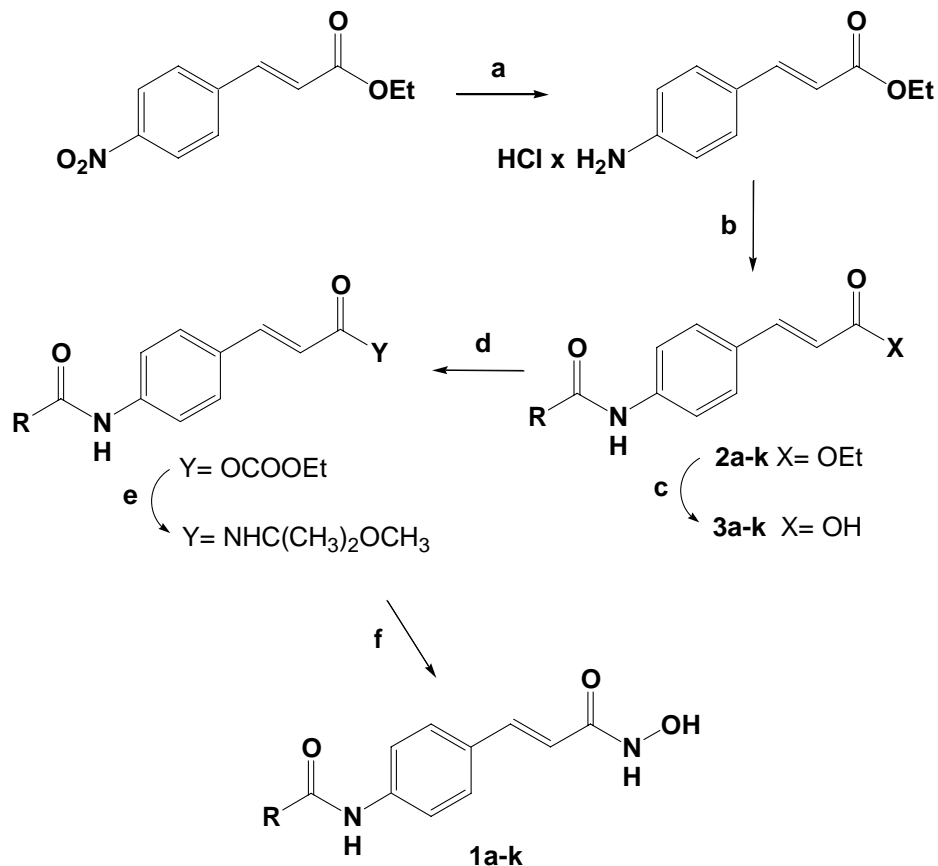
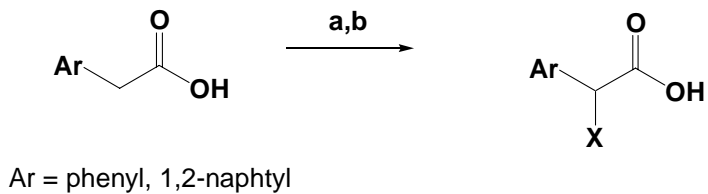


**Figure 40.** Optimization's study of 3b.

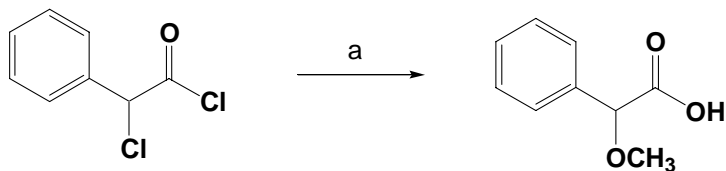
18.10. Chemistry.



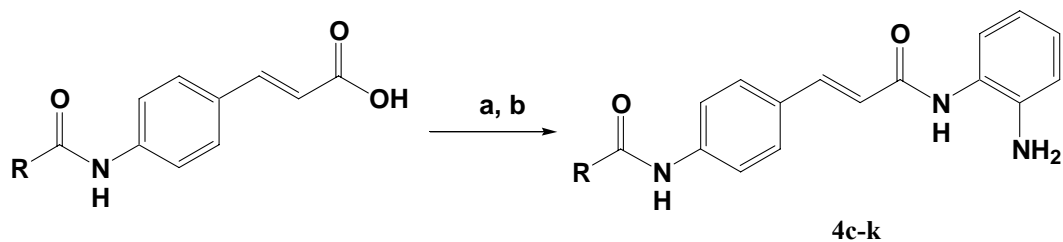
**Scheme 1.** a)  $\text{SnCl}_2 \cdot 2\text{H}_2\text{O}$ ,  $\text{HCl}$ ,  $\text{EtOH}$ . b)  $\text{RCOCl}$ ,  $(\text{C}_2\text{H}_5)_3\text{N}$ ,  $\text{CH}_2\text{Cl}_2$ , room temp. c)  $\text{LiOH}$ ,  $\text{H}_2\text{O}$ , room temp. d)  $\text{ClCOOC}_2\text{H}_5$ ,  $(\text{C}_2\text{H}_5)_3\text{N}$ ,  $\text{THF}$ ,  $0^\circ\text{C}$ . e)  $\text{NH}_2\text{OC}(\text{CH}_3)_2\text{OCH}_3$ , room temp. f) Amberlyst 15,  $\text{CH}_3\text{OH}$ , room temp.



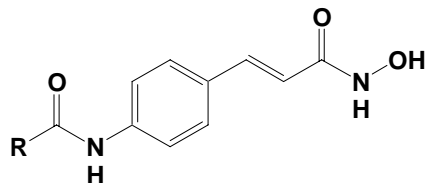
**Scheme 2.** a) n-BuLi 2.5 M,  $\text{Et}_2\text{NH}$ , THF,  $-78^\circ\text{C}$ , b) alkyl bromide or iodide,  $-78^\circ\text{C}$ .



**Scheme 3.** a) MeONa, MeOH, THF,  $70^\circ\text{C}$ , 5 h.

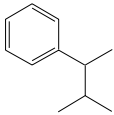
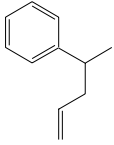
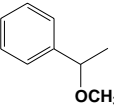
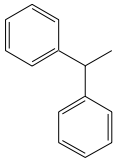
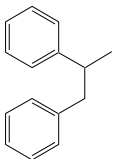


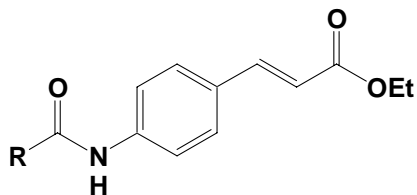
**Scheme 4.** a)  $\text{Et}_3\text{N}$ , BOP reagent, DMF, r.t., b) 1,2-phenylenediamine, DMF, r.t.



**Table 21.** Chemical and physical data of compound **1a-k**.

Compound	R	m.p. (°C)	Recrystallization solvent	Yield (%)
<b>1a</b>		103-105	Benzene	65.7
<b>1b</b>		95-97	Benzene	68.4
<b>1c</b>		133-135	Benzene	67.3
<b>1d</b>		128-130	Benzene	59.8
<b>1e</b>		180-182	Benzene/acetonitrile	61.0
<b>1f</b>		179-181	Benzene/acetonitrile	63.8

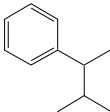
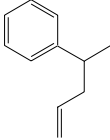
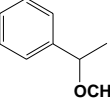
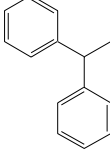
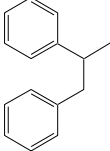
<b>1g</b>		162-164	Benzene/acetonitrile	67.6
<b>1h</b>		110-112	Benzene	58.3
<b>1i</b>		146-148	Benzene/acetonitrile	54.9
<b>1j</b>		238-240	Acetonitrile/methanol	61.3
<b>1k</b>		182-184	Acetonitrile	59.2

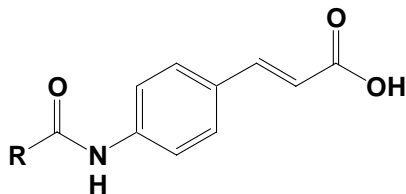


**Table 22.** Chemical and physical data of compound **2a-k**.

Compound	R	m.p. (°C)	Recrystallization solvent	Yield (%)
<b>2a</b>		144-146	Cyclohexane/benzene	85.0
<b>2b</b>		105-107	Cyclohexane	78.4
<b>2c</b>		114-116	Cyclohexane	87.3
<b>2d</b>		109-111	Cyclohexane	88.2
<b>2e</b>		135-137	Cyclohexane/benzene	79.6
<b>2f</b>		125-127	Cyclohexane/benzene	82.8

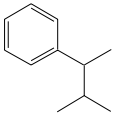
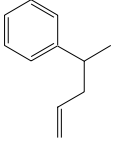
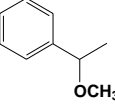
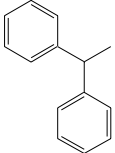
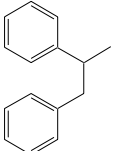


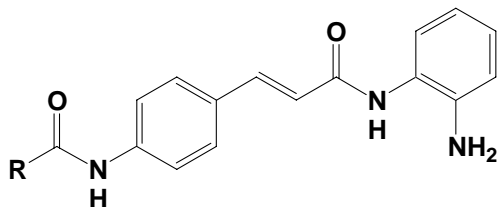
<b>2g</b>		95-97	Cyclohexane	83.6
<b>2h</b>		114-116	Cyclohexane/benzene	77.5
<b>2i</b>		133-135	Cyclohexane/benzene	78.7
<b>2j</b>		151-153	Cyclohexane/benzene	73.4
<b>2k</b>		143-145	Cyclohexane/benzene	83.4



**Table 23.** Chemical and physical data of compound **3a-k**.

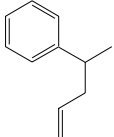
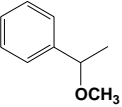
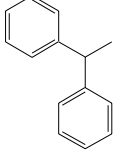
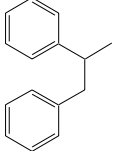
Compound	R	m.p. (°C)	Recrystallization solvent	Yield (%)
<b>3a</b>		>250	Acetonitrile/methanol	86.7
<b>3b</b>		>250	Acetonitrile/methanol	95.7
<b>3c</b>		224-226	Acetonitrile/methanol	94.5
<b>3d</b>		210-212	Acetonitrile/methanol	88.6
<b>3e</b>		186-188	Acetonitrile	89.4
<b>3f</b>		187-189	Acetonitrile	83.8

<b>3g</b>		162-164	Benzene/acetonitrile	89.0
<b>3h</b>		171-173	Benzene/acetonitrile	82.3
<b>3i</b>		198-200	Benzene/acetonitrile	85.7
<b>3j</b>		>250	Acetonitrile/methanol	81.
<b>3k</b>		168-170	Benzene/acetonitrile	83.4



**Table 24.** Chemical and physical data of compound **4c-k**.

Compound	R	m.p. (°C)	Recrystallization solvent	Yield (%)
<b>4c</b>		228-230	Acetonitrile/methanol	87.0
<b>4d</b>		200-202	Acetonitrile/methanol	78.5
<b>4e</b>		206-208	Acetonitrile/methanol	76.9
<b>4f</b>		205-207	Acetonitrile/methanol	73.4
<b>4g</b>		240-242	Methanol	74.6

<b>4h</b>		240-242	Methanol	72.8
<b>4i</b>		180-182	Benzene/acetonitrile	75.7
<b>4j</b>		>250	Methanol	77.4
<b>4k</b>		244-246	Methanol	78.5

### 18.11. Experimental section.

#### **Synthesis of Ethyl 3-(4-aminophenyl)-2-propenoate.**

To a solution of ethyl 4-nitrocinnamate (18.08 mmol, 4g) in ethanol (30 mL) stannous chloride dihydrate (64 mmol, 14.44 g) was added. Then concentrated HCl was dropwise added and the resulting suspension was stirred overnight. The precipitate salt was filtered, washed with ether and dried to afford the pure amine hydrochloride.

#### **General procedure for the synthesis of ethyl 3-(4-acylamino)phenyl)-2-propenoates 2a-k.**

**Example: Ethyl 3-[4-(2-phenylbutyryl)aminophenyl]-2-propenoate (2d).** 3-Phenylbutyryl chloride (6.1 mmol, 1 g) and triethylamine (15.22 mmol, 2.12 mL) were added to a solution of ethyl 3-(4-aminophenyl)-2-propenoate hydrochloride (6.1 mmol, 1.39 g) in dry dichloromethane (20 mL) at 0 °C under nitrogen atmosphere. After stirring at room temperature for 4 h, the reaction mixture was poured into water (50 mL), the organic layer was separated, and the aqueous one was extracted with chloroform (2 x 50 mL). The combined organic solution was washed with water (100 mL) and brine (100 mL), and was dried and evaporated to dryness. The residual solid was purified by crystallization from dichloromethane/*n*-hexane to yield pure **2d**. <sup>1</sup>H NMR (CDCl<sub>3</sub>) δ 0.93 (m, 3H, CH<sub>2</sub>CH<sub>3</sub>), 1.32 (m, 3H, OCH<sub>2</sub>CH<sub>3</sub>), 1.85-2.25 (m, 2H, CH<sub>2</sub>CH<sub>3</sub>), 3.40 (m, 3H, PhCHCO), 4.25 (OCH<sub>2</sub>CH<sub>3</sub>), 6.34 (d, 1H, PhCH=CHCOOEt), 7.26-7.49 (m, 9H, benzene protons), 7.60 (d, 1H, PhCH=CHCOOEt).

#### **General procedure for the synthesis of 3-(4-acylamino)phenyl)-2-propenoic acids 3a-k.**

##### **Example: 3-[4-(2-Phenyl-pent-4-en-oylamino)phenyl]-2-propenoic acid (3h).**

A mixture of ethyl 3-[4-(2-Phenyl-pent-4-en-oylamino)phenyl]-2-propenoate (**2h**) (0.57 mmol, 0.20 g), lithium hydroxide hydrate (1.14 mmol, 0.048 g), and tetrahydrofuran (15 mL) was stirred at room temperature. After 24 h, 2 N HCl was added to the mixture until the pH was 5, and the obtained solid was filtered and recrystallized to yield pure **3h**. <sup>1</sup>H NMR (DMSO-*d*<sub>6</sub>) δ 2.48-2.76 (m, 2H, CH<sub>2</sub>CH=CH<sub>2</sub>), 3.50 (m, 1H, PhCHCO), 5.00 (m, 2H, CH<sub>2</sub>CH=CH<sub>2</sub>), 5.72 (m, 1H, CH<sub>2</sub>CH=CH<sub>2</sub>), 6.35 (d, 1H, PhCH=CHCOOEt), 7.31-7.60 (m, 10 H, benzene protons and PhCH=CHCOOEt), 10.30 (s, 1H, CONHPh).

**General procedure for the synthesis of 3-(4-acylamino-phenyl)-*N*-hydroxy-2-propenamides 1a-k. Example: 3-[4-(2,3-Diphenyl-propionylamino)-phenyl]- *N*-hydroxy-2-propenamide (1k).**

Ethyl chloroformate (1.26 mmol, 0.12 mL) and triethylamine (1.37 mmol, 0.19 mL) were added to a cooled (0 °C) solution of 3-[4-(2,3-Diphenyl-propionylamino)-phenyl]-2-propenoic acid **3k** (1.05 mmol, 0.42 g) in dry THF (10 mL), and the mixture was stirred for 10 min. The solid was filtered off, and *O*-(2-methoxy-2-propyl)hydroxylamine (3.15 mmol, 0.23 mL) was added to the filtrate. The solution was stirred for 15 min at 0 °C, then was evaporated under reduced pressure, and the residue was diluted in methanol (10 mL). Amberlyst® 15 ion-exchange resin (42 mg) was added to the solution of the *O*-protected hydroxamate, and the mixture was stirred at room temperature for 1 h. After, the reaction was filtered and the filtrate was concentrated in vacuo to give the crude **1k** which was purified by crystallization. <sup>1</sup>H NMR (DMSO-*d*<sub>6</sub>) δ 3.05 (m, 1H, PhCH<sub>2</sub>), 3.60 (m, 1H, PhCH<sub>2</sub>), 3.75 (m, 1H, PhCHCO), 6.36 (d, 1H, PhCH=CHCOOEt), 7.15-7.70 (m, 15H, benzene protons and PhCH=CHCOOEt), 9.00 (s, 1H, OH), 10.23 (s, 1H, CONHPh), 10.85 (s, 1H, NHOH).

**General procedure for the synthesis of *N*-(2-Amino-phenyl)-3-[4-(acylamino)-phenyl]-2-propenamide 4c-k. Example: *N*-(2-Amino-phenyl)-3-[4-(2-naphthalen-2-yl-butyrylamino)-phenyl]-2-propenamide (4f).**

To a solution of 3-[4-(2-naphthalen-2-yl-butyrylamino)-phenyl]-2-propenoic acid (**3f**) (0.55 mmol, 0.20 g) in anhydrous dimethylformamide (5mL) triethylamine (2.2 mmol) and BOP reagent (0.66 mmol, 0.29 g) were added under nitrogen atmosphere. The resulting mixture was stirred for 30 min at room temperature. The reaction was quenched by water, extracted with ethyl acetate (3 x 30 mL), then the organic layers were dried with sodium sulfate and concentrated to afford a solid that was chromatographed by SiO<sub>2</sub> eluting with acetate/chloroform 1:1. The pure product **4f** was obtained as a yellow solid. <sup>1</sup>H NMR (DMSO-*d*<sub>6</sub>) δ 0.90 (m, 3H, CH<sub>2</sub>CH<sub>3</sub>), 1.75-2.25 (m, 2H, CH<sub>2</sub>CH<sub>3</sub>), 3.77 (m, 1H, 2-napht-CHCO), 6.56-6.74 (m, 4H, 2-aminoanilide C3-5 and PhCH=CHCONHPh), 7.30 (d, 1H, 2-aminoanilide C6), 7.44-7.89 (m, 12H, 2-naphthalene and benzene protons and PhCH=CHCONHPh), 9.29 (s, 1H, PhCH=CHCONHPh), 10.33 (s, 1H, 2-napht-CHCONH).

**General procedure for the synthesis of the  $\alpha$ -alkyl-arylacetic acids. Example: 3-Methyl-2-phenyl-butyric acid.**

A solution of diethylamine (16.16 mmol, 1.68 mL) in anhydrous tetrahydrofuran (10 mL) was dropwise added to a solution of n-butyllithium 2.5 M in hexane (32.32 mmol, 12.93 mL) cooled at  $-78^{\circ}\text{C}$  and under nitrogen atmosphere. The resulting solution was stirred at  $0^{\circ}\text{C}$  for 30 min, then cooled again at  $-78^{\circ}\text{C}$  and a solution of phenylacetic acid in tetrahydrofuran (10 mL) was dropwise added under nitrogen atmosphere. The mixture was stirred at  $0^{\circ}\text{C}$  for others 30 min, afterwards it was cooled at  $-78^{\circ}\text{C}$  and a solution of 2-iodopropane (16.16 mmol, 1.613 mL) was slowly added. The reaction was left stirring at room temperature overnight, was quenched by water (50 mL) and the aqueous layer was extracted with ethyl acetate (3 x 30 mL), acidified with concentrated HCl and extracted again with ethyl acetate (3 x 30 mL). The organic layers was washed with NaCl solution (3 x 30 mL). dried with sodium sulfate and concentrated to afford an oil that was purified by chromatography eluting with ethyl acetate/ chloroform 1:5. The pure product was obtained as a white solid.

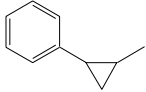
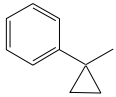
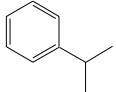
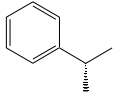
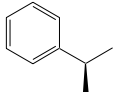
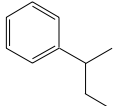
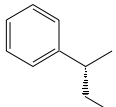
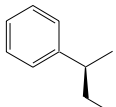
**General procedure for the synthesis of the  $\alpha$ -methoxy-phenylacetic acid.**

To a cooled at  $0^{\circ}\text{C}$  solution of sodium methoxide (63.48 mmol, 1.46 g Na) in methanol (20 mL) a solution of  $\alpha$ -chloro-phenylacetyl chloride (7.93 mmol, 1.25 mL) in tetrahydrofuran (10 mL) was slowly added. The mixture was stirred at  $70^{\circ}\text{C}$  for 5 h, then the solvent was evaporated, the residue was eluted with water (50 mL) and extracted with ethyl acetate (3 x 30 mL), the aqueous layer was acidified and extracted again with ethyl acetate (3 x 30 mL). The organic layers was dried and concentrated to afford the pure product that slowly solidify.

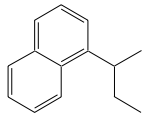
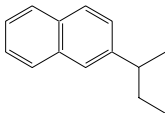
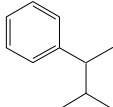
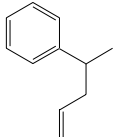
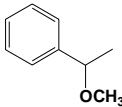
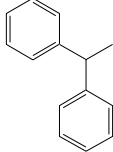
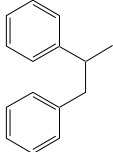
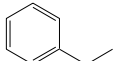


**19. Biological evaluation.**

**Table 25.** HD1-B, HD1-A and mouse HDAC1 inhibiting activity of compounds **1a-k**.

Compound	R	IC <sub>50</sub> (μM)		
		<i>zm</i> -HD1-B	<i>zm</i> -HD1-A	<i>mouse</i> -HDAC1
<b>1a</b>		0.064	0.132	0.198
<b>1b</b>		0.065	0.196	0.334
<b>1c</b>		0.033	0.057	0.102
<b>1c (2)</b>		0.056	0.073	0.258
<b>1c (1)</b>		0.170	0.125	0.406
<b>1d</b>		0.028	0.068	0.055
<b>1d (2)</b>		0.040	0.070	0.045
<b>1d (1)</b>		0.101	0.063	0.328

Design, synthesis and biological validation of epigenetic modulators of histone/protein deacetylation and methylation.

<b>1e</b>		0.058	0.042	0.620
<b>1f</b>		0.062	0.069	0.560
<b>1g</b>		0.187	0.057	0.296
<b>1h</b>		0.126	0.057	0.115
<b>1i</b>		0.083	0.140	0.150
<b>1j</b>		0.162	0.055	0.128
<b>1k</b>		0.133	0.074	0.083
<b>lead compound</b>		0.092	0.072	-
<b>SAHA</b>	-	0.030	0.200	-

Compounds **1a-k** have been evaluated for their inhibiting activities against two maize HDAC enzymes, HD1-B, HD1-A and for the first time against the mouse HDAC1. As reference we used the *lead compound* and SAHA.

The results showed that all alkylic groups are well tolerated but the best branching is resulted by the methyl and ethyl groups, introduced in the compound **1c** and **1d**, respectively, that endowed with most potency, comparable with SAHA. All derivatives **1a-k** have a chiral center, then on the basis of good results obtained we have separated two enantiomers *R*-(-) and *S*-(+) of raceme **1c** and **1d**, with the aim to have a different activity between two enantiomers. The inhibitory activity of the enantiomers **1c(1)** and **1d(1)**, that are the enantiomers *R*-(-), are better than the inhibitory activity of **1c(2)** and **1d(2)**. This result is more evident analysing the biological assays below reported.

#### *19.1. Granulocytic Differentiation on human U937 leukemia Cells.*

The most potent derivatives, **1c**, **1c(1)**, **1c(2)**, **1d**, **1d(1)**, **1d(2)**, **1g**, **4c**, **4d**, **4g**, **4e**, **4f** were assayed on human U937 leukemia cells to value the granulocytic differentiating capacity. We considered as reference SAHA and MS-275. The results are represented in the following figure 41 and 42.

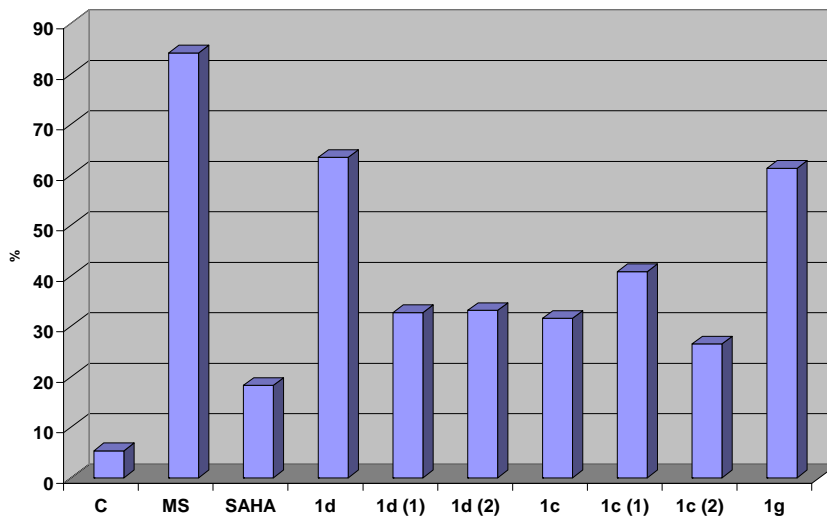


**Figure 41 (a).** Differentiation of the human U937 leukemia Cells (30 hours) by HDAC inhibitors (idoxammates derivatives).

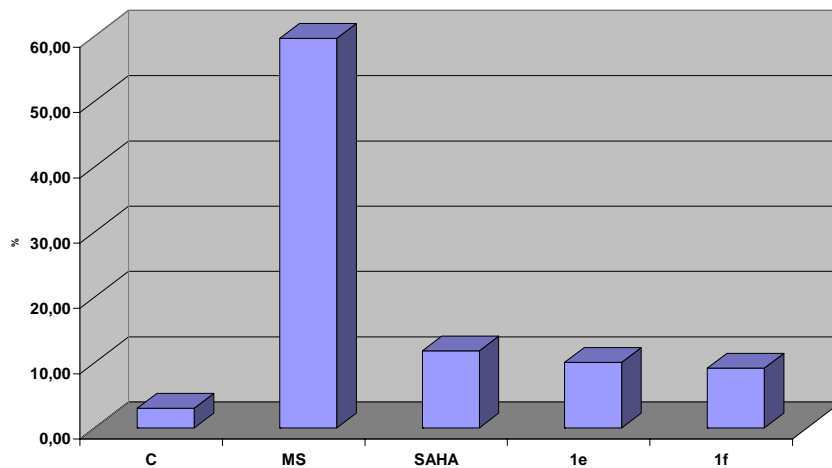


**Figure 41 (b).** Differentiation of the human U937 leukemia Cells (30 hours) by HDAC inhibitors (idoxammates derivatives).

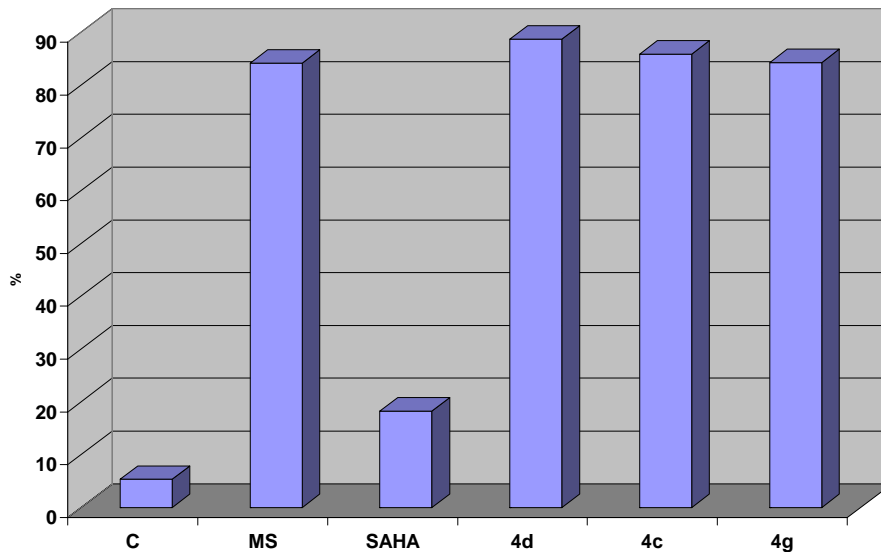


**Figure 42 (a).** Differentiation of the human U937 leukemia Cells (30 hours) by HDAC inhibitors (2-aminoanilides derivatives).

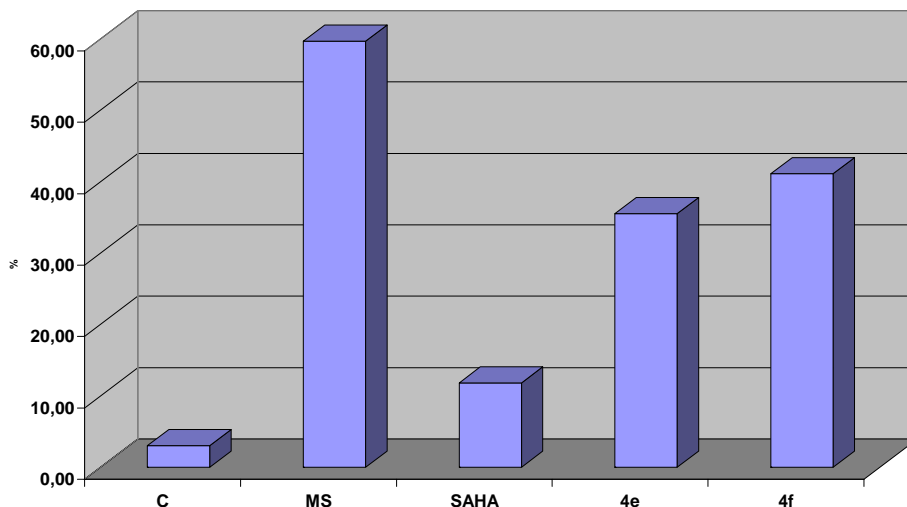


**Figure 42 (b).** Differentiation of the human U937 leukemia Cells (30 hours) by HDAC inhibitors (2-aminoanilides derivatives).

Granulocytic differentiation of human leukemia U937 cells was determined by CD11c expression level upon 30 h of stimulation with selected compounds. To this end, cell cultures were treated with compounds at 5  $\mu$ M concentration together with SAHA and MS-275 as the reference drugs, and after 30 h, the percent values of CD11c positive PI negative cells were determined.

**Granulocytic Differentiation on U937 Cells.** Granulocytic differentiation was carried out as previously described.<sup>66</sup> Briefly, U937 cells were harvested and resuspended in 10  $\mu$ L of phycoerythrine-conjugated CD11c (CD11c-PE). Control samples were incubated with 10  $\mu$ L of PE conjugated mouse IgG1, incubated for 30 min at 4 °C in the dark, washed in PBS, and resuspended in 500  $\mu$ L of PBS containing PI (0.25 *ig*/mL). Samples were analyzed by FACS with Cell Quest technology (Becton Dickinson). PI positive cells have been excluded from the analysis.

*19.2. Effects on human U937 leukemia cells cycle.*

The derivatives **1c**, **1c(1)**, **1c(2)**, **1d**, **1d(1)**, **1d(2)**, **1g**, **4c**, **4d**, **4g**, **4e**, **4f** were tested against the human U937 leukemia cells to estimate the antiproliferative effect considering cell cycle arrest in the phases G1, G2, M and the pro-apoptotic effect.

The results of these assays are showed in the below figure 43 and 44.

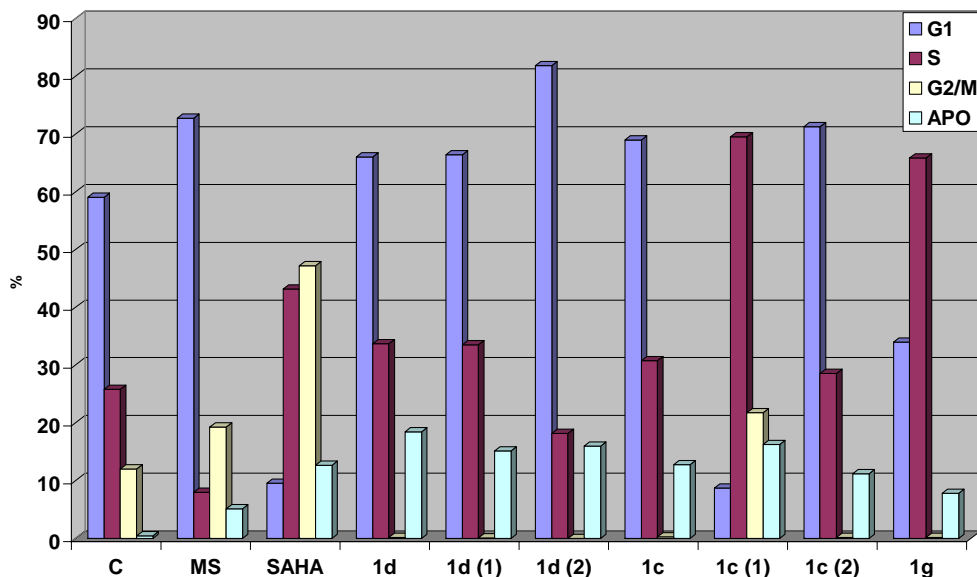


**Figure 43 (a).** Effect on human U937 leukemia Cells cycle (24 hours) by HDAC inhibitors (idroxammates derivatives).



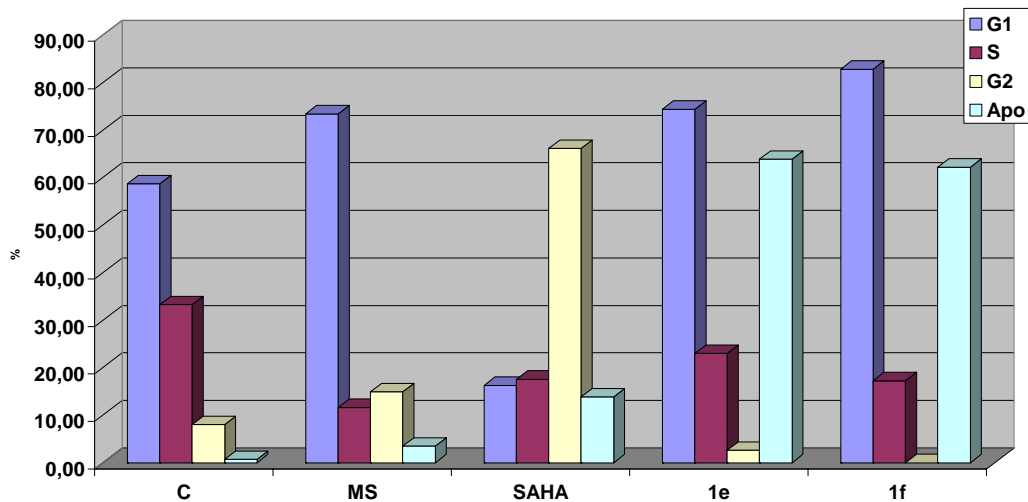


**Figure 43 (b).** *Effect on human U937 leukemia Cells cycle (24 hours) by HDAC inhibitors (idroxammates derivatives).*

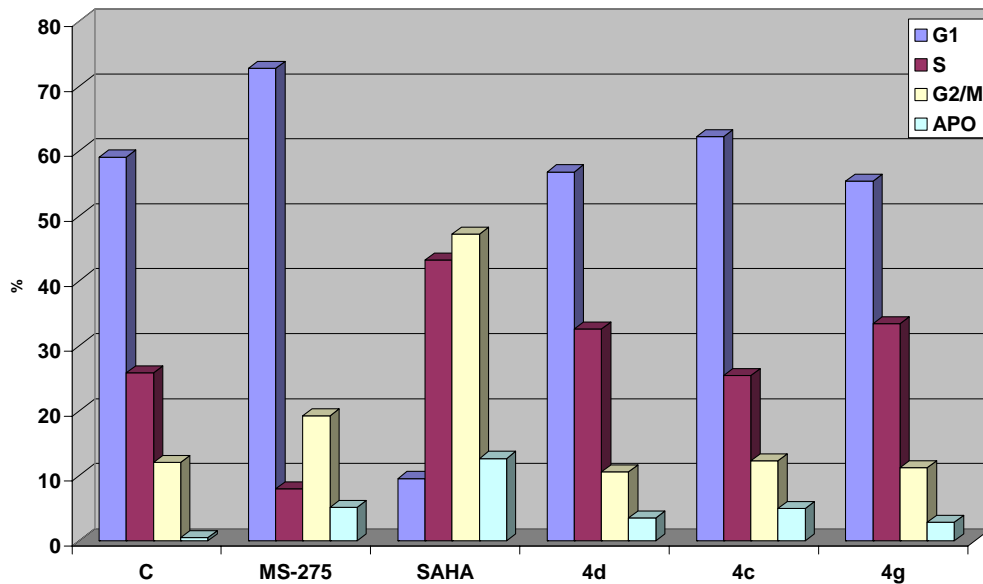


**Figure 44 (a).** Effect on human U937 leukemia Cells cycle (24 hours) by HDAC inhibitors (2-aminoanilides derivatives).

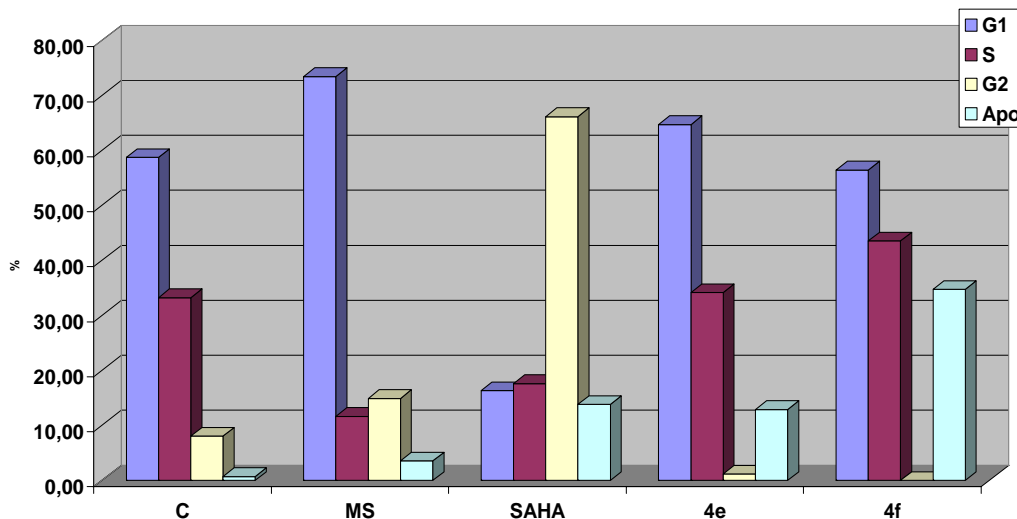


**Figure 44 (b).** *Effect on human U937 leukemia Cells cycle (24 hours) by HDAC inhibitors (2-aminoanilides derivatives).*

To evaluate the effects of HDAC inhibitors on cell cycle and apoptosis in the human leukemia U937 cell line, cell cultures were treated with 5  $\mu\text{M}$  concentration of selected derivatives in comparison with SAHA (5  $\mu\text{M}$ ) and MS-275 (5  $\mu\text{M}$ ), and after 24 h the cell cycle analysis was determined. Apoptosis, measured as caspase 3 cleavage (data not shown) and AnnexinV/propidium iodide (PI) double staining by FACS analyses, was checked after 24 h of treatment with selected compounds used at 5  $\mu\text{M}$ .

**Cell Cycle Analysis on U937 Cells.** Cells ( $2.5 \times 10^5$ ) were collected and resuspended in 500  $\mu\text{L}$  of hypotonic buffer (0.1% Triton X-100, 0.1% sodium citrate, 50  $\mu\text{g}/\text{mL}$  of propidium iodide (PI), and RNase A). Cells were incubated in the dark for 30 min. Samples were

acquired on a FACS-Calibur flow cytometer using the Cell Quest software (Becton Dickinson) and analyzed with standard procedures using the Cell Quest software (Becton Dickinson) and the ModFit LT version 3 Software (Verity). All of the experiments were performed three times.

### 19.3. p21 Induction and $\alpha$ -Tubulin Acetylation.

Taking the cyclin dependent kinase inhibitor p21<sup>WAF1/CIP1</sup> (p21) induction as well as the acetylation extents of  $\alpha$ -tubulin as markers of HDACi activity in U937 cells, we performed Western blot analyses to test the activity of selected derivatives.

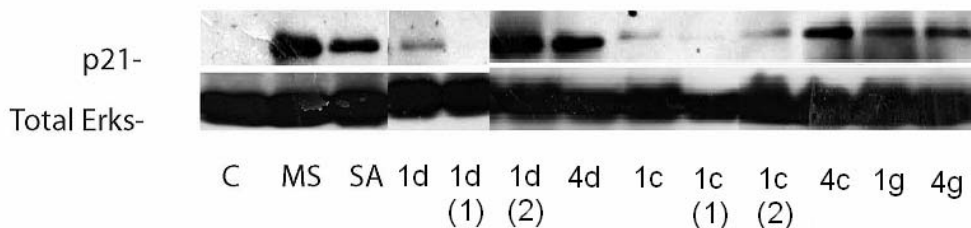


**Figure 45.** p21 oncosuppressor expression by HDAC inhibition.

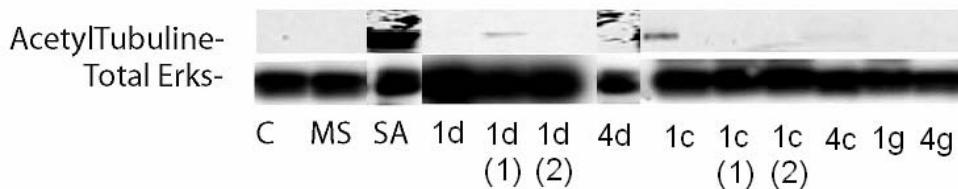


**Figure 46.**  $\alpha$ -tubulin acetylation.

Taking the cyclin dependent kinase inhibitor p21<sup>WAF1/CIP1</sup> (p21) induction as well as the acetylation extents of  $\alpha$ -tubulin as markers of HDACi activity in U937 cells, we performed Western blot analyses to test the activity of selected HDAC inhibitors. Figure 46 shows that **1d (2)**, but not **1d (1)**, increased the p21 expression more than MS-275 and SAHA. No compound induced  $\alpha$ -tubulin acetylation.  $\alpha$ -tubulin acetylation is a functional test for the evaluation of HDAC6 activity, a class IIb HDAC, whereas p21 induction represents a feature of HDAC class I inhibitors.

## 20. HMT inhibitors design.

In 2004, a series of dyes and dye-like compounds were evaluated as small molecule modulators of PRMT and HKMT activity. In this screen, AMI-1 has been described as the first specific PRMT inhibitor, and AMI-5 was one of the most potent, though less selective, compound (Figure 47).<sup>357</sup> Recently, the fungal metabolite chaetocin was identified and characterized as first specific inhibitor of the HKMT SU(VAR)3-9 (figure 47).<sup>358</sup>

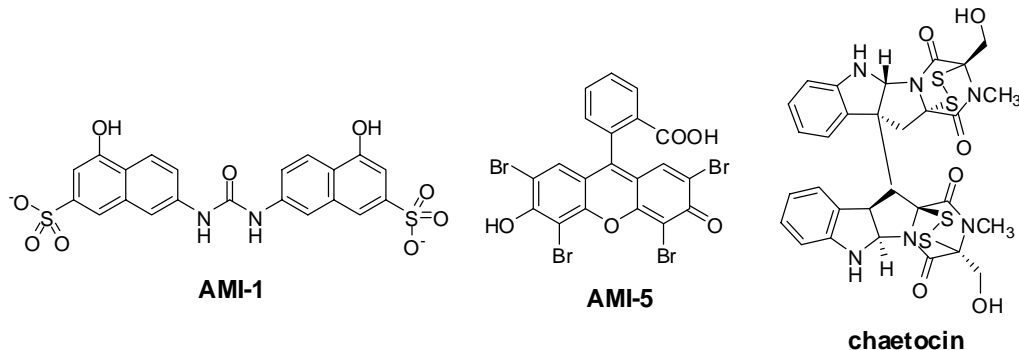


*Figure 47. PRMT inhibitors and HKMT SU(VAR)3-9 specific inhibitor.*

As a part of our medicinal chemistry project aimed to discover new entities as small molecule modulators of epigenetic targets, we chose the AMI-5 chemical structure as a template and designed a new series of simplified analogues starting from a pharmacophore hypothesis. In this hypothesis, we identified the presence of two *o*-bromo- or *o,o*-dibromophenol moieties as crucial for having anti-methyltransferase activity, and inserted a hydrophobic spacer between the above fragments (figure 48).

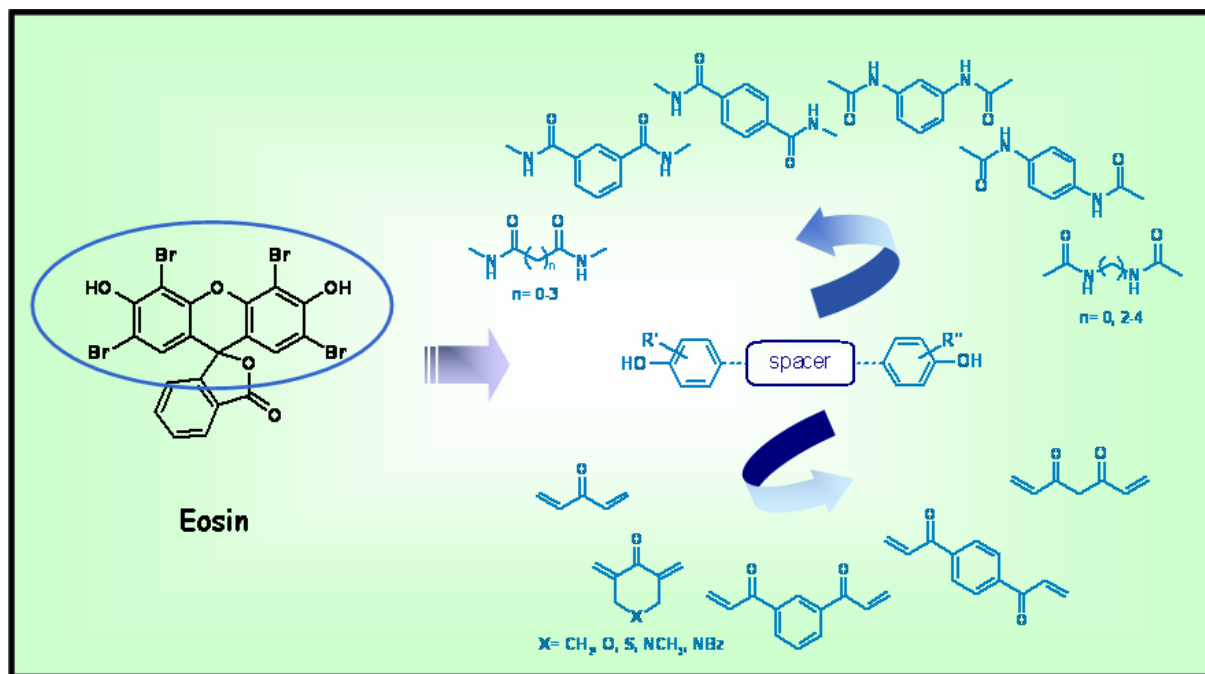
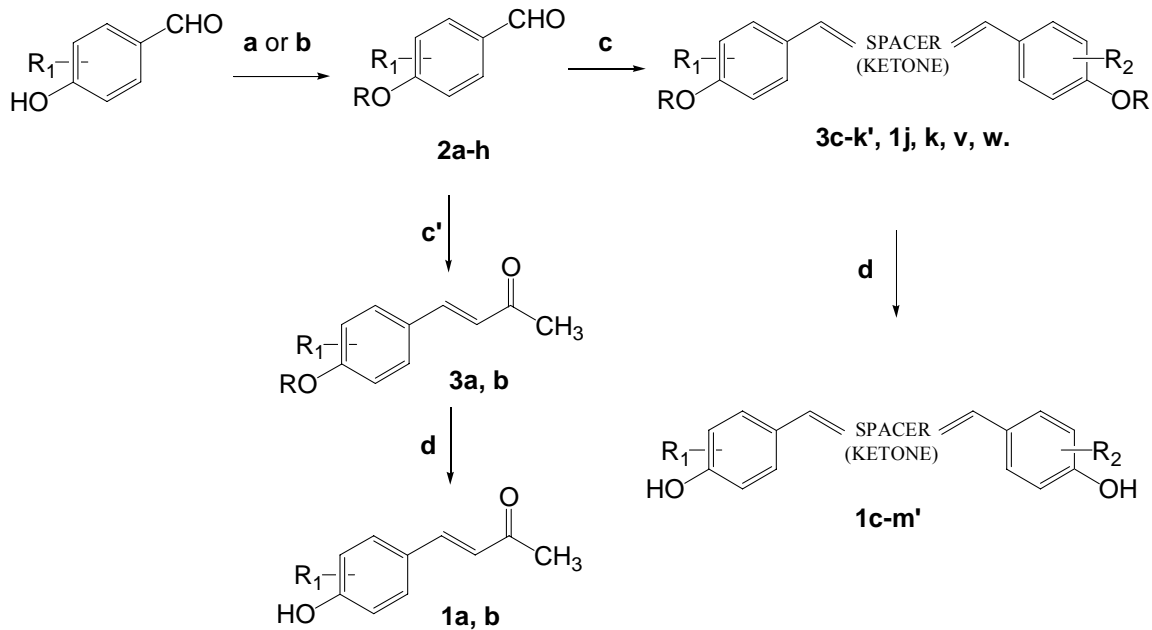
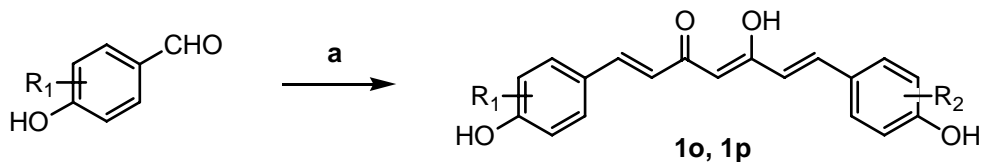


**Figure 48.** Rational design for development of HMT inhibitors.

20.1. Chemistry.

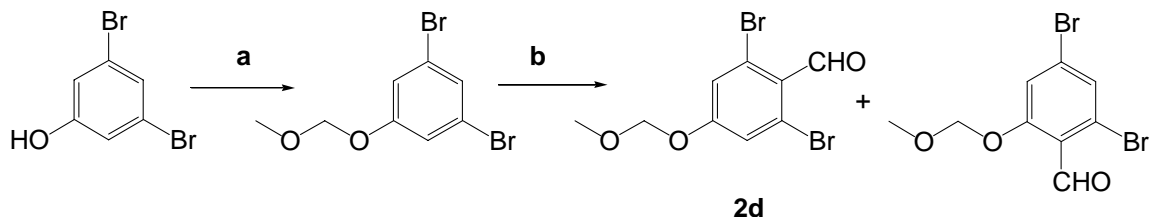


**Scheme 1.** **a:** NaH, CH<sub>3</sub>OCH<sub>2</sub>Br, THF, 0°C, 30 min; **b:** K<sub>2</sub>CO<sub>3</sub>, CH<sub>3</sub>I, CH<sub>3</sub>CN, 80°C; **c:** ketone, Ba(OH)<sub>2</sub> X 8H<sub>2</sub>O, r. t., 2h; **c':** CH<sub>3</sub>COCH<sub>3</sub>, Ba(OH)<sub>2</sub> X 8H<sub>2</sub>O, r. t., 2h; **d:** HCl 3N, MeOH, 70°C, 3h.

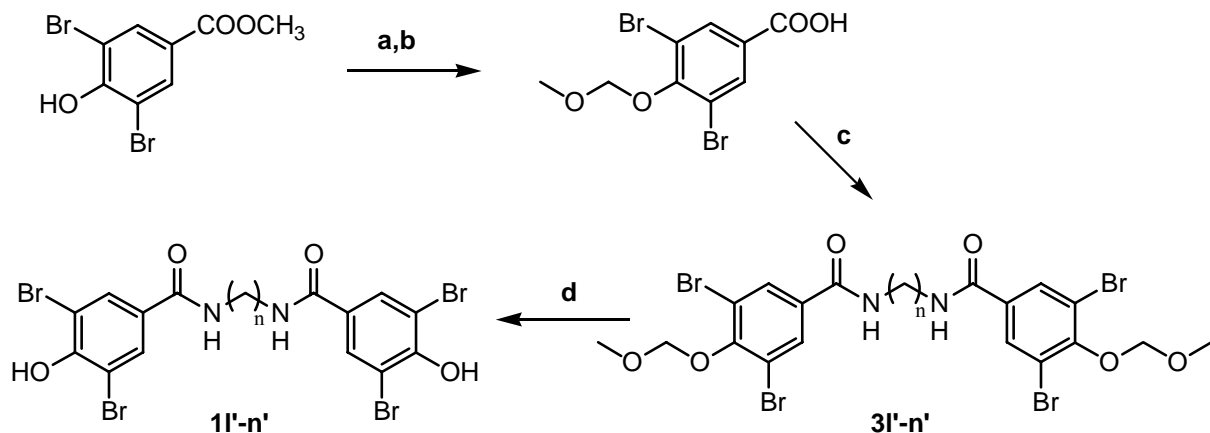


**Scheme 2.** **a:** 2,4-pentanedione, B<sub>2</sub>O<sub>3</sub>, B(OBu)<sub>3</sub>, BuNH<sub>2</sub>, AcOEt, 80°C.

*Design, synthesis and biological validation of epigenetic modulators of histone/protein deacetylation and methylation.*

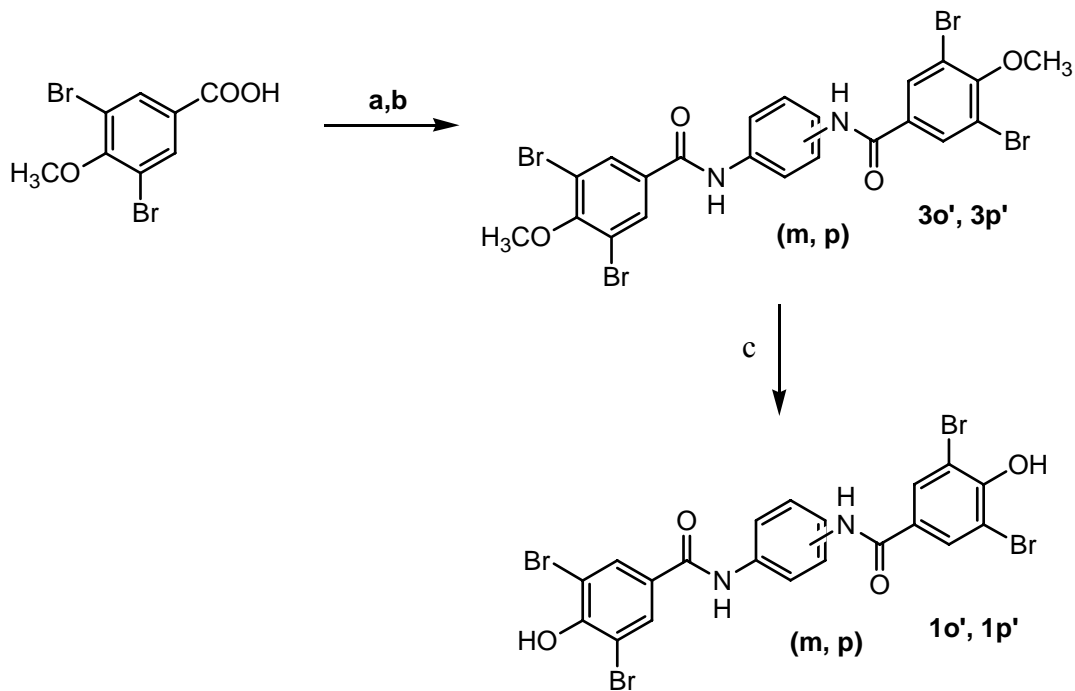


**Scheme 3.** a: NaH, CH<sub>3</sub>OCH<sub>2</sub>Br, THF, 0°C, 30 min. b: LDA, DMF, THF, -80°C, 30 min.

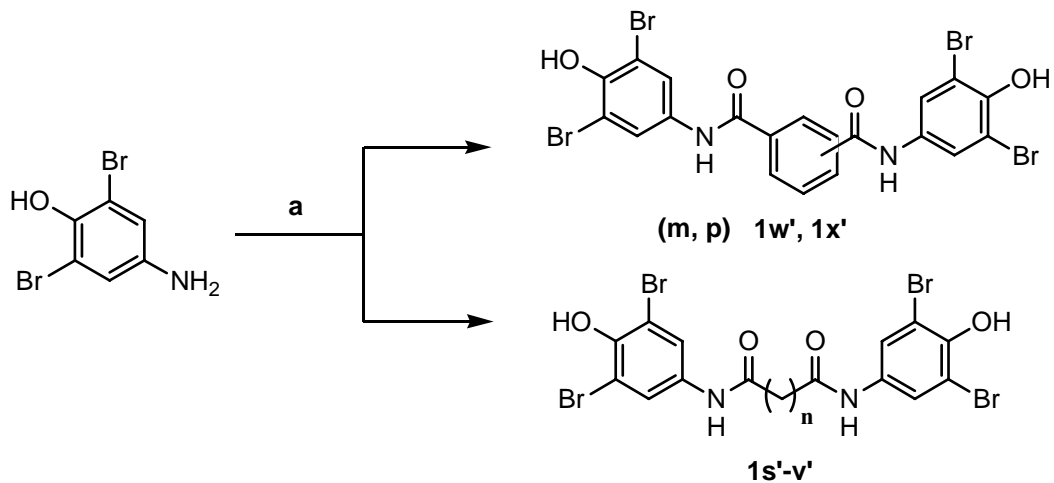


**Scheme 4.** a: NaH, CH<sub>3</sub>OCH<sub>2</sub>Br, THF, 0°C; b: KOH 2N, MeOH; c: 1) TEA, ClCOOEt, THF, 0°C, 2) diamine, THF, 0°C; d: HCl 3N, MeOH, 50°C.





**Scheme 5.** **a:** SOCl<sub>2</sub>, 70°C; **b:** TEA, 1,3 or 1,4-phenyldiamine, THF, 0°C; **c:** BBr<sub>3</sub>, CH<sub>2</sub>Cl<sub>2</sub>, -78°C.



**Scheme 6. a:** TEA, opportune acylic dichloride, THF, 0°C.

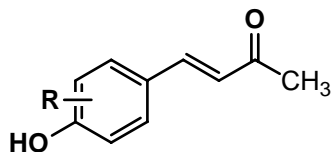


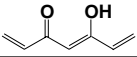
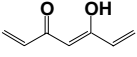
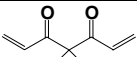
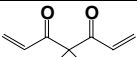
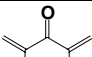
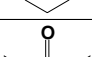
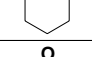
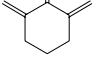
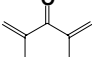
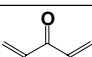
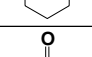
**Table 26.** Chemical and physical data of the compounds **1a-b**.

<b>Compounds</b>	<b>R</b>	<b>Melting Point (°C)</b>	<b>Recrystallization solvent</b>	<b>Yield (%)</b>
<b>1a</b>	3-Br	100-102	Ethanol	94.0
<b>1b</b>	3,5-di-Br	142-144	Ethanol	93.0

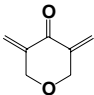
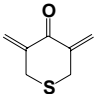
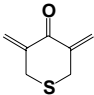
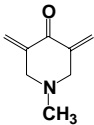
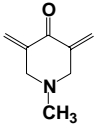
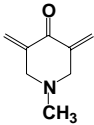
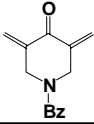
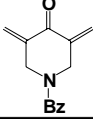


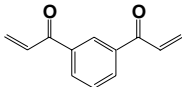
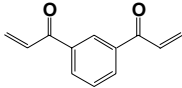
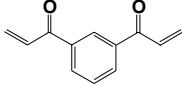
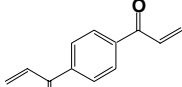
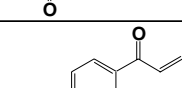
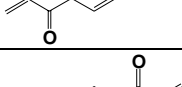
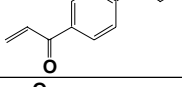
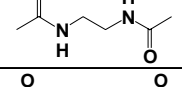
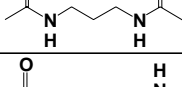
**Table 27.** Chemical and physical data of the compound **1c-x'**.

Compounds	R <sub>1</sub> , R <sub>2</sub>	Spacer	Melting Point (°C)	Recrystalliz. solvent	Yield (%)
<b>1c</b>	Bis-3-Br-4-OH		248-250	methanol	84.5
<b>1d</b>	Bis-3,5-di-Br-4-OH		274-276	methanol	92.5
<b>1e</b>	3-Br-4-OH, 3,5-di-Br-4-OH		240-242	methanol	86.0
<b>1f</b>	Bis-3-Br		118-120	methanol	97.3
<b>1g</b>	Bis-4-OH		246-248	methanol	100.0
<b>1h</b>	Bis-2-Br-4-OH		>250	methanol	78.1
<b>1i</b>	Bis-2,6-di-Br-4-OH		>250	methanol	82.8
<b>1j</b>	Bis-3-Br-4-OCH <sub>3</sub>		170-172	methanol	93.7
<b>1k</b>	Bis-3,5-di-Br-4-OCH <sub>3</sub>		218-220	methanol	89.4
<b>1l</b>	Bis-3-NO <sub>2</sub> -4-OH		239-241	methanol	87.8
<b>1m</b>	Bis-3-F-4-OH		240-242	methanol	95.0
<b>1n</b>	Bis-3,5-di-CH <sub>3</sub> -4-OH		229-231	methanol	91.6

<b>1o</b>	Bis-3-Br-4-OH		238-240	methanol	45.0
<b>1p</b>	Bis-3,5-di-Br-4-OH		244-246	methanol	26.0
<b>1q</b>	Bis-3-Br-4-OH		130-132	methanol	67.5
<b>1r</b>	Bis-3,5-di-Br-4-OH		146-148	methanol	59.6
<b>1s</b>	Bis-3-Br-4-OH		151-153	methanol	96.5
<b>1t</b>	Bis-3,5-di-Br-4-OH		198-200	methanol	92.4
<b>1u</b>	Bis-4-OH		>250	methanol	98.3
<b>1v</b>	Bis-3-Br-4-OCH <sub>3</sub>		156-158	methanol	89.4
<b>1w</b>	Bis-3,5-di-Br-4-OCH <sub>3</sub>		200-202	methanol	78.0
<b>1x</b>	Bis-3-Br-4-OH		220-222	methanol	86.0
<b>1y</b>	Bis-3,5-di-Br-4-OH		>250	methanol	76.7

*Design, synthesis and biological validation of epigenetic modulators of histone/protein deacetylation and methylation.*

<b>1z</b>	Bis-4-OH		>250	methanol	88.2
<b>1a'</b>	Bis-3-Br-4-OH		168-170	methanol	86.0
<b>1b'</b>	Bis-3,5-di-Br-4-OH		230-232	methanol	76.8
<b>1c'</b>	Bis-3-Br-4-OH		>250	methanol	75.4
<b>1d'</b>	Bis-3,5-di-Br-4-OH		>250	methanol	73.8
<b>1e'</b>	3,5-di-Br-4-OH, 3-Br-4-OH		>250	methanol	86.0
<b>1f'</b>	Bis-3-Br-4-OH		>250	methanol	68.5
<b>1g'</b>	Bis-3,5-di-Br-4-OH		>250	methanol	56.7

<b>1h'</b>	Bis-3-Br-4-OH		>250	methanol	79.8
<b>1i'</b>	Bis-3,5-di-Br-4-OH		>250	methanol	64.7
<b>1j'</b>	Bis-4-OH		>250	methanol	75.6
<b>1k'</b>	Bis-3-Br-4-OH		>250	methanol	77.4
<b>1l'</b>	Bis-3,5-di-Br-4-OH		>250	methanol	68.0
<b>1m'</b>	Bis-4-OH		>250	methanol	78.0
<b>1n'</b>	Bis-3,5-di-Br-4-OH		>250	methanol	98.7
<b>1o'</b>	Bis-3,5-di-Br-4-OH		238-240	methanol	96.5
<b>1p'</b>	Bis-3,5-di-Br-4-OH		246-248	methanol	89.0

*Design, synthesis and biological validation of epigenetic modulators of histone/protein deacetylation and methylation.*

<b>1q'</b>	Bis-3,5-di-Br-4-OH		>250	methanol	88.6
<b>1r'</b>	Bis-3,5-di-Br-4-OH		>250	methanol	75.4
<b>1s'</b>	Bis-3,5-di-Br-4-OH		>250	methanol	78.3
<b>1t'</b>	Bis-3,5-di-Br-4-OH		230-232	methanol	66.5
<b>1u'</b>	Bis-3,5-di-Br-4-OH		215-217	methanol	75.7
<b>1v'</b>	Bis-3,5-di-Br-4-OH		198-200	methanol	84.6
<b>1w'</b>	Bis-3,5-di-Br-4-OH		196-198	methanol	92.3
<b>1x'</b>	Bis-3,5-di-Br-4-OH		>250	methanol	90.1



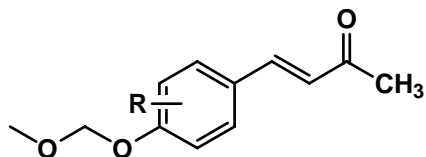


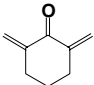
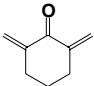
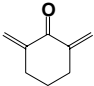
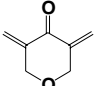
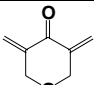
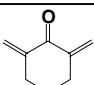
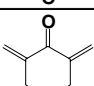
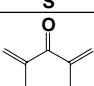
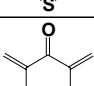
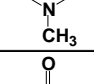
**Table 28.** Chemical and physical data of the compound **3a-b**.

<b>Compounds</b>	<b>R</b>	<b>Melting Point (°C)</b>	<b>Recrystallization solvent</b>	<b>Yield (%)</b>
<b>3a</b>	3-Br	115-117	cyclohex/benz	96.0
<b>3b</b>	3,5-di-Br	112-114	cyclohex/benz	82.7

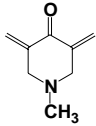
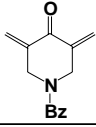
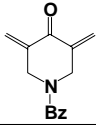
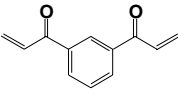
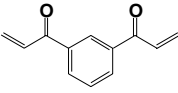
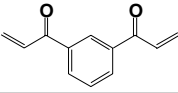
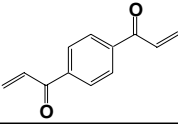
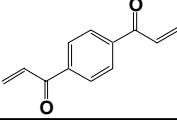


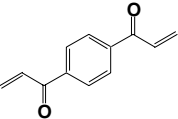
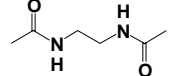
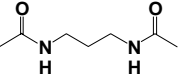
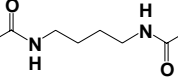
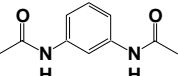
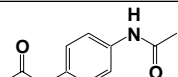
**Table 29.** Chemical and physical data of the compound **3c-p'**.

Compounds	R <sub>1</sub> R <sub>2</sub>	Spacer	Melting Point (°C)	Recrystalliz. solvent	Yield (%)
<b>3c</b>	Bis-3-Br-4-OCH <sub>2</sub> OCH <sub>3</sub>		121-123	methanol	90.3
<b>3d</b>	Bis-3,5-di-Br-4-OCH <sub>2</sub> OCH <sub>3</sub>		140-142	methanol	88.2
<b>3g</b>	Bis-4-OCH <sub>2</sub> OCH <sub>3</sub>		84-86	cyclohex/benz	95.0
<b>3h</b>	Bis-2-Br-4-OCH <sub>2</sub> OCH <sub>3</sub>		133-135	methanol	74.0
<b>3i</b>	Bis-2,6-di-Br-4-OCH <sub>2</sub> OCH <sub>3</sub>		138-140	methanol	76.7
<b>3l</b>	Bis-3-NO <sub>2</sub> -4-OCH <sub>2</sub> OCH <sub>3</sub>		154-156	methanol	83.5
<b>3m</b>	Bis-3-F-4-OCH <sub>2</sub> OCH <sub>3</sub>		90-92	methanol	95.0
<b>3n</b>	Bis-3,5-di-CH <sub>3</sub> -4-OCH <sub>2</sub> OCH <sub>3</sub>		101-103	methanol	93.0
<b>3q</b>	Bis-3-Br-4-OCH <sub>2</sub> OCH <sub>3</sub>		78-80	cyclohexane	64.0
<b>3r</b>	Bis-3,5-di-Br-4-OCH <sub>2</sub> OCH <sub>3</sub>		90-92	cyclohexane	60.3

<b>3s</b>	Bis-3-Br-4-OCH <sub>2</sub> OCH <sub>3</sub>		116-118	methanol	93.2
<b>3t</b>	Bis-3,5-di-Br-4-OCH <sub>2</sub> OCH <sub>3</sub>		155-157	methanol	86.8
<b>3u</b>	Bis-4-OCH <sub>2</sub> OCH <sub>3</sub>		171-173	methanol	95.4
<b>3v</b>	Bis-3-Br-4-OCH <sub>2</sub> OCH <sub>3</sub>		162-164	methanol	87.6
<b>3w</b>	Bis-3,5-di-Br-4-OCH <sub>2</sub> OCH <sub>3</sub>		164-166	methanol	84.0
<b>3x</b>	Bis-4-OCH <sub>2</sub> OCH <sub>3</sub>		174-176	methanol	95.6
<b>3y</b>	Bis-3-Br-4-OCH <sub>2</sub> OCH <sub>3</sub>		150-152	methanol	93.7
<b>3z</b>	Bis-3,5-di-Br-4-OCH <sub>2</sub> OCH <sub>3</sub>		162-164	methanol	88.5
<b>3a'</b>	Bis-3-Br-4-OCH <sub>2</sub> OCH <sub>3</sub>		184-186	methanol	96.4
<b>3b'</b>	Bis-3,5-di-Br-4-OCH <sub>2</sub> OCH <sub>3</sub>		166-168	methanol	86.8

*Design, synthesis and biological validation of epigenetic modulators of histone/protein deacetylation and methylation.*

<b>3c'</b>	3,5-di-Br-4-OCH <sub>2</sub> OCH <sub>3</sub> , 3-Br-4-OCH <sub>2</sub> OCH <sub>3</sub>		182-184	methanol	84.3
<b>3d'</b>	Bis-3-Br-4-OCH <sub>2</sub> OCH <sub>3</sub>		164-166	methanol	75.7
<b>3e'</b>	Bis-3,5-di-Br-4-OCH <sub>2</sub> OCH <sub>3</sub>		178-180	methanol	64.5
<b>3f'</b>	Bis-3-Br-4-OCH <sub>2</sub> OCH <sub>3</sub>		174-176	methanol	73.0
<b>3g'</b>	Bis-3,5-di-Br-4-OCH <sub>2</sub> OCH <sub>3</sub>		179-181	methanol	76.7
<b>3h'</b>	Bis-4-OCH <sub>2</sub> OCH <sub>3</sub>		166-168	methanol	79.8
<b>3i'</b>	Bis-3-Br-4-OCH <sub>2</sub> OCH <sub>3</sub>		182-184	methanol	67.4
<b>3j'</b>	Bis-3,5-di-Br-4-OCH <sub>2</sub> OCH <sub>3</sub>		189-191	methanol	62.3

<b>3k'</b>	Bis-4-OCH <sub>2</sub> OCH <sub>3</sub>		197-199	methanol	76.7
<b>3l'</b>	Bis-3,5-di-Br-4-OCH <sub>2</sub> OCH <sub>3</sub>		174-176	methanol	96.5
<b>3m'</b>	Bis-3,5-di-Br-4-OCH <sub>2</sub> OCH <sub>3</sub>		150-152	methanol	94.3
<b>3n'</b>	Bis-3,5-di-Br-4-OCH <sub>2</sub> OCH <sub>3</sub>		126-128	methanol	89.0
<b>3o'</b>	Bis-3,5-di-Br-4-OCH <sub>3</sub>		248-250	methanol	92.0
<b>3p'</b>	Bis-3,5-di-Br-4-OCH <sub>3</sub>		>250	methanol	76.4

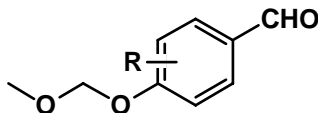


**Table 30.** Chemical and physical data of the compound **2a-h**.

Compounds	R	Melting Point (°C)	Recrystallization solvent	Yield (%)
<b>2a</b>	3-Br	72-74	cyclohexane	98.0
<b>2b</b>	3,5-di-Br	66-68	cyclohexane	94.0
<b>2c</b>	2-Br	62-64	cyclohexane	89.4
<b>2d</b>	2,6-di-Br	96-98	cyclohexane	25.6
<b>2e</b>	H	oil	-	100.0
<b>2f</b>	3,5-di-CH <sub>3</sub>	oil	-	100.0
<b>2g</b>	3-F	oil	-	96.7
<b>2h</b>	3-NO <sub>2</sub>	95-97	cyclohexane	98.0

## 20.2. Experimental Section.

*Chemistry.* Melting points were determined on a Büchi 530 melting point apparatus and are uncorrected. Infrared (IR) spectra (KBr) were recorded on a Perkin-Elmer Spectrum One instrument. <sup>1</sup>H NMR spectra were recorded at 200 MHz on a Bruker AC 200 spectrometer; chemical shifts are reported in  $\delta$  (ppm) units relative to the internal reference tetramethylsilane (Me<sub>4</sub>Si). All compounds were routinely checked by TLC and <sup>1</sup>H NMR. TLC was performed on aluminum-backed silica gel plates (Merck DC-Alufolien Kieselgel 60 F<sub>254</sub>) with spots visualized by UV light. All solvents were reagent grade and, when necessary, were purified and dried by standard methods. Concentration of solutions after reactions and extractions involved the use of a rotary evaporator operating at a reduced pressure of *ca.* 20 Torr. Organic solutions were dried over anhydrous sodium sulfate. Analytical results are within  $\pm 0.40\%$  of the theoretical values.

All chemicals were purchased from Aldrich Chimica, Milan (Italy) or Lancaster Synthesis GmbH, Milan (Italy) and were of the highest purity.

**General Procedure for the Synthesis of 4-(Methoxymethoxy)benzaldehydes (2a-h) and of 1,3-dibromo-5-(methoxymethoxy)benzene. Example: 3,5-Dibromo-4-(methoxymethoxy)benzaldehyde (1b).**

To a suspension of sodium hydride in mineral oil 60% (14.3 mmol, 572 mg) in anhydrous tetrahydrofuran (20 mL) at 0 °C (ice bath), 3,5-dibromo-4-hydroxybenzaldehyde (7.15 mmol, 2 g) was slowly added and the resulting mixture was stirred for 30 min. Then, a solution of bromomethyl(methyl)ether (14.3 mmol, 1.17 mL) in anhydrous tetrahydrofuran (5 mL) was added dropwise at 0 °C, and the mixture was stirred for further 30 min. The reaction was quenched with water (30 mL) and extracted with diethyl ether (3 × 50 mL). The organic phases were washed with 2 N sodium hydroxide (3 × 50 mL) and sodium chloride (3 × 50 mL), and dried with sodium sulfate. The residual oil was purified by column chromatography on silica gel by eluting with a 1:5 mixture of ethyl acetate and chloroform to furnish the pure product **2b** as a solid. <sup>1</sup>H NMR (CDCl<sub>3</sub>, 400 MHz, δ; ppm) δ 9.86 (s, 1H), 8.04 (s, 2H), 5.28 (s, 2H), 3.72 (s, 3H).

**Synthesis of 2,6-dibromo-4-(methoxymethoxy)benzaldehyde (2d).**

A 2 M solution of lithium diisopropylamide (LDA) in heptane/THF/ethylbenzene (14.87 mmol, 7.43 mL) was added dropwise (ca. 15 min) to a solution of 1,3-dibromo-5-(methoxymethoxy)benzene (7.43 mmol, 2.2 g) in anhydrous THF (20 mL) cooled to -80 °C. The resultant solution was stirred for 15 min, then anhydrous *N,N*-dimethylformamide (DMF, 14.87 mmol, 1.15 mL) was slowly added. The mixture was stirred for additional 30 min and then the reaction was quenched with water (30 mL) and extracted with diethyl ether (3 × 50 mL). The collected organic phases were washed with sodium chloride (3 × 50 mL) and dried with sodium sulfate. Evaporation of solvent afforded a mixture of 1,4-dibromo-6-(methoxymethoxy)benzaldehyde and 2,6-dibromo-4-(methoxymethoxy)benzaldehyde (**2d**), which were separated by column chromatography on silica gel by eluting with ethyl acetate:*n*-hexane 1:10. For **2d**: <sup>1</sup>H NMR (CDCl<sub>3</sub>, 400 MHz, δ; ppm) δ 10.22 (s, 1H), 7.34 (s, 2H), 5.22 (s, 2H), 3.49 (s, 3H).

**General Procedure for the Synthesis of the compounds 3a-k'. Example: 1,5-Bis-(4-(methoxymethoxy)-3-nitrophenyl)penta-1,4-dien-3-one (3l).**

To a suspension of barium hydroxide octahydrate (6.62 mmol, 2.08 g) in methanol (20 mL) 2-propanone (1.65 mmol, 0.12 mL) was added, and the mixture was stirred for 5 min. Then a solution of 4-(methoxymethoxy)-3-nitrobenzaldehyde **2h** (3.31 mmol, 0.7 g) in methanol (10 mL) was added, and the resultant mixture was stirred for 2 h at room temperature. The precipitate was filtered, washed with water, and dried to afford the pure product **3l**. <sup>1</sup>H NMR (DMSO-*d*<sub>6</sub>, 400 MHz, δ; ppm) δ 8.32 (s, 2H), 8.03 (d, 2H), 7.77 (d, 2H), 7.47 (d, 2H), 7.34 (d, 2H), 5.42 (s, 4H), 3.49 (s, 6H).

**General Procedure for the Synthesis of the compounds 1a-m'. Example: 3,5-Bis-(3-bromo-4-hydroxy-benzylidene)-1-methyl-piperidin-4-one (1c').**

A 3 N hydrochloric acid solution (5mL) was added to a solution of 3,5-Bis-(3-bromo-4-methoxymethoxy-benzylidene)-1-methyl-piperidin-4-one **3a'** (0.53 mmol, 0.3 g) in methanol (5 mL), and the resulting mixture was refluxed for 3 h. The reaction was cooled at room temperature, then the precipitate was filtered, washed with water and dried to afford the pure product **1c'**. <sup>1</sup>H NMR (DMSO-*d*<sub>6</sub>, 400 MHz, δ; ppm) δ 11.22 (s, 2H), 7.73 (d, 4H), 7.39 (s, 2H), 7.13 (s, 2H), 4.60 (s, 4H), 2.98 (s, 3H).

**Synthesis of 3,5-di-Br-4-methoxymethoxybenzoic acid.**

To a suspension of sodium hydride in mineral oil 60% ( 9.67 mmol, 0.387 g) in anhydrous tetrahydrofuran (20 ml) cooled to 0°C slowly methyl-3,5-dibromo-4-hydroxy-benzoate ( 6.45 mmol, 2 g) was added and resulting mixture was stirred for 30 min. Then a solution of bromomethylmethylether (9.67 mmol, 0.79 mL) in anhydrous tetrahydrofuran (5 ml) was added dropwise at 0°C and the mixture was stirred for 30 min. The reaction was quenched by water (30 ml) and extracted with diethyl ether (3x50 ml). The organic layers were washed with a solution of sodium hydroxide 2N (3x50 ml) before and with a solution of sodium chloride (3x50 ml) and finally dried with sodium sulfate. The crude product was eluted with methanol and hydrolyzed with 2N KOH ( 12.43 mmol, 0.697 g) to afford the pure product as a white solid.



**General procedure for the synthesis of the N,N'-[bis-(3,5-di-Br-4-methoxymethoxy-alkylen-benzamides)] (3l'-n'). Example: synthesis of N,N'-[bis-(3,5-di-Br-4-methoxymethoxy-ethylen-benzamide)] (3l').**

Ethyl chloroformate (2.93 mmol, 0.28 mL) and triethylamine (3.17 mmol, 0.45 mL) were added to a cooled (0°C) solution of 3,5-di-Br-4-methoxymethoxybenzoic acid (2.44 mmol, 0.83 g) in dry THF (10 mL), and the mixture was stirred for 10 min. The solid was filtered off, and ethylenediamine (1.22 mmol, 0.082 mL) was added to the filtrate. The solution was stirred for 15 min at 0°C, evaporated under decreased pressure to afford pure product **3l** as a white solid. <sup>1</sup>H NMR (DMSO-*d*<sub>6</sub>, 400 MHz, δ; ppm) δ 8.55 (s, 2H), 8.09 (s, 4H), 5.18 (s, 4H), 3.59 (s, 6H), 3.36 (s, 4H).

**General procedure for the synthesis of the N,N'-[bis-(3,5-di-Br-4-hydroxy-alkylen-benzamides)] (1l'-n'). Example: synthesis of N,N'-[bis-(3,5-di-Br-4-hydroxy-propylen-benzamide)] (1m').**

To a solution of N,N'-[bis-(3,5-di-Br-4-methoxymethoxy-propylen-benzamide)] (**3m'**)(0.70 mmol, 0.5 g) in methanol (10 mL) 3N HCl solution was added and the resulting mixture was stirred at 60°C for 1h. The solvent was evaporated and the solid residue was washed with water and dried to furnish the pure product **1m'**. <sup>1</sup>H NMR (DMSO-*d*<sub>6</sub>, 400 MHz, δ; ppm) δ 10.5 (s, 2H), 8.55 (s, 2H), 8.00 (s, 4H), 3.31 (s, 4H).

**General procedure for the synthesis of the N,N'- phenylen-[bis-(3,5-di-Br-4-methoxy-benzamides)] (3o', 3p'). Example: synthesis of N,N'-1,3-phenylen-[bis-(3,5-di-Br-4-methoxy-benzamide)] (3o').**

3,5-di-Br-4-methoxybenzoic acid (2.58 mmol, 0.8 g) was eluted with thionyl chloride and refluxed for 1h. Then the solution was concentrated on vacuum, eluted with tetrahydrofuran (10 mL) and added dropwise to a cooled (0°C) solution of 1,3-phenylenediamine (1.29 mmol, 0.139 g), triethylamine (3.87 mmol, 0.54 mL) and the resulting mixture was stirred for 30 min. The suspension was concentrated on vacuum, eluted with water (50 mL) and the precipitated solid was filtered and finally dried to afford pure **3o'**. <sup>1</sup>H NMR (DMSO-*d*<sub>6</sub>, 400 MHz, δ; ppm) δ 10.70 (s, 2H), 10.24 (s, 2H), 8.25 (s, 1H), 8.19 (s, 4H), 7.45 (d, 2H), 7.30 (m, 1H), 3.70 (s, 6H).

**General procedure for the synthesis of the N,N'-phenylen [bis-(3,5-di-Br-4-hydroxy-benzamides)] (1o', 1p'). Example: synthesis of N,N'-1,3-phenylen-[bis-(3,5-di-Br-4-methoxy-benzamide)] (1o').**

To a suspension of diether **3o'** (0.29 mmol, 0.2 g) in methylene chloride (5 mL) cooled at -78°C a BBr<sub>3</sub> solution in methylene chloride (5 mL) was slowly added. The reaction mixture, which immediately became clear, was allowed to warm to room temperature and was stirred for 5h. Water (30 mL) was added to quench the reaction. The off-solid that formed was removed by filtration to afford diphenol **1o'** as a white solid. <sup>1</sup>H NMR (DMSO-*d*<sub>6</sub>, 400 MHz, δ; ppm) δ 10.70 (s, 2H), 10.24 (s, 2H), 8.25 (s, 1H), 8.19 (s, 4H), 7.45 (d, 2H), 7.30 (m, 1H).

**General procedure for the synthesis of the compounds 1s'-x'. Example: synthesis of N,N'-Bis-(3,5-dibromo-4-hydroxy-phenyl)-isophthalamide 1w'.**

To a cooled (0°C) solution of 4-Amino-2,6-dibromo-phenol (3.75 mmol, 1g) and triethylamine (5.61 mmol, 0.78 mL) in tetrahydrofuran (10 mL) isophthaloyl dichloride (1.87 mmol, 0.38g), eluted in tetrahydrofuran (10 mL), was slowly added. The reaction mixture was stirred for 1h, then the solvent was distilled on vacuum and the solid residue was washed with HCl 2N, then with water (50 mL) and at last dried to afford pure product **1w'**. <sup>1</sup>H NMR (DMSO-*d*<sub>6</sub>, 400 MHz, δ; ppm) δ 11.0 (s, 2H), 10.39 (s, 2H), 8.50 (s, 1H), 8.10 (d, 2H), 7.98 (s, 4H), 7.67 (m, 1H).

**Synthesis of the 1,7-Bis-(3-bromo-4-hydroxy-phenyl)-5-hydroxy-hepta-1,4,6-trien-3-one (1o) and 1,7-Bis-(3,5-di-bromo-4-hydroxy-phenyl)-5-hydroxy-hepta-1,4,6-trien-3-one (1p). Example: synthesis of 1,7-Bis-(3,5-di-bromo-4-hydroxy-phenyl)-5-hydroxy-hepta-1,4,6-trien-3-one (1p).**

2,4-pentanedione (4.97 mmol, 0.51 mL) and boric anhydride (3.48 mmol, 0.24 g) were dissolved in EtOAc (15 mL). The solution was stirred at 70°C for 30 min. 3-bromo-4-hydroxybenzaldehyde (9.95 mmol, 2 g) and tributyl borate (9.95 mmol, 2.68 mL) were added. After stirring for 30 min, butylamine (7.45 mmol, 0.73 mL) dissolved in 4 mL of EtOAc was added dropwise over 15 min. The stirring continued for 5 h at 85°C. The mixture was then hydrolyzed by adding 1 N HCl (8 mL) and stirring for 30 min at 60°C. The organic layer was separated, and the aqueous layer was extracted with EtOAc. The combined organic layers were washed until neutral and dried over anhydrous sodium sulfate. The solvent was removed

in vacuo, and the crude product was purified by column chromatography eluting with hexane-EtOAc 1:1 to give the pure product (**1o**) as an orange solid. <sup>1</sup>H NMR (DMSO-*d*<sub>6</sub>, 400 MHz, δ; ppm) δ 10.48 (s, 2H), 7.96 (s, 4H), 7.49 (d, 2H), 6.95 (d, 2H), 6.00 (s, 1H).

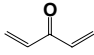
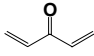
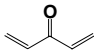
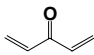
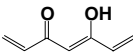
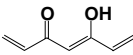
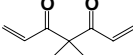
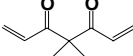
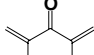
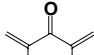
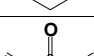
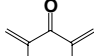
### *20.3. Biological evaluation.*

Compounds **1a-x** were tested against RmtA, an arginine methyltransferase from *Aspergillus nidulans* with significant sequence homology to human PRMT1 and specific for methylation at Arg3 of H4.<sup>13</sup> Histones H4 were used as substrate. The results have been reported as percent of inhibition at a fixed dose and IC<sub>50</sub> (50% inhibitory concentration) values (Table 30).

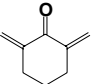
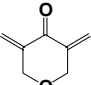
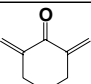
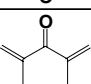
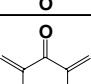
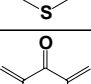
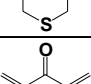
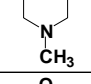
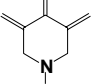


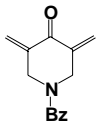
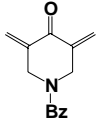
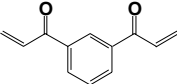
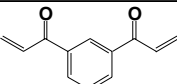
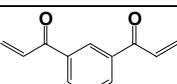
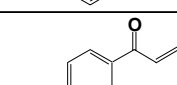
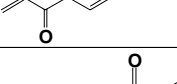
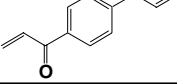
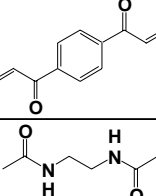
**Table 30.** Inhibiting activity of the new HMT inhibitors against RmtA.<sup>a</sup>

Compounds	R <sub>1</sub> , R <sub>2</sub>	Spacer	RmtA (μM)
<b>1a</b>	3-Br	-	No inhibition at 73 μM
<b>1b</b>	3,5-di-Br	-	No inhibition at 73 μM
<b>1c</b>	Bis-3-Br-4-OH		162
<b>1d</b>	Bis-3,5-di-Br-4-OH		69
<b>1e</b>	3-Br-4-OH, 3,5-di-Br-4-OH		40
<b>1f</b>	Bis-3-Br		Inactive up to 90 μM
<b>1g</b>	Bis-4-OH		Inactive up to 90 μM
<b>1h</b>	Bis-2-Br-4-OH		114
<b>1i</b>	Bis-2,6-di-Br-4-OH		215
<b>1j</b>	Bis-3-Br-4-OCH <sub>3</sub>		Inactive up to 90 μM

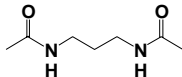
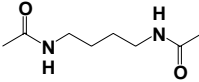
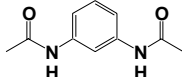
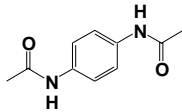
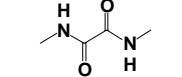
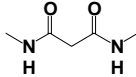
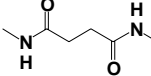
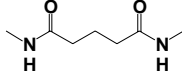
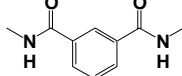
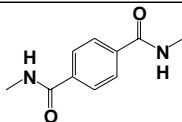
<b>1k</b>	Bis-3,5-di-Br-4-OCH <sub>3</sub>		Inactive up to 90 μM
<b>1l</b>	Bis-3-NO <sub>2</sub> -4-OH		249
<b>1m</b>	Bis-3-F-4-OH		No inhibition at 28.3 μM
<b>1n</b>	Bis-3,5-di-CH <sub>3</sub> -4-OH		206
<b>1o</b>	Bis-3-Br-4-OH		
<b>1p</b>	Bis-3,5-di-Br-4-OH		48 μM
<b>1q</b>	Bis-3-Br-4-OH		no inhib. at 91,8 μM
<b>1r</b>	Bis-3,5-di-Br-4-OH		no inhib. at 13,0 μM
<b>1s</b>	Bis-3-Br-4-OH		90 μM
<b>1t</b>	Bis-3,5-di-Br-4-OH		14 μM
<b>1u</b>	Bis-4-OH		no inhib. at 27,7 μM
<b>1v</b>	Bis-3-Br-4-OCH <sub>3</sub>		Inactive up to 90 μM

Design, synthesis and biological validation of epigenetic modulators of histone/protein deacetylation and methylation.

<b>1w</b>	Bis-3,5-di-Br-4-OCH <sub>3</sub>		Inactive up to 90 μM
<b>1x</b>	Bis-3-Br-4-OH		132 μM
<b>1y</b>	Bis-3,5-di-Br-4-OH		29 μM
<b>1z</b>	Bis-4-OH		no inhib. at 27,5 μM
<b>1a'</b>	Bis-3-Br-4-OH		No inhibition at 17.7 μM
<b>1b'</b>	Bis-3,5-di-Br-4-OH		45 μM
<b>1c'</b>	Bis-3-Br-4-OH		no inhib. at 17,7 μM
<b>1d'</b>	Bis-3,5-di-Br-4-OH		39 μM
<b>1e'</b>	3,5-di-Br-4-OH, 3-Br-4-OH		no inhib. at 15,2 μM

<b>1f'</b>	Bis-3-Br-4-OH		No inhibition at 15.4 μM
<b>1g'</b>	Bis-3,5-di-Br-4-OH		210 μM
<b>1h'</b>	Bis-3-Br-4-OH		59 μM
<b>1i'</b>	Bis-3,5-di-Br-4-OH		10 μM
<b>1j'</b>	Bis-4-OH		no inhib. at 22,9 μM
<b>1k'</b>	Bis-3-Br-4-OH		47 μM
<b>1l'</b>	Bis-3,5-di-Br-4-OH		37 μM
<b>1m'</b>	Bis-4-OH		no inhib. at 22,9 μM
<b>1n'</b>	Bis-3,5-di-Br-4-OH		no inhib. at 13,8 μM

*Design, synthesis and biological validation of epigenetic modulators of histone/protein deacetylation and methylation.*

<b>1o'</b>	Bis-3,5-di-Br-4-OH		no inhib. at 13.6 μM
<b>1p'</b>	Bis-3,5-di-Br-4-OH		616 μM
<b>1q'</b>	Bis-3,5-di-Br-4-OH		no inhib. at 13,8 μM
<b>1r'</b>	Bis-3,5-di-Br-4-OH		no inhib. at 13,8 μM
<b>1s'</b>	Bis-3,5-di-Br-4-OH		32,6 μM
<b>1t'</b>	Bis-3,5-di-Br-4-OH		no inhib. at 14,2 μM
<b>1u'</b>	Bis-3,5-di-Br-4-OH		no inhib. at 13,8 μM
<b>1v'</b>	Bis-3,5-di-Br-4-OH		no inhib. at 13,8 μM
<b>1w'</b>	Bis-3,5-di-Br-4-OH		13,8 μM
<b>1x'</b>	Bis-3,5-di-Br-4-OH		no inhib. at 12,8 μM

<sup>a</sup>Data represent mean values of at least three separate experiments.



RmtA from *A. nidulans* showed high homology to human PRMT1 and is specific for Arg3 of H4 methylation. To acquire information on their effect and selectivity on human PRMTs and HKMTs, compounds **1a-x'** have been tested at 100  $\mu$ M against human recombinant PRMT1 using the *Saccharomyces cerevisiae* RNA-binding protein Npl3p as a substrate, against human recombinant CARM1/PRMT4 using poly(A)binding protein 1 (PABP1) as a substrate, and against the lysine methyltransferase SET7 with histones H3 as a substrate (Figure 49 and 50).

**Top panels.**

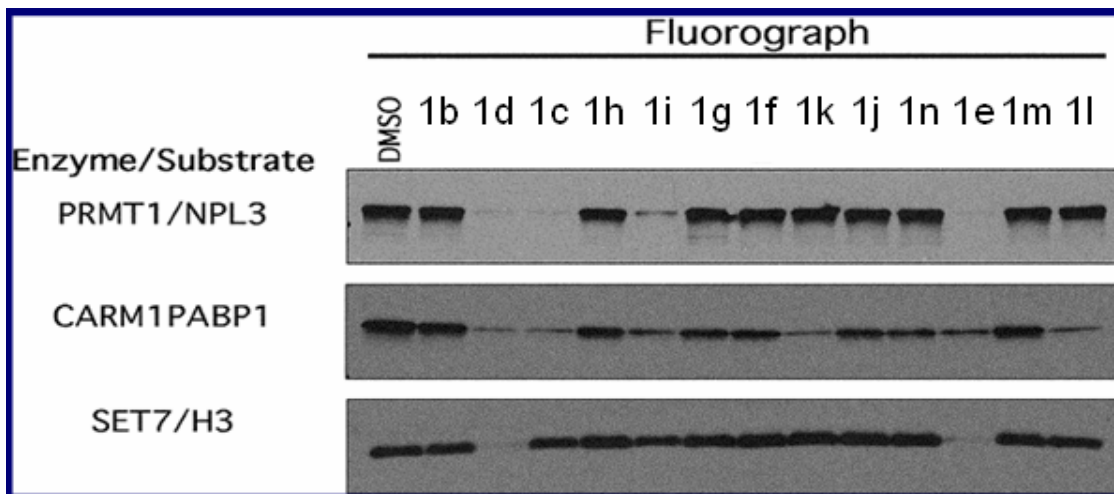


**Figure 49 (a).** Fluorographs. Inhibition assay against PRMT1, CARM1, SET7 at 100  $\mu$ M concentration of each of the compounds.

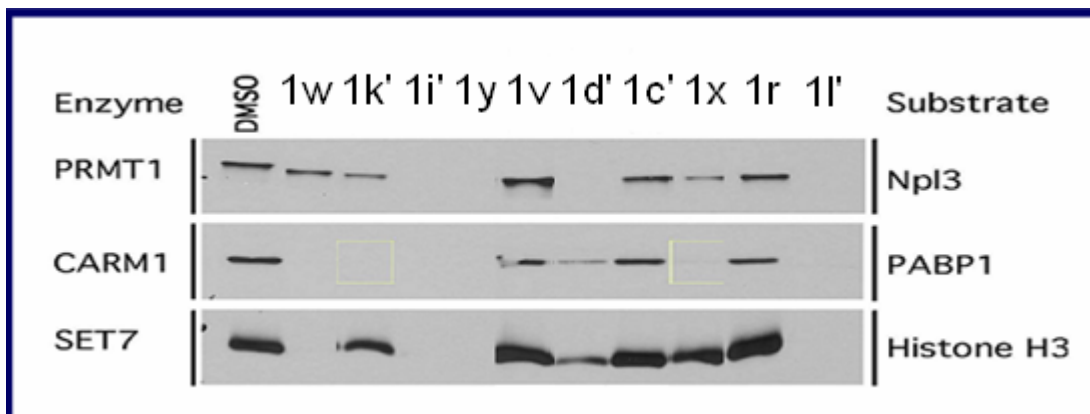


**Figure 49 (b).** Fluorographs. Inhibition assay against PRMT1, CARM1, SET7 at 100  $\mu\text{M}$  concentration of each of the compounds.

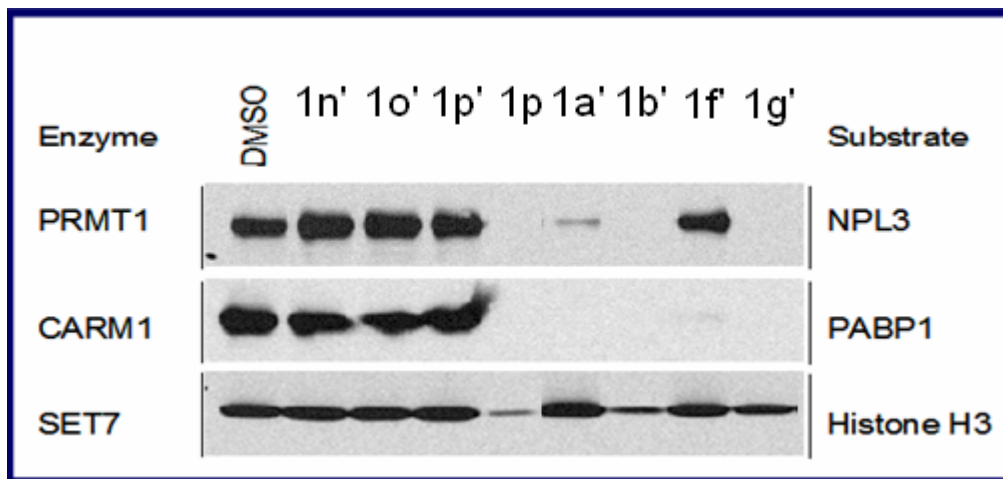


**Figure 49 (c).** Fluorographs. Inhibition assay against PRMT1, CARM1, SET7 at 100  $\mu\text{M}$  concentration of each of the compounds.

**Bottom panel.**

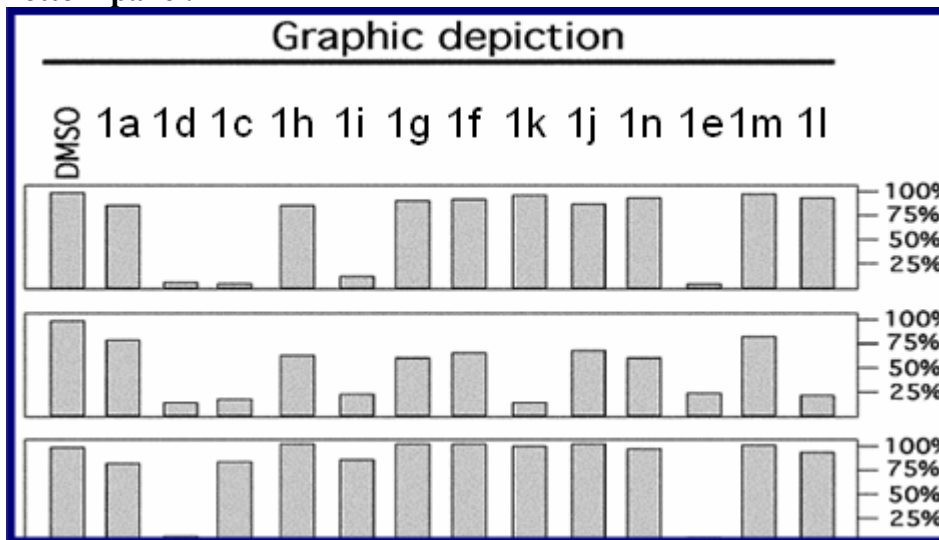


**Figure 50.** *Graphic depiction. Inhibition assay expressed in percentual decrease of the enzyme activity at 100  $\mu$ M concentration of each of the compounds.*

*20.3.1. Preparation of GST-RmtA Fusion Proteins.*

The coding sequence of RmtA was cloned into a pGEX-5X-1 expression vector (Amersham Pharmacia Biotech). RmtA-Protein was expressed in BL21 cells in LB-medium. 250 mL cultures with an  $A_{600}$  of 0.4 were induced with a final concentration of 1mM IPTG and grown for 4h at 37 °C. After centrifugation of cells at 4000g, the pellet was resuspended in 6 mL of GST-binding buffer (140 mM NaCl, 2.7 mM KCl, 10 mM  $\text{Na}_2\text{HPO}_4$ , 1.8 mM  $\text{KH}_2\text{PO}_4$ , pH 7.3) containing one protease inhibitor tablet (Complete, Roche, Mannheim, Germany) for 50 mL of buffer. For cell lysis, lysozyme was added at a final concentration of 5 mg/mL binding buffer and cells were passed through a french press with pressure setting of 1000 psi. The

resulting lysate was centrifuged at 20000g for 10 min at 4 °C. GST fusion protein was purified from soluble extracts by binding to a GST-HiTrap column (Amersham Pharmacia Biotech). Proteins were eluted with 50 mM Tris-HCl, 10 mM reduced glutathione, pH 8.0 and assayed for histone methyltransferase activity.

### 20.3.2. RmtA Inhibitory assay.

For inhibition assays, affinity purified GST-RmtA fusion proteins were used as enzyme source. HMT activities were assayed using chicken erythrocyte core histones as substrate. 500 ng of GST-RmtA fusion proteins were incubated with different concentrations of compounds for 15 min at room temperature and 20 µg of chicken core histones and 0.55 µCi of [<sup>3</sup>H]-S-adenosyl-L-methionine (SAM) were added. This mixture was incubated for 30 min at 30 °C. Reaction was stopped by TCA precipitation (25% final concentration) and samples were kept on ice for 20 min. Whole sample volumes were collected onto glass fibre filter (Whatman GF/F) preincubated with 25% TCA. Filters were washed three times with 3 mL of 25% TCA and then three times with 1 mL of ethanol. After drying the filters for 10 min at 70 °C, radioactivity was measured by liquid scintillation spectrophotometry (3 mL scintillation cocktail).

### 20.3.3. PRMT1, CARM1/PRMT4, and SET7 Inhibitory Assay.

*In vitro* methylation reactions have been described in detail previously.<sup>359</sup> Briefly, all methylation reactions were carried out in the presence of *S*-adenosyl-L-[methyl-<sup>3</sup>H]methionine([<sup>3</sup>H]AdoMet, 79 Ci/mmol from a 12.6 µM stock solution in dilute HCl/ethanol 9:1, pH 2.0–2.5, Amersham Biosciences) and PBS (137 mM NaCl, 2.7 mM KCl, 4.3 mM Na<sub>2</sub>HPO<sub>4</sub>, 1.4 mM KH<sub>2</sub>PO<sub>4</sub>, pH 7.4). To determine the specificity of the small molecules, compounds were incubated with GST-PRMT1 and Npl3p, GST-PRMT4 and PABP1, GST-SET7 and histone H3, respectively. Substrates (0.5 µg) were incubated with recombinant enzymes (0.2 µg) in the presence of 0.5 µM [<sup>3</sup>H]AdoMet and 100 µM concentration of each of the compound for 90 min at 30 °C in a final volume of 30 µL PBS. Reactions were run on a 10% SDS-PAGE, transferred to a PVDF membrane, sprayed with Enhance<sup>TM</sup>, and exposed to film overnight. The fluorographs are shown in the *top panels*, and the quantification of the

methylation levels is depicted in the *bottom panel*. Reactions were performed in the presence of Me<sub>2</sub>SO at 3.3% v/v.

#### 20.4. Docking study of the compounds **1c**, **1d** and **1k**.

In order to elucidate the binding possibilities of selected HMT inhibitors, compounds **1c** (PRMTs-selective), **1d** (no selective), and **1k** (CARM1-selective) were docked (Autodock program)<sup>360</sup> into the crystal structures of PRMT1<sup>361</sup> and SET7,<sup>362</sup> and into the modeled structures of RmtA and CARM1. The analysis of the Autodock-proposed binding modes for **1c**, **1d**, **1k** revealed that the compounds are able to bind in the *S*-adenosylmethionine (SAM) or in the Arg/Lys substrate binding sites (Figure 51).

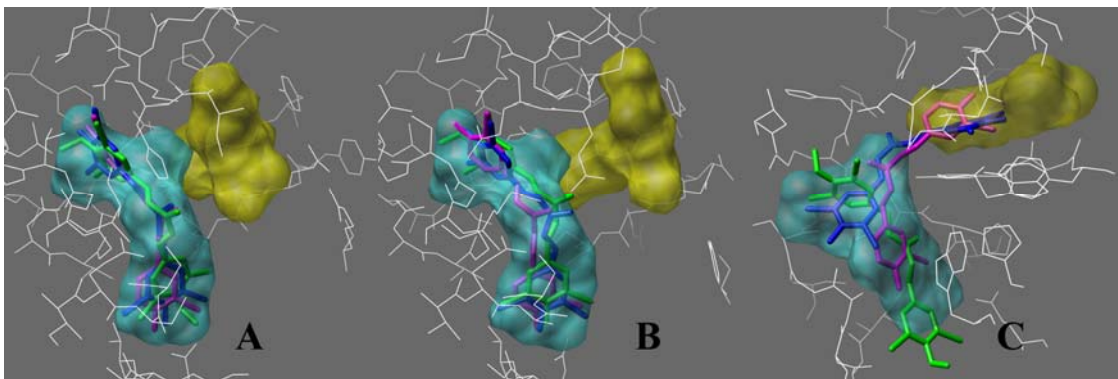


**Figure 51.** Compounds **1c** (magenta), **1d** (blue), and **1k** (green) docked into PRMT1 (A), CARM1 (B) and SET7 (C). The Arg/Lys and SAM binding sites are represented in red and yellow, respectively. The enzymes residues within 5.0 Å from the substrates are reported in white wire. For the sake of clarity hydrogen atoms are not displayed.

The **1c**, **1d**, **1k** inhibition constants (p*K<sub>i</sub>*s) calculated by the Autodock internal scoring function largely agree with the experimental values. Although the absolute values are by far overestimated, the overall inhibition selectivity trend is respected. Thus, **1c** was calculated to be more active against PRMTs (PRMT1, CARM1, and RmtA) than against SET7, **1d** was predicted to be no selective, and **1k** was predicted to be slightly selective for CARM1.

#### *20.4.1. Molecular Docking.*

All the tested molecules were built, starting from ASCII text, using the stand alone version of PRODRG, in conjunction with the GROMACS suite. The docking studies were performed by means of the Autodock 3.0.5 program using a grid spacing of 0.375 Å and 39 × 50 × 56 number of points that embraced both the SAM and Arg/Lys binding sites. The grid was centred on the mass centre of the experimental bound SAM and Arg substrates. The GA-LS method was adopted using the default setting except for the maximum number of energy evaluations that was set to 2500000. Autodock generated 100 possible binding conformations for each molecule that were clustered using a tolerance of 2.0 Å. The AutoDockTool (ADT) graphical interface was used to prepare the enzyme PDBQS file. The protein atom charges as calculated during the complex minimization were retained for the docking calculations. To analyze the docking results the ADT was used and the Chimera 1.2176 program was used to produce the images.

#### *20.5. Results and discussion.*

As depicted in Figure 49 and 50 the 1,5-bis(3-bromo-4-hydroxyphenyl)penta-1,4-dien-3-one **1c** was highly efficient and selective in inhibiting PRMTs, while it was ineffective against the HKMT SET7. The introduction of further bromine atoms at 5,5' or just at the 5 position (compound **1d** or **1e**) increased the inhibiting power of the derivatives but abated the selectivity. By shifting the bromine from C3- to C2-benzene position an inactive compound (**1h**) was obtained. Nevertheless, the introduction of bromine atoms at both 2,6 and 2',6' positions gave a further molecule (**1i**) which was highly active and selective against PRMTs. The 1,5-bis(4-hydroxyphenyl)penta-1,4-dien-3-one **1g** and the 1,5-bis(3-bromophenyl)penta-1,4-dien-3-one **1f** were ineffective in inhibiting all the tested HMTs. The replacement of the 4-hydroxy group of **1c** with the 4-methoxy one (compound **1j**) gave similar results. Interestingly, the bis(3,5-dibromo-4-methoxy) analogue **1k** behaved as a very potent and selective CARM1/PRMT4 inhibitor (84% inhibition). The replacement of 3-bromo with 3,5-dimethyl or 3-fluoro substituent (compounds **1n** and **1m**) furnished inactive derivatives, while the 1,5-bis(3-nitro-4-hydroxyphenyl) penta-1,4-dien-3-one **1l** showed high activity and selectivity against CARM1/PRMT4 (80% inhibition). Finally, the monomer 4-(3,5-dibromo-4-hydroxyphenyl)but-3-en-2-one **1b** failed in inhibiting all the tested enzymes.

After this study we replaced the “ketonic spacer group” with others to evaluate its importance in the pharmacophore model.

All the ketonic spacer groups, except N-benzyl-4-piperidone, were tolerated, but the most functional were represented by cyclohexanone (compound **1t**) and 1,3-diacetylbenzene (compound **1i'**), both bis 3,5-di-bromo substituted. These compounds were the most potent against RmtA, in fact endowed with  $IC_{50}$  : 14  $\mu$ M (**1t**) and 10  $\mu$ M (**1i'**), but also against PRMT1, PRMT4 (CARM 1) and SET7, yet didn't show enzyme selectivity.

So we reported the first synthetic HMT (PRMT1, CARM1 and SET7) inhibitors obtaining the satisfactory results, yet further synthetic and biological studies are underway on both the pharmacophore motif and the linker moiety that connects the two phenyl rings.

## **References.**

1. Lengauer C, Issa JP. The role of epigenetics in cancer: DNA methylation, imprinting, and the epigenetics of cancer. *Mol Med Today* 1998;4:102–103.
2. Jones PA, Laird PW. Cancer epigenetics comes of age. *Nat Genet* 1999;21:163–167.
3. Mukesh V, Sudhir S. Epigenetics in cancer: Implications for early detection and prevention. *Lancet Oncol* 2002;3:755–763.
4. Fire A. Potent and specific genetic interference by double-stranded RNA in *Caenorhabditis elegans*. *Nature* 1998;391:806–811.
5. Baylin SB. Tying it all together: Epigenetics, genetics, cell cycle, and cancer. *Science* 1997;277: 1948–1949.
6. Jones PA, Baylin SB. The fundamental role of epigenetic events in cancer. *Nat Rev Genet* 2002;3: 415–428.
7. Takacs M, Salamon D, Myohanen S. Epigenetics of latent Epstein–Barr virus genomes: High resolution methylation analysis of the bidirectional promoter region of latent membrane protein 1 and 2B genes. *Biol Chem* 2001;382:699–705.
8. Tierney RJ, Kirby HE, Nagra JK. Methylation of transcription factor binding sites in the Epstein–Barr virus latent cycle promoter Wp coincides with promoter down-regulation during virus-induced B-cell transformation. *J Virol* 2000;74:10468–10479.
9. Robertson KD. The role of DNAmethylation in modulating Epstein–Barr virus gene expression. *Curr Top Microbiol Immunol* 2000;249:21–34.
10. Tao Q, Swinnen LJ, Yang J. Methylation status of the Epstein–Barr virus major latent promoter C in iatrogenic B cell lymphoproliferative disease: Application of PCR-based analysis. *Am J Pathol* 1999;155:619–625.
11. Hagan CR, Rudin CM. Mobile genetic element activation and genotoxic cancer therapy: Potential clinical implications. *Am J Pharmacogenomics* 2002;2:25–35.
12. Nelson WG, De Marzo AM, De Weese TL. Preneoplastic prostate lesions: An opportunity for prostate cancer prevention. *Ann NY Acad Sci* 2001;952:135–144.
13. Rideout WM, Eggan K, Jaenisch R. Nuclear cloning and epigenetic reprogramming of the genome. *Science* 2001;293:1093–1098.
14. Nelson WG, De Marzo AM, De Weese TL. The molecular pathogenesis of prostate cancer: Implications for prostate cancer prevention. *Urology* 2001;57:39–45.
15. Howell CY, Bestor TH, Ding F. Genomic imprinting disrupted by a maternal effect mutation in the Dnmt 1 gene. *Cell* 2001;104:829–838.
16. El-Osta A, Wolffe AP. DNAmethylation and histone deacetylation in the control of gene expression: Basic biochemistry to human development and disease. *Gene Exp* 2000;9:63–75.
17. Zuccotti M, Garagna S, Redi CA. Nuclear transfer, genome reprogramming, and novel opportunities in cell therapy. *J Endocrinol Invest* 2000;23:623–629.



18. Avner P, Heard E. X-chromosome inactivation: Counting, choice, and initiation. *Nat Rev Genet* 2001; 2:59–67.
19. Feinberg AP. Cancer epigenetics takes center stage. *Proc Natl Acad Sci USA* 2001;98:392–394.
20. Dennis C. Altered states. *Nature* 2003;421:686–688.
21. Maier S, Olek A. Diabetes: A candidate disease for efficient DNA methylation profiling. *J Nutr Sci* 2002;132:2440–2443.
22. Lumey LH. Decreased birth weights in infants after maternal in utero exposure to the dutch famine of 1944–1945. *Paediatr Perinat Epidemiol* 1992;6:240–253.
23. Kaati G, Bygren LO, Edvisson S. Cardiovascular and diabetes mortality determined by nutrition during parents' and grandparents' slow growth period. *Eur J Hum Genet* 2002;10:682–688.
24. Morgan HD, Sutherland HGE, Martin DIK, Whitelaw E. Epigenetic inheritance at the agouti locus in the mouse. *Nat Genet* 1999;23:314–318.
25. Sollars V. Evidence for an epigenetic mechanism by which Hsp90 act as a capacitor for morphological evolution. *Nat Genet* 2003;33:70–74.
26. Bestor T, Laudano A, Mattaliano R, Ingram V. Cloning and sequencing of a cDNA encoding DNA methyltransferases of mouse cell. The carboxyl-terminal domain of the mammalian enzymes is related to bacterial restriction methyltransferases. *J Mol Biol* 1988;203:971–983.
27. Okano M, Xie S, Li E. Cloning and characterization of a family of novel mammalian DNA (cytosine-5) methyltransferases. *Nat Genet* 1998;19:219–220.
28. Larsen F, Gundersen G, Lopez R, Prydz H. CpG islands as gene markers in the human genome. *Genomics* 1992;13:1095–1107.
29. Jones PL. Methylated DNA and MeCP2 recruit histone deacetylase to repress transcription. *Nat Genet* 1998;19:187–191.
30. Nan X. Transcriptional repression by the methyl-CpG-binding protein MeCP2 involves a histone deacetylase complex. *Nature* 1998;393:386–389.
31. Constancia M, Dean W, Lopes S, Moore T, Kelsey G, Reik W. Deletion of a silencer element in IgA2 results in loss of imprinting independent H19. *Nat Genet* 2000;26:203–206.
32. Eden S. An upstream repressor element plays a role in IgA2 imprinting. *EMBO J* 2001;20:3518–3525.
33. Hark AT. CTCF mediated methylation-sensitive enhancer-blocking activity at the H19/IgA2 locus. *Nature* 2000;405:486–489.
34. Cooper DN, Youssoufian H. The CpG dinucleotide and human genetic disease. *Hum Genet* 1988;78:151–155.
35. Rideout WM, Coetzee GA, Olumi AF, Jones PA. 5-Methylcytosine as an endogenous mutagen in the human LDL receptor and p53 genes. *Science* 1990;249:1288–1290.
36. Esteller M, Catusas L, Matias-Guiu X. hMLH1 promoter hypermethylation is an early event in human endometrial tumorigenesis. *Am J Pathol* 1999;155:1767–1772.
37. Esteller M, Hamilton SR, Burger PC. Inactivation of the DNA repair gene O6-methylguanine-DNA methyltransferase by promoter hypermethylation is a common event in primary human neoplasia. *Cancer Res* 1999;59:793–797.

38. Esteller M, Sanchez-Cespedes M, Rosell R. Detection of aberrant promoter hypermethylation of tumour suppressor genes in serum DNA from non-small cell lung cancer patients. *Cancer Res* 1999;59:67–70.
39. Tycko B. Epigenetic gene silencing in cancer. *J Clin Invest* 2000;105:401–407.
40. Akhtar M, Cheng Y, Magno RM. Promoter methylation regulates Helicobacter pylori-stimulated cyclooxygenase-2 expression in gastric epithelial cells. *Cancer Res* 2001;61:2399–2403.
41. Ahluwalia A, Yan P, Hurteau JA. DNA methylation and ovarian cancer I: Analysis of CpG island hypermethylation in human ovarian cancer using differential methylation hybridization. *Gynecol Oncol* 2001;82:261–268.
42. Ahluwalia A, Hurteau JA, Bigsby RM, Nephew KP. DNA methylation in ovarian cancer. II: Expression of DNA methyltransferases in ovarian cancer cell lines and normal ovarian epithelial cells. *Gynecol Oncol* 2001;82:299–304.
43. Barbieri R, Mischiati C, Piva R. DNA methylation of the Haras-1 oncogene in neoplastic cells. *Anticancer Res* 1989;9:1787–1791.
44. Hanada M, Delia D, Aiello A. Bcl-2 gene hypomethylation and high-level expression in B-cell chronic lymphocytic leukemia. *Blood* 1993;82:1820–1828.
45. Ray JS, Harbison ML, McClain RM, Goodman JI. Alterations in the methylation status and expression of the raf oncogene in phenobarbital-induced and spontaneous B6C3F1 mouse live tumours. *Mol Carcinog* 1994;9:155–166.
46. Stephenson J, Akdag R, Ozbek N, Mufti GJ. Methylation status within exon 3 of the c-myc gene as a prognostic marker in myeloma and leukemia. *Leuk Res* 1993;17:291–293.
47. Cameron EE, Bachman KE, Myohanen S, Herman JG, Baylin SB. Synergy of demethylation and histone deacetylase inhibition in the re-expression of genes silenced in cancer. *Nat Genet* 1999;21:103–107.
48. Suzuki H, Gabrielson E, Chen W, Anbazhagan R, Van Engeland M, Weijnenberg MP, Herman JG, Baylin SB. A genomic screen for genes upregulated by demethylation and histone deacetylase inhibition in human colorectal cancer. *Nat Genet* 2002;31:141–149.
49. Yamashita K, Upadhyay S, Osada M, Hoque OM, Xiao Y, Mori M, Sato F, Meltzer SJ, Sidransky D. Pharmacologic unmasking of epigenetically silenced tumor suppressor genes in esophageal squamous cell carcinoma. *Cancer Cell* 2002;2:485–495.
50. Belinsky SA, Klinge DM, Stidley CA, Issa JP, Herman JG, March TH, Baylin SB. Inhibition of DNA methylation and histone deacetylation prevents murine lung cancer. *Cancer Res* 2003;63:7089–7093.
51. Momparler RL, Cote S, Eliopoulos N. Pharmacological approach for optimization of the dose schedule of 5-aza-2'-deoxycytidine (decitabine) for the therapy of leukemia. *Leukemia* 1997;11:1–6.
52. Wu J, Grunstein M. 25 Years after the nucleosome model: chromatin modifications. *Trends Biochem. Sci.* 2000;25:612–623.
53. Luger K, Mader AW, Richmond RK, Sargent DF, Richmond TJ. Crystal structure of the nucleosome core particle at 2.8 Å resolution. *Nature* 1997;389:251–260.
54. Jendwein T, Allis CD. Translating the histone code. *Science* 2001;293:1074–1080.
55. Turner BM. Histone acetylation and an epigenetic code. *BioEssay* 2000;22:836–845.
56. Van Holde KE. *Chromatin*. New York: Springer; 1998. p111–148

57. Wolffe AP, Hayes JJ. Chromatin disruption and modification. *Nucleic Acid Res* 1999;27:711-720.
58. Hecht A, Laroche T, Strahl-Bolsinger S, Gasser SM, Grunstein M. Histone H3 and H4 N-termini interact with SIR3 and SIR4 proteins: a molecular model for the formation of heterochromatin in yeast. *Cell* 1995;80:583-592.
59. Edmonson DG, Smith MM, Roth SY. Repression domain of the yeast global repressor Tup1 interacts directly with histones H3 and H4. *Genes Dev.* 1996;10:1247-1259.
60. Bird A. Methylation talk between histones and DNA. *Science* 2001;294:2113-2115.
61. Bannister AJ, Zegerman P, Partridge JF. Selective recognition of methylated lysine 9 on histone H3 by the HP1 chromo domain. *Nature* 2001;410:120-124.
62. Nakayama JI, Rice JC, Strahl BD. Role of histone H3 lysine 9 methylation in epigenetic control of heterochromatin assembly. *Science* 2001;292:110-113.
63. Kouzarides T. Acetylation: a regulatory modification to rival phosphorylation? *EMBO J* 2000;19:1176-1179.
64. Grunstein M. Histone acetylation in chromatin structure and transcription. *Nature* 1997;389:349-352.
65. Struhl K. Histone acetylation and transcriptional regulatory mechanisms. *Genes Dev* 1998;12:599-606.
66. Kouzarides T. Histone acetylases and deacetylases in cell proliferation. *Curr Opin Genet Dev* 1999;9:40-48.
67. Davie JR. Covalent modifications of histones expression from chromatin templates. *Curr Opin Genet Dev* 1998;8:173-178.
68. Davie JR, Spencer VA. Control of histone modifications. *J Cell Biochem* 1999; Suppl:141-148.
69. Turner BM. Histone acetylation and epigenetic code. *Bioessays* 2000;22:836-845.
70. Turner BM, Birley AJ, Lavender J. Histone H4 isoforms acetylated at specific lysine residues define individual chromosomes and chromatin domains in *Drosophila Polytene* nuclei. *Cell* 1992;69:375-384.
71. Brownell, J. E. et al. Tetrahymena histone acetyltransferase A: a homolog of yeast Gcn5p linking histone acetylation to gene activation. *Cell.* 1996, 84, 843-851.
72. Bannister, A. J. & Kouzarides, T. The CBP co-activator is a histone acetyltransferase. *Nature* 1996, 384, 641-643.
73. Neal, K. C., Pannuti, A., Smith, E. R. & Lucchesi, J. C. A new human member of the MYST family of histone acetyl transferases with high sequence similarity to *Drosophila* MOF. *Biochim. Biophys. Acta.* 2000, 1490, 170-174.
74. Gray SG, Ekstrom TJ. The human histone deacetylase family. *Exp Cell Res* 2001;262:75-83.
75. Kao H-Y, Lee C-H, Komarov A. Isolation and characterization of mammalian HDAC10, a novel histone deacetylase. *J Biol Chem* 2002;277:187-193.
76. Gao L, Cueto MA, Asselbergs F, Ataoja P. Clonino and functional characterization of HDAC11, a novel member of the human histone deacetylase family. *J Biol Chem* 2002;277:25748-25755.
77. Grozinger CM, Hassig CA, Schreiber SL. Three proteins define a class of human histone deacetylases related to yeast Hda1p. *Proc Natl Acad Sci USA* 1999;96:4868-4873
78. Bertos NR, Wang AH, Yang XY. Class II histone deacetylases: structure, function and regulation. *Biochem Cell Biol* 2001;79:243-252.

Design, synthesis and biological validation of epigenetic modulators of histone/protein deacetylation and methylation.

79. Yang XY, Seto E. Collaborative spirit of histone deacetylases in regulating chromatin structure and gene expression. *Curr Opin Genet Dev* 2003;13:143-153.
80. Fischle W, Kiermer V, Dequiedt F, Verdin E. The emerging role of class II histone deacetylases. *Biochem Cell Biol* 2001;79:337-348.
81. Zhang CL, McKinsey TA, Chang S, Antos CL, Hill JA, Olson EN. Class II histone deacetylase act as signal-responsive repressors of cardiac hypertrophy. *Cell* 2002;110:479-488.
82. Yoon HG, Chan DW, Huang ZQ, Li J, Fondell JD, Quin J, Wong J. Purification and functional characterization of the human N-CoR complex: the roles of HDAC3, TBL1 and TBLR1. *EMBO J* 2003;22:1336-1346.
83. Frye RA. Phylogenetic classification of prokaryotic and eukaryotic Sir2-like proteins. *Biochem Biophys Res Commun* 2000;273:793-798.
84. Chang JH, Kim HC, Hwang KY, Lee JW, Jackson SP, Bell SD, Cho Y. Structural basis for the NAD-dependent deacetylase mechanism of Sir 2. *J Biol Chem* 2002;277:34489-34498.
85. Luo G. Negative control of p53 by Sir2 $\alpha$  promoters cell survival under stress. *Cell* 2001;107:137-148.
86. Vaziri H. hSIR2(SIRT1) Functions as an NAD-dependent p53 deacetylase. *Cell* 2001;107:149-159.
87. Afshar G, Murnane JP. Characterization of a human gene with sequence homology to *Saccharomyces cerevisiae* SIR2. *Gene* 1999;234:161-168.
88. Taplick, J., Kurtev, V., Kroboth, K., Posch, M., Lechner, T. and Seiser, C. Homo oligomerisation and nuclear localisation of mouse histone deacetylase 1. *J.Mol.Biol.* 2001, 308, 27-38
89. Yao, Y. L., Yang, W. M. and Seto, E. Regulation of transcription factor YY1 by acetylation and deacetylation. *Mol. Cell. Biol.* 2001, 21, 5979-5991
90. Koipally, J., Renold, A., Kim, J. and Georgopoulos, K. Repression by Ikaros and Aiolos is mediated through histone deacetylase complexes. *EMBO J.* 1999, 18,3090-3100
91. Wu, X., Li, H., Park, E. J. and Chen, J. D. SMRTE inhibits MEF2C transcriptional activation by targeting HDAC4 and 5 to nuclear domains. *J. Biol. Chem.* 2001, 276, 24177-24185
92. Nair, A. R., Boersma, L. J., Schiltz, L., Chaudry, A. and Muschel, R. J. Paradoxical effects of trichostatin A: inhibition of NF-Y-associated histone acetyltransferase activity, phosphorylation of hGCN5 and downregulation of cyclin A and B1 mRNA. *Cancer Lett.* 2001, 166, 55-64.
93. Pflum, M. K., Tong, J. K., Lane, W. S. and Schreiber, S. L. Histone deacetylase 1 phosphorylation promotes enzymatic activity and complex formation. *J. Biol. Chem* (2001), 276, 47733-47741.
94. Guenther, M. G., Barak, O. and Lazar, M. A. The SMRT and N-CoR corepressors are activating cofactors for histone deacetylase 3. *Mol. Cell. Biol.* 2001, 21,6091-6101.
95. Yoshida, M., Furumai, R., Nishiyama, M., Komatsu, Y., Nishino, N. and Horinouchi, S. Histone deacetylase as a new target for cancer chemotherapy. *Cancer Chemother. Pharmacol.* 2001, 48 (Suppl. 1), S20-S26.
96. Vannini, A, Volpari C., Filocamo G., Caroli Casavola E., Brunetti M., Renzoni D., Chakravarty P., Paolini C., De Francesco R., Gallinari P., Steinkuhler C., Di Marco S. Crystal structure of a eukaryotic zinc-dependent histone deacetylase, human HDAC8, complexed with a hydroxamic acid inhibitor. *PNAS* 2004, 42, 15064-15069.

97. Zhou, X., Marks, P. A., Rifkind, R. A. and Richon, V. M. Cloning and characterization of a histone deacetylase, HDAC9. *Proc. Natl. Acad. Sci. U.S.A.* 2001, 98, 10572-10577.
98. Bertos, N. R., Wang, A. H. and Yang, X. J. Class II histone deacetylases: structure, function, and regulation. *Biochem. Cell Biol.* 2001, 79, 243-252.
99. Haggarty S., Koeller K., Wong J., Grozinger C., Schreiber S.L. Domain-selective small-molecule inhibitor of histone deacetylase 6 (HDAC6)-mediated tubulin deacetylation. *PNAS*, 2003, 8, 4389-4394.
100. Guardiola, A. R. and Yao, T. P. Molecular cloning and characterization of a novel histone deacetylase HDAC10. *J. Biol. Chem.* 2002, 277, 3350-3356.
101. McKinsey, T. A., Zhang, C.-L., Lu, J. & Olson, E. N. Signal-dependent nuclear export of a histone deacetylase regulates muscle differentiation. *Nature*, 2000, 408, 106-111.
102. Pflum MK, Tong JK, Lane WS, Schreiber SL. Histone deacetylase 1 phosphorylation promotes enzymatic activity and complex formation. *J Biol Chem* 2001, 276, 47733-47741.
103. David G, Neptune MA, DePinho RA. SUMO-1 modification of histone deacetylase 1 (HDAC1) modulates its biological activities. *J Biol Chem* 2002, 277:23658-23663.
104. Colombo R, Boggio R, Seiser C, Draetta GF, Chiocca S. The adenovirus protein Gam1 interferes with sumoylation of histone deacetylase 1. *EMBO Rep.* 2002, 3: 1062-1068.
105. Lin SJ, Ford E, Haigis M, Liszt G, Guarente L.. Calorie restriction extends yeast life span by lowering the level of NADH. *Genes Dev.* 2004, 18, 12-16.
106. Anderson RM, Bitterman KJ, Wood JG, Medvedik O, Sinclair DA. Nicotinamide and PNC1 govern lifespan extension by calorie restriction in *Saccharomyces cerevisiae*. *Nature.* 2003, 423, 181-185.
107. Jacobson S, Pillus L. Modifying chromatin and concepts of cancer. *Curr Opin Genet Dev* 1999;9:175-184.
108. Kouzarides T. Histone acetylases and deacetylases in cell proliferation. *Curr Opin Genet Dev* 1999;9:40-48.
109. Jones PA, Baylin SB. The fundamental role of epigenetic events in cancer. *Nature Rev Genet* 2002;3:415-428.
110. Mahiknecht U, Hoelzer D. Histone acetylation modifiers in the pathogenesis of malignant disease. *Mol Med* 2000;6:623-644.
111. Moller C, Leutz A. Chromatin remodelling in development and differentiation. *Curr Opin Genet Dev* 2001;11:167-174.
112. Ito K, Barnes PJ, Adcock IM. Glucocorticoid receptor recruitment of histone deacetylase 2 inhibits interleukin-1- $\beta$  induced histone H4 acetylation on lysines 8 and 12. *Mol Cell Biol* 2000;20:6891-6903.
113. Cai RL, Yan-Neale Y, Cueto MA, Xu H, Cohen D. HDAC1 a histone deacetylase, forms a complex with Hus 1 and Rad 9, two G<sub>2</sub>/ M checkpoint Rad proteins. *J Biol Chem* 2000;275:27909-27916.
114. Robertson KD, Ait-Si-Ali S, Yokochi T, Wade PA, Jones PL, Wolffe AP. DNMT1 forms a complex with Rb, E2F1 and HDAC1 and represses transcription from E2F-responsive promoters. *Nat Genet* 2000;25:338-342.
115. Smirnov DA, Hou S, Ricciardi RP. Association of histone deacetylase with COUP-TF in tumorigenic Ad 12-transformed cells and its potential role in shut-off of MHC class I transcription. *Virology* 2000;268:319-328.

Design, synthesis and biological validation of epigenetic modulators of histone/protein deacetylation and methylation.

116. Giles RH, Peters DJ, Breuning MH. Conjunction dysfunction: CBP/p300 in human disease. *Trends Genet* 1998;14:178-183.
117. Gayther SA, Batley SJ, Linger L, Bannister A. Mutations truncating the EP300 acetylase in human cancers. *Nat Genet* 2000;24:300-303.
118. Murata T, Kurokawa R, Krones A. Defect of histone acetyltransferase activity of the nuclear transcriptional coactivator CBP in Rubinstein-Taybi syndrome. *Hum Mol Genet* 2001;10:1071-1076.
119. Goodman RH, Smolik S. CBP/p300 in cell growth, transformation, and development. *Genes Dev* 2000;14:1553-1577.
120. Urnov FD, Wolffe A. Chromatin organization and human disease. *Emerg Ther Targets* 2000;4:665-685.
121. Cress WD, Seto E. Histone deacetylases, transcriptional control and cancer. *J Cell Physiol* 2000;184:1-16.
122. Chan HM, Kastic-Demonacos M, Smith L. Acetylation control of the retinoblastoma tumour-suppressor protein. *Mol Cell Biol* 2001;3:667-674.
123. Magnaghi-Jaulin L, Groisman R, Naguibneva I. Retinoblastoma protein represses transcription by recruiting a histone deacetylase. *Nature* 1998;391:601-605.
124. Murphy M, Ahn J, Walker KK. Transcriptional repression by wild-type p53 utilizes histone deacetylases, mediated by interaction with mSin3a. *Genes Dev* 1999;13:2490-2501.
125. Yarden RI, Brody LC. BRCA1 interacts with components of the histone deacetylase complex. *Proc Natl Acad Sci USA* 1999;96:4983-4988.
126. Fenick R, Hiebert SW. Role of histone deacetylase in acute leukemia. *J Cell Biochem* 1998;31:194-202.
127. He L-Z, Tolentino T, Grayson P. Histone deacetylase inhibitors induce remission in transgenic models of therapy-resistant acute promyelocytic leukemia. *J Clin Invest* 2001;108:321-1330.
128. Marks PA, Rifkind RA. Erythroleukemic differentiation. *Ann Rev Biochem* 1978;47:419-478.
129. Marks PA, Rifkind RA, Richon VM. Deacetylase inhibitors: inducers of differentiation or apoptosis of transformed cells. *J Natl Cancer I* 2000;92:1210-1216.
130. Kramer OH, Gottlicher M, Heinzel T. Histone deacetylase as a therapeutic target. *Trends Endocrinol Metab* 2001;12:294-300.
131. Marks PA, Richon VM, Breslow R. Histone deacetylase inhibitors as new cancer drugs. *Curr Opin Oncol* 2001;13:477-485.
132. Vigushin DM, Coombes RC. Histone deacetylase inhibitors in cancer treatment. *Anti-Cancer Drug* 2002;13:1-13.
133. Butler LM, Agus D, Scher HI. Suberoylanilide hydroxamic acid, an inhibitor of histone deacetylase, suppresses the growth of prostate cancer cells *in vitro* and *in vivo*. *Cancer Res* 2000;60:5165-5170.
134. Butler LM, Webb Y, Agus DB. Inhibition of transformed cell growth and induction of cellular differentiation by piroxamide, an inhibitor of histone deacetylase. *Clin Cancer Res* 2001;7:962-970.
135. Qui L, Kelso MJ, Hansen C, West ML, Fairlie DP, Parson PG. Antitumor activity *in vitro* and *in vivo* of selective differentiating agents containing hydroxamate. *Br J Cancer* 1999;80:1252-1258.
136. Parson PG, Hansen C, Fairlie DP. Tumor selectivity and transcriptional activation by azelaic bishydroxamic acid in human melanocytic cells. *Biochem Pharmacol* 1997;53:1719-1724.

137. Van Lint C, Emiliani S, Verdin E. The expression of a small fraction of cellular gene is changed in response to histone hyperacetylation. *Gene Expr* 1996;5:245-254.
138. Suzuki H, Gabrielson E, Chen W. A genomic screen for genes upregulated by and histone deacetylase inhibitors in human colorectal cancer. *Nature Genet* 2002;31:141-149.
139. Marladason JM, Corner GA, Augenlicht LH. Genetic reprogramming in pathways of colonic cell maturation induced by short chain fatty acids: comparison with trichostatin A, sulindac, and curcumin and implications for chemoprevention of colon cancer. *Cancer Res* 2000;60:4561-4572.
140. Huang L, Pardee AB. Suberoylanilide hydroxamic acid as a potential therapeutic agent for human breast cancer treatment. *Mol Med* 2000;6:849-866.
141. Xiao H, Horinouchi S, Beppu T. Both Sp1 and Sp3 are responsible for p21waf1 promoter activity induced by histone deacetylase inhibitor in NIH3T3 cells. *J Cell Biochem* 1999;73:291-302.
142. Zhang Y, Reinberg D. Transcription regulation by histone methylation: interplay between different covalent modifications of the core histone tails. *Genes Dev* 2001;15:2343-2360.
143. Richon VM, Sandhoff TW, Rifkind RA. Histone deacetylase inhibitors selectively induce p21waf1 expression and gene-associated histone acetylation. *Proc Natl Acad Sci USA* 2000;97:10014-10019.
144. Butler LM, Zhou X, Xu WS. The histone deacetylase inhibitor SAHA arrests cancer cell growth, up-regulates thioredoxin-binding protein-2, and-regulates thioredoxin. *Proc Natl Acad Sci USA* 2002;99:11700-11705.
145. Mishra N, Brown DR, Olorenshaw IM, Kammer GM. Trichostatin A reverses skewed expression of CD 154, interleukin 10, and interferon- $\gamma$  gene and protein expression in lupus T cells. *Proc Natl Acad Sci USA* 2001;98:2628-2633.
146. Magner WJ. Activation of MHC class I, II, and CD40 gene expression by histone deacetylase inhibitors. *J Immunol* 2000;165:7017-7024.
147. Maeda T, Towatani M, Kosugi H, Saito H. Up-regulation of costimulatory/adhesion molecules by histone deacetylase inhibitors in acute myeloid leukemia cells. *Blood* 2000;96:3847-3856.
148. Kim MS. Histone deacetylases induce angiogenesis by negative regulation of tumour suppressor genes. *Nature Med* 2001;7:437-443.
149. Histone deacetylase inhibitor FK228 inhibits tumor angiogenesis. *J Int Cancer* 2002;97:290-296.
150. HDAC inhibitors as anti-angiogenic agents altering vascular endothelial growth factor signaling. *Oncogene* 2002;21:427-436.
151. Longhurst HJ, Holder AA. The histones of Plasmodium falciparum: identification, purification and a possible role in the pathology of malaria. *Parasitology* 1997;114:413-419.
152. Darkin-Rattray SJ, Gurnett AM, Myers RW. Apicidin: a novel antiprotozoal agent that inhibits parasite histone deacetylase. *Proc Natl Acad Sci USA* 1996;93:13143-13147.
153. Belli SI. Chromatin remodelling during life cycle of trypanosomatids. *Int J Parasitol* 2000;30:679-687.
154. Han JW, Ahn SH, Park SH, Wang SY, Bae GU, Lee YW, Lee HW. Apicidin, a histone deacetylase inhibitor, inhibits proliferation of tumour cells via induction of p21WAF1/Cip1 and gelsolin. *Cancer Research* 2000;60:6068-6074.

Design, synthesis and biological validation of epigenetic modulators of histone/protein deacetylation and methylation.

155. Andrews KT, Walduck A, Kelso MJ, Fairlie DP, Saul A, Parsons PG. Anti-malarial effect of histone deacetylation inhibitors and mammalian tumour cytodifferentiating agents. *Int J Parasitol* 2000;30:761-768.
156. Impagnatiello F, Guidotti AR, Pesold C. A decrease of reelin expression as a putative vulnerability factor in schizophrenia. *Proc Natl Acad Sci USA* 1998;95:15718-15723.
157. Lewis DA, Lieberman JA. Catching up on schizophrenia: natural history and neurobiology. *Neuron* 2000;28:325-334.
158. Costa E, Chen Y, Davis J, Dong E, Noh JS, Tremolizzo L, Veldic M, Grayson DR, Guidotti A. Reelin and schizophrenia: a disease at the interface of genome and epigenome. *Mol Interv* 2002;2:47-57.
159. Hakimi MA, Dong Y, Lane WS, Speicher DW, Shiekhattar R. A candidate X-linked mental retardation gene is a component of a new family of histone deacetylase-containing complexes. *J Biol Chem* 2003;278:7234-7239.
160. Steffan JS, Bodai L, Palios J, Kazantsev A, Schmidt E, Greenwald M, Kurokawa R, Housman DE, Jackson GR, Marsh JL, Thompson LM. Histone deacetylase inhibitors arrest polyglutamine-dependent neurodegeneration in *Drosophila*. *Nature* 2001;413:739-743.
161. Wagner M, Brosch G, Zwerschke W, Seto E, Loidl P, Jansen P. Histone deacetylase in replicative senescence: evidence for a senescence-specific form of HDAC-2. *Febs Lett* 2001;499:101-106.
162. Chang KT, Min K-T. Regulation of lifespan by histone deacetylase. *Ageing Res Rev* 2002;1:313-326.
163. Bitterman KJ, Anderson RM, Cohen HY, Latorre-Esteves M, Sinclair DA. Inhibition of silencing and accelerated aging by nicotinamide, a putative negative regulator of yeast Sir2 and human SIRT1. *J Biol Chem* 2002;277:45099-45107.
164. Finnin MS, Pavletich NP. Structures of a histone deacetylase homologue bound to the TSA and SAHA inhibitors. *Nature* 1999;401:188-193.
165. Borra MT, O'Neill FJ, Jackson MD, Marshall B, Verdin E, Foltz KR, Denu JM. Conserved enzymatic production and biological effect of O-acetyl-ADP-ribose by silent information regulator 2-like NAD<sup>+</sup>-dependent deacetylases. *J Biol Chem* 2002;277:12632-12641.
166. Gary, J. D.; and Clarke, S. *Prog. Nucleic Acids Res. Mol. Biol.* 1998; 61: 65-131.
167. Scott, H. S.; Antonarakis, S. E.; Lalioti, M. D.; Rossier, C.; Silver, P. A.; and Henry, M.F. *Genomics* 48, 1998, 330-340.
168. Lin, W. J.; Gary, J. D.; Yang, M. C.; Clarke, S.; and Herschman, H. R. *J. Biol. Chem.* 271, 1996, 15034-15044.
169. Tang, J.; Gary, J. D.; Clarke, S.; and Herschman, H. R. *J. Biol. Chem.* 273, 1998, 16935-16945.
170. Chen, D.; Ma, H.; Hong, H.; Koh, S. S.; Huang, S. M.; Schurter, B. T.; Aswad, D. W.; and Stallcup, M. R. *Science* 284, 1999, 2174-2177.
171. Frankel, A.; Yadav, N.; Lee, J.; Branscombe, T. L.; Clarke, S.; and Bedford, M. T. *J. Biol. Chem.* 277, 2002, 3537-3543.
172. Scorilas, A.; Black, M.H.; Talieri, M.; and Diamandis, E.P. *Biochem. Biophys. Res. Commun.* 278, 2000, 349-359.
173. Najbauer, J.; Johnson, B.A.; Young, A.L.; and Aswad, D.W. *J. Biol. Chem.* 268, 1993, 10501-10509.



174. Weiss, V.H.; McBride, A.E.; Soriano, M.A.; Filman, D.J.; Silver, P.A.; and Hogle, J.M. *Nat. Struct. Biol.* 7, 2000, 1165-1171.
175. Zhang, X.; and Cheng, X. *Structure* (Camb). 11, 2003, 509-520.
176. Zhang, X.; Zhou, L.; and Cheng, X. *EMBO J.* 19, 2000, 3509-3519.
177. Cote, J.; Boisvert, F.M.; Boulanger, M.C.; Bedford, M.T.; and Rich, S. *Mol. Biol. Cell* 14, 2003, 274-287.
178. Paik, W.K.; and Kim, S. *Biochem. Biophys. Res. Commun.* 1967, 29, 14-20.
179. McBride, A.E.; and Silver, P.A. *Cell.* 2001, 106, 5-8.
180. Pal, S.; Vishwanath, S.N.; Erdjument-Bromage, H.; Tempst, P.; and Sif, S. *Mol. Cell. Biol.* 2004, 24, 9630-9645.
181. Jenuwein, T.; and Allis, C.D. *Science* 2001, 293, 1074-1080.
182. McBride, A. E.; and Silver, P. A. *Cell.* 2001, 106, 5-8.
183. An, W.; Kim, J.; and Roeder, R.G. *Cell.* 2004, 117, 735-748.
184. Rezai-Zadeh, N.; Zhang, X.; Namour, F.; Fejer, G.; Wen, Y.D.; Yao, Y.L.; Gyory, I.; Wright, K.; and Seto, E. *Genes Dev.* 2003, 17, 1019-1029.
185. Covic, M.; Hassa, P.O.; Saccani, S.; Buerki, C.; Meier, N.I.; Lom-bardi, C.; Imhof, R.; Bedford, M.T.; Natoli, G.; and Hottiger, M.O. *EMBO J.* 2004, 24, 85-96.
186. Lee, D.Y.; Teyssier, C.; Strahl, B.D.; and Stallcup, M.R. *Endocr. Rev.* 2004a, 2, 147-170.
187. Chevillard-Briet, M.; Trouche, D.; and Vandel, L. *EMBO J.* 2002, 21, 5457-5466.
188. Xu, W.; Chen, H.; Du, K.; Asahara, H.; Tini, M.; Emerson, B.M.; Montminy, M.; and Evans, R.M. *Science* 2001, 294, 2507-2511.
189. Boisvert, F.M.; Cote, J.; Boulanger, M.C.; and Richard, S. *Mol. Cell. Proteomics* 2003, 2, 1319-1330.
190. Abramovich, C.; Jakobson, B.; Chebath, J.; and Revel, M. *EMBO J.* 1997, 16, 260-266.
191. Singh, V.; Miranda, T.B.; Jiang, W.; Frankel, A.; Roemer, M.E.; Robb, V.A.; Gutmann, D.H.; Herschman, H.R.; Clarke, S.; and Newsham, I.F. *Oncogene* 2004, 23, 7761-7771.
192. Bauer, U.M.; Daujat, S.; Nielsen S.J.; Nightingale, K.; Kouzarides, T. *EMBO Rep.* 2002, 3, 39-44.
193. Ma, H.; Baumann, C.T.; Li, H.; Strahl, B.D.; Rice, R.; et al. *Curr. Biol.* 2001, 11, 1981-85.
194. Schurter, B.T.; Koh, S.S.; Chen, D.; Bunick, G.J.; Harp, J.M.; et al. *Biochemistry* 2001, 40, 5747-56.
195. Strahl, B.D.; Briggs, S.D.; Brame, C.J.; Caldwell, J.A.; Koh, S.S.; et al. *Curr. Biol.* 2001, 11, 996-1000.
196. Wang, H.; Huang, Z.Q.; Xia, L.; Feng, Q.; Erdjument-Bromage, H.; et al. *Science* 2001, 293, 853-57.
197. Kouzarides, T. *Curr. Opin. Genet. Dev.* 2002, 12, 198-209.
198. Strahl, B.D.; Allis, C.D. *Nature* 2000, 403, 41-45.
199. Lee, Y.H.; Koh, S.S.; Zhang, X.; Cheng, X.; Stallcup, M.R. *Mol. Cell. Biol.* 2002, 22, 3621-32.
200. Daujat, S.; Bauer, U.M.; Shah, V.; Turner, B.; Berger, S.; Kouzarides, T. *Curr. Biol.* 2002, 12, 2090-97.
201. Tang, J.; Kao, P.N.; Herschman, H.R. *J. Biol. Chem.* 2000, 275, 19866-76.
202. Pawlak, M.R.; Scherer, C.A.; Chen, J.; Roshon, M.J.; Ruley, H.E. *Mol. Cell. Biol.* 2000, 20, 4859-69.
203. Cimato, T.R.; Tang, J.; Xu, Y.; Guarnaccia, C.; Herschman, H.R.; et al. *J. Neurosci. Res.* 2002, 67, 435-42.
204. Smith, J.J.; Rucknagel, K.P.; Schierhorn, A.; Tang, J.; Nemeth, A.; et al. *J. Biol. Chem.* 1999, 274, 13229-34.

Design, synthesis and biological validation of epigenetic modulators of histone/protein deacetylation and methylation.

205. Klein, S.; Carroll, J.A.; Chen, Y.; Henry, M.F.; Henry, P.A.; et al. *J. Biol. Chem.* 2000, 275, 3150-57.
206. Mowen, K.A.; Tang, J.; Zhu, W.; Schurter, B.T.; Shuai, K.; et al. *Cell.* 2001, 104, 731-41.
207. Kwak, Y.T.; Guo, J.; Prajapati, S.; Park, K.J.; Surabhi, R.M.; et al. 2003. *Mol. Cell.* 2003, 11, 1055-66.
208. Stallcup, M.R. *Oncogene* 2001, 20, 3014-20.
209. Stallcup, M.R.; Kim, J.H.; Teyssier, C.; Lee, Y.H.; Ma, H.; Chen, D. *J. Steroid Biochem. Mol. Biol.* 2003, 85, 139-45.
210. Cheng, X.; Roberts, R.J. *Nucleic Acids Res.* 2001, 29, 3784-95.
211. Schubert, H.L.; Blumenthal, R.M.; Cheng, X. *Trends Biochem. Sci.* 2003, 28, 329-35.
212. Jenuwein, T.; Laible, G.; Dorn, R.; Reuter, G. *Cell. Mol. Life Sci.* 1998, 54, 80-93.
213. Rea, S.; Eisenhaber, F.; O'Carroll, D.; Strahl, B.D.; Sun, Z.W.; et al. *Nature* 2000, 406, 593-99.
214. Baumbusch, L.O.; Thorstensen, T.; Krauss, V.; Fischer, A.; Naumann, K.; et al. *Nucleic Acids Res.* 2001, 29, 4319-33.
215. Zhang, X.; Tamaru, H.; Khan, S.I.; Horton, J.R.; Keefe, L.J.; et al. *Cell.* 2002, 111, 117-27.
216. Zhang, X.; Yang, Z.; Khan, S.I.; Horton, J.R.; Tamaru, H.; et al. *Mol. Cell.* 2003, 12, 177-85.
217. Min, J.; Zhang, X.; Cheng, X.; Grewal, S.I.; Xu, R.M. *Nat. Struct. Biol.* 2002, 9, 828-32.
218. Jacobs, S.A.; Harp, J.M.; Devarakonda, S.; Kim, Y.; Rastinejad, F.; Khorasanizadeh, S. *Nat. Struct. Biol.* 2002, 9, 833-38.
219. Kwon, T.; Chang, J.H.; Kwak, E.; Lee, C.W.; Joachimiak, A.; et al. *EMBO J.* 2003, 22, 292-303.
220. Wilson, J.R.; Jing, C.; Walker, P.A.; Martin, S.R.; Howell, S.A.; et al. *Cell* 2002, 111, 105-15.
221. Xiao, B.; Jing, C.; Wilson, J.R.; Walker, P.A.; Vasisht, N.; et al. *Nature* 2003, 421, 652-56.
222. Santos-Rosa, H.; Schneider, R.; Bannister, A.J.; Sherriff, J.; Bernstein, B.E.; et al. *Nature* 2002, 419, 407-11.
223. Czermin, B.; Melfi, R.; McCabe, D.; Seitz, V.; Imhof, A.; Pirrotta, V. *Cell* 2002, 111, 185-96.
224. Tamaru, H.; Zhang, X.; McMillen, D.; Singh, P.B.; Nakayama, J.; et al. *Nat. Genet.* 2003, 34, 75-79.
225. Trievel, R.C.; Beach, B.M.; Dirk, L.M.; Houtz, R.L.; Hurley, J.H. *Cell* 2002, 111, 91-103.
226. Shi, Y., Lan, F., Matson, C., Mulligan, P., Whetstine, J.R., Cole, P.A., and Casero, R.A. Histone demethylation mediated by the nuclear amine oxidase homolog LSD1. *Cell* 2004; 119, 941-953.
227. Hong, H., Kao, C., Jeng, M.H., Eble, J.N., Koch, M.O., Gardner, T.A., Zhang, S., Li, L., Pan, C.X., Hu, Z., et al. Aberrant expression of CARM1, a transcriptional coactivator of androgen receptor, in the development of prostate carcinoma and androgen-independent status. *Cancer* 2004; 101: 83-89.
228. Cheng, D., Yadav, N., King, R.W., Swanson, M.S., Weinstein, E.J., and Bedford, M.T. Small molecule regulators of protein arginine methyltransferases. *J. Biol. Chem.* 2004; 279: 23892-23899.
229. Yadav, N., Lee, J., Kim, J., Shen, J., Hu, M.C., Aldaz, C.M., and Bedford, M.T. Specific protein methylation defects and gene expression perturbations in coactivator-associated arginine methyltransferase 1-deficient mice. *Proc. Natl. Acad. Sci. USA* 2003; 100: 6464-6468.
230. Pal, S., Vishwanath, S.N., Erdjument-Bromage, H., Tempst, P., and Sif, S. Human SWI/SNF-associated PRMT5 methylates histone H3 arginine 8 and negatively regulates expression of ST7 and NM23 tumor suppressor genes. *Mol. Cell. Biol.* 2004; 24: 9630-9645.

231. Hamamoto, R., Furukawa, Y., Morita, M., Iimura, Y., Silva, F.P., Li, M., Yagyu, R., and Nakamura, Y. SMYD3 encodes a histone methyltransferase involved in the proliferation of cancer cells. *Nat. Cell Biol.* 2004; 6: 731–740.
232. Marmorstein, R. Structure of SET domain proteins: a new twist on histone methylation. *Trends Biochem. Sci.* 2003, 28: 59–62.
233. Balint L. Balint, Attila Szanto, Andras Madi, Uta-Maria Bauer, Petra Gabor, Szilvia Benko, Laszlo G. Puska's, Peter J. A. Davies, and Laszlo Nagy. Arginine Methylation Provides Epigenetic Transcription Memory for Retinoid-Induced Differentiation in Myeloid Cells. *Mol. and Cell. Biol.* 2005; 25: 5648–5663.
234. Wei Jiang, Martha E. Roemer, Irene F. Newsham. The tumor suppressor DAL-1/4.1B modulates protein arginine *N*-methyltransferase 5 activity in a substrate-specific manner *Biochemical and Biophysical Research Communications* 2005; 329: 522–530.
235. Chuikov S, Kurash JK, Wilson JR, Xiao B, Justin N, et al. Regulation of p53 activity through lysine methylation. *Nature* 2004; 432: 353–60.
236. Shute RE, Dunlap B, Rich DH. Analogues of the cytostatic and antimetabolic agents chlamydocin and HC-toxin: synthesis and biological activity of chloromethyl ketone and diazomethyl ketone functionalized cyclic tetrapeptides. *J Med Chem* 1987;30:71-78.
237. Grozinger CM, Schreiber SL. Deacetylase enzymes: biological functions and the use of small-molecule inhibitors. *Chem Biol* 2002;9:3-16.
238. Yoshida M, Kijima M, Akita M, Beppu T. Potent and specific inhibition of mammalian histone deacetylase both *in vivo* and *in vitro* by trichostatin A. *J Biol Chem* 1990;265:17174-17179.
239. Kijima M, Yoshida M, Suguta K, Horinouchi S, Beppu T. Trapoxin, an antitumor cyclic tetrapeptide, is an irreversible inhibitor of mammalian histone deacetylase. *J Biol Chem* 1993;268:22429-22435.
240. Closse A, Hugenin R. Isolation and structure elucidation of chlamydocin. *Helv Chim Acta* 1974;57:533-545.
241. Hirota A, Suzuki A, Aizawa K, Tamura S. Mass spectrometric determination of amino acid sequence in Cyl-2, a novel cyclotetrapeptide from *Cylindrocladium scoparium*. *Biomed Mass Spectrom* 1974;1:15-19.
242. Umehara K, Nakahara K, Kiyoto S, Iwami M, Okamoto M, Tanaka H, Kohsaka M, Aoki H, Imanaka H. Studies on WF-3161, a new antitumor antibiotic. *J Antibiot* 1983;36:478-483.
243. Ueda H, Nakajima H, Hori Y, Fujita T, Nishimura M, Goto T, Okuhara M. FR901228, a novel antitumor bicyclic depsipeptide produced by *Chromobacterium violaceum* No. 968. I. Taxonomy, fermentation, isolation, physico-chemical and biological properties, and antitumor activity. *J Antibiot* 1994;47:301-310.
244. Kwon HJ, Owa T, Hassig CA, Shimada J, Schreiber SL. Depudecin induces morphological reversion of transformed fibroblasts via the inhibition of histone deacetylase. *Proc Natl Acad Sci USA* 1998;95:3356-3361.
245. Kruh J. Effects of sodium butyrate, a new pharmacological agent, on cells in culture. *Mol Cell Biochem* 1982;42:65-82.
246. Richon VM, Emiliani S, Verdin E, Webb Y, Breslow R, Rifkind RA, Marks PA. A class of hybrid polar inducers of transformed cell differentiation inhibits histone deacetylases. *Proc Natl Acad Sci USA* 1998;95:3003-3007.

247. Jung M, Brosch G, Kölle D, Scherf H, Gerhäuser C, Loidl P. Amide analogues of trichostatin A as inhibitors of histone deacetylase and inducers of terminal cell differentiation. *J Med Chem* 1999;42:4669-4679.
248. Remiszewski SW, Sambucetti LC, Atadja P, Bair KW, Cornell WD, Green MA, Howell K L, Jung M, Known P, Trogani N, Walker H. Inhibitors of human histone deacetylase: synthesis and enzyme and cellular activity of straight chain hydroxamates. *J Med Chem* 2002;45:753-757.
249. Woo SH, Frechette S, Khalil EA, Bouchain G, Vaisburg A, Bernstein N, Moradei O, Leit S, Allan M, Fournel M, Trachy-Bourget MC, Li Z, Besterman JM, Delorme D. Structurally simple trichostatin A-like straight chain hydroxamates as potent histone deacetylase inhibitors. *J Med Chem* 2002;45:2877-2885.
250. Uesato S, Kitagawa M, Nagaoka Y, Maeda T, Kuwajima H, Yamori T. Novel histone deacetylase inhibitors: N-hydroxycarboxamides possessing a terminal bicyclic aryl group. *Bioorg Med Chem Lett* 2002;12:1347-1349.
251. Su GH, Sohn TA, Ryu B, Kern SE. A novel histone deacetylase inhibitor identified by high-throughput transcriptional screening of a compound library. *Cancer Res* 2000;60:3137-3142.
252. Kim YB, Lee KH, Sugita K, Yoshida M, Horinouchi S. Oxamflatin is a novel antitumor compound that inhibits mammalian histone deacetylase. *Oncogene* 1999;18:2461-2470.
253. Lavoie R, Bouchain G, Frechette S, Woo SH, Khalil EA, Leit S, Fournel M, Yan PT, Trachy-Bourget MC, Beaulieu C, Li Z, Besterman JM, Delorme D. Design and synthesis of a novel class of histone deacetylase inhibitors. *Bioorg Med Chem Lett* 2001;11:2847-2850.
254. Furumai R, Komatsu Y, Nishino N, Khochbin S, Yoshida M, Horinouchi S. Potent histone deacetylase inhibitors built from trichostatin A and cyclic tetrapeptide antibiotics including trapoxin. *Proc Natl Acad Sci USA* 2001;98:87-92.
255. Remiszewski SW, Sambucetti LC, Bair KW, Bontempo J, Cesarz D, Chandramouli N, Chen R, Cheung M, Cornell-Kennon S, Dean K, Diamantidis G, France D, Green MA; Howell KL, Kashi R, Kwon P, Lassota P, Martin MS, Mou Y, Perez LB, Sharma S, Smith T, Sorensen E, Taplin F, Trogani N, Versace R, Walker H, Weltchek-Engler S, Wood A, Wu A, Atadja P. N-hydroxy-3-phenyl-2-propenamides as novel inhibitors of human histone deacetylase with *in vivo* antitumour activity: discovery of (2E)-N-hydroxy-3-[4-[[2-(2-hydroxyethyl)[2-(1H-indol-3-yl)ethyl]amino]methyl]phenyl]-2-propenamide (NVP-LAQ824). *J Med Chem* 2003;46:4609-4624.
256. Saito A, Yamashita T, Mariko Y, Nosaka Y, Tsuchiya K, Ando T, Suzuki T, Tsuruo T, Nakanishi O. A synthetic inhibitor of histone deacetylase, MS-275, with marked *in vivo* antitumour activity against human tumors. *Proc Natl Acad Sci USA* 1999;96:4592-4597.
257. Frey RR, Wada CK, Garland RB, Davidsen SK. Trifluoromethyl ketones as inhibitors of histone deacetylase. *Bioorg Med Chem Lett* 2002;12:3443-3447.
258. Vasudevan A, Ji Z, Frey RR, Wada CK, Steinman D, Heyman HR, Guo Y, Curtin ML, Guo J, Li J, Pease L, Glaser KB, Marcotte PA, Bouska JJ, Davidsen SK, Michaelides MR. Heterocyclic ketones as inhibitors of histone deacetylase. *Bioorg Med Chem Lett* 2003;13:3909-3913.
259. Carducci MA, Bowling MK, Eisenberger M. Phenylbutyrate (PB) for refractory solid tumours: phase I clinical and pharmacologic evaluation of intravenous and oral PB. *Anticancer Res* 1997;17:3972-3973.

260. Gottlicher M, Minucci S, Zhu P, Kramer OH, Schimpf A, Giavara S, Sleeman JP, Lo Coco F, Nervi C, Pelicci PG, Heinzel T. Valproic acid defines a novel class of HDAC inhibitors inducing differentiation of transformed cells. *EMBO J* 2001;20:6969-6978.
261. Tsuji N, Kobayashi M, Nagashima K, Wakisaka Y, Koizumi K. A new antifungal antibiotic, trichostatin. *J Antibiot* 1976;29:1-6.
262. Tsuji N, Kobayashi M. Trichostatin C, a glucopyranosyl hydroxamate. *J Antibiot* 1978;31:939-944.
263. Yoshida M, Nomura S, Beppu T. Effects of trichostatins on differentiation of murine erythroleukemia cells. *Cancer Res* 1987;47:3688-3691.
264. Yoshida M, Horinouchi S, Beppu T. Trichostatin and trapoxin: novel chemical probes for the role of histone acetylation in chromatin structure and function. *Bioessays* 1995;17:423-430.
265. Yoshida M, Hoshikawa Y, Koseki K, Mori K, Beppu T. Structural specificity for biological activity of trichostatin, a specific inhibitor of mammalian cell cycle with potent differentiation-inducing activity in Friend leukemia cells. *J Antibiot* 1990;43:1101-1106.
266. Yoshida M, Beppu T. Reversible arrest of proliferation of rat 3Y1 fibroblasts in both G1 and G2 phases by trichostatin A. *Exp Cell Res* 1988;177:122-131.
267. Breslow R, Jursic B, Yan ZF, Friedman E, Leng L, Ngo L, Rifkind RA, Marks PA. Potent cytodifferentiating agents related to hexamethylenebisacetamide. *Proc Natl Acad Sci USA* 1991;88:5542-5546.
268. Marks P, Rifkind RA, Richon VM, Breslow R, Miller T, Kelly WK. Histone deacetylases and cancer: causes and therapies. *Nat Rev Cancer* 2001;1:194-202.
269. Richon, V. M.; Webb, Y.; Merger, R.; Sheppard, T.; Jursic, B.; et al. Second generation hybrid polar compounds are potent inducers of transformed cell differentiation. *PNAS*. 1996, 93, 5705-5708.
270. Richon, V. M.; Emiliani, S.; Verdin, E.; Webb, Y.; Breslow, R.; et al. A class of hybrid polar inducers of transformed cell differentiation inhibits histone deacetylases. *PNAS*. 1998, 95, 3003-3007.
271. Van Ommeslaeghe, K. E. G.; Brecx, V.; Papeleu, P.; Iterbeke, K.; Geerlings, P.; Tourwe, D.; Rogiers, V. Amide analogues of TSA: synthesis, binding mode analysis and HDAC inhibition. *Bioorg. Med. Chem. Lett.* 2003, 13, 1861-1864.
272. Kim, Y. B.; Lee, K. H.; Sugita, K.; Yoshida, M.; Horinouchi, S. Oxamflatin is a novel antitumor compound that inhibits mammalian histone deacetylase. *Oncogene* 1999, 18, 2461-2470.
273. Ohtani, M.; Matsuura, T.; Shirahase, K.; Sugita, K. (2E)-5-[3-[(Phenylsulfonyl)amino]phenyl]-pent-2-en-4-ynohydroxamic acid and its derivatives as novel and potent inhibitors of ras transformation. *J. Med. Chem.* 1996, 39, 2871-2873.
274. Su, G. H.; Sohn, T. A.; Ryu, B.; Kern, S. E. A Novel Histone Deacetylase Inhibitor Identified by High-Throughput Transcriptional Screening of a Compound Library. *Cancer Res.* 2000, 60, 3137-3142.
275. Jung, M.; Hoffmann, K.; Brosch, G.; Loid, P. Analogues of trichostatin A and trapoxin B as histone deacetylase inhibitors. *Bioorg. Med. Chem. Lett.* 1997, 7, 1655-1658.
276. Wittich, S.; Scherf, H.; Xie, C.; Brosch, G.; Loidl, P.; et al. Structure-activity relationships on phenylalanine-containing inhibitors of histone deacetylase: in vitro enzyme inhibition, induction of

- differentiation, and inhibition of proliferation in Friend leukemic cells. *J. Med. Chem.* 2002, *45*, 3296-3309.
277. Jung, M.; Brosch, G.; Ko"lle, D.; Scherf, H.; Gerha"user, C.; et al. Amide Analogues of Trichostatin A as Inhibitors of Histone Deacetylase and Inducers of Terminal Cell Differentiation. *J. Med. Chem.* 1999, *42*, 4669-4679.
278. Breslow, R.; Marks, P. A.; Rifkind, R. Potent inducers of terminal differentiation and methods of use thereof. U.S. Patent 5,700,811, 1997.
279. Glaser, K. B.; Li, J.; Aakre, M. E.; Morgan, D. W.; Sheppard, G.; et al. Transforming growth factor beta mimetics: discovery of 7-[4-(4-cyanophenyl)phenoxy]-heptanohydroxamic acid, a biaryl hydroxamate inhibitor of histone deacetylase. *Mol. Cancer Ther.* 2002, *1*, 759-768.
280. Curtin, M. L.; Garland, R. B.; Heyman, H. R.; Frey, R. R.; Michaelides, M. R.; et al. Succinimide hydroxamic acids as potent inhibitors of histone deacetylase (HDAC). *Bioorg. Med. Chem. Lett.* 2002, *12*, 2919-2923.
281. Sternson, S. M.; Wong, J. C.; Grozinger, C. M.; Schreiber, S. L. Synthesis of 7200 small molecules based on a substructural analysis of the histone deacetylase inhibitors trichostatin and trapoxin. *Org. Lett.* 2001, *3*, 4239-4242.
282. Lavoie, R.; Bouchain, G.; Frechette, S.; Woo, S. H.; Khalil, E. A.; et al. Design and synthesis of a novel class of histone deacetylase inhibitors. *Bioorg. Med. Chem. Lett.* 2001, *11*, 2847-2850.
283. Perez, L. B.; Remiszewski, S. W.; Sambucetti, L. C.; Atadja, P.; Blair, K. W.; et al. Discovery and SAR of NVP-LAQ824: novel histone deacetylase inhibitor with in vitro and in vivo antitumor activity. Presented at the Meeting of the American Association for Cancer Research, San Francisco, CA, 2002; Abstract 3671.
284. Kim, D.K.; Lee, J.Y.; Kim, J.S.; Ryu, J.H.; Choi, J.Y.; Lee, J.W.; Im, G.J.; Kim, T.K.; Seo, J.W.; Park, H.J.; Yoo, J.; Park, J.H.; Kim, T.Y., and Bang, Y.J. Synthesis and biological evaluation of 3-(4-substituted-phenyl)-N-hydroxy-2-propenamides, a new class of histone deacetylase inhibitors. *J. Med. Chem.* 2003; *46*: 5745-5751.
285. Chen, J. S.; Faller, D. V. Short-chain fatty acid inhibitors of histone deacetylases: promising anticancer. *Curr. Cancer Drug Targets* 2003, *3*, 219-236.
286. Cummings, J. I. Short chain fatty acids in the human colon. *Gut* 1981, *22*, 763-779.
287. Watson, J.; Glasg, M. B. Butyric acid in the treatment of cancer. *Lancet* 1933, 746-748.
288. Johnstone, R. W. Histone-deacetylase inhibitors: novel drugs for the treatment of cancer. *Nat. Rev. Drug Discovery* 2002, *1*, 287-299.
289. Warrell, R. P., Jr.; He, L. Z.; Richon, V.; Calleja, E.; Pandolfi, P.P. Therapeutic targeting of transcription in acute promyelocytic leukemia by use of an inhibitor of histone deacetylase. *J. Natl. Cancer Inst.* 1998, *90*, 1621-1625.
290. Rephaeli, A.; Zhuk, R.; Nudelman, A. Prodrugs of butyric acid from bench to bedside: synthetic design, mechanism of action, and clinical applications. *Drug Dev. Res.* 2000, *50*, 379-391.
291. Suzuki, T.; Ando, T.; Tsuchiya, K.; Fukazawa, N.; Saito, A.; et al. Synthesis and histone deacetylase inhibitory activity of new benzamide derivatives. *J. Med. Chem.* 1999, *42*, 3001-3003.

292. El-Beltagi, H. M.; Martens, A. C. M.; Lelieveld, P.; Haroun, E. A.; Hagenbeek, A. Acetyldinaline: a new oral cytostatic drug with impressive differential activity against leukemic cells and normal stem cellspreclinical studies in a relevant rat model for human acute myelocytic leukemia. *Cancer Res.* 1993, *53*, 3008-3014.
293. Seelig, M. H.; Berger, M. R. Efficacy of dinaline and its methyl and acetyl derivatives against colorectal cancer in vivo and in vitro. *Eur. J. Cancer* 1996, *32A*, 1968-1976.
294. Saito, A.; Yamashita, T.; Mariko, Y.; Nosaka, Y.; Tsuchiya, K.; et al. A synthetic inhibitor of histone deacetylase, MS-27-275, with marked in vivo antitumor activity against human tumors. *Proc. Natl. Acad. Sci. U.S.A.* 1999, *96*, 4592-4597.
295. Prakash, S.; Foster, B. J.; Meyer, M.; Wozniak, A.; Heilbrun, L. K.; et al. Chronic oral administration of CI-994: a phase I study. *Invest. New Drugs* 2001, *19*, 1-11.
296. Wong, J. C.; Hong, R.; Schreiber, S. L. Structural biasing elements for in-cell histone deacetylase paralog selectivity. *J. Am. Chem. Soc.* 2003, *125*, 5586-5587.
297. Christianson, D. W.; Lipscomb, W. N. The complex between carboxypeptidase A and a possible transition-state analogue: mechanistic inferences from high-resolution X-ray structures of enzyme-inhibitor complexes. *J. Am. Chem. Soc.* 1986, *108*, 4998-5003.
298. Walter, M. W.; Felici, A.; Galleni, M.; Soto, R. P.; Adlington, R. M.; et al. Trifluoromethyl alcohol and ketone inhibitors of metallo-beta-lactamases. *Bioorg. Med. Chem. Lett.* 1996, *6*, 2455-2458.
299. Frey, R. R.; Wada, C. K.; Garland, R. B.; Curtin, M. L.; Michaelides, M. R.; et al. Trifluoromethyl ketones as inhibitors of histone deacetylase. *Bioorg. Med. Chem. Lett.* 2002, *12*, 3443-3447.
300. Frey, R. R.; Curtin, M. L.; Garland, R. B.; Wada, C. K.; Vasudevan, A.; et al. Electrophilic ketone-based histone deacetylase (HDAC) inhibitors as cancer chemotherapeutic agents. Presented at the 224th National Meeting of the American Chemical Society, Boston, MA, 2002.
301. Marshall, J. L.; Rizvi, N.; Kauh, J.; Dahut, W.; Figuera, M.; et al. A phase I trial of depsipeptide (FR901228) in patients with advanced cancer. *J. Exp. Ther. Oncol.* 2002, *2*, 325-332.
302. Kijima, M.; Yoshida, M.; Sugita, K.; Horinouchi, S.; Beppu, T. Trapoxin, an antitumor cyclic tetrapeptide, is an irreversible inhibitor of mammalian histone deacetylase. *J. Biol. Chem.* 1993, *268*, 22429-22435.
303. Gross, M. L.; McCrery, D.; Crow, F.; Tomer, K. B. The structure of the toxin from *Helminthosporium carbonum*. *Tetrahedron Lett.* 1982, *23*, 5381-5384.
304. Itazaki, H.; Nagashima, K.; Sugita, K.; Yoshida, H.; Kawamura, Y.; Yasuda, Y.; Matsumoto, K.; Ishii, K.; Uotani, N.; Nakai, H.; Terui, A.; Yoshimatsu, S.; Ikenishi, Y.; Nakawaga, Y. Isolation and structural elucidation of new cyclotetrapeptides, trapoxin A and B, having detransformation activities as antitumor agents. *J. Antibiot.* 1990, *63*, 1524-1532.
305. Closse, A.; Huguenin, R. Isolation and structural clarification of chlamydocin. *Helv. Chim. Acta* 1974, *57*, 533-545.
306. Singh, S. B.; Zink, D. L.; Polishook, J. D.; Dombrowski, A. W.; Darkin-Rattray, S. J.; Schmatz, D. M.; Goetz, M. A. Apicidins: novel cyclic tetrapeptides as coccidiostats and antimalarial agents from *Fusarium pallidoroseum*. *Tetrahedron Lett.* 1996, *37*, 8077-8080.

Design, synthesis and biological validation of epigenetic modulators of histone/protein deacetylation and methylation.

307. Colletti, S. L.; Myers, R. W.; Darkin-Rattray, S. J.; Gurnett, A. M.; Dulski, P. M.; et al. Broad spectrum antiprotozoal agents that inhibit histone deacetylase: structure-activity relationships of apicidin. Part 1. *Bioorg. Med. Chem. Lett.* 2001, *11*, 107-111.
308. Furumai, R.; Komatsu, Y.; Nishino, N.; Khochbin, S.; Yoshida, M.; et al. Potent histone deacetylase inhibitors built from trichostatin A and cyclic tetrapeptide antibiotics including trapoxin. *Proc. Natl. Acad. Sci. U.S.A.* 2001, *98*, 87-92.
309. Colletti, S. L.; Myers, R. W.; Darkin-Rattray, S. J.; Gurnett, A. M.; Dulski, P. M.; et al. Broad spectrum antiprotozoal agents that inhibit histone deacetylase: structure-activity relationships of apicidin. Part 2. *Bioorg. Med. Chem. Lett.* 2001, *11*, 113-117.
310. Ueda, H.; Nakajima, H.; Hori, Y.; Fujita, T.; Nishimura, M.; Goto, T.; Okuhara, M. FR901228, A novel antitumor bicyclic depsipeptide produced by *Chromobacterium violaceum* no. 968. *J. Antibiot.* 1994, *47*, 301-310.
311. Furumai, R.; Matsuyama, A.; Kobashi, N.; Lee, K. H.; Nishiyama, M.; et al. FK228 (depsipeptide) as a natural prodrug that inhibits class I histone deacetylases. *Cancer Res.* 2002, *62*, 4916-4921.
312. Suzuki T., Kouketsu A., Matsuura A., Kohara A., Ninomiya S., Kohdaa K. and Miyataa N. Thiol-based SAHA analogues as potent histone deacetylase inhibitors. *Bioorg. Med. Chem. Lett.* 2004, *14*, 3313-3317.
313. Grozinger MC, Chao ED, Blackwell HE, Moazed D, Schreiber SL. Identification of a class of small molecule inhibitors of the sirtuin family of NAD-dependent deacetylases by phenotypic screening. *J Biol Chem* 2001;276:38837-38843.
314. Bedalov A, Gatbonton T, Irvine WP, Gottschling DE, Simon JA. Identification of a small molecule inhibitor of Sir2p. *Proc Natl Acad Sci USA* 2001;98:15113-15118.
315. O. H. Kramer, M. G. Göttlicher, T. Heinzel. *Trends Endocrinol. Metab.* 2001, *12*, 294-300.
316. P. A. Marks, V. M. Richon, R. Breslow, R. A. Rifkind. *Curr. Opin. Oncol.* 2001, *13*, 477-483.
317. P. A. Marks, R. A. Rifkind, V. M. Richon, R. Breslow, T. Miller, W. K. Kelly. *Nat. Rev. Cancer* 2001, *1*, 194-202.
318. D. M. Vigushin, R. C. Coombes. *Anti-Cancer Drugs* 2002, *13*, 1-13.
319. R. W. Johnstone. *Nat. Rev. Drug Discovery* 2002, *1*, 287-299.
320. W. K. Kelly, O. A. O'Connor, P. A. Marks. *Expert Opin. Investig. Drugs* 2002, *11*, 1695-1713.
321. T. A. Miller, D. J. Witter, S. Belvedere. *J. Med. Chem.* 2003, *46*, 5097-5116.
322. A.Mai, S. Massa, D. Rotili, I. Cerbara, S. Valente, R. Pezzi, S. Simeoni, R. Ragno. *Med. Res. Rev.* 2005, *25*, 261-309.
323. N. R. Bertos, A. H. Wang, X.-J. Yang. *Biochem. Cell Biol.* 2001, *79*, 243-252.
324. W. Fischle, V. Kiermer, F. Dequiedt, E. Verdin. *Biochem. Cell Biol.* 2001, *79*, 337-348.
325. A.R. Guardiola, T.-P. Yao. *J. Biol. Chem.* 2002, *277*, 3350-3356.
326. M. Göttlicher, S. Minucci, P. Zhu, O. H. Krämer, A. Schimpf, S. Giavara, J. P. Sleeman, F. Lo Coco, C. Nervi, P. G. Pelicci, T. Heinzel. *EMBO J.* 2001, *20*, 6969-6978.
327. T. Suzuki, T. Ando, K. Tsuchiya, N. Fukazawa, A. Saito, Y. Mariko, T. Yamashita, O. Nakanishi. *J. Med. Chem.* 1999, *42*, 3001-3003.



328. A. Saito, T. Yamashita, Y. Mariko, Y. Nosaka, K. Tsuchiya, T. Ando, T. Suzuki, T. Tsuruo, O. Nakanishi. Proc. Natl. Acad. Sci. USA 1999, 96, 4592-4597.
329. J. C. Wong, R. Hong, S. L. Schreiber. J. Am. Chem. Soc. 2003, 125, 5586-5587.
330. J.-H. Park, Y. Jung, T. Y. Kim, S. G. Kim, H.-S. Jong, J. W. Lee, D.-K. Kim, J.-S. Lee, N. K. Kim, T.-Y. Kim, Y.-J. Bang. Clin. Cancer Res. 2004, 10, 5271-5281.
331. R. Fumurai, A. Matsuyama, N. Kobashi, K.-H. Lee, M. Nishiyama, H. Nakajima, A. Tanaka, Y. Komatsu, N. Nishino, M. Yoshida, S. Horinouchi. Cancer Res. 2002, 62, 4916-4921.
332. R. Fumurai, Y. Komatsu, N. Nishino, S. Khochbin, M. Yoshida, S. Horinouchi. Proc. Natl. Acad. Sci. USA 2001, 98, 87-92.
333. S. M. Sternson, J. C. Wong, C. M. Grozinger, S. L. Schreiber. Org. Lett. 2001, 3, 4239-4242.
334. S. J. Haggarty, K. M. Koeller, J. C. Wong, Butcher, R. A.; Schreiber, S. L. Multidimensional Chemical Genetic Analysis of Diversity-Oriented Synthesis-Derived Deacetylase Inhibitors Using Cell-Based Assays. Chem. Biol. 2003, 10, 383-396.
335. S. J. Haggarty, K. M. Koeller, J. C. Wong, C. M. Grozinger, S. L. Schreiber. Proc. Natl. Acad. Sci. USA 2003, 100, 4389-4394.
336. A. Mai, S. Massa, R. Pezzi, D. Rotili, P. Loidl, G. Brosch. J. Med. Chem. 2003, 46, 4826-4829.
337. S. Massa, A. Mai, G. Sbardella, M. Esposito, R. Ragno, P. Loidl, G. Brosch. J. Med. Chem. 2001, 44, 2069-2072.
338. A. Mai, S. Massa, R. Ragno, M. Esposito, G. Sbardella, G. Nocca, R. Scatena, F. Jesacher, P. Loidl, G. Brosch. J. Med. Chem. 2002, 45, 1778-1784.
339. A. Mai, S. Massa, R. Ragno, I. Cerbara, F. Jesacher, P. Loidl, G. Brosch. J. Med. Chem. 2003, 46, 512-524.
340. A. Mai, S. Massa, I. Cerbara, S. Valente, R. Ragno, P. Bottoni, R. Scatena, P. Loidl, G. Brosch. J. Med. Chem. 2004, 47, 1098-1109.
341. R. Ragno, A. Mai, S. Massa, I. Cerbara, S. Valente, P. Bottoni, R. Scatena, F. Jesacher, P. Loidl, G. Brosch. J. Med. Chem. 2004, 47, 1351-1359.
342. M. Jung, G. Brosch, D. Kölle, H. Scherf, C. Gerhäuser, P. Loidl. J. Med. Chem. 1999, 42, 4669-4679.
343. S. Wittich, H. Scherf, C. Xie, G. Brosch, P. Loidl, C. Gerhäuser, M. Jung. J. Med. Chem. 2002, 45, 3296-3309.
344. D. Kölle, G. Brosch, T. Lechner, A. Pipal, W. Helliger, J. Taplick, P. Loidl. Biochemistry 1999, 38, 6769-6773.
345. T. Lechner, A. Lusser, A. Pipal, G. Brosch, A. Loidl, M. Goralik-Schramel, R. Sendra, S. Wegener, J. D. Walton, P. Loidl. Biochemistry 2000, 39, 1683-1692.
346. G. Brosch, M. Goralik-Schramel, P. Loidl. FEBS Lett. 1996, 393, 287-291.
347. G. Brosch, E. Georgieva, G. Lopez-Rodas, H. Lindner, P. Loidl. J. Biol. Chem. 1992, 267, 20561-20564.
348. W. Pendergast, J. V. Johnson, S. H. Dickerson, I. K. Dev, D. S. Duch, R. Ferone, W. R. Hall, J. Humphreys, J. M. Kelly, D. C. Wilson. J. Med. Chem. 1993, 36, 2279-2291.
349. M. Kijima, M. Yoshida, K. Sugata, S. Horinouchi, T. Beppu. J. Biol. Chem. 1993, 268, 22429-22435.

Design, synthesis and biological validation of epigenetic modulators of histone/protein deacetylation and methylation.

350. M. Yoshida, M. Kijima, M. Akita, T. Beppu. *J. Biol. Chem.* 1990, 265, 17174-17179.
351. C. J. Phiel, F. Zhang, E. Y. Huang, M. G. Guenther, M. A. Lazar, P. S. Klein. *J. Biol. Chem.* 2001, 76, 36734-36741.
352. V. M. Richon, S. Emiliani, E. Verdin, Y. Webb, R. Breslow, R. A. Rifkind, P. A. Marks. *Proc. Natl. Acad. Sci. USA* 1998, 95, 3003-3007.
353. M. Kijima, M. Yoshida, K. Suguta, S. Horinouchi, T. Beppu. *J. Biol. Chem.* 1993, 268, 22429-22435.
354. G. Brosch, R. Ransom, T. Lechner, J. Walton, P. Loidl. *Plant Cell* 1995, 33, 1941-1950.
355. O. Lund, M. Nielsen, C. Lundegaard, P. Worning. Abstract at the CASP5 conference A102, 2002, <http://www.cbs.dtu.dk/services/CPHmodels/>.
356. A. Pipal, M. Goralik-Schramel, A. Lusser, C. Lanzanova, B. Sarg, A. Loidl, H. Lindner, V. Rossi, P. Loidl. *Plant Cell* 2003, 15, 1904-1917.
357. Cheng, D.; Yadav, N.; King, R. W.; Swanson, M. S.; Weinstein, E. J.; Bedford, M. T. Small molecule regulators of protein arginine methyltransferases. *J. Biol. Chem.* 2004, 279, 23892-23899.
358. Greiner, D.; Bonaldi, T.; Eskeland, R.; Roemer, E.; Imhof, A. Identification of a specific inhibitor of the histone methyltransferase SU(VAR)3-9. *Nat. Chem. Biol.* 2005, 1, 143-145.
359. Schneider, R.; Bannister, A. J.; Kouzarides, T. Unsafe SETs: histone lysine methyltransferases and cancer. *Trends Biochem.* 2002, 27, 396-402.
360. Goodsell, D. S.; Morris, G. M.; Olson, A. J., Automated docking of flexible ligands: applications of AutoDock. *J. Mol. Recognit.* 1996, 9, 1-5.
361. Zhang, X.; Cheng, X. Structure of the predominant protein arginine methyltransferase PRMT1 and analysis of its binding to substrate peptides. *Structure* 2003, 11, 509-520.
362. Xiao, B.; Jing, C.; Wilson, J. R.; Walker, P. A.; Vasisht, N.; Kelly, G.; Howell, S.; Taylor, I. A.; Blackburn, G. M.; Gamblin, S. J., Structure and catalytic mechanism of the human histone methyltransferase SET7/9. *Nature* 2003, 421, 652-656.